

Post  
OK

GEORGIA INSTITUTE OF TECHNOLOGY  
OFFICE OF RESEARCH ADMINISTRATION  
RESEARCH PROJECT INITIATION

Date: July 15, 1975

Project Title: Investigation of Long Term, High Temperature Changes in the  
Calcia-Stabilized Zirconia-Alumina System

Project No: E-18-612

Principal Investigator: Dr. J. E. Cochran and Dr. J. F. Banial

Sponsor: U. S. Bureau of Mines

Agreement Period: From June 16, 1975 Until June 15, 1976

Type Agreement: Grant No. G0155129

Amount: \$18,203 Bureau of Mines  
10,635 GIT (E-18-312)  
\$28,838 Total

Reports Required: Quarterly Technical Letter, Quarterly Financial Letter,  
Intermediate (if contract is extended), Final Technical

Sponsor Contact Person (s):

Technical Matters

Mr. M. H. Stanczyk  
Technical Project Officer  
Tuscaloosa Metallurgy  
P.O. Box L  
University, Alabama 35346

Administrative Matters

Mr. William B. Fulton, Jr.  
Contract Specialist  
U. S. Dept. of the Interior  
Bureau of Mines, Interior Bldg.  
Br. of Contracts & Grants, Room 2759  
18th & E Sts., N.W.  
Washington, D. C. 20240  
(202) 343-9393

Assigned to: Ceramic Engineering

COPIES TO:

Principal Investigator	Library
School Director	Rich Electronic Computer Center
Dean of the College	Photographic Laboratory
Director, Research Administration	Project File
Director, Financial Affairs (2)	
Security Reports-Property Office	
Patent Coordinator	Other

GEORGIA INSTITUTE OF TECHNOLOGY  
OFFICE OF CONTRACT ADMINISTRATION

## SPONSORED PROJECT TERMINATION

Date: 9/15/77

Project Title: "Investigation of Long Term, High Temperature Changes in Calcia-Stabilized Zirconia-Alumina System."

Project No: E-18-612

Project Director: J. K. Cochran and J. F. Benzel

Sponsor: U. S. Bureau of Mines

Effective Termination Date: 6/15/77Clearance of Accounting Charges: 6/15/77

Grant/Contract Closeout Actions Remaining:

- ☐ Final Invoice and Closing Documents
- ☐ Final Fiscal Report
- ☒ Final Report of Inventions
- ☒ Govt. Property Inventory & Related Certificate
- ☐ Classified Material Certificate
- ☐ Other \_\_\_\_\_

Assigned to: Ceramic Engineering (School/Laboratory)

## COPIES TO:

Project Director  
Division Chief (EES)  
School/Laboratory Director  
Dean/Director-EES  
Accounting Office  
Procurement Office  
Security Coordinator (OCA)  
Reports Coordinator (OCA)

Library, Technical Reports Section  
Office of Computing Services  
Director, Physical Plant  
EES Information Office  
Project File (OCA)  
Project Code (GTRI)  
Other \_\_\_\_\_

INVESTIGATION OF LONG TERM,  
HIGH TEMPERATURE CHANGES IN THE  
CALCIA-STABILIZED ZIRCONIA-ALUMINA SYSTEM

Quarterly Progress Report No. 1  
June 16 through August 31, 1975

Submitted to  
U. S. Bureau of Mines -- Metallurgy  
Washington, D. C. 20240

Grant No. G0155189

Submitted by  
Joe K. Cochran, Jr.  
School of Ceramic Engineering  
Georgia Institute of Technology  
Atlanta, Georgia 30332

INVESTIGATION OF LONG TERM,  
HIGH TEMPERATURE CHANGES IN THE  
CALCIA-STABILIZED ZIRCONIA-ALUMINA SYSTEM

Quarterly Progress Report No. 1  
June 16 through August 31, 1975

Introduction

The purpose of this investigation is to measure microstructural and phase changes in the CaO stabilized  $\text{ZrO}_2\text{-Al}_2\text{O}_3$  system after heat treatment as high as  $1300^\circ\text{C}$  for up to 2000 hours. In addition, high temperature flexural strength, thermal expansion, and room temperature microhardness will be investigated in an attempt to correlate these properties to microstructure and crystal structure changes.

The original intent of this work was to investigate compositions of high stabilized zirconia content plus  $\alpha\text{-Al}_2\text{O}_3$ . Phase relations for the  $\text{CaO-Al}_2\text{O}_3\text{-ZrO}_2$  ternary are not available. Thus, prior to selection of compositions for long term heat treatment, the high zirconia (greater than or equal to 55%) portion of the ternary is being investigated.

From the results to date, a preliminary ternary of the high  $\text{ZrO}_2$  portion of the  $\text{CaO-Al}_2\text{O}_3\text{-ZrO}_2$  system is presented below. In addition, raw material selection, experimental procedure, and comments on observed microstructure are discussed.

Raw Material Selection

Samples of zirconia were obtained from the Zirconium Corporation of America and the TAM Division of N L Industries. The samples from Zircoa were labeled Zircoa-B and Zircoa-C. Both samples were -325

mesh; B was a fully calcia-stabilized  $\text{ZrO}_2$  and C was a partially stabilized  $\text{ZrO}_2$ . TAM supplied CP  $\text{ZrO}_2$ -Milled, which is +99.0  $\text{ZrO}_2$  with an average particle size of 1.4  $\mu\text{m}$ , and CP-40, which is partially stabilized and -325 mesh. Pellets of all four were pressed and fired to 1500°C in a SiC furnace. Densities obtained from these tests were: Zircoa-B, 4.99 gm/cc; Zircoa-C, 5.59; CP  $\text{ZrO}_2$ , 5.82; and CP-40, 4.96. From density and observation of microstructures, CP  $\text{ZrO}_2$  exhibited the least porosity and was selected as the  $\text{ZrO}_2$  source for these studies. The calcia and alumina sources selected were calcium carbonate from Fisher Scientific and A-16 Superground  $\text{Al}_2\text{O}_3$  from Alcoa.

#### Tentative Phase Diagram of $\text{CaO-Al}_2\text{O}_3\text{-ZrO}_2$ System

Experimental Procedure. Nine compositions, Table I, in the high  $\text{ZrO}_2$  end of the  $\text{CaO-Al}_2\text{O}_3\text{-ZrO}_2$  ternary have been prepared and analyzed. The samples were weighed using the above described raw materials and mixed in an automatic  $\text{Al}_2\text{O}_3$  mortar and pestle for thirty minutes. Pellets 0.75 inches in diameter and 0.25 inches thick were pressed at 5000 psi. The samples were prefired to 1200°C in a SiC resistance furnace, gas fired to approximately 1700°C for one hour, and allowed to cool in the furnace. Bulk density was measured by water immersion, and crystalline phases were analyzed by x-ray diffraction. Optical examination consisted of polishing to a one  $\mu\text{m}$  diamond finish and photographing in reflected light at 600x. Observations on all samples showed three distinct phases: (a) closed porosity, (b) a white discontinuous phase assumed to be cubic ss mostly and/or monoclinic  $\text{ZrO}_2$ , and (c) a gray phase thought to be  $\text{CA}_6$  or  $\text{CA}_2$ . Relative amounts of these three phases were measured from the micrographs using point counting with a minimum of 300 points.

TABLE I. Composition, Crystalline Phases, Density, Porosity, and Quantitative Optical Data on Samples in the  $\text{CaO-Al}_2\text{O}_3\text{-ZrO}_2$  System

Sample No.	ZrO (m/o)	$\text{Al}_2\text{O}_3$ (m/o)	CaO (m/o)	Crystalline Phases	Bulk Density (g/cc)	Porosity %	Optical	
							% White	% Gray
1-1	64.0	20.0	16.0	Cubic SS, $\text{CA}_6$ , $\text{CA}_2$	4.31	13	61	39
1-2	68.0	20.0	12.0	Cubic SS, $\text{ZrO}_2$ , $\text{CA}_2$	4.08	25	79	21
1-3	72.0	20.0	8.0	$\text{ZrO}_2$ , Cubic SS, $\text{CA}_6$	4.72	13	62	38
1-4	69.6	13.0	17.4	Cubic SS, $\text{CA}_2$	4.40	21	76	24
1-5	74.0	13.0	13.0	Cubic SS, $\text{CA}_2$	4.59	7	69	31
1-6	78.3	13.0	8.7	Cubic SS, $\text{ZrO}_2$	4.94	11	78	22
1-7	76.2	4.8	19.0	Cubic SS, $\text{CA}_2$ , CZ	4.60	10	84	16
1-8	80.9	4.8	14.3	Cubic SS	4.83	10	89	11
1-9	85.7	4.8	9.5	Cubic SS, $\text{ZrO}_2$	5.18	16	94	6

## Results and Discussion

The crystalline phases detected by x-ray are listed in Table I and a tentative phase diagram for the high  $\text{ZrO}_2$  end of the  $\text{CaO-Al}_2\text{O}_3\text{-ZrO}_2$  system is shown in Figure 1. The exact position of the phase regions has not been determined and 25 additional samples have been prepared and are being analyzed to provide a more definitive phase diagram. It is important to note that no free alumina was detected in any of the samples. Apparently only a small amount of  $\text{Al}_2\text{O}_3$  will exist in solid solution in cubic or monoclinic  $\text{ZrO}_2$ . Once the solubility has been exceeded, the alumina forms calcium aluminates.

Due to the much greater mass absorption coefficient of zirconium, calcium aluminates and alumina are difficult to detect in the presence of a major zirconia phase. Mixtures of  $\text{CA}_2$ ,  $\text{CA}_6$ , and  $\text{Al}_2\text{O}_3$  with cubic and monoclinic  $\text{ZrO}_2$  are being prepared to establish the detectability limits.

Except for Sample 1-3, the microstructure of all the compositions were similar, consisting of grains of cubic and/or monoclinic  $\text{ZrO}_2$  in a continuous minor phase of  $\text{CA}_2$  and/or  $\text{CA}_6$ . The porosity consisted of isolated pores. From point counting, the relative amounts of the "white" zirconia phases and gray calcium aluminates were determined (Table 1). As would be expected, the relative amount of white zirconia phases increased with  $\text{ZrO}_2$  content, but even at the highest  $\text{ZrO}_2$  content (Sample 1-9), 6% of a gray phase was measured optically. X-ray analysis of this sample indicated no phases other than cubic and monoclinic zirconia.

After the phase regions have been established with more precision, three compositions will be selected for long term firing studies. At this point, it appears that one composition from the cubic ss region and two from the cubic ss- $\text{CA}_2$  region will be investigated.

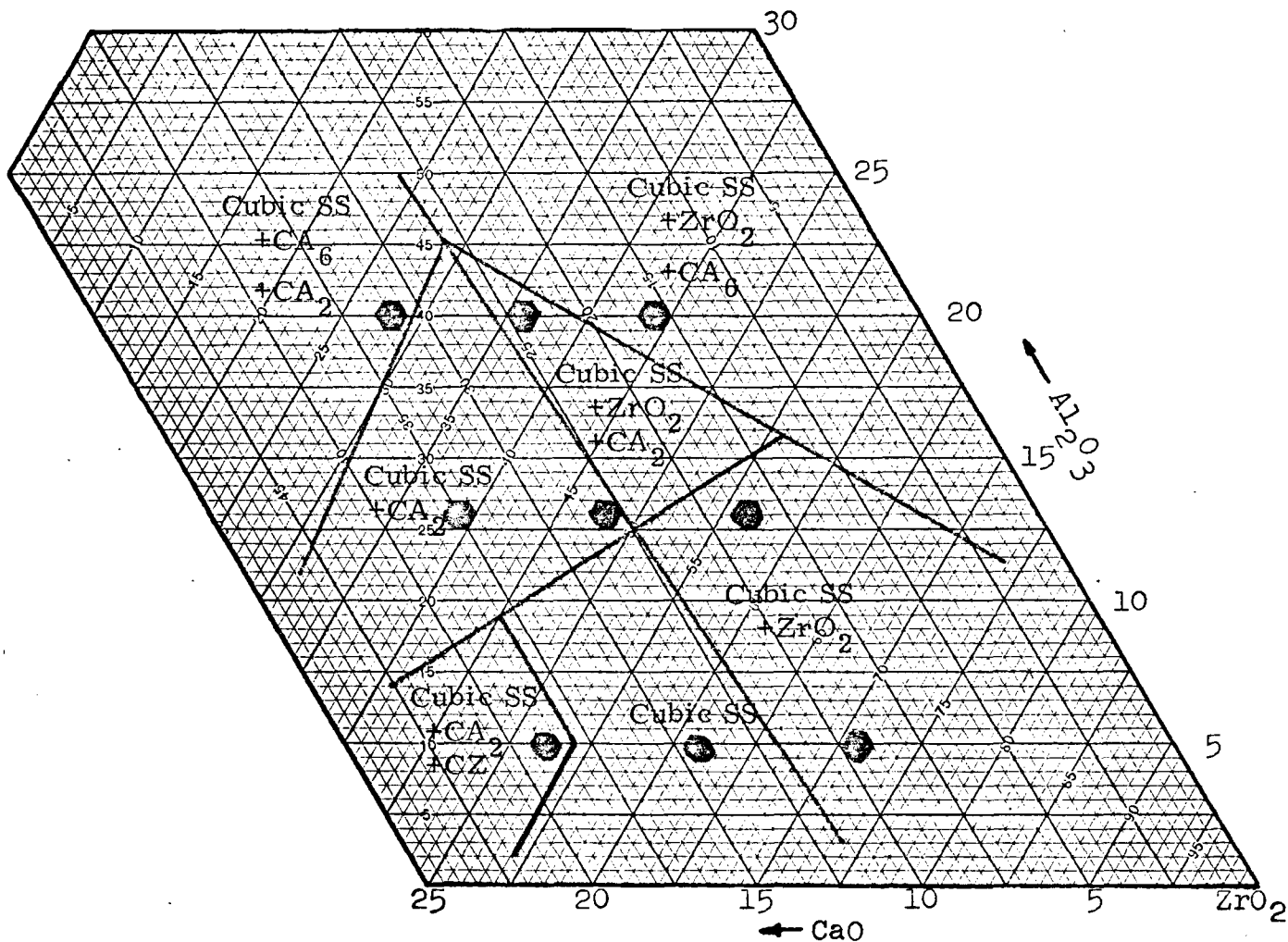


Figure 1. Tentative Phase Diagram for High ZrO<sub>2</sub> End of  
CaO-Al<sub>2</sub>O<sub>3</sub>-ZrO<sub>2</sub> System.



### Personnel

In addition to Dr. James F. Benzel and myself, two graduate students are working on this investigation. One, Mr. Jae Do Lee, is a Ph. D. candidate and has an M. S. degree in Ceramic Engineering. The other, Mr. John Day, is a candidate for a Masters degree.

E-18-612

INVESTIGATION OF LONG TERM,  
HIGH-TEMPERATURE CHANGES IN THE  
CALCIA-STABILIZED ZIRCONIA-ALUMINA SYSTEM

Quarterly Progress Report No. 2  
September 1, 1975 through November 30, 1975

Submitted to:

U.S. Bureau of Mines -- Metallurgy  
Washington, D.C. 20240

Grant Number G0155189

Submitted by:

Joe K. Cochran, Jr.  
School of Ceramic Engineering  
Georgia Institute of Technology  
Atlanta, Georgia 30332

INVESTIGATION OF LONG TERM,  
HIGH-TEMPERATURE CHANGES IN THE  
CALCIA-STABILIZED ZIRCONIA-ALUMINA SYSTEM

Quarterly Progress Report No. 2  
September 1 through November 30, 1975

Introduction

The purpose of this investigation is to measure microstructural and phase changes in the CaO-stabilized  $\text{ZrO}_2\text{-Al}_2\text{O}_3$  system after heat treatment as high as  $1300^\circ\text{C}$  for up to 2000 hours. In addition, high temperature flexural strength, thermal expansion, and room temperature microhardness will be investigated in an attempt to correlate these properties to microstructure and crystal structure changes.

The original intent of this work was to investigate compositions of high stabilized zirconia content plus  $\alpha\text{-Al}_2\text{O}_3$ . Phase relations for the CaO- $\text{Al}_2\text{O}_3$ - $\text{ZrO}_2$  ternary were not available. Thus, prior to selection of compositions for long term heat treatment, the phase relations in the high zirconia (greater than or equal to 55%) portion of the ternary had to be established.

From results to date, the ternary of the high  $\text{ZrO}_2$  portion of the CaO- $\text{Al}_2\text{O}_3$ - $\text{ZrO}_2$  system, both slow cooled ( $\sim 1^\circ\text{C}/\text{min}$ ) and quenched from  $1500^\circ\text{C}$ , is presented below as determined from 39 compositions. In addition, porosity, volume fraction of  $\text{ZrO}_2$  containing phases, and microstructure were determined from optical micrographs of selected compositions

to aid in selection of long term compositions. Based on these results, three compositions in the  $\text{CaO}-2\text{Al}_2\text{O}_3$ , Cubic  $\text{ZrO}_2$ , Monoclinic  $\text{ZrO}_2$  region of the ternary were selected for long term firing studies. The long term compositions were selected to contain a constant weight ratio of cubic/monoclinic equal to three.

### Phase Diagram of the $\text{CaO}-\text{Al}_2\text{O}_3-\text{ZrO}_2$ System at $1500^\circ\text{C}$

Experimental Procedure. Thirty-nine compositions, Table 1, in the high  $\text{ZrO}_2$  end of the  $\text{CaO}-\text{Al}_2\text{O}_3-\text{ZrO}_2$  ternary were prepared and analyzed using raw materials described in Quarterly Progress Report No. 1. Samples were weighed, mixed in an automatic  $\text{Al}_2\text{O}_3$  mortar and pestle for thirty minutes, and calcined at  $1200^\circ\text{C}$  for 20 hours to prereact the components. The calcined powder was reground for 30 minutes, pressed into pellets of 0.75 inch diameter and 0.25 inch thickness at 5000 psi, and fired to  $1700^\circ\text{C}$  for 20 hours. The pellets were slow cooled to room temperature at  $\sim 1^\circ\text{C}/\text{min}$  and analyzed as described below. After analysis, the same pellets were refired to  $1500^\circ\text{C}$  for 20 hours and water quenched.

Both qualitative and quantitative phase analyses were accomplished using x-ray diffraction. Standards for determining weight ratios of cubic/monoclinic zirconia were prepared from pure cubic zirconia (15 m/o  $\text{CaO}$ ) and pure monoclinic  $\text{ZrO}_2$  (0 m/o  $\text{CaO}$ ) using cubic/monoclinic weight ratios of 4, 1, and 0.25. From x-ray diffraction theory, it can be shown that there is a linear relation between the intensity ratios of x-ray

Table 1. Compositions and Qualitative Phases Present In  
The  $\text{CaO-ZrO}_2\text{-Al}_2\text{O}_3$  System at  $1500^\circ\text{C}$

Composition	CaO (m/o)	$\text{Al}_2\text{O}_3$ (m/o)	$\text{ZrO}_2$ (m/o)	Phases Present*
C-1	16	20	64	Cubic, $\text{CA}_2$ , Mono
C-2	12	20	68	Cubic, $\text{CA}_2$ , Mono
C-3	8	20	72	Mono, $\text{CA}_2$ , $\text{CA}_6$
C-4	17.4	13	69.6	Cubic, $\text{CA}_2$
C-5	13.0	13	74.0	Cubic, Mono, $\text{CA}_2$
C-6	8.7	13	78.3	Cubic, Mono, $\text{CA}_2$
C-7	19.0	4.8	76.2	Cubic, $\text{CA}_2$
C-8	14.3	4.8	80.9	Cubic, $\text{CA}_2$
C-9	9.5	4.8	85.7	Cubic, Mono, $\text{CA}_2$
C-10	20	0	80	Cubic
C-11	15	0	85	Cubic
C-12	10	0	90	Cubic, Mono
C-13	12.5	0	87.5	Cubic, Mono
C-14	17.5	0	82.5	Cubic
2-1	20	25	55	Cubic, $\text{CA}_2$
2-2	17.5	25	57.5	Cubic, Mono, $\text{CA}_2$
2-3	15	25	60.0	Cubic, Mono, $\text{CA}_2$
2-4	12.5	25	62.5	Mono, Cubic, $\text{CA}_2$
2-5	10	25	65	Mono, $\text{CA}_2$ , $\text{CA}_6$
2-6	20	20	60	Cubic, $\text{CA}_2$
2-7	17.5	20	62.5	Cubic, $\text{CA}_2$

Table 1. (Continued)

Composition	CaO (M/o)	Al <sub>2</sub> O <sub>3</sub> (m/o)	ZrO <sub>2</sub> (m/o)	Phases Present*
2-8	15	20	65	Cubic, Mono, CA <sub>2</sub>
2-9	125	20	67.5	Cubic, Mono, CA <sub>2</sub>
2-10	10	20	70	Mono, Cubic, CA <sub>2</sub>
2-11	20	15	65	Cubic, CA <sub>2</sub>
2-12	17.5	15	67.5	Cubic, CA <sub>2</sub>
2-13	15	15	70	Cubic, CA <sub>2</sub> , Mono
2-14	12.5	15	72.5	Cubic, Mono, CA <sub>2</sub>
2-15	10	15	75	Cubic, Mono, CA <sub>2</sub>
2-16	20	10	70	Cubic, CA <sub>2</sub>
2-17	17.5	10	72.5	Cubic, CA <sub>2</sub>
2-18	15	10	75	Cubic, CA <sub>2</sub>
2-19	12.5	10	77.5	Cubic, Mono, CA <sub>2</sub>
2-20	10	10	80	Cubic, Mono, CA <sub>2</sub>
2-21	20	5	75	Cubic, CA <sub>2</sub>
2-22	17.5	5	77.5	Cubic, CA <sub>2</sub>
2-23	15	5	80	Cubic, CA <sub>2</sub>
2-24	12.5	5	82.5	Cubic, Mono, CA <sub>2</sub>
2-25	10	5	85	Cubic, Mono, CA <sub>2</sub>

\* (1) Compositions 2-11, 2-12, 2-16, 2-17, 2-21, 2-22, C-4, and C-7 contain small quantities of 4 CaO·3Al<sub>2</sub>O<sub>3</sub>·SO<sub>3</sub> in addition to the phases above. This sulfate phase was concentrated on the surface of the samples. Chemical analysis of the TAM zirconia raw material listed a SO<sub>2</sub> content of 0.1%, which apparently is enough SO<sub>2</sub> to produce the calcium-alumino-sulfate that was identified.

(2) Cubic = Cubic ZrO<sub>2</sub>, Mono = Monoclinic ZrO<sub>2</sub>, CA<sub>2</sub> = CaO·2Al<sub>2</sub>O<sub>3</sub>, CA<sub>6</sub> = CaO·6Al<sub>2</sub>O<sub>3</sub>.

peaks from two components and their weight ratios. Using the peak heights ( $I$ ) from the  $11\bar{1}$  and  $111$  planes of monoclinic  $ZrO_2$  ( $I_{M11\bar{1}}$  and  $I_{M111}$ , respectively) and the  $111$  planes of cubic zirconia ( $I_{C111}$ ), the intensity ratios for cubic / monoclinic ( $I_{C111}/I_{M11\bar{1}}$  and  $I_{C111}/I_{M111}$ ) were plotted versus weight ratio cubic/monoclinic, Figure 1. Intensity ratios were measured for all samples containing both cubic and monoclinic  $ZrO_2$ , and weight ratios of cubic to monoclinic were determined from the least squares equations for the two lines of Figure 1, Table 2. Since two weight ratios were measured for each sample ( $I_{C111}/I_{M11\bar{1}}$  and  $I_{C111}/I_{M111}$ ), the average of these two weight ratios was used for the calculations described below.

Phase Diagram at 1500°C. The phase diagram for the  $CaO-Al_2O_3-ZrO_2$  system both slow cooled and quenched from 1500°C is presented in Figures 2-3. The results of the qualitative x-ray identification were identical except that cubic  $ZrO_2$  x-ray intensities were slightly greater and monoclinic  $ZrO_2$  and  $Ca_2$  x-ray intensities were slightly less in the quenched samples. This indicates that at high temperatures both  $CaO$  and  $Al_2O_3$  have greater solubility in  $ZrO_2$  than at lower temperatures. The increased solubility of  $CaO$  and  $Al_2O_3$  with increasing temperature is probably responsible for the differences between the phase diagram at 1500°C reported here and the 1700°C phase diagram reported in Quarterly Progress Report No. 1.

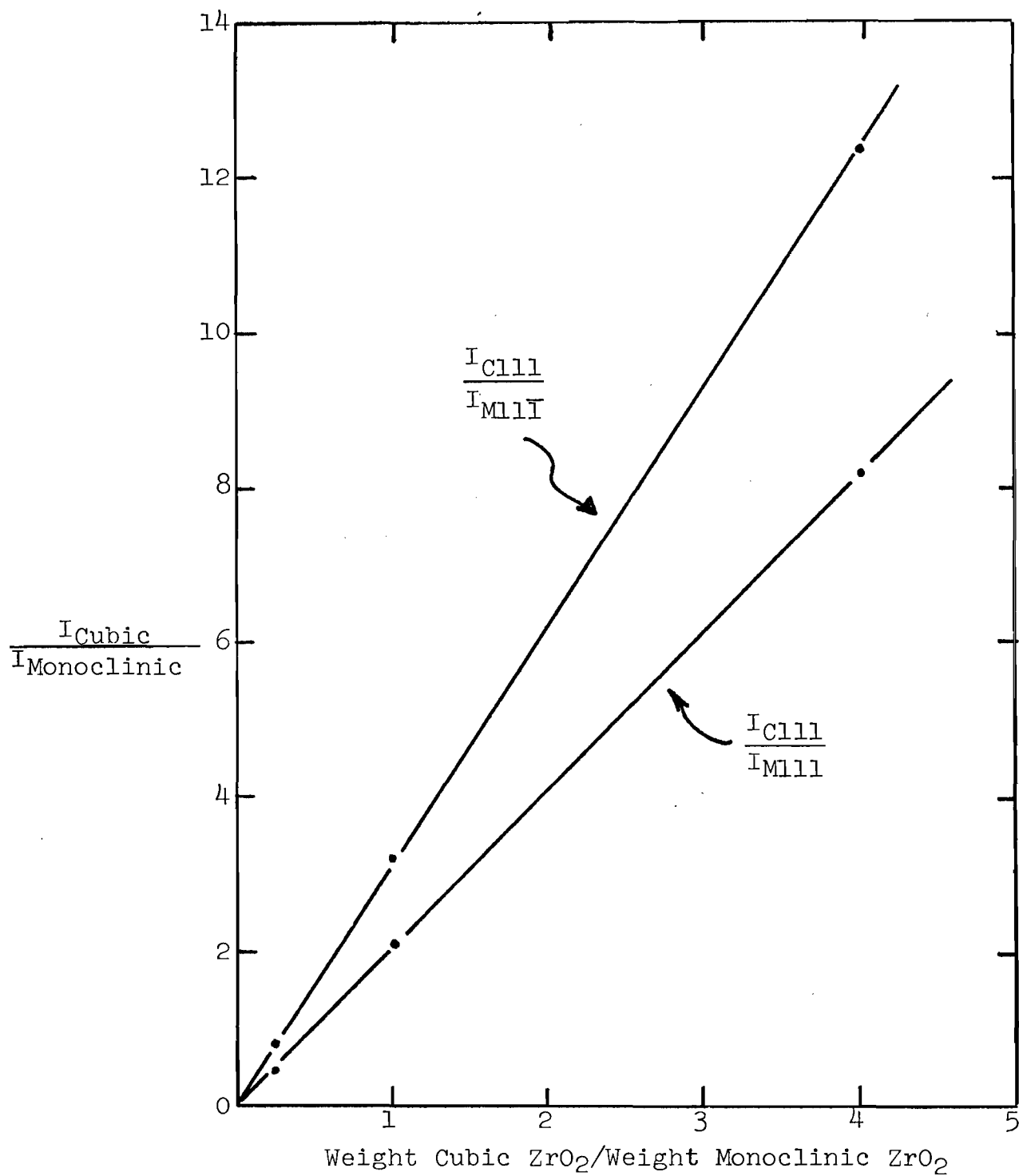


Figure 1. X-ray Diffraction Standard Curve for Determining Weight Ratio of Cubic to Monoclinic  $\text{ZrO}_2$  Based on X-ray Peak Heights.



TABLE 2. Quantitative Analysis of the  $\text{Ca}_2\text{O} + \text{Cubic ZrO}_2 + \text{Monoclinic ZrO}_2$  Region of the  $\text{CaO-Al}_2\text{O}_3\text{-ZrO}_2$  System.

Composition	Weight Ratio of Cubic to Monoclinic	Al <sub>2</sub> O <sub>3</sub> /CaO Molar Ratio	
		Assuming Cubic = 16% CaO Mono = 2% CaO	Assuming Cubic = 14% CaO Mono = 2% CaO
C-1	2.94	3.0	2.88
C-2	0.36	2.6	2.49
C-5	2.13	4.6	2.99
C-6	0.32	3.3	2.97
C-9	1.65	<del>3.0</del>	27.85
2-2	3.74	2.8	2.46
2-3	1.04	2.8	2.59
2-4	0.08	2.4	2.38
2-8	2.90	3.6	2.98
2-9	1.46	4.5	3.70
2-10	0.16	2.9	2.79
2-13	17.92	6.6	3.82
2-14	2.77	7.3	4.47
2-15	0.87	5.6	4.25
2-19	7.25	<del>8.0</del>	9.20
2-20	1.59	<del>6.0</del>	4.64
2-24	29.43	<del>10.0</del>	<del>3.0</del>
2-25	3.16	<del>8.0</del>	<del>2.0</del>



Figure 3. Phase Diagram for  $\text{CaO-Al}_2\text{O}_3\text{-ZrO}_2$  System at  $1500^\circ\text{C}$ .

The cubic to monoclinic weight ratios, Table 1, were used to estimate the position of the lines separating the cubic  $\text{ZrO}_2$ - $\text{CA}_2$ ,  $\text{CA}_2$ - $\text{CA}_6$  regions of the diagram. These weight ratios are plotted in Figure 4 and a constant cubic/monoclinic weight ratio line of 3.0 was drawn. Compositions on this 3.0 weight ratio line were selected for long term firing samples.

Attempts were made to determine the CaO solubility in Cubic  $\text{ZrO}_2$  in the  $\text{CA}_2$ -Cubic-Monoclinic region of the phase diagram. Literature indicates that the minimum solubility of CaO in cubic  $\text{ZrO}_2$  is 14 m/o. However, using cubic to monoclinic weight ratios for the CaO- $\text{ZrO}_2$  samples, C-12 and C-13, CaO contents of  $\sim 13$  m/o were calculated for cubic  $\text{ZrO}_2$  with monoclinic  $\text{ZrO}_2$  present. (The assumption was made that monoclinic  $\text{ZrO}_2$  contained 2 m/o CaO.)

By assuming that monoclinic  $\text{ZrO}_2$  contains 2 m/o CaO and no  $\text{Al}_2\text{O}_3$  solubility exists in cubic or monoclinic  $\text{ZrO}_2$ , the  $\text{Al}_2\text{O}_3$ /CaO mole ratios available to form  $\text{CA}_2$  were calculated using the weight ratios in the Cubic  $\text{ZrO}_2$ -Monoclinic  $\text{ZrO}_2$ - $\text{CA}_2$  region and assuming a fixed CaO content in cubic  $\text{ZrO}_2$ . These  $\text{Al}_2\text{O}_3$ /CaO mole ratios were calculated for calcia solubilities of 16 and 14 m/o in cubic  $\text{ZrO}_2$ , Table 2. Since available literature shows no solid solution for  $\text{CA}_2$ , it is probable that the correct CaO solubility in cubic  $\text{ZrO}_2$  would correspond to that necessary to calculate an  $\text{Al}_2\text{O}_3$  to CaO mole ratio of 2. By decreasing the CaO solubility in cubic  $\text{ZrO}_2$  from 16 to 14 m/o, the  $\text{Al}_2\text{O}_3$ /CaO ratios were approaching 2 for some compositions, but were still greater than 2 at 14 m/o. In

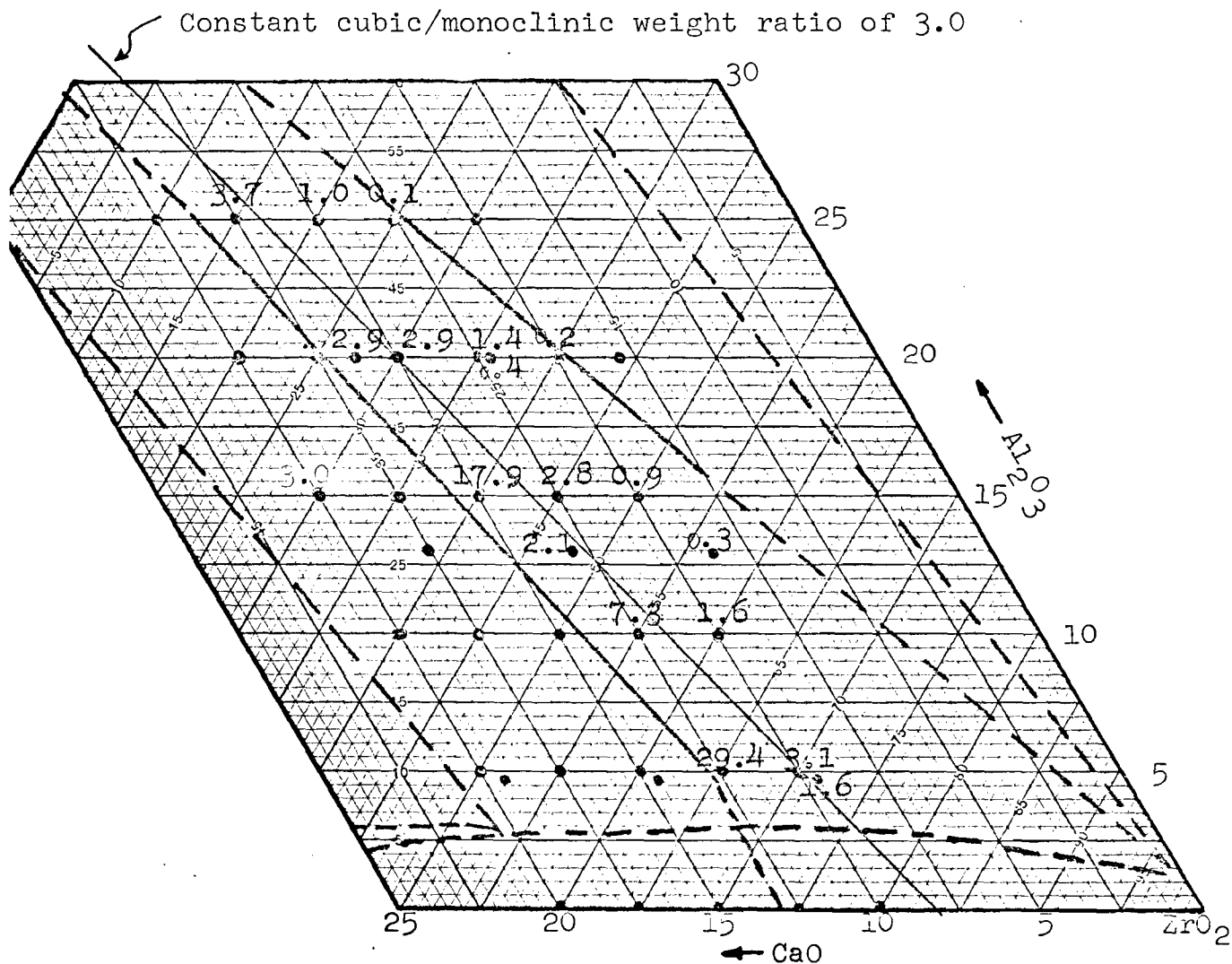


Figure 4. Weight Ratios of Cubic ZrO<sub>2</sub> to Monoclinic ZrO<sub>2</sub> in the CA<sub>2</sub>, Cubic ZrO<sub>2</sub>, Monoclinic ZrO<sub>2</sub> Region of the CaO-Al<sub>2</sub>O<sub>3</sub>-ZrO<sub>2</sub> System.

addition, it may be seen that as both monoclinic and cubic  $\text{ZrO}_2$  contents increase, the calculated  $\text{Al}_2\text{O}_3/\text{CaO}$  ratios also increase. Thus, to obtain  $\text{Al}_2\text{O}_3/\text{CaO}$  ratios compatible with  $\text{CA}_2$  in this region, solubilities of less than 14 m/o CaO in cubic  $\text{ZrO}_2$  and less than 2 m/o CaO in monoclinic will have to be assumed. Further calculations will be made to estimate more precisely the CaO solubilities in the two zirconia structures.

### Microstructure Analysis

Microstructural analyses were made from reflected light micrographs of selected samples at 600x. Observations on all samples showed, as reported previously, three distinct phases: a) closed porosity, b) a white continuous phase (at 1700°C the white phase had been discontinuous) assumed to be cubic  $\text{ZrO}_2$  and/or monoclinic  $\text{ZrO}_2$ , and c) a gray discontinuous phase assumed to be  $\text{CA}_2$  and/or  $\text{CA}_6$ . Relative volumes of these phases were estimated from the micrographs using point counting with a minimum of 300 points, Table 3. The average grain size of all phases was estimated to be well under 10  $\mu\text{m}$ , but quantitative grain size analysis was not performed.

A plot of porosity on the phase diagram, Figure 5, showed a sharp break between a region of high porosity and a region of low porosity. The line separating the two regions probably is parallel to constant temperature liquidus lines on the phase diagram. Volume fractions of zirconia containing phases Table 3, increased as would be expected with increasing  $\text{ZrO}_2$  content.

Table 3. Quantitative Microstructural Analysis of Selected  
 $\text{CaO-Al}_2\text{O}_3\text{-ZrO}_2$  Compositions Fired to  $1500^\circ\text{C}$  for  
 20 Hours and Slow Cooled

Composition	Porosity (%)	Volume Fraction $\text{ZrO}_2$ Phases Excluding Porosity	Volume Fraction $\text{CA}_2+\text{CA}_6$ Excluding Porosity
C-1	7	0.52	0.48
C-2	6	0.56	0.44
C-3	38	0.65	0.35
C-4	7	0.67	0.33
C-5	24	0.70	0.30
C-6	24	0.71	0.29
C-7	9	0.81	0.19
C-8	33	0.87	0.13
C-9	26	0.80	0.20
2-1	6	0.49	0.51
2-3	8	0.52	0.49
2-5	13	0.49	0.51
2-9	11	0.54	0.46
2-11	4	0.65	0.35
2-21	10	0.79	0.21
2-25	20	0.79	0.21

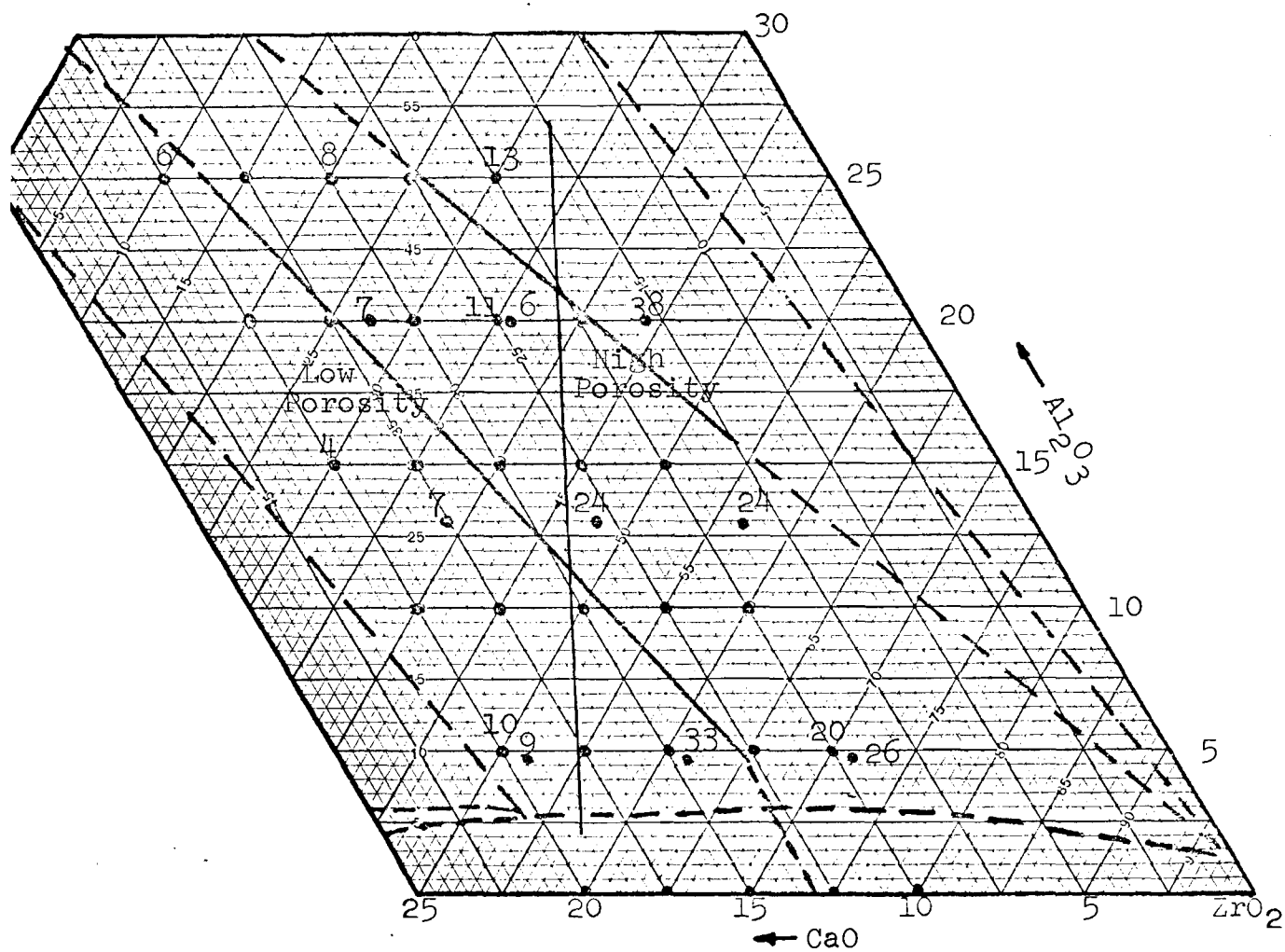


Figure 5. Porosity Diagram for  $\text{CaO-Al}_2\text{O}_3\text{-ZrO}_2$  Compositions  
Fired to  $1500^\circ\text{C}$  and Slow Cooled.



### Selection of Long Term Compositions

Three compositions were selected for long term firing studies to contain a cubic to monoclinic weight ratio of 3.0 and varying  $\text{CA}_2$  contents. This was done to approximate a two-component system since with a constant cubic/monoclinic ratio the  $\text{ZrO}_2$  phases should act as a single phase of varying amount. The compositions selected from the 3.0 weight ratio line of Figure 4 were:

Composition	CaO (m/o)	$\text{Al}_2\text{O}_3$ (m/o)	$\text{ZrO}_2$ (m/o)
A	12.5	10	77.5
B	14.5	17.5	68.0
C	17.5	25.0	57.5

Preparation of a four-kilogram batch of each composition is underway and will be reported in the next quarterly report.

E-18-612

INVESTIGATION OF LONG TERM,  
HIGH-TEMPERATURE CHANGES IN THE  
CALCIA-STABILIZED ZIRCONIA-ALUMINA SYSTEM

QUARTERLY PROGRESS REPORT NO. 3  
DECEMBER 1, 1975 THROUGH FEBRUARY 29, 1976

SUBMITTED TO:  
U.S. BUREAU OF MINES -- METALLURGY  
WASHINGTON, D.C. 20240

GRANT NUMBER G0155189

SUBMITTED BY:  
JOE K. COCHRAN, JR.,  
SCHOOL OF CERAMIC ENGINEERING  
GEORGIA INSTITUTE OF TECHNOLOGY  
ATLANTA, GEORGIA 30332

Investigation of Long Term,  
High-Temperature Changes In The  
Calcia-Stabilized Zirconia-Alumina System

Quarterly Progress Report No. 3  
December 1, 1975 through February 29, 1976

INTRODUCTION

The purpose of this investigation is to measure micro-structural and phase changes in the CaO-stabilized  $ZrO_2$ - $Al_2O_3$  system after heat treatment as high as  $1300^{\circ}C$  for up to 2000 hours. In addition, high temperature flexural strength, thermal expansion, and room temperature microhardness will be investigated in an attempt to correlate these properties to microstructure and crystal changes.

The original intent of this work was to investigate compositions of high stabilized zirconia content plus  $Al_2O_3$ . Phase relations for the CaO- $Al_2O_3$ - $ZrO_2$  ternary were not available. Thus, prior to selection of compositions for long term heat treatment, the phase relations in the high zirconia (greater than or equal to 55%) portion of the ternary were established and were reported in Quarterly 1 and 2. It should be noted that work is continuing in refining the phase diagram and will be reported in the future.

Based on the results from the phase diagram study, three compositions in the  $CA_2$ -cubic  $ZrO_2$ -Monoclinic  $ZrO_2$ , compatibility triangle were selected for long term firing studies. During this

quarter, the long term firing compositions were fabricated and firings were initiated. In addition, initial physical property measurements were made as reported below. The three compositions are presented in Table I, as are estimated weight and volume percentages.

#### LONG TERM FIRING STUDIES

Sample Preparation and Firing. Four kilogram batches of each composition, Table 1, were prepared. Each batch was mixed in a polyethylene jar with alumina balls for 24 hours and the powder was calcined at  $1200^{\circ}\text{C}$  for 20 hours. The calcined powder was examined by x-ray diffraction to determine if a stable ratio of cubic to monoclinic zirconia had been achieved. The batches were reground in the polyethylene jars and recalcined twice before a constant cubic to monoclinic zirconia ratio was obtained. Batches were lightly ground after the final calcining prior to sample fabrication. One hundred pellets of (0.75 in diameter and 0.25 in. thick), each composition were dry pressed in a Stokes Model F. Tablet Press and 50 (0.25 x 0.25 x 4 in.) bars were dry pressed at 5000 psi. Three weight percent kerosene was added to both the bars and pellets as a lubricant. Both the bars and pellets were fired at  $1550^{\circ}\text{C}$  for 24 hours on stabilized  $\text{ZrO}_2$  setter plates. Both heating and cooling was carried out at  $1^{\circ}\text{C}/\text{min}$ . After firing, the bars were cut with a diamond saw to 1.5 in. lengths.

Samples were subjected to long term heat treatment at 900 and  $1300^{\circ}\text{C}$ . Thirty-two bars and 18 pellets of each composition were placed in covered alumina saggers and 12 pellets of each

Table I. Chemical and Crystallographic Contents of CaO-Al<sub>2</sub>O<sub>3</sub> - ZrO<sub>2</sub> Composition Used in Long Term Firing Studies<sup>2,3</sup>

Oxide and Phase	Composition (Mole %)		
	A	B	C
CaO	12.5	14.5	17.5
Al <sub>2</sub> O <sub>3</sub>	10.0	17.5	25.0
ZrO <sub>2</sub>	77.5	68.0	57.5
Composition (Wt. %)*			
Cubic ZrO <sub>2</sub>	65.7	58.4	50.7
Mono ZrO <sub>2</sub>	21.9	19.5	16.9
CA <sub>2</sub>	12.4	22.1	32.4
Composition (Vol. %)*			
Cubic ZrO <sub>2</sub>	57.0	46.3	36.8
Mono ZrO <sub>2</sub>	20.1	16.3	13.0
CA <sub>2</sub>	22.9	37.4	50.2
Theoretical Density*			
	5.33	4.87	4.47

\* Weight and volume percentage and density calculations were based on densities of 6.15, 5.83, and 2.88 g/cc for cubic ZrO<sub>2</sub>, Mono ZrO<sub>2</sub>, and CA<sub>2</sub>, respectively, and assuming all the Al<sub>2</sub>O<sub>3</sub> forms CA<sub>2</sub> and a Cubic/Mono ZrO<sub>2</sub> weight ratio of 3:1 is achieved.

composition were placed on top of the saggers. The samples were heated to temperature at  $1^{\circ}\text{C}/\text{min}$ . After 200, 400, 600 and 800 hours, three pellets of each composition were withdrawn from the furnace and air quenched. Samples inside the sagger thus were not thermal shocked by removal of the pellets. At 1000 hours, the furnaces were cooled at  $1^{\circ}\text{C}/\text{min}$ , 16 bars and 3 pellets were removed, 12 pellets from inside the saggers were placed on top, and the furnaces were reheated to temperature at  $1^{\circ}\text{C}/\text{min}$ . Pellets were withdrawn at 1200, 1400, 1600, and 1800 hours and after 2000 hours, the furnaces were cooled at  $1^{\circ}\text{C}/\text{min}$ .

Flexure Strength Measurement. Flexure strength measurements were made in three point loading on an Instron Universal Tester using a span of 1.25 inches and a head speed of 0.01 cm/min. Samples were broken as fired with no surface treatment.

Thermal Expansion Measurement. Thermal expansion measurements were made on an Orton Automatic Recording Dilatometer using an  $\text{Al}_2\text{O}_3$  sample tube and push rod. Maximum temperature was limited to  $1200^{\circ}\text{C}$  which was sufficient to observe the monoclinic to tetragonal inversion in  $\text{ZrO}_2$ . The thermal expansion on both heating and cooling was recorded.

Physical Property Results. The flexure strength, bulk density, porosity, and volume of  $CA_2$  present in the "as fired" compositions prior to heat treatment have been measured, Table II. The results, particularly flexure strength, are interesting. Strengths show a large increase as the  $CA_2$  content increases and the Cubic and Monoclinic  $ZrO_2$  decreases. It is not known at this point whether the strength increase is due to the increases in  $CA_2$  or to a reduction of monoclinic  $ZrO_2$ . The reduction in monoclinic content from composition A to B to C was greater than indicated by the values in Table I (which were estimated from chemical composition) because x-ray analysis showed a greater cubic to monoclinic  $ZrO_2$  ratio than had been measured at  $1500^{\circ}C$ . No monoclinic  $ZrO_2$  was detected by x-ray diffraction for composition C fired at  $1550^{\circ}C$ .

Thermal expansion results, Figure 1, confirmed the absence of monoclinic  $ZrO_2$  in composition C at  $1550^{\circ}C$  and as was expected, both composition A and B showed the presence of monoclinic  $ZrO_2$ .

The x-ray results indicated increased cubic stability resulting from changes in solution of  $CaO$  and/or  $Al_2O_3$  in Cubic  $ZrO_2$  at  $1550^{\circ}C$  compared to  $1500^{\circ}C$ . This was even more evident when the volume of  $CA_2$  measured optically in C was compared to that calculated from chemical composition. The observed (optical) value for  $CA_2$  in C was 42.8% compared to a calculated value of 50.2%, Table II. This again indicated significantly

Table II. Room Temperature Properties of Long Term Firing  
Compositions As Fired to 1550°C for 20 Hours

Composition	Flexure	Bulk	Porosity	Theoretical*		CA <sub>2</sub> (Vol.%)	
	Strength	Density	(Optically)	Density			
	(psi)			Measured*	Table I	(optically)	(Table 1)
A	6,700	5.218	4.5	5.46	5.33	22.0	22.9
B	11,400	4.777	4.1	4.98	4.87	39.7	37.4
C	15,380	4.546	2.8	4.68	4.47	42.8	50.2

\* Measured Theoretical Density was determined from Bulk Density/(1-Pore Fraction)



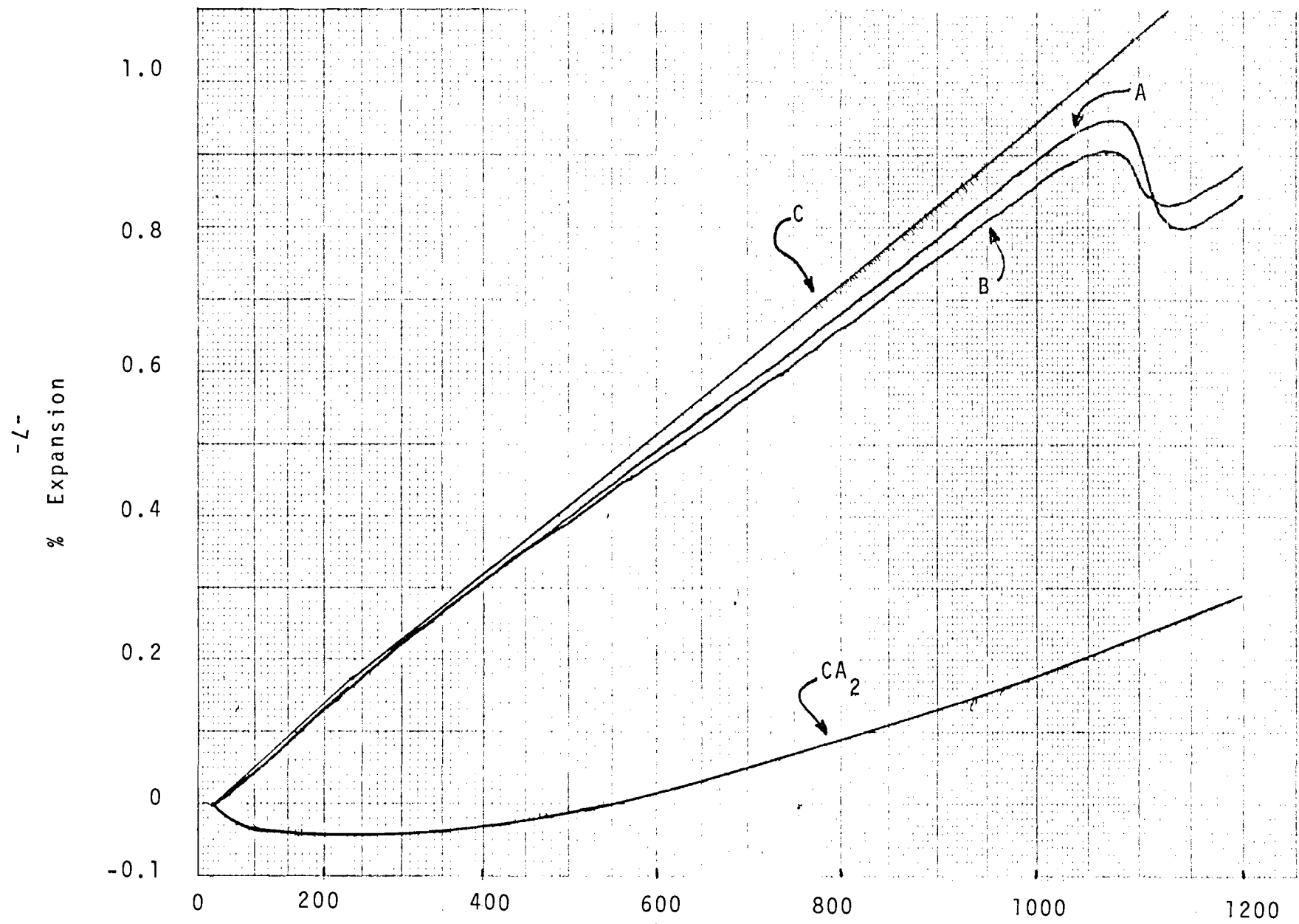


Figure 1. Thermal Expansion of CA<sub>2</sub> and Compositions A, B, and C as Fired to 1550°C.

less  $CA_2$  present in the 1550°C samples than was expected.

Final explanations for variations in strengths and  $CA_2$  contents will probably depend on the physical property information available for  $CA_2$ . Very little  $CA_2$  information has been found in the literature and it would be beneficial to develop physical property data on  $CA_2$ . An attempt was made to synthesize a small quantity of  $CA_2$  for thermal expansion measurements. A mixture of  $CaCO_3$  and  $Al_2O_3$  to produce  $CA_2$  was melted in a SiC crucible and x-ray analysis indicated a high fraction of  $CA_2$  with only a small quantity of CA. Thermal expansion values for the  $CA_2$ , Table III, were very low,  $2.5 \times 10^{-6}/^{\circ}C$  at 1200°C. Thus, with the low thermal expansion,  $CA_2$  should be beneficial in reducing the thermal shock of  $CAO-Al_2O_3-ZrO_2$  refractories. Thermal expansion values for compositions A, B, and C, Table III, were higher than expected since they are comparable to pure cubic  $ZrO_2$ . Considering the low expansion values for  $CA_2$  and the quantity of  $CA_2$  present, particularly in C, the additive thermal expansion equation would predict a much lower expansion.

Table III. Thermal Expansion of  $CA_2$  and Compositions  
A, B, and C as Fired to  $1550^{\circ}C$

T ( $^{\circ}C$ )	$CA_2$	% Expansion		
		A	B	C
200	-0.050	0.120	0.135	0.140
400	-0.030	0.310	0.310	0.320
600	+0.010	0.490	0.475	0.515
800	+0.085	0.680	0.660	0.720
1000	+0.175	0.895	0.860	0.945

Monoclinic Inversion

Length Change (%)	0.14	0.08	0
-------------------	------	------	---

T ( $^{\circ}C$ )	$CA_2$	$a_{Eng} \times 10^{-6}/^{\circ}C$		
		A	B	C
200	-2.8	6.7	7.2	7.8
400	-0.8	8.2	8.2	8.4
600	0.2	8.4	8.2	8.9
800	1.1	8.7	8.5	9.2
1000	1.8	9.1	8.8	9.6

INVESTIGATION OF LONG TERM,  
HIGH-TEMPERATURE CHANGES IN THE  
CALCIA-STABILIZED ZIRCONIA-ALUMINA SYSTEM

Quarterly Progress Report No. 4  
March 1 through May 31, 1976

Submitted to:

U.S. Bureau of Mines -- Metallurgy  
Washington, D.C. 20240

Grant Number G0155189

Submitted by:

Joe K. Cochran, Jr.  
School of Ceramic Engineering  
Georgia Institute of Technology  
Atlanta, Georgia 30332

Investigation of Long Term,  
High-Temperature Changes in the  
Calcium-Stabilized Zirconia-Alumina System

Quarterly Progress Report No. 4  
March 1 through May 31, 1976

The purpose of this investigation is to measure microstructural and phase changes in the CaO-stabilized  $ZrO_2-Al_2O_3$  system after heat treatment as high as  $1300^{\circ}C$  for up to 2000 hours. In addition, high temperature flexural strength, thermal expansion, and room temperature microhardness will be investigated in an attempt to correlate these properties to microstructure and crystal changes.

The original intent of this work was to investigate compositions of high stabilized  $ZrO_2$  content plus  $\alpha-Al_2O_3$ . Phase relations for the CaO- $Al_2O_3$ - $ZrO_2$  ternary were not available. Thus, prior to selection of compositions for long term heat treatment, the phase relations in the high zirconia portion of the ternary were established. Based on the results from the phase diagram study, three compositions in the CA<sub>2</sub>-cubic  $ZrO_2$ -monoclinic  $ZrO_2$  compatibility triangle were selected for long term firing studies. Long term firing has been completed at  $900^{\circ}C$  and  $1300^{\circ}C$  for 2000 hours. Crystalline phase changes have been analyzed as a function of time and temperature. The results of the phase equilibria studies at  $1500^{\circ}C$  and long term phase stability at  $900^{\circ}C$  and  $1300^{\circ}C$  have been compiled and analyzed in a Masters Degree thesis entitled, "Phase Relationships and Long Term Temperature Stability in the High Zirconia Region of the Calcium-Alumina-Zirconia System," by Mr. John Day. This

thesis is submitted as a portion of Quarterly Progress Report No. 4 since it covers the bulk of the work completed in the first year of Grant Number G0155189.

Physical property measurements, room temperature and high temperature flexure strength, thermal expansion, and room temperature microhardness for the long term high temperature samples are near completion and will be reported in Quarterly Progress Report No. 5.

E-18-612

INVESTIGATION OF LONG TERM,  
HIGH-TEMPERATURE CHANGES IN THE  
CALCIA-STABILIZED ZIRCONIA-ALUMINA SYSTEM

QUARTERLY PROGRESS REPORT NO. 5  
JUNE 1, 1976 THROUGH AUGUST 31, 1976

SUBMITTED TO:  
U.S. BUREAU OF MINES -- METALLURGY  
WASHINGTON, D.C. 20240

GRANT NUMBER G0155189

SUBMITTED BY:  
JOE K. COCHRAN, JR.  
SCHOOL OF CERAMIC ENGINEERING  
GEORGIA INSTITUTE OF TECHNOLOGY  
ATLANTA, GEORGIA 30332

Investigation of Long Term,  
High-Temperature Changes in the  
Calcia-Stabilized Zirconia-Alumina System

Quarterly Progress Report No. 5  
June 1, 1976 through August 31, 1976

INTRODUCTION

The purpose of this investigation is to measure microstructural and phase changes in the CaO-stabilized  $\text{ZrO}_2\text{-Al}_2\text{O}_3$  system after heat treatment as high as  $1300^\circ\text{C}$  for up to 2000 hours. In addition, high temperature flexural strength, thermal expansion, and room temperature microhardness has been investigated in an attempt to correlate these properties to microstructure and crystal changes.

The original intent of this work was to investigate compositions of high stabilized zirconia content plus  $\text{Al}_2\text{O}_3$ . Phase relations for the  $\text{CaO-Al}_2\text{O}_3\text{-ZrO}_2$  ternary were not available. Thus, prior to selection of compositions for long term heat treatment, the phase relations in the high zirconia (greater than or equal to 55%) portion of the ternary were established and were reported in Quarterly 1-4.

Based on the results from the phase diagram study, three compositions in the  $\text{CA}_2$ -cubic  $\text{ZrO}_2$ -Monoclinic  $\text{ZrO}_2$ , compatibility triangle were selected for long term firing studies. The phase changes found on heat treating these composition at 900 and  $1300^\circ\text{C}$  for 2000 hours were reported in Quarterly No. 4. During this



quarter, room temperature and high temperature flexure strength were measured for the compositions "as fired" at 1550°C, after heat treatment at 900°C for 1000 and 2000 hours, and after heat treatment at 1300°C for 1000 and 2000 hours. In addition, room temperature Knoop's microhardness was measured for the "as fired", 900°C, and 1300°C heat treatments.

#### PRODECURE

Flexure Strength Measurement. Sample preparation and heat treatment for the flexure strength samples was described in Quarterly Report No. 3. The final sample geometry for flexure strength were bars ~ 0.20 x 0.20 x 1.50 in. Measurement of flexure strength was made in three point loading on an Instron Universal Tester using a span 1.25 inches and a head speed of 0.01 cm/min. Samples were broken as fired with no surface treatment.

For high temperature flexure strength measurements a furnace was constructed using molybdenum disilicide heating elements and temperature control was accomplished using a proportional band controller with rate and reset.

Temperature during flexure strength measurement was maintained  $\pm 5^{\circ}\text{C}$ . The furnace was a pusher type design with high  $\text{Al}_2\text{O}_3$  sample sleds pushed in tandem through the furnace on 0.5 inch diameter  $\text{Al}_2\text{O}_3$  tubes. Each sample sled had slots for five samples and 0.125 in. diameter sapphire rods served as the knife edge on which the samples were broken. The load was applied via a 0.5 inch diameter  $\text{Al}_2\text{O}_3$  tube that had been ground to a knife edge with an approximately 0.05 inch radius on the knife edge. The samples were broken at five minute intervals and each sample was at the breaking temperature

for a minimum of 20 minutes prior to loading.

Samples were broken at room temperature, 900°C, 1100°C, and 1300°C for each heat treatment condition ("as fired" at 1550°C, 900°C-1000 hours, 900°C-2000 hours, 1300°C-1000 hours, and 1300°C-2000 hours.) Four samples were broken for each composition, heat treatment condition, and breaking temperature. The average flexure strength, standard deviation, and percent standard deviation

(standard deviation/flexure strength) x100 are tabulated in Tables I-IV.

Microhardness Measurements. As fired and heat treated samples were mounted in clear resin and ground for twenty minutes utilizing 180, 320, and 600 grit grinding paper. The samples were polished for 48 hours on a vibratory grinder incorporating one micron diamond paste.

A Reichhart metalograph was set up with a Knoop microhardness tester\* under a power of 480x. Three indentations measurements were made at each of the following loads: 30.5, 34, 39, 42.5, 46, 51, and 59 grams. Fracturing occurred often at the higher loads, requiring re-indentation and measurement. The testing device determines the indentation length in drum divisions of which each is equal to 0.167 microns.

The three values for length were averaged for each load and sample and the Knoop hardness was determined by a computer using the following equation:

\*Model Number 40931/39400.

TABLE I

Flexure Strength of As-Fired  $\text{CaO-Al}_2\text{O}_3\text{-ZrO}_2$   
Compositions A, B, and C  
As a Function of Breaking Temperature

Breaking Temperature (°C)	Flexure Strength (10 <sup>3</sup> psi)	Standard Deviation (10 <sup>3</sup> psi)	Percent Standard Deviation
<u>Composition A</u>			
20	6.70	0.43	6.4
900	7.18	1.46	20.3
1100	7.74	1.64	21.2
1300	8.52	1.48	17.4
<u>Composition B</u>			
20	11.40	0.05	0.4
900	7.96	0.99	12.4
1100	8.14	1.80	22.1
1300	9.92	0.23	2.3
<u>Composition C</u>			
20	15.58	0.20	1.7
900	11.79	1.39	11.8
1100	12.82	2.70	21.0
1300	11.48	0.89	7.8

TABLE II

Flexure Strength of Composition A  
As a Function of Breaking Temperature  
For Various Heat Treatment Conditions

Breaking Temperature (°C)	Flexure Strength (10 <sup>3</sup> psi)	Standard Deviation (10 <sup>3</sup> psi)	Percent Standard Deviation
<u>100°C Heat Treatment - 1000 Hours</u>			
20	7.78	0.73	9.5
900	7.83	1.07	13.6
1100	6.53	0.98	15.0
1300	9.42	1.32	14.0
<u>100°C Heat Treatment - 2000 Hours</u>			
20	7.75	0.56	7.3
900	7.21	0.74	10.3
1100	6.49	0.66	10.2
1300	8.63	2.68	31.1
<u>300°C Heat Treatment - 1000 Hours</u>			
20	9.42	0.77	8.2
900	7.88	1.17	14.5
1100	8.07	1.08	13.3
1300	9.25	1.84	19.9
<u>300°C Heat Treatment - 2000 Hours</u>			
20	7.23	0.42	5.8
900	7.07	0.89	12.6
1100	5.78	1.05	18.2
1300	7.20	1.20	16.7

TABLE III

Flexure Strength of Composition B  
As a Function of Breaking Temperature  
For Various Heat Treatment Conditions

Breaking Temperature (°C)	Flexure Strength (10 <sup>3</sup> psi)	Standard Deviation (10 <sup>3</sup> psi)	Percent Standard Deviation
<u>900°C Heat Treatment - 1000 Hours</u>			
20	8.99	0.61	6.8
900	8.57	0.80	9.4
1100	8.34	0.96	11.5
1300	9.54	1.69	17.7
<u>900°C Heat Treatment - 2000 Hours</u>			
20	9.14	1.16	12.7
900	8.89	1.38	15.5
1100	7.93	0.69	8.7
1300	10.28	1.99	19.4
<u>1300°C Heat Treatment - 1000 Hours</u>			
20	10.66	0.29	2.7
900	9.55	1.11	11.6
1100	9.22	1.61	17.5
1300	9.41	1.65	17.5
<u>1300°C Heat Treatment - 2000 Hours</u>			
20	9.15	0.82	9.0
900	8.65	0.48	5.5
1100	10.85	3.84	35.4
1300	9.72	0.94	9.7

TABLE IV

Flexure Strength of Composition C  
As a Function of Breaking Temperature  
For Various Heat Treatment Conditions

Breaking Temperature (°C)	Flexure Strength (10 <sup>3</sup> psi)	Standard Deviation (10 <sup>3</sup> psi)	Percent Standard Deviation
<u>900°C Heat Treatment - 1000 Hours</u>			
20	13.71	2.87	20.9
900	9.91	0.89	9.0
1100	11.62	1.67	14.3
1300	13.33	1.37	10.3
<u>900°C Heat Treatment - 2000 Hours</u>			
20	14.55	2.79	19.2
900	8.72	0.80	9.2
1100	12.75	2.19	17.2
1300	13.21	1.64	12.4
<u>1300°C Heat Treatment - 1000 Hours</u>			
20	27.02	5.27	19.5
900	20.56	1.98	9.6
1100	12.60	4.67	37.0
1300	15.23	2.49	16.3
<u>1300°C Heat Treatment - 2000 Hours</u>			
20	14.43	1.87	13.0
900	11.97	0.40	3.3
1100	15.68	3.11	19.8
1300	14.79	2.12	14.4

$$KHN = \frac{P}{0.07028 L^2}$$

where KHN = Knoop Hardness Number

P = load in kilograms

L = indentation length in millimeters

The average microhardness values as a function of load are tabulated in Tables V-VII.

### Discussion of Results

Flexure Strength. Results of room temperature and high temperature flexure strengths of compositions A, B, and C from the  $Ca_2$  Cubic  $ZrO_2$ -Monoclinic  $ZrO_2$  compatibility triangle are reported in this section. Prior to a discussion of the flexure strength data, a review of the chemical and crystallographic compositions of A, B, and C will help to provide an explanation the changing compositions of A, B, and C with time.

The change in chemical composition from A to B to C, Table VIII, is to larger  $CaO$  and  $Al_2O_3$  contents and to smaller  $ZrO_2$  contents. These compositions are near the tie line between  $Ca_2$  and the lower  $CaO$  content Cubic  $ZrO_2$  SS composition, Crystallographic contents "as fired" at  $1550^\circ C$  for A, B, and C on a weight basis; Table VIII, shows increases in  $Ca_2$  quantity from A to B to C. Composition A contained the most cubic  $ZrO_2$  at 78.6 w/o and Composition B the least cubic  $ZrO_2$  at 65.9 w/o. On heat treatment at 900 and  $1300^\circ C$ , the monoclinic  $ZrO_2$  content

Table V. Room Temperature Microhardness of Composition A  
After Various Heat Treatments

Load (grams)	Knoop Microhardness (kg/mm <sup>2</sup> )				
	As-fired 1550°C	900°C 1000 hrs	900°C 2000 hrs	1300°C 1000 hrs	1300°C 2000 hrs
30.5	1377	2330	1815	2409	1566
34.0	1309	1840	1592	2492	1366
39.0	1117	1639	1687	1427	1337
42.5	1036	1584	1565	1368	1271
46.0	1080	1603	1593	1297	1211
51.0	985	1771	1395	1327	1163
59.0	657	1252	1239	1237	1005



Table VI. Room Temperature Microhardness of Composition B  
After Various Heat Treatments

Load (grams)	Knoop Microhardness (kg/mm <sup>2</sup> )				
	As-fired 1550°C	900°C 1000 hrs	900°C 2000 hrs	1300°C 1000 hrs	1300°C 2000 hrs
30.5	1377	2294	1529	2154	1654
34.0	1309	2288	1291	1854	1316
39.0	1117	1889	1373	1592	1393
42.5	1036	1567	1334	1462	1297
46.0	1080	1562	1240	1325	1166
51.0	985	1726	1161	1299	1171
59.0	657	1175	981	1123	957

Table VII. Room Temperature Microhardness of Composition C  
After Various Heat Treatments

Load (grams)	Knoop Microhardness ( $\text{kg/mm}^2$ )				
	As-fired 1550°C	900°C 1000 hrs	900°C 2000 hrs	1300°C 1000 hrs	1300°C 2000 hrs
30.5	2149	2966	2159	2936	1675
34.0	1955	2988	1938	2499	1429
39.0	1697	2010	1719	2053	1384
42.5	1657	2216	1587	1970	1275
46.0	1500	2134	1616	1786	1333
51.0	1583	1765	1611	1682	1160
59.0	1506	1857	1551	1619	1119

TABLE VIII. COMPOSITIONS OF  $\text{CaO-AL}_2\text{O}_3\text{-ZrO}_2$   
 SAMPLES A, B, AND C.

OXIDE	MOLE %		
	A	B	C
CaO	12.5	14.5	17.5
$\text{AL}_2\text{O}_3$	10.0	17.5	25.0
$\text{ZrO}_2$	77.5	68.0	57.5

PHASE	WEIGHT %		
	A	B	C
CUBIC $\text{ZrO}_2$	78.6	65.9	67.7
MONOCLINIC $\text{ZrO}_2$	8.0	12.0	0
$\text{CaO-2AL}_2\text{O}_3$	12.4	22.1	32.4

of all compositions increased with time and the cubic  $\text{ZrO}_2$  content decreased correspondingly. At  $900^\circ\text{C}$ , Figure 1, the change in monoclinic  $\text{ZrO}_2$  content was small (2-3 wt%) and probably would not effect flexure strength. However, the increase in monoclinic  $\text{ZrO}_2$  at  $1300^\circ\text{C}$ , Figure 2, was approximately 12-16 wt% for all three compositions and if this quantity change in monoclinic  $\text{ZrO}_2$  content significantly affects flexure strength it should be detectable between "as fired" samples and samples heat treated at  $1300^\circ\text{C}$  for 1000 for 2000 hours.

Comparisons of the flexure strength of compositions A, B, and C may be seen in Figure 3 where each data point represents the average strength of all heat treatment conditions. Significant strength increases occurred as the  $\text{CA}_2$  content increased from A to B to C. The strength of all three was relatively constant with temperature up to  $1300^\circ\text{C}$  showing a slight decrease at  $900$  and  $1100^\circ\text{C}$  ( $\sim 10\%$ ) as compared to  $20$  and  $1300^\circ\text{C}$  strengths. A slight strength decrease is probably to be expected around the  $1000^\circ\text{C}$  monoclinic  $\text{ZrO}_2$  phase inversion. The higher average strength of composition C at  $20^\circ\text{C}$  is misleading as a strength of 27 Kpsi for samples heat treated at  $1300^\circ\text{C}$  for 1000 hours is included in this average and will be discussed below.

The effect of heat treatment at  $900^\circ\text{C}$  and  $1300^\circ\text{C}$  for up to 2000 hours is presented in Figures 4-6. Other than composition C- $1300^\circ\text{C}$ -1000 hour heat treatment, there were no significant effects produced by the heat treatments. The standard deviation

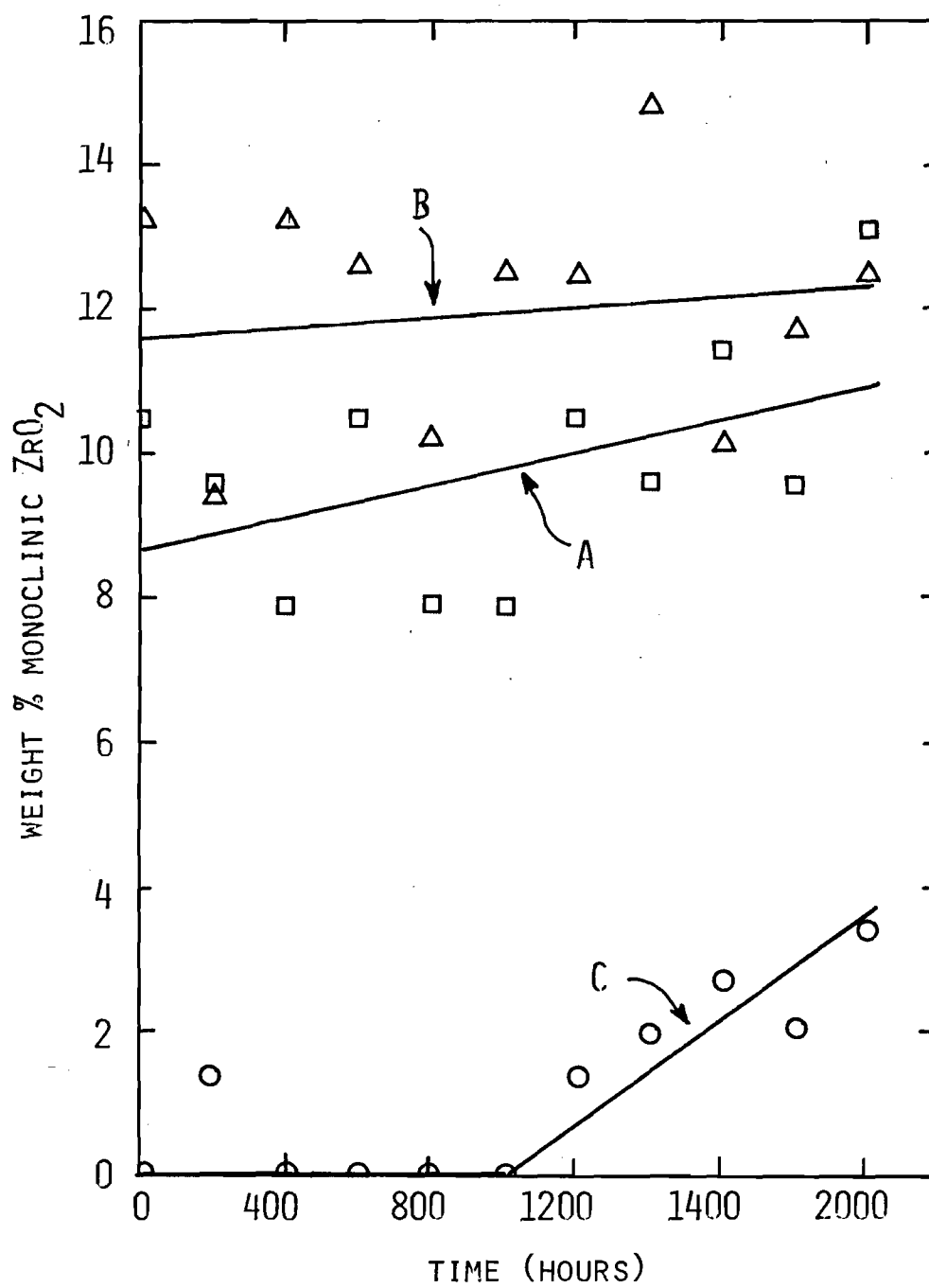


FIGURE 1. CHANGE IN MONOCLINIC  $ZrO_2$  CONTENT WITH TIME AT  $900^{\circ}C$  FOR  $CaO-Al_2O_3-ZrO_2$  COMPOSITIONS A, B, AND C.

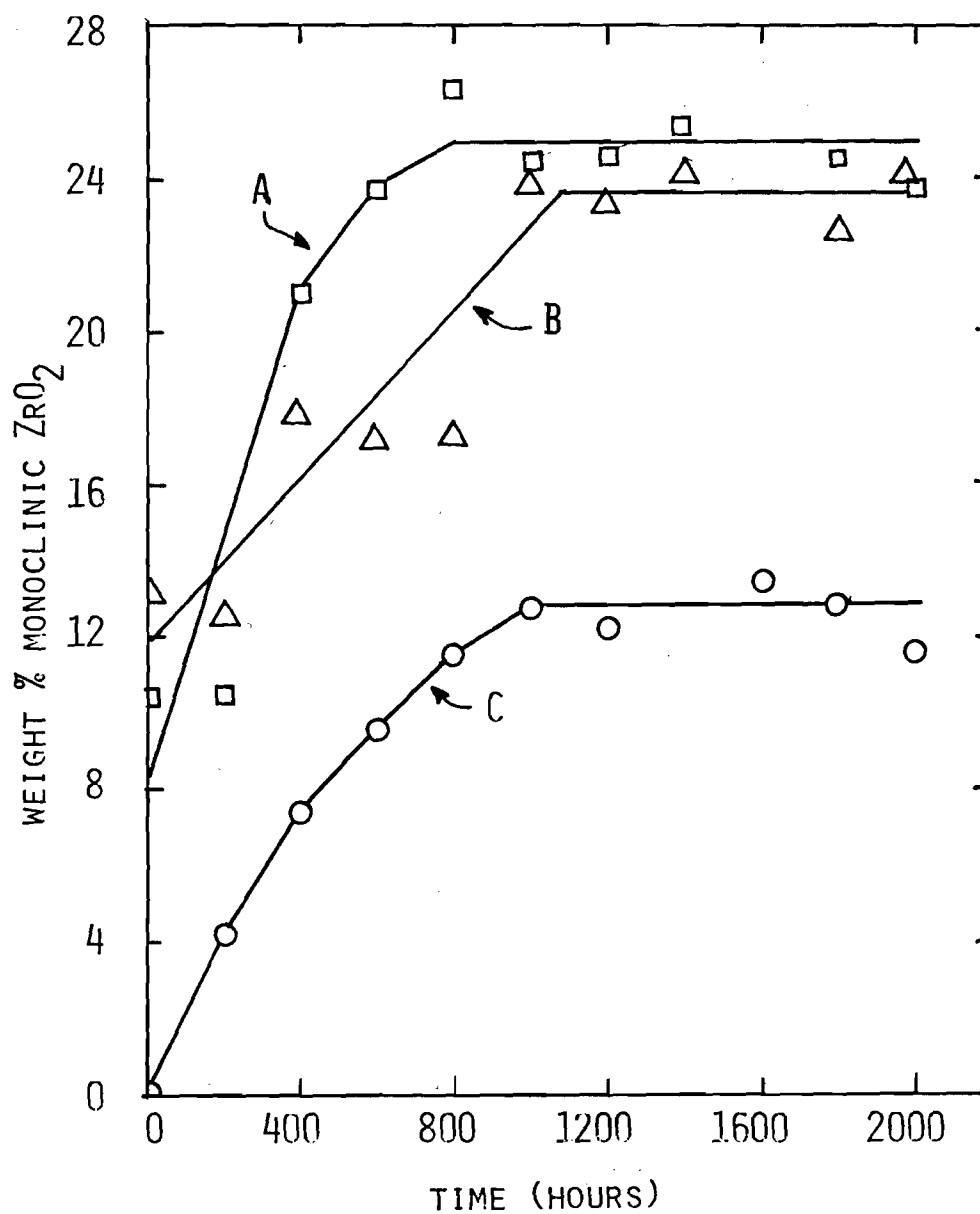


FIGURE 2. CHANGE IN MONOCLINIC  $ZrO_2$  CONTENT WITH TIME AT  $1300^{\circ}C$  FOR  $CaO-Al_2O_3-ZrO_2$  COMPOSITIONS A, B, AND C.

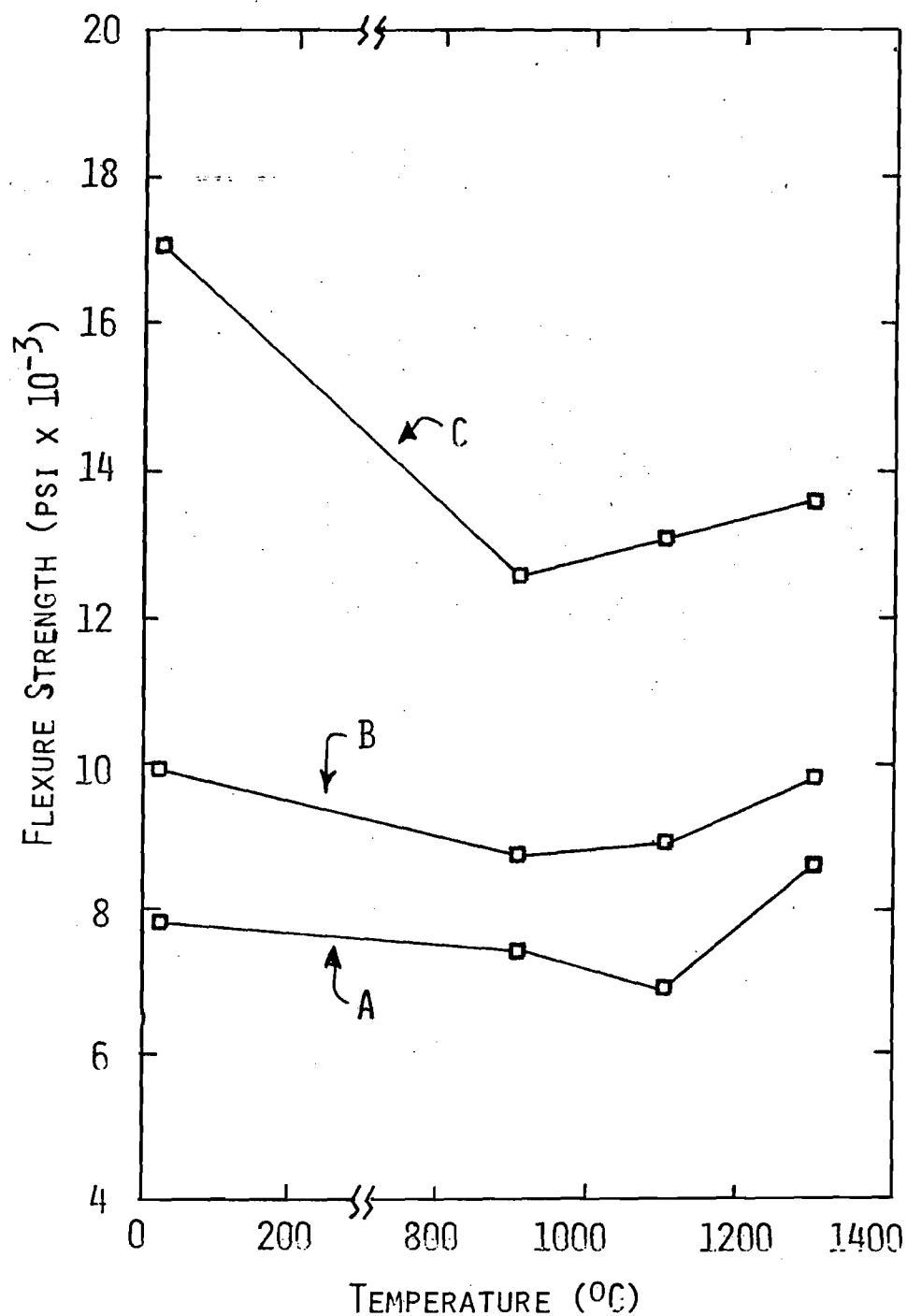


FIGURE 3. EFFECT OF TEMPERATURE ON FLEXURE STRENGTH OF  $\text{CaO-Al}_2\text{O}_3\text{-ZrO}_2$  COMPOSITIONS A, B, AND C. EACH POINT REPRESENTS THE AVERAGE OF ALL HEAT TREATMENT CONDITIONS.

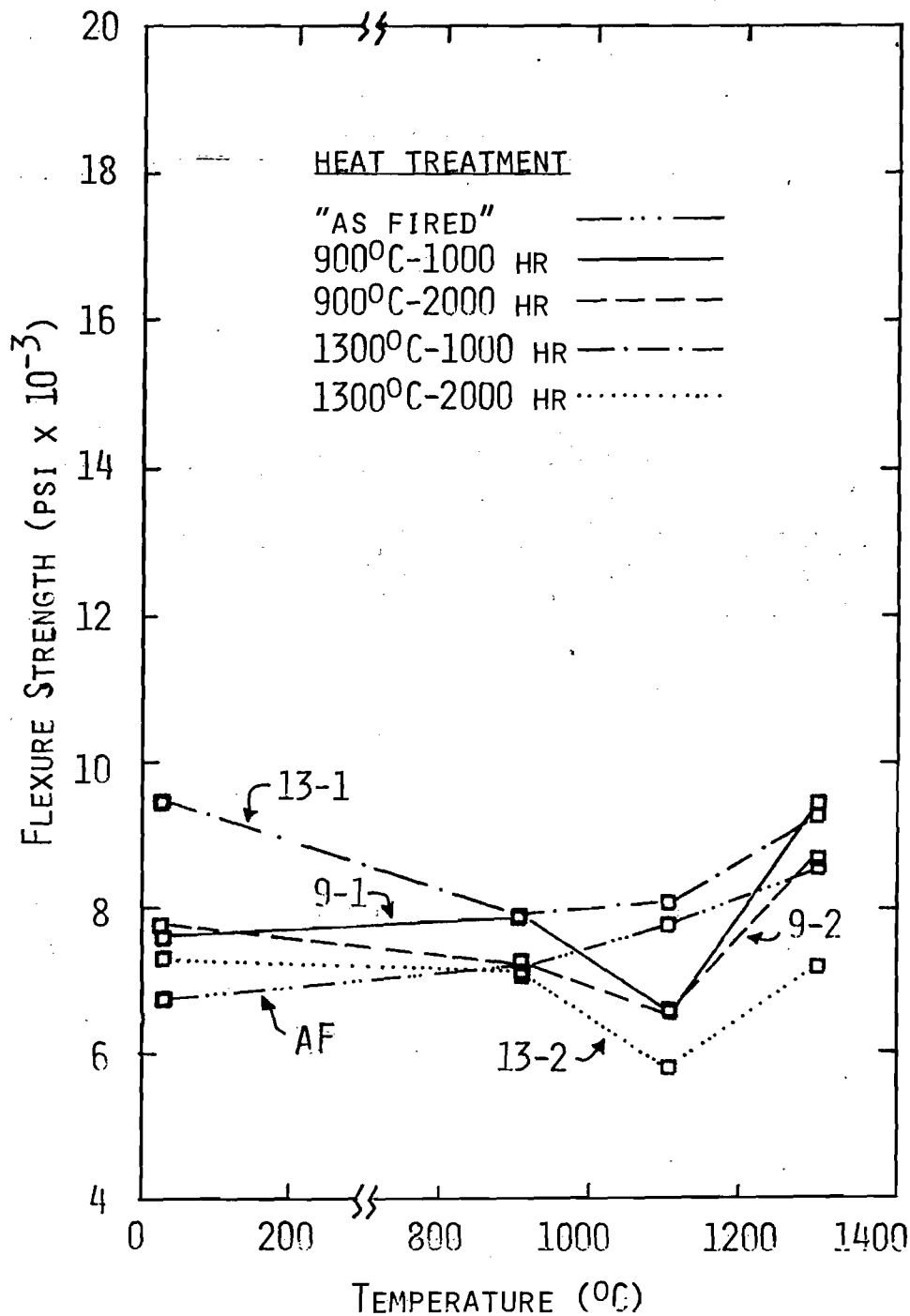


FIGURE 4. EFFECT OF TEMPERATURE ON FLEXURE STRENGTH OF  $\text{CAO-AL}_2\text{O}_3\text{-ZrO}_2$  COMPOSITION A AFTER HEAT TREATMENTS.



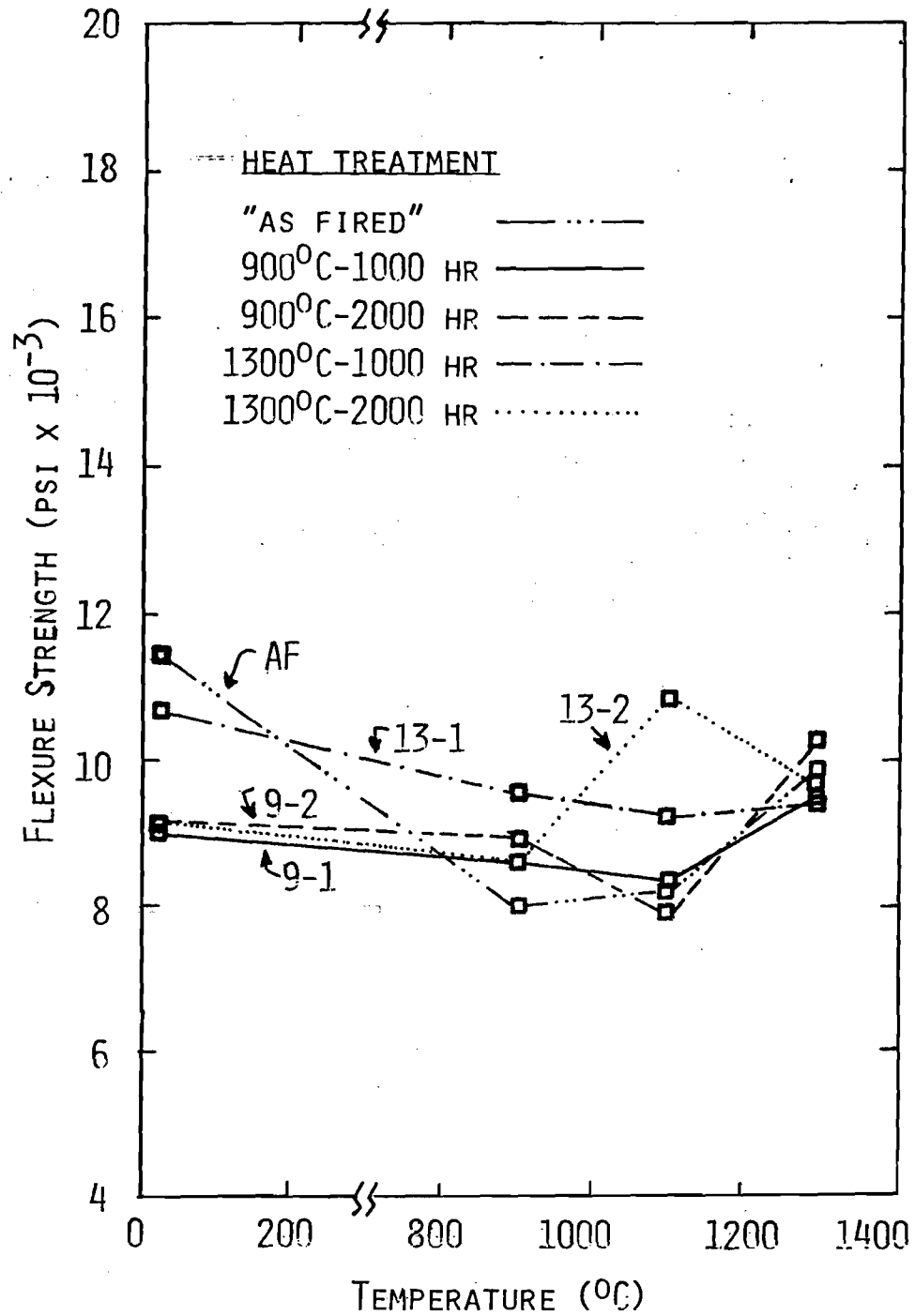


FIGURE 5 . EFFECT OF TEMPERATURE ON FLEXURE STRENGTH OF  $\text{CaO-Al}_2\text{O}_3\text{-ZrO}_2$  COMPOSITION B FOR VARIOUS HEAT TREATMENT CONDITIONS.

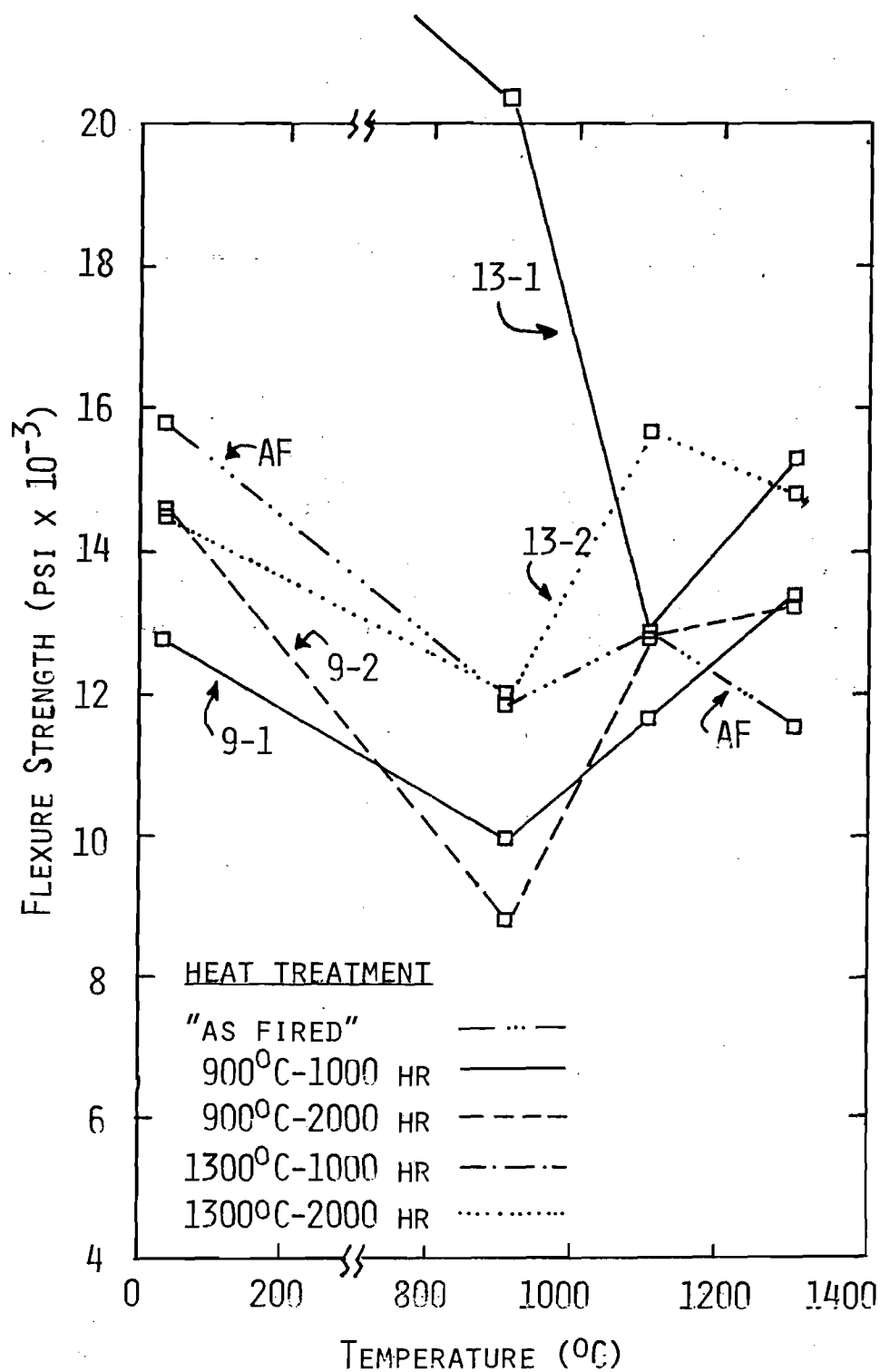


FIGURE 6, EFFECT OF TEMPERATURE ON FLEXURE STRENGTH OF  $\text{CaO-Al}_2\text{O}_3\text{-ZrO}_2$  COMPOSITION C FOR VARIOUS HEAT TREATMENT CONDITIONS.

of all the data points in Figures 4-6 was approximately 5 to 20% which covers the ranges of strengths produced by the heat treatments. Thus, heat treatment was not detrimental to flexure strength.

In considering the effect of monoclinic  $\text{ZrO}_2$  on flexure strength, it must be concluded that for the variations in monoclinic  $\text{ZrO}_2$  exhibited by these compositions, the effect is negligible. If increases in monoclinic  $\text{ZrO}_2$  weakened the samples, the  $1300^\circ\text{C}$  heat treatment should have produced weaker samples compared to the "as fired" and  $900^\circ\text{C}$  samples. Heat treatment at  $1300^\circ\text{C}$  did not degrade flexure strength and thus the increased monoclinic  $\text{ZrO}_2$  produced by heat treatment was not detrimental.

The strength produced by heat treatment of sample C at  $1300^\circ\text{C}$  for 1000 hours is worthy of special note. The average strength of composition C for all heat treatments was approximately 14 Kpsi. The average strength for samples of composition C heat treated at  $1300^\circ\text{C}$  for 1000 hours was 27 Kpsi when broken at  $20^\circ\text{C}$  and 20.5 Kpsi when broken at  $900^\circ\text{C}$ . No adequate explanation is apparent for the significantly higher strengths. They were fired and strength tested with other compositions that showed no significant variations and thus lack of control of testing procedures must be eliminated as an explanation. The most significant difference in sample history is that the "as fired" "C" contained no monoclinic  $\text{ZrO}_2$ ; on heating treating at  $1300^\circ\text{C}$  for 1000 hours, 12% monoclinic  $\text{ZrO}_2$  was formed; and cooling to

room temperature was the only time that the monoclinic  $\text{ZrO}_2$  of these samples went through the tetragonal-monoclinic inversion prior to strength testing at  $20^\circ\text{C}$  and  $900^\circ\text{C}$ . For all other samples of all compositions and testing conditions, there was monoclinic  $\text{ZrO}_2$  present that went through the inversion a minimum of two times.

In summary, the strengths of compositions A, B, and C increased in that order with increasing  $\text{Ca}_2$  contents as can be seen by the strength ranges in Figure 7. Both heat treatment at  $900^\circ\text{C}$  and  $1300^\circ\text{C}$  and breaking temperature up to  $1300^\circ\text{C}$  had little effect on flexure strength of these  $\text{CaO-Al}_2\text{O}_3\text{-ZrO}_2$  compositions. From a practical aspect, the lack of effect of heat treatment and breaking temperature is important in that "as fired" room temperature property measurement is indicative of higher temperature properties.

#### Microhardness

Microhardness of the "as-fired" compositions, Figure 8, were analogous to the flexural strength data in that hardness increased from composition A to B to C. Again, increasing the  $\text{Ca}_2$  content also improved microhardness. In analyzing the effect of heat treatment on microhardness for the three compositions, Figure 9-11, there are several trends apparent. Heat treatment for 1000 hours both at 900 and  $1300^\circ\text{C}$  produced higher microhardness values than did heat treatment at 2000 hours. In general, heat treatment increased microhardness of compositions A, B, and C possibly due to annealing. Except for the "as-fired" samples, the microhardness of compositions A and B were almost identical.

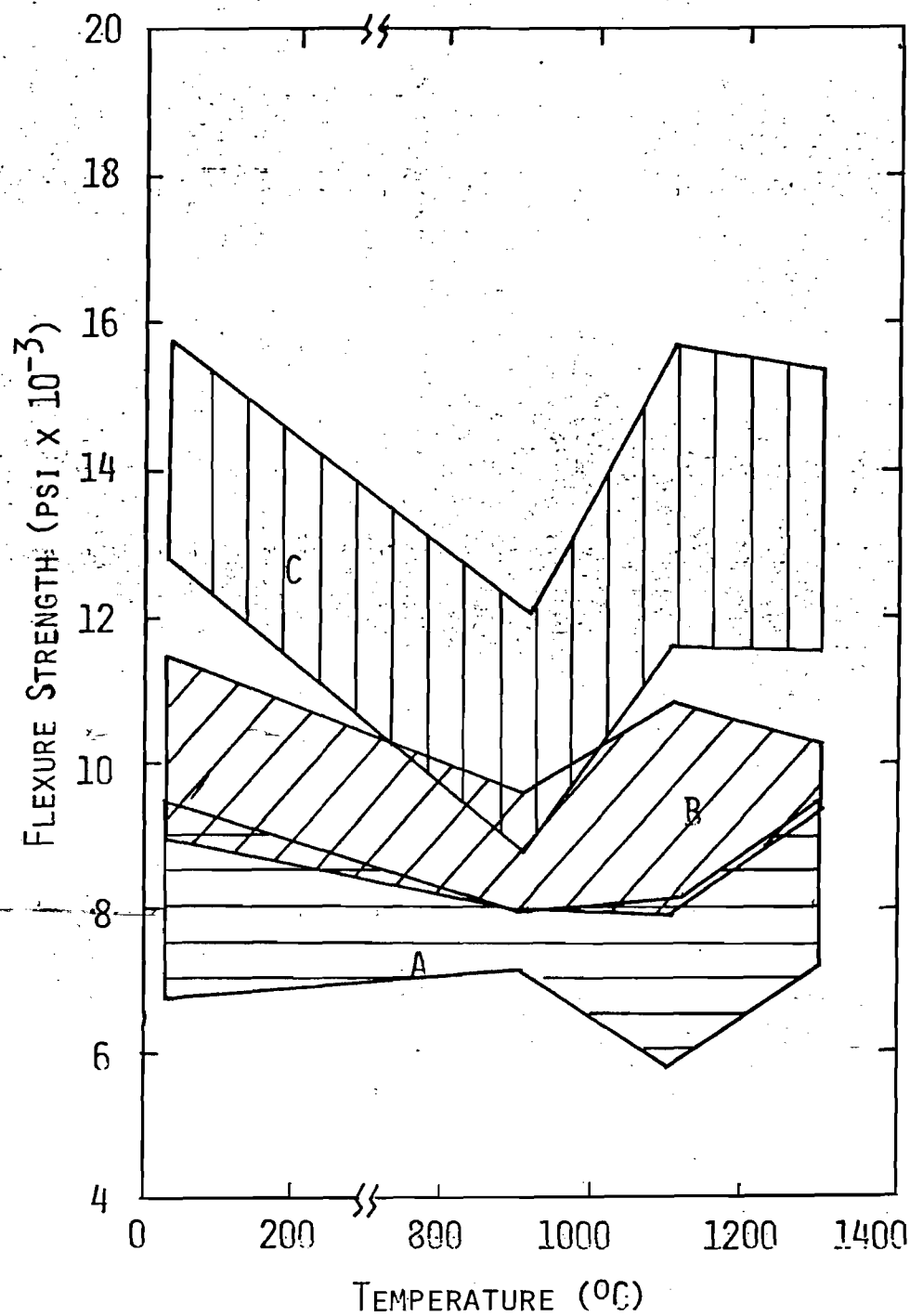


FIGURE 7 . RANGE OF FLEXURE STRENGTH AS A FUNCTION OF TEMPERATURE FOR  $\text{CaO-Al}_2\text{O}_3\text{-ZrO}_2$  COMPOSITIONS A, B, AND C FOR VARIOUS HEAT TREATMENT CONDITIONS.

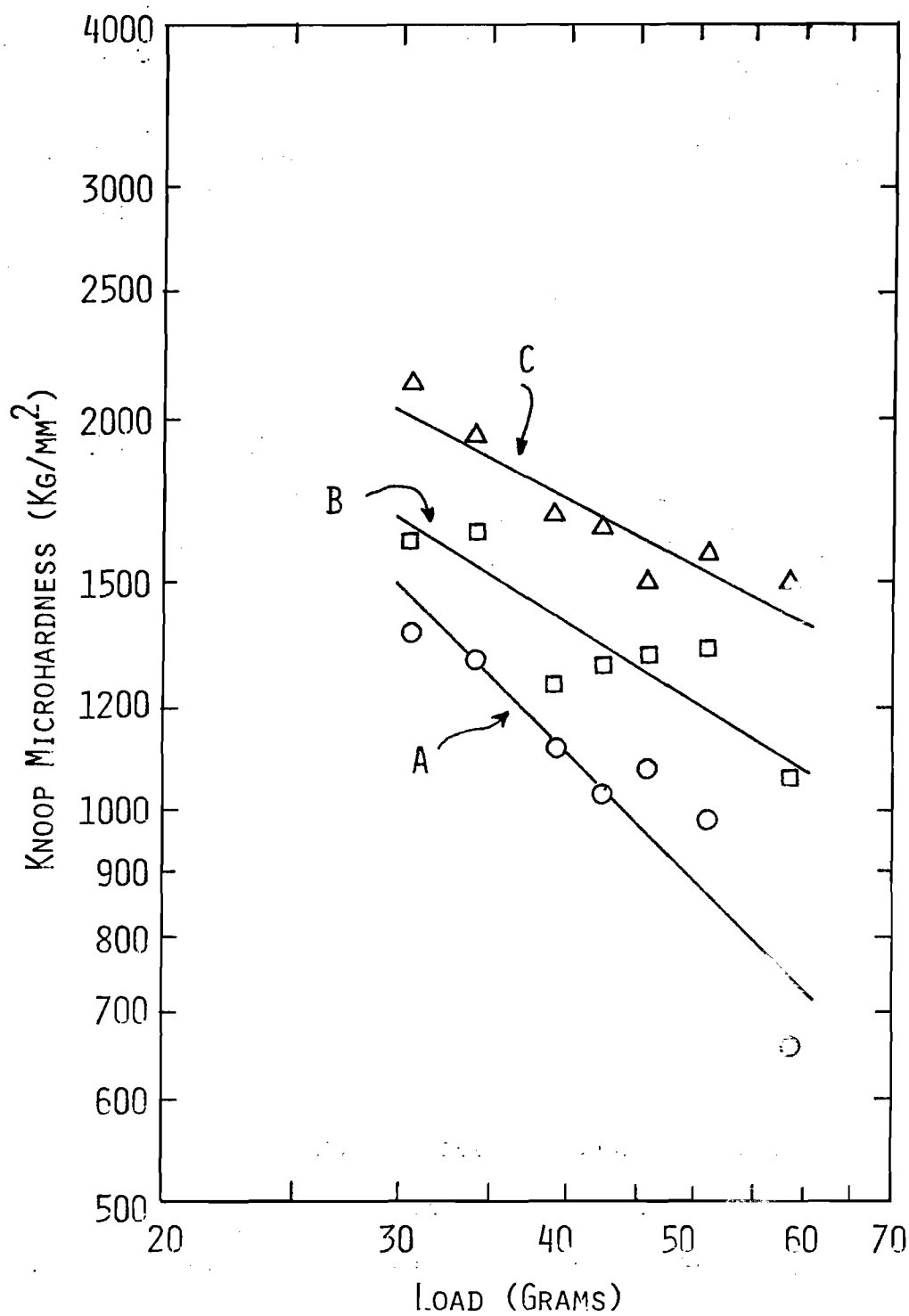


FIGURE 8. ROOM TEMPERATURE MICROHARDNESS OF  
"AS FIRED"  $\text{CaO-Al}_2\text{O}_3\text{-ZrO}_2$  COMPOSITIONS  
A, B, AND C.

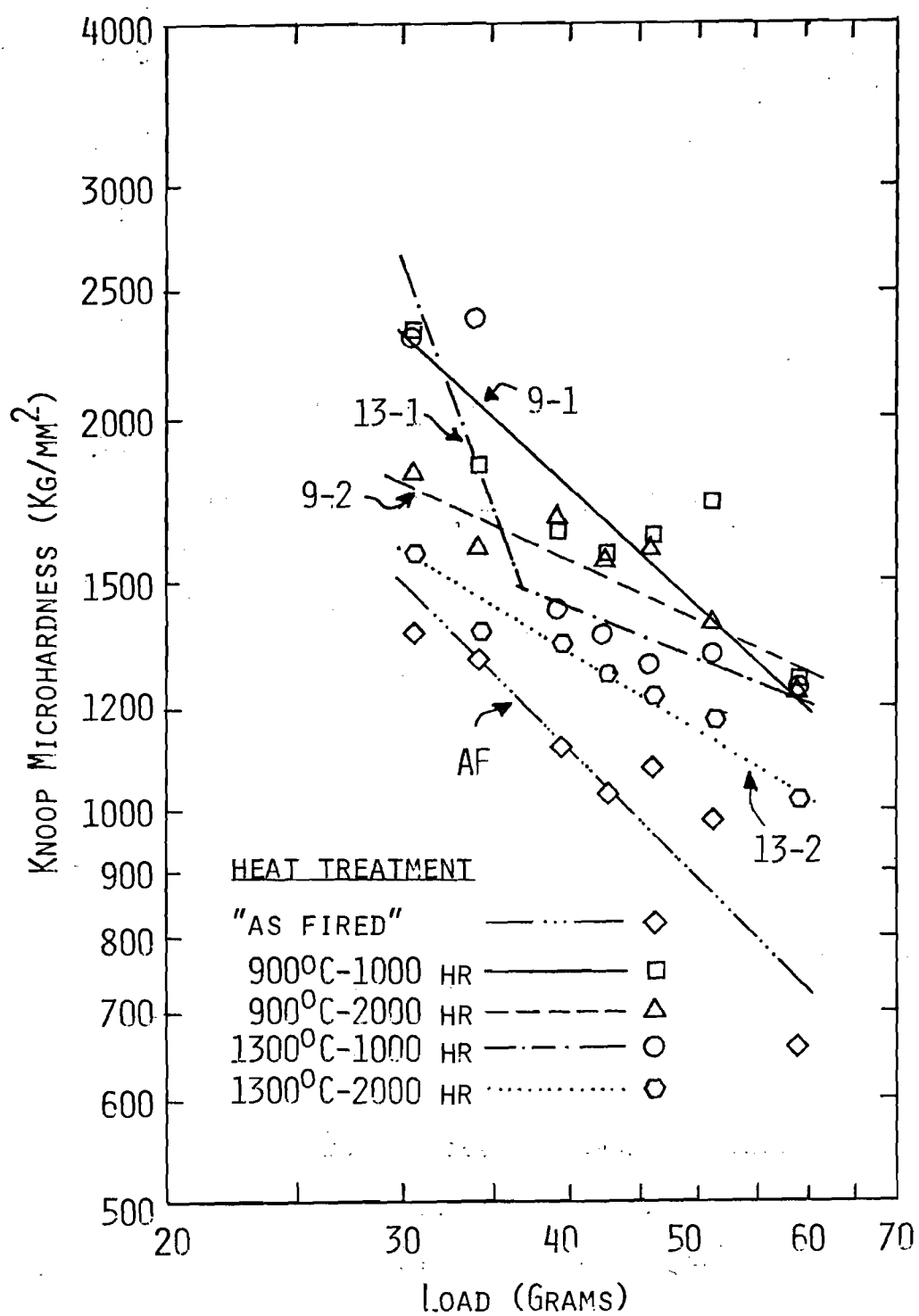


FIGURE 9 . ROOM TEMPERATURE MICROHARDNESS OF  $\text{CaO-Al}_2\text{O}_3\text{-ZrO}_2$  COMPOSITION A AFTER VARIOUS HEAT TREATMENTS.

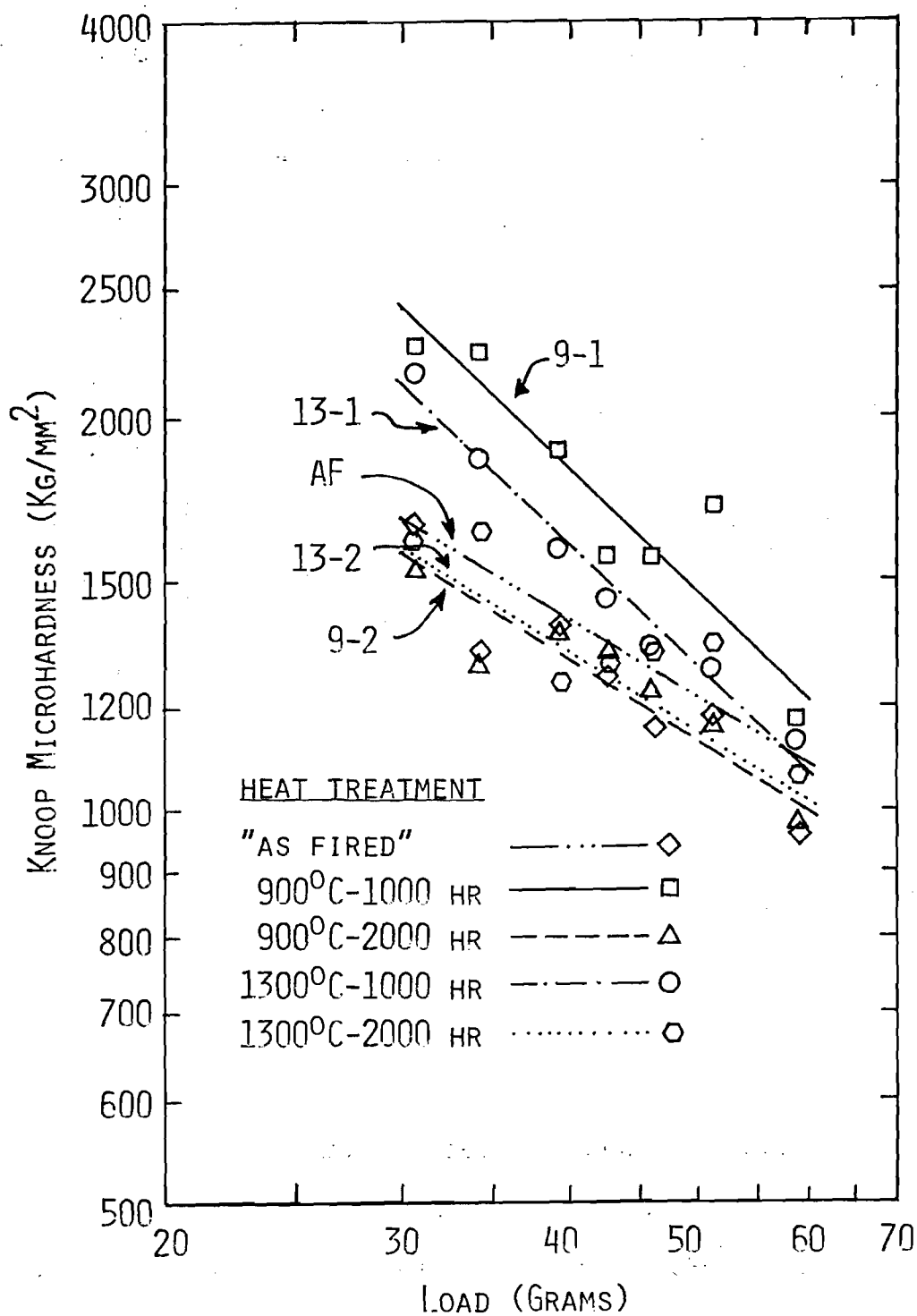


FIGURE 10. ROOM TEMPERATURE MICROHARDNESS OF  $\text{CaO-Al}_2\text{O}_3\text{-ZrO}_2$  COMPOSITION B AFTER VARIOUS HEAT TREATMENTS.



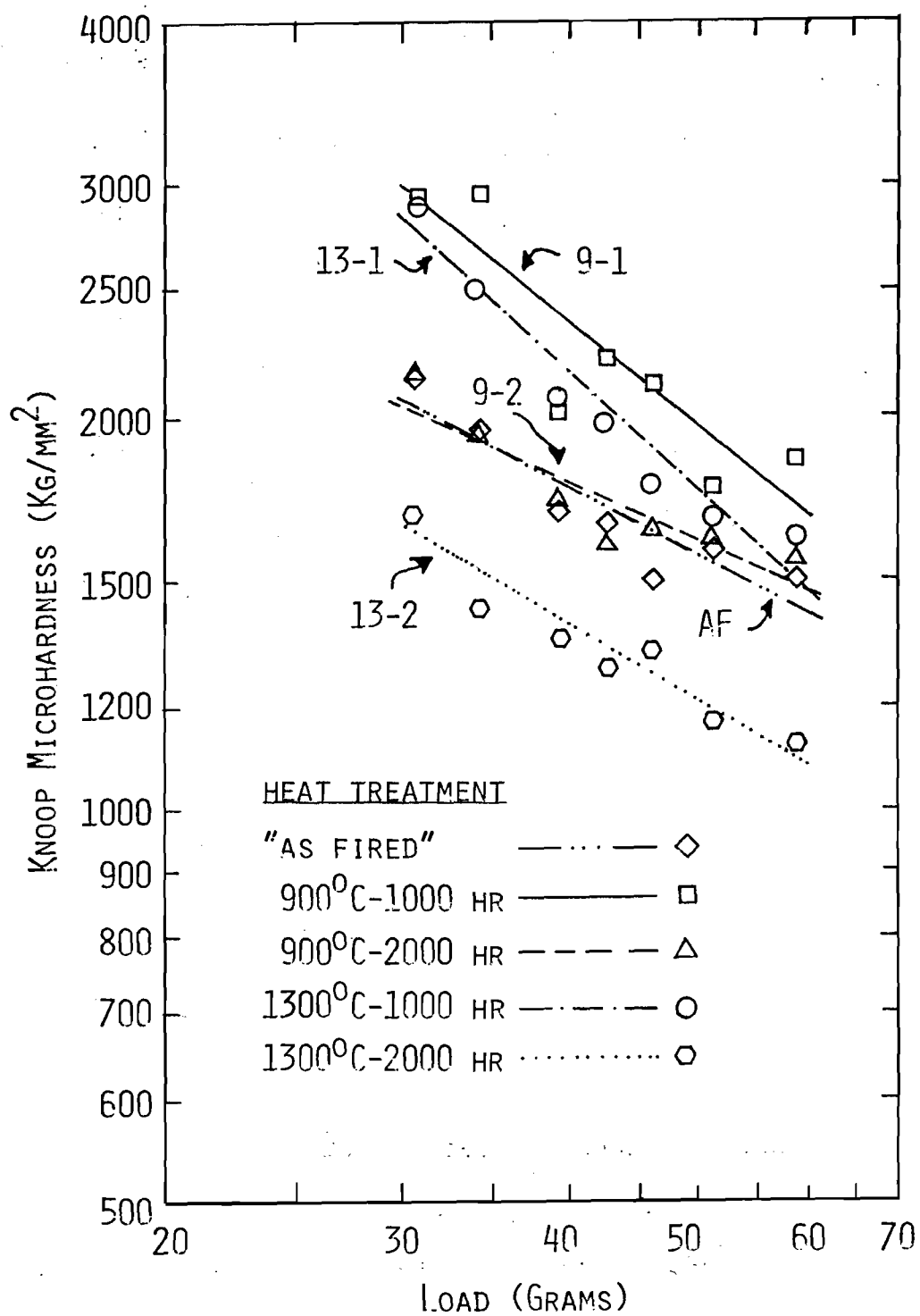


FIGURE 11. ROOM TEMPERATURE MICROHARDNESS OF  $\text{CaO-Al}_2\text{O}_3\text{-ZrO}_2$  COMPOSITION C AFTER VARIOUS HEAT TREATMENTS.

E-18-612

INVESTIGATION OF LONG TERM,  
HIGH-TEMPERATURE CHANGES IN THE  
CALCIA-STABILIZED ZIRCONIA-ALUMINA SYSTEM

Quarterly Progress Report No. 6

September 1, 1976 through December 31, 1976

Submitted to:

U.S. Bureau of Mines -- Metallurgy  
Washington, D.C. 20240

Grant Number G0155189

Submitted by:

Joe K. Cochran, Jr.  
School of Ceramic Engineering  
Georgia Institute of Technology  
Atlanta, Georgia 30332

Investigation of Long Term,  
High-Temperature Changes in the  
Calcia-Stabilized Zirconia-Alumina System

Quarterly Progress Report No. 6  
September 1, 1976 through December 31, 1976

INTRODUCTION

The purpose of this investigation is to measure microstructural and phase changes in the CaO-stabilized  $ZrO_2$ - $Al_2O_3$  system after heat treatment as high as  $1300^{\circ}C$  for up to 2000 hours. In addition, high temperature flexural strength, thermal expansion, and room temperature microhardness has been investigated in an attempt to correlate these properties to microstructure and crystal changes.

The original intent of this work was to investigate compositions of high stabilized zirconia content plus  $Al_2O_3$ . Phase relations for the CaO- $Al_2O_3$ - $ZrO_2$  ternary were not available. Thus, prior to selection of compositions for long term heat treatment, the phase relations in the high zirconia (greater than or equal to 55%) portion of the ternary were established and were reported in Quarterly 1-4.

Based on the results from the phase diagram study, three compositions in the CA<sub>2</sub>-cubic  $ZrO_2$ -Monoclinic  $ZrO_2$ , compatibility triangle were selected for long term firing studies. The phase changes found on heat treating these compositions at 900 and  $1300^{\circ}C$  for 2000 hours were reported in Quarterly No. 4. Room temperature and high temperature flexure strength were measured for the

compositions "as fired" at 1550°C, after heat treatment at 900°C for 1000 and 2000 hours, and after heat treatment at 1300°C for 1000 and 2000 hours. In addition, room temperature Knoop's microhardness was measured for the "as fired", 900°C, and 1300°C heat treatments. Flexure strengths and microhardness were reported. in Quarterly No. 5.

Very little of the properties of  $CA_2$  is reported in the literature with information only on the crystal structure and thermal expansion having been found. Thus in an effort to characterize  $CA_2$  more fully, the stoichiometry, flexure strength, thermal expansion, and microhardness of  $CA_2$  was investigated this quarter for comparison to results compiled for compositions A, B, and C.

#### PROCEDURE

$CA_2$  Stoichiometry. Earlier results in this investigation indicated that the molar composition of  $CA_2$  was 69%  $Al_2O_3$  and 31% m/o CaO rather than the reported 67.7 and 33.3 m/o respectively. In an attempt to determine more accurately the composition of  $CA_2$  for our raw materials, fifteen compositions of CaO- $Al_2O_3$ - $ZrO_2$ , Table 1, were prepared from  $CaCO_3$  (Fisher),  $Al_2O_3$  (Alcoa A-16 Super Ground) and  $ZrO_2$  (TAM C.P. Milled). The compositions were pressed into pellets, fired to 1500°C for four hours, ground after cooling, repressed and fired again to 1500°C for 20 hours. Samples were analyzed by qualitative x-ray diffraction to determine the phases present.

$CA_2$  Properties. After analyzing the  $CA_2$  stoichiometry results, a composition, 67.5 m/o  $Al_2O_3$ -32.0 m/o CaO-0.5 m/o  $ZrO_2$ , was selected for physical property determination.

A 200 gram batch was prepared by pressing into pellets, firing

Table 1. Qualitative Phase Analysis of  $\text{CaO} \cdot \text{Al}_2\text{O}_3 \cdot \text{ZrO}_2$  Compositions Near Composition  $\text{CA}_2$ \*

Sample	Composition (Oxide)			Crystalline Phases
	CaO	$\text{Al}_2\text{O}_3$	$\text{ZrO}_2$	
5-1	29	71	0	$\text{CA}_2$ , $\text{CA}_6$
5-2	28.4	69.6	2	$\text{CA}_2$ , $\text{CA}_6$ , Mono, CA <sup>+</sup>
5-3	27.9	68.3	3.8	$\text{CA}_2$ , $\text{CA}_6$ , Mono, CA <sup>+</sup>
5-4	31	69	0	$\text{CA}_2$ , $\text{CA}_6$
5-5	30.4	67.6	2	$\text{CA}_2$ , $\text{CA}_6$ , Mono, CA <sup>+</sup>
5-6	29.8	66.3	3.8	$\text{CA}_2$ , $\text{CA}_6$ , Mono, CA <sup>+</sup>
5-7	33.3	66.7	0	$\text{CA}_2$ , CA
5-8	32.6	65.4	2	$\text{CA}_2$ , CA, CZ
5-9	32.0	64.1	3.8	$\text{CA}_2$ , Cubic, CA <sup>+</sup>
5-10	35.3	64.7	0	$\text{CA}_2$ , CA
5-11	34.6	63.4	2	$\text{CA}_2$ , CA, CZ
5-12	33.9	62.2	3.8	$\text{CA}_2$ , CA, CZ
5-13	37.5	62.5	0	$\text{CA}_2$ , CA
5-14	36.8	61.3	2	$\text{CA}_2$ , CA, CZ
5-15	36.1	60.1	3.8	$\text{CA}_2$ , CA, CZ

\*Fired to 1500°C, 20 hours slow cooled.

<sup>+</sup>CA present in samples -2, -3, -5, -6, and -9 indicate that equilibrium was not achieved.

to 1200°C for four hours, grinding to a powder after cooling and repressing into bars 4" x 0.25" x 0.25". The bars were fired to 1500°C for 50 hours on ZrO<sub>2</sub> sleds and slow cooled. Flexure strength (room temperature and high temperature), microhardness, and thermal expansion was measured for the CA<sub>2</sub> bars as previously reported.

## RESULTS AND DISCUSSION

CA<sub>2</sub> Stoichiometry. The phases detected in the CA<sub>2</sub> stoichiometry samples are reported in Table 1 and the compatibility triangles near CA<sub>2</sub> were constructed from the determined phases, Figure 1. CA<sub>2</sub> was the major phase in all compositions and the x-ray intensity of the major peak of the remaining phases (CA, CA<sub>6</sub>, Cubic ZrO<sub>2</sub>, Monoclinic ZrO<sub>2</sub>, and calcium zirconate, relative to CA<sub>2</sub> were noted, Table 2, to confirm that the quantity of the phases were changing in the correct order. The phases detected were as expected except for compositions 2, 3, 5, 6 and 9 where CA was present. Apparently these compositions are difficult to take to equilibrium.

For the raw materials used in this study, the composition of CA<sub>2</sub> appears to occur at 68 m/o Al<sub>2</sub>O<sub>3</sub>, 32 m/o CaO. To show this, the relative intensity of CA<sub>6</sub>/CA<sub>2</sub> for compositions 5-1 and 5-3 and CA/CA<sub>2</sub> for compositions 5-7, 5-10 and 5-13 was plotted vs Al<sub>2</sub>O<sub>3</sub> content, Figure 2. The relative intensities of CA and CA<sub>6</sub> were extrapolated to zero in an effort to pinpoint the composition of CA<sub>2</sub>. CA extrapolated to zero at 67% Al<sub>2</sub>O<sub>3</sub> and CA<sub>6</sub> at 68.7 for an average of 67.9% Al<sub>2</sub>O<sub>3</sub>. In addition, composition 5-8 contained

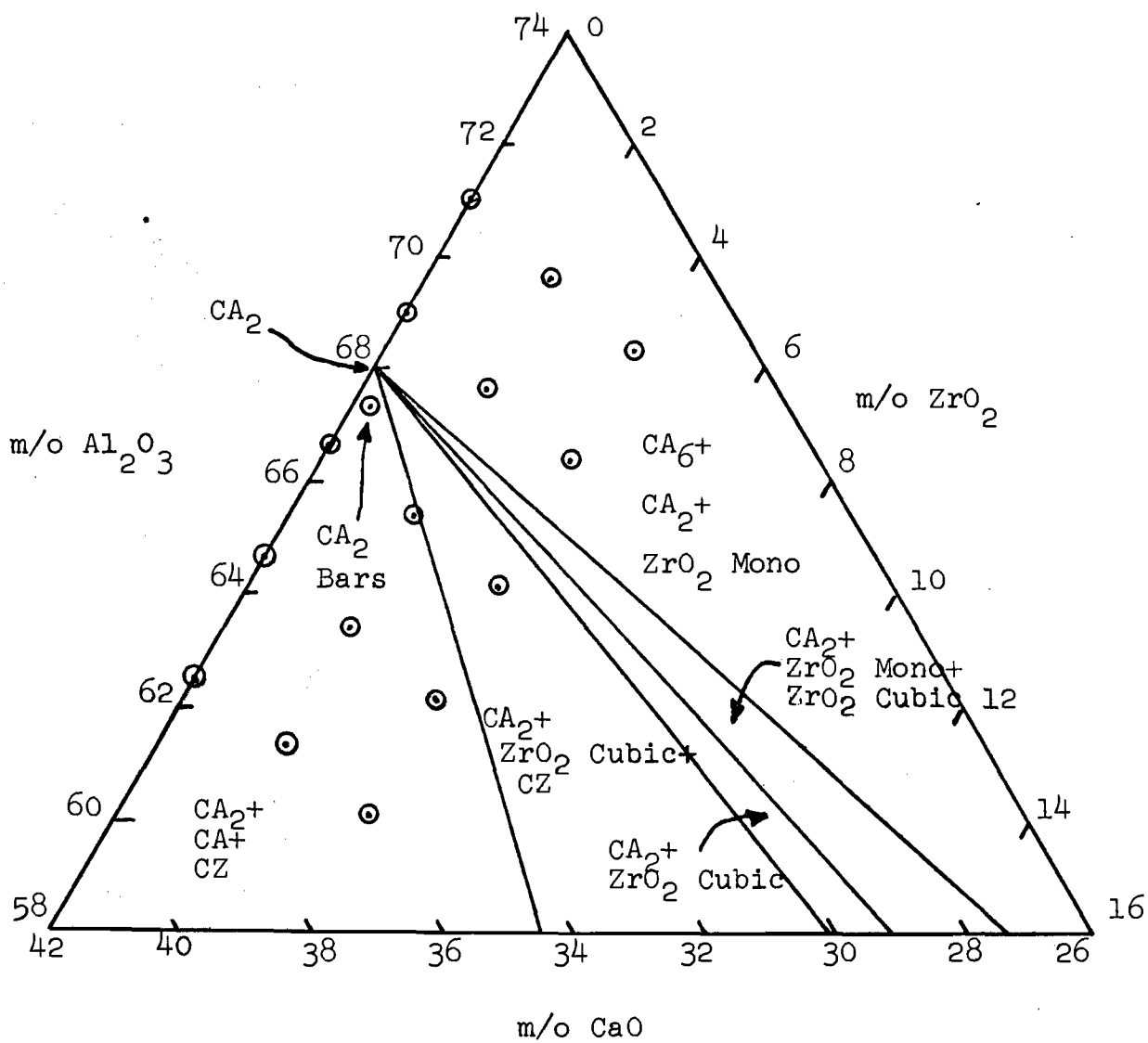


Figure 1. Phase Diagram of the  $\text{CaO}-\text{Al}_2\text{O}_3-\text{ZrO}_2$  System for Compositions Surrounding  $\text{CA}_{2.3}$

Table 2. Relative Intensities of the Major X-ray Diffraction Peaks From Phases Present in Samples Near the Composition  $CA_2^*$ .

Sample	$CA_2$	CA	$CA_6$	Cubic	Mono	CZ
5-1	100	0	37	0	0	0
5-2	100	11	16	0	5	0
5-3	100	18	15	0	11	0
5-4	100	0	5	0	0	0
5-5	100	20	7	0	3	0
5-6	100	30	7	0	0	0
5-7	100	4	0	0	0	0
5-8	100	18	0	0	0	0
5-9	100	38	0	Trace	0	0
5-10	100	20	0	0	0	0
5-11	100	20	0	0	0	4
5-12	100	5	0	0	0	26
5-13	100	44	0	0	0	0
5-14	100	36	0	0	0	22
5-15	100	15	0	0	0	34

\*Samples fired at  $1500^{\circ}C$  for 20 hours and slow cooled.



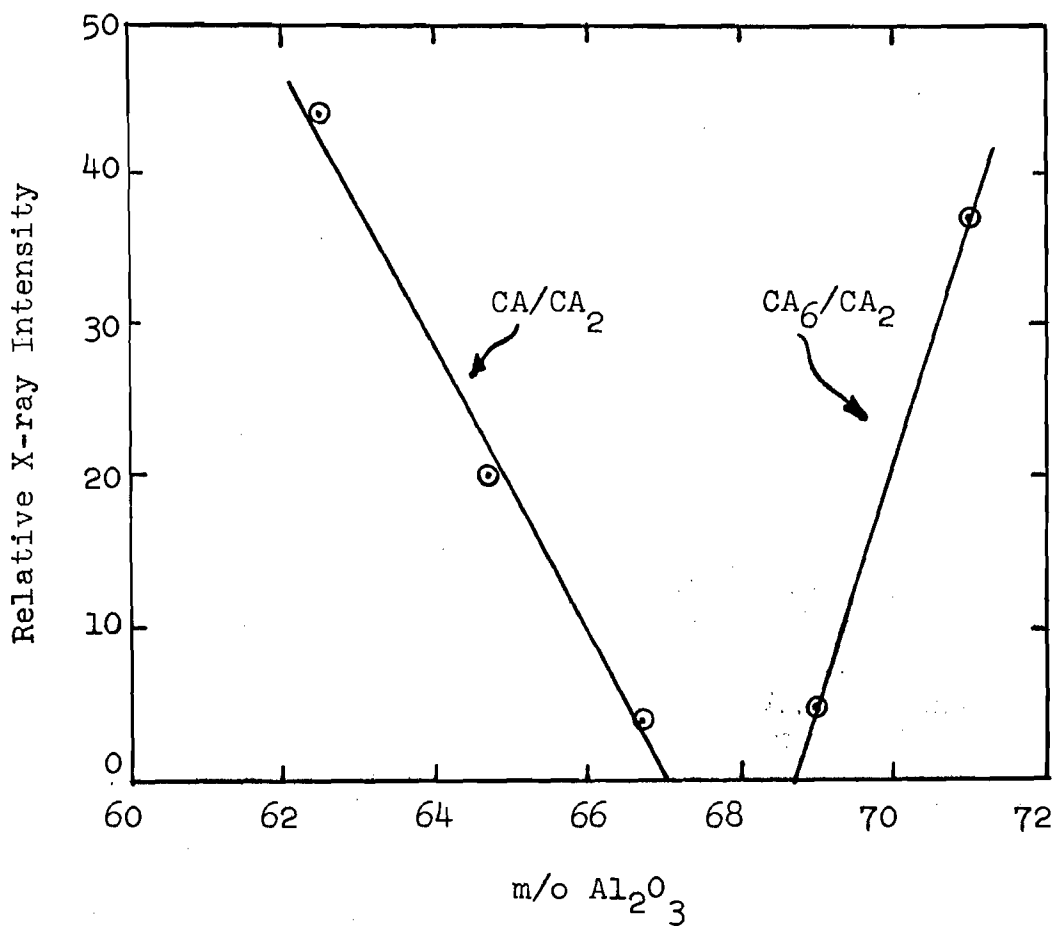


Figure 2. Relative X-ray Intensity of  $CA_6/CA_2$  and  $CA/CA_2$  for  $CaO-Al_2O_3$  Composition. Note: Lines Should Extrapolate to Zero at  $CA_2$  Composition.

CA and no cubic  $\text{ZrO}_2$ . Thus the join between  $\text{CA}_2$  and calcium zirconate must be drawn to 68%  $\text{Al}_2\text{O}_3$ , 32%  $\text{CaO}$ .

In summary, the data reported here and that extrapolated from high  $\text{ZrO}_2$  compositions reported earlier indicated that the composition of  $\text{CA}_2$  is 68%  $\text{Al}_2\text{O}_3$  and 32%  $\text{CaO}$  for our raw materials.

$\text{CA}_2$  Properties. The composition 67.5 m/o  $\text{Al}_2\text{O}_3$ -32.0 m/o  $\text{CaO}$ -0.5 m/o  $\text{ZrO}_2$  was selected for physical property determination of  $\text{CA}_2$ . X-ray diffraction analysis of the fired  $\text{CA}_2$  bars, Figure 3, indicated a trace of CA as the only other crystalline phase. Either the  $\text{ZrO}_2$  went into solid solution or was below the detectability level of x-ray diffraction.

Flexure strength and microhardness of the  $\text{CA}_2$  bars is reported in Tables 3 and 4. Comparison of flexure strength and microhardness of  $\text{CA}_2$  to "as fired" values for compositions A, B, and C, Figures 4 and 5, show that  $\text{CA}_2$  values are lower for both properties. This is interesting, since as  $\text{CA}_2$  content increased for compositions A, B, and C, both flexure strength and microhardness increased. Flexure strength may be porosity and grain size controlled which could provide an explanation for the strength variations but microhardness indentations are in non-porous areas and there is no satisfactory explanation for the microhardness variations.

Thermal expansions measurements on the  $\text{CA}_2$  bars and composition 5-7 is reported in Table 6 and Figure 6. Composition 5-7 contained a trace of  $\text{CA}_6$  and the  $\text{CA}_2$  bars contained a trace of CA. The expansion of the two compositions agreed well with each other and with values reported in literature being approximately  $5.0 \times 10^{-6}/^\circ\text{C}$  at  $1200^\circ\text{C}$ .

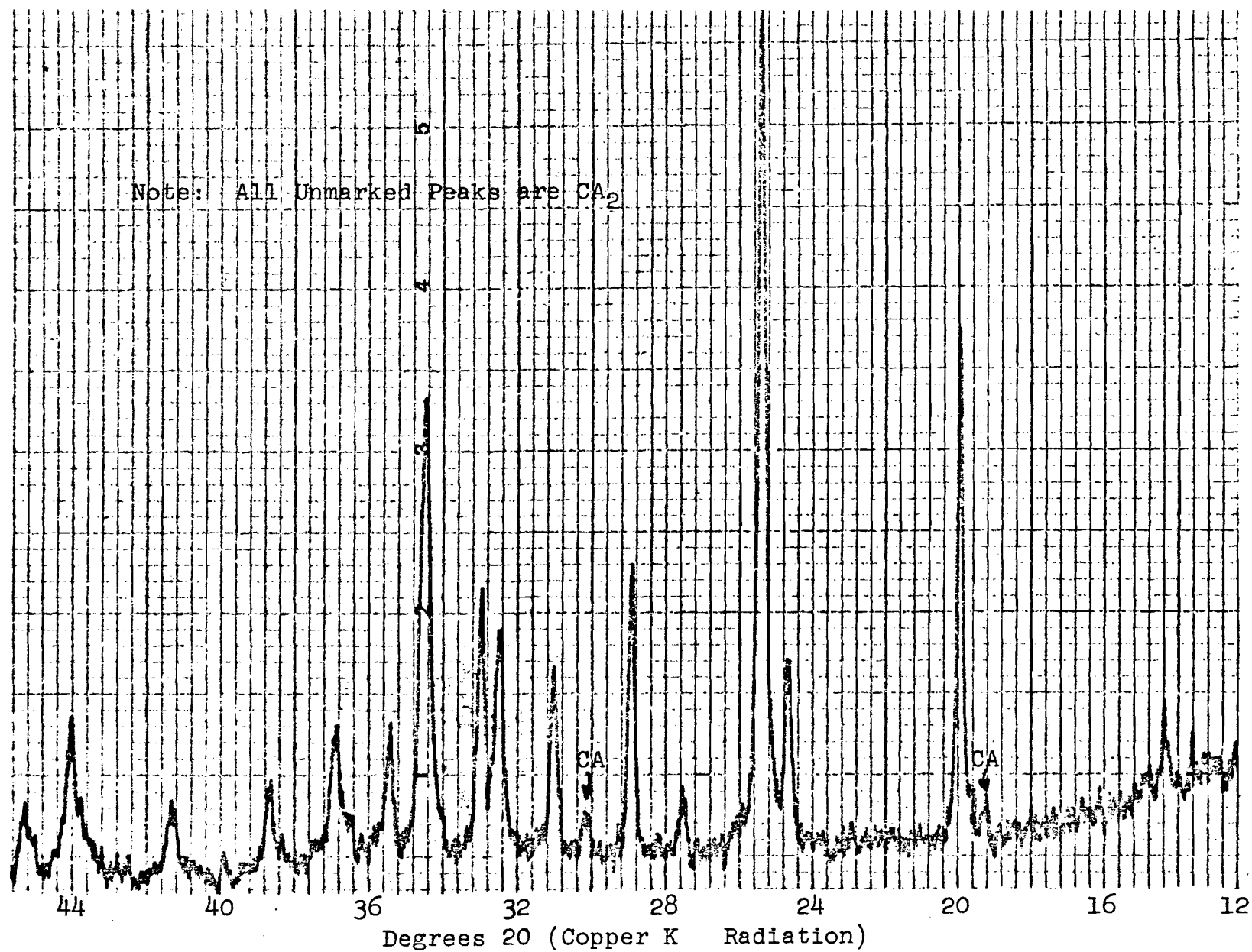


Figure 3. X-ray Diffraction Trace of  $\text{CA}_2$  Bars Showing Peaks for  $\text{CA}_2$  and a Trace of CA (Marked Peaks).

Table 3. Flexure Strength of  $\text{CaO} \cdot 2\text{Al}_2\text{O}_3$  as a Function of Temperature

Temperature (°C)	Flexure Strength (psi)	Standard Deviations (psi)	Percent Standard Deviations
20	5040	1010	20.0
900	5780	800	13.8
1100	5770	910	15.8
1300	6340	920	14.5

Table 4. Room Temperature Microhardness of  $\text{CaO} \cdot 2\text{Al}_2\text{O}_3$ 

Load (grams)	Knoop Hardness (kg/mm <sup>2</sup> )
30.5	1006
34.0	984
39.0	917
42.5	906
46.0	770
51.0	651
59.0	528

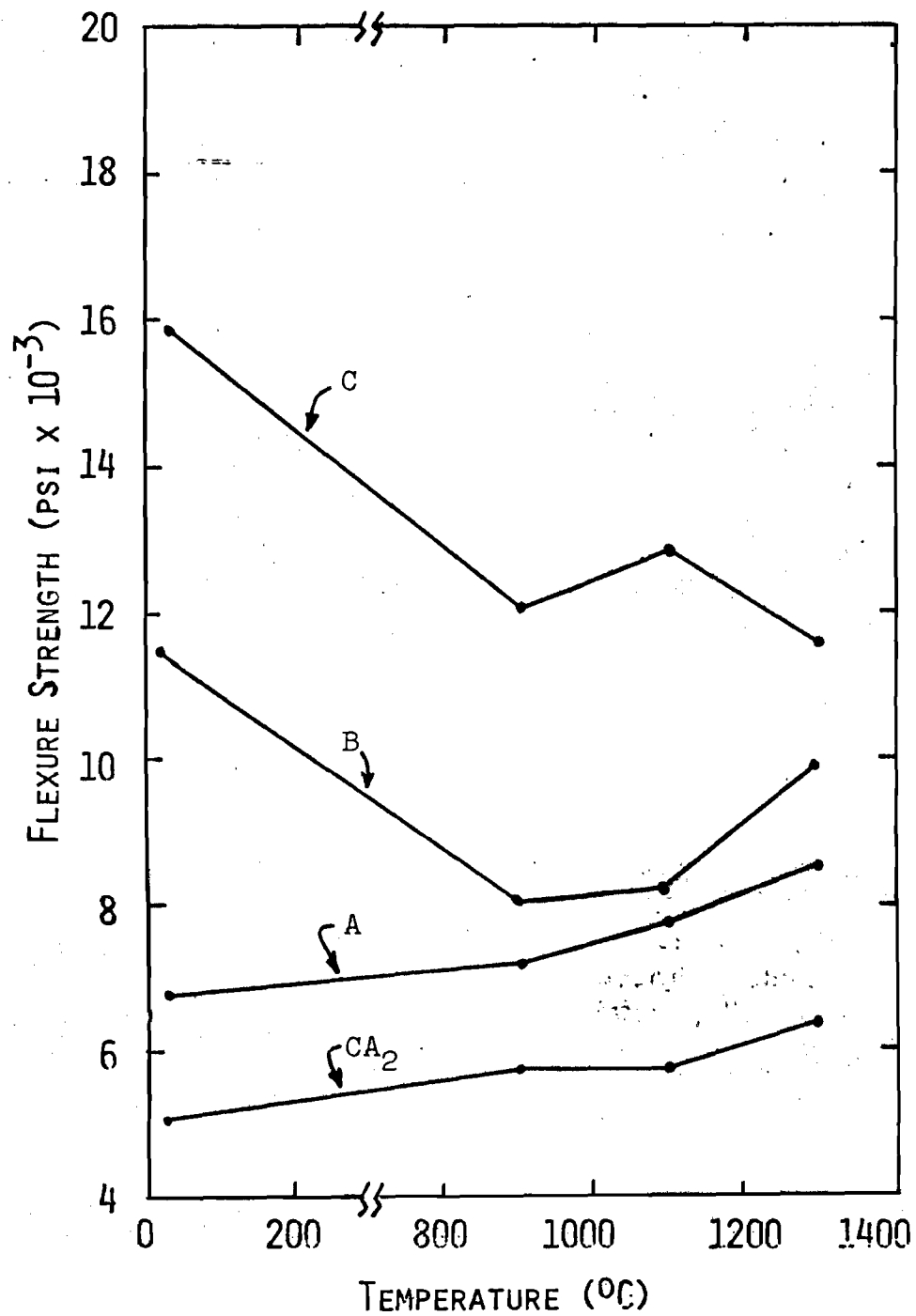


Figure 4. Flexure Strength of CA<sub>2</sub> Compared to "As Fired" Compositions A, B and C.

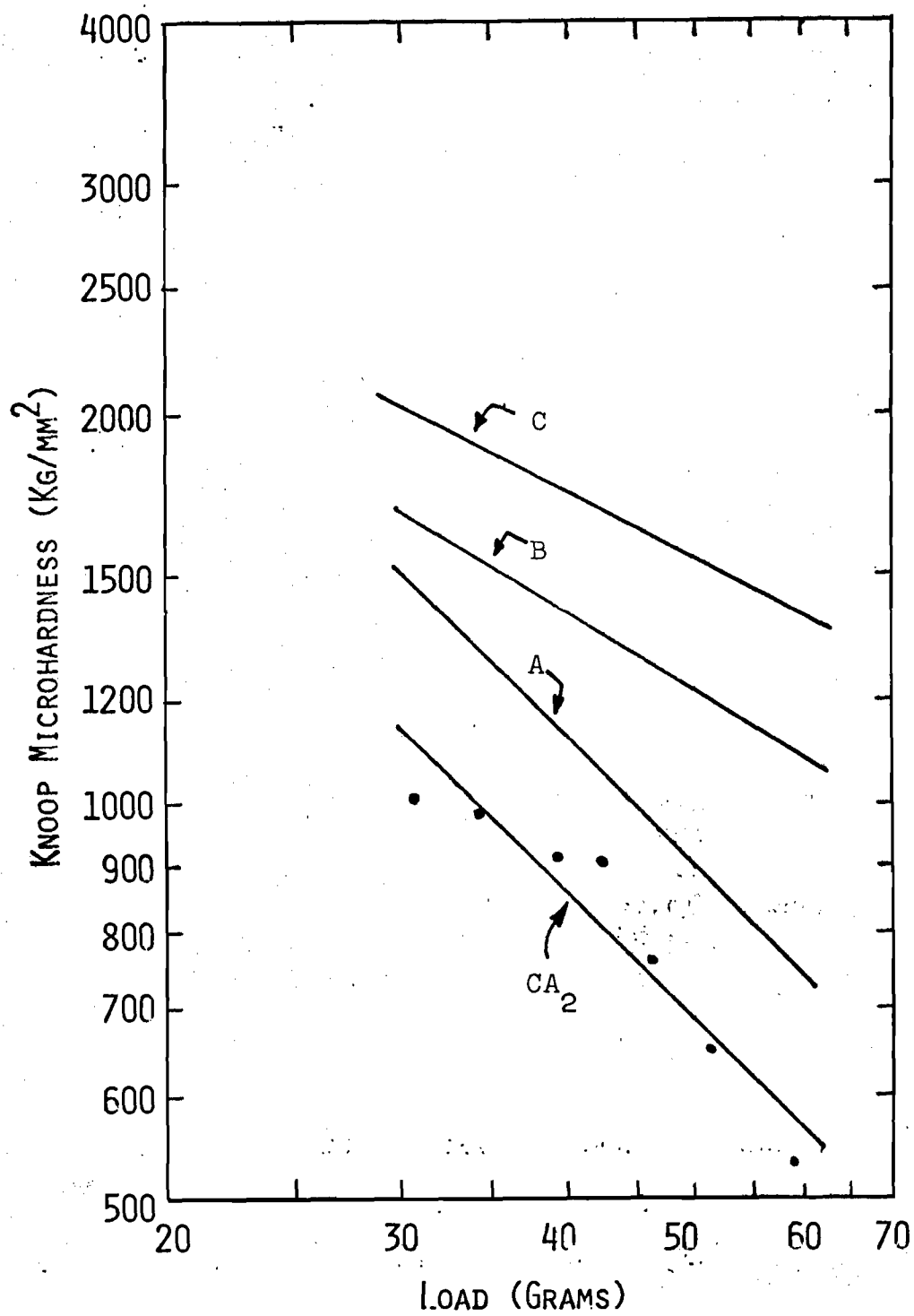


Figure 5. Microhardness of CA<sub>2</sub> Compared to "As Fired" Compositions A, B and C.

Table 5. Thermal Expansion of  $CA_2$ .

Temperature $^{\circ}C$	$CA_2$ Bars*		Composition 5-7 <sup>1</sup>	
	% Expansion	$a_{Eng}$ $\times 10^{-6}/^{\circ}C$	% Expansion	$a_{Eng}$ $\times 10^{-6}/^{\circ}C$
200	0.058	3.22	0.058	3.22
400	0.148	3.90	0.130	3.42
600	0.240	4.14	0.230	3.96
800	0.360	4.61	0.335	4.30
1000	0.490	5.00	0.460	4.69
1200	0.610	5.16	0.565	4.79

\*

$CA_2$  Bars - Composition (m/o), 67.5  $Al_2O_3$ , 32.0 CaO, 0.5  $ZrO_2$   
Phases,  $CA_2$  and trace of CA.

<sup>1</sup>Composition 5-7 - Composition (m/o), 69.0  $Al_2O_3$ , 31.0 CaO  
Phases,  $CA_2$  and trace of  $CA_6$ .

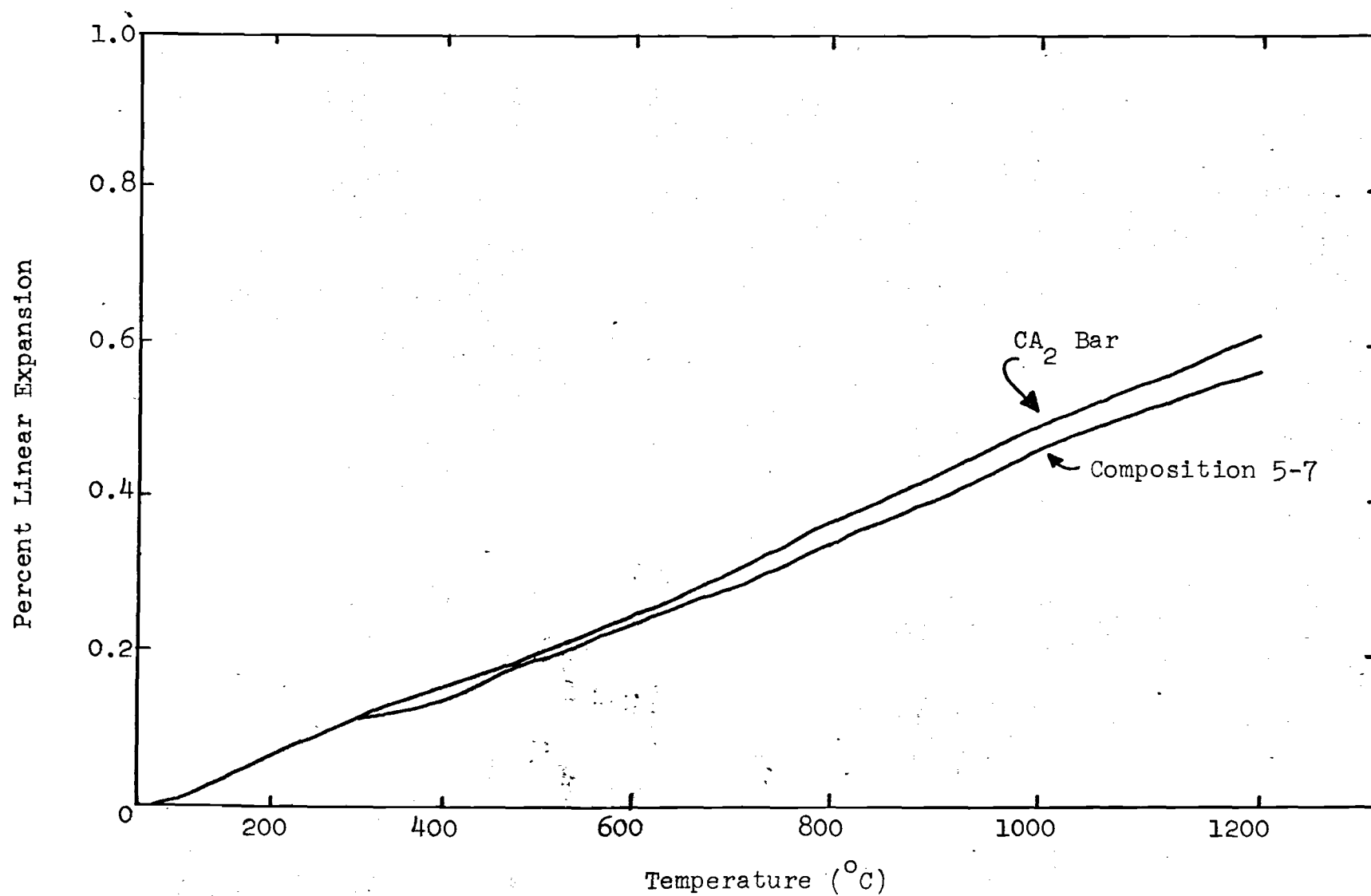


Figure 6. Thermal Expansion of CA<sub>2</sub> Containing a Trace of CA (CA<sub>2</sub> Bar) and CA<sub>2</sub> Containing a Trace of CA<sub>6</sub> (Composition 5-7).



PHASE RELATIONSHIPS AND LONG-TERM TEMPERATURE STABILITY  
IN THE HIGH ZIRCONIA REGION OF THE  
CALCIA-ALUMINA-ZIRCONIA SYSTEM

A THESIS

Presented to

The Faculty of the Division of Graduate  
Studies and Research

By

John Day


In Partial Fulfillment  
of the Requirements for the Degree  
Master of Science  
in the School of Ceramic Engineering

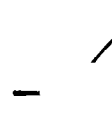
Georgia Institute of Technology


December, 1976

PHASE RELATIONSHIPS AND LONG-TERM TEMPERATURE STABILITY  
IN THE HIGH ZIRCONIA REGION OF THE  
CALCIA-ALUMINA-ZIRCONIA SYSTEM

Approved:

 \_\_\_\_\_  
Joe K. Cochran, Jr., Chairman

 \_\_\_\_\_  
Alan T. Chapman

 \_\_\_\_\_  
James F. Benzel

Date Approved by Chairman: 10-26-76

## ACKNOWLEDGEMENTS

I wish to give special thanks to the U.S. Bureau of Mines for its sponsorship and to Dr. Joe K. Cochran, Jr., for his encouragement and direction throughout the pursuit of this research investigation. Thanks also go to Dr. Chapman and Dr. Benzel for their reading of this thesis and for their advice. I also wish to thank Mr. Jae Do Lee and Mr. B. H. Kim for their able assistance in collecting and interpreting portions of the data. Thanks go also to Mr. Tom Mackrovich for his help in fabricating the samples. Above all, I thank my wife Margaret for her faithful encouragement and prayers throughout the undertaking of this project. Only through her steadfastness and through the grace and strength of our Savior and Lord Jesus Christ was this project completed.

## TABLE OF CONTENTS

	Page
ACKNOWLEDGEMENTS . . . . .	ii
LIST OF TABLES . . . . .	v
LIST OF ILLUSTRATIONS. . . . .	vi
SUMMARY. . . . .	viii
GLOSSARY OF ABBREVIATIONS. . . . .	ix
CHAPTER	
I. INTRODUCTION . . . . .	1
II. SURVEY OF LITERATURE. . . . .	2
CaO-Al <sub>2</sub> O <sub>3</sub> -ZrO <sub>2</sub>	
ZrO <sub>2</sub> -CaO	
CaO-Al <sub>2</sub> O <sub>3</sub>	
Al <sub>2</sub> O <sub>3</sub> -ZrO <sub>2</sub>	
The Disappearing Phase Method of Phase Diagram Determination	
III. PROCEDURE . . . . .	22
Sample Preparation	
Qualitative X-Ray Analysis	
Quantitative X-Ray Analysis	
Lattice Parameter Measurement	
Quantitative Optical Determination	
Density Determination	
IV. RESULTS AND DISCUSSION OF RESULTS . . . . .	35
Qualitative Phase Diagram at 1500 °C	
Calculation of Alkemade Lines and Verification of	
Equilibrium at 1500 °C	
Alumina Solubility in Cubic and Monoclinic Zirconia	
CaO-Al <sub>2</sub> O <sub>3</sub> -ZrO <sub>2</sub> Phase Equilibria at 1500 °C	
Long Term Phase Equilibria Stability	
Analysis of Series 1 Fired at 1700 °C	
V. CONCLUSIONS . . . . .	64

## TABLE OF CONTENTS (Continued)

VI. RECOMMENDATIONS . . . . .	66
APPENDICES	
A. SYSTEMATIC POINT COUNTING TECHNIQUE . . . . .	67
B. PHASE ANALYSIS OF COMPOSITIONS FIRED AT 1500 °C . . . . .	69
C. DATA FOR CALCULATING $Ca_2$ - CUBIC $ZrO_2$ AND $Ca_2$ - MONOCLINIC $ZrO_2$ ALKEMADE LINES . . . . .	72
D. QUANTITATIVE CHANGES IN CUBIC TO MONOCLINIC ZIRCONIA CONTENTS FOR LONG TERM FIRING . . . . .	76
REFERENCES . . . . .	77

## LIST OF TABLES

Table	Page
1. X-Ray $d$ Spacings for $\text{Ca}_{76}\text{Al}_6\text{ZrO}_{18}$ . . . . .	4
2. Decomposition of the Solid Solutions during Heating in Air . .	14
3. Ionic Crystal Radii. . . . .	13
4. Powder Diffraction Data for $\text{CaO} \cdot 2\text{Al}_2\text{O}_3$ . . . . .	19
5. Composition of Series 1 . . . . .	23
6. Composition of Series 2 . . . . .	24
7. Composition of Series 3 . . . . .	25
8. Composition of Series 4 . . . . .	25
9. Composition of Batches for Long Term Firing . . . . .	27
10. Optical Data for $\text{CA}_2$ Stoichiometry Determination . . . . .	46
11. Phase Composition and Optically Determined Phase Volume of Series 1, 1700 °C . . . . .	62
12. Accuracy of Systematic Point Counting Technique . . . . .	67
13. Phase Analysis of Series 2 . . . . .	70
14. Phase Analysis of Series 3 . . . . .	71
15. Quantitative X-Ray Data for Series 2 and 3, Slow-Cooled. . .	73
16. Quantitative X-Ray Data for Series 2, Quenched . . . . .	74
17. Quantitative X-Ray Data for Long Term Samples at 1550 °C . .	75
18. Quantitative X-Ray Data for Long Term Samples at 1300 °C . .	75
19. Ratios of Cubic to Cubic Plus Monoclinic Zirconia for Compositions A, B, and C Fired at 900 °C and 1300 °C for up to 2000 Hours . . . . .	76

## LIST OF ILLUSTRATIONS

Figure	Page
1. Phase Diagram of the $\text{CaO-Al}_2\text{O}_3\text{-ZrO}_2$ System as Determined by Berezhnoi . . . . .	3
2. Linear Thermal Expansion of Monoclinic Zirconia . . . . .	6
3. Phase Diagram of the $\text{CaO-ZrO}_2$ System as Determined by Duwez . .	8
4. Effect of the Amount of Calcia on Transformation Temperature from Cubic to Monoclinic Zirconia . . . . .	9
5. Lattice Parameter Variations with Solid Solution Changes in Cubic Zirconia . . . . .	10
6. Phase Diagram and Lattice Parameter Data for the $\text{CaO-ZrO}_2$ System after Garvie. . . . .	12
7. Phase Diagram of the $\text{CaO-Al}_2\text{O}_3$ System as Determined by Lea and Desch. . . . .	17
8. Relationship between Peak Intensities and Weight Ratios of Cubic to Monoclinic Zirconia. . . . .	30
9. Lattice Parameter Extrapolation for Composition A before Heat Treatment . . . . .	33
10. Phase Analysis of Samples Slow-Cooled from 1500 °C . . . . .	36
11. Extrapolation of Calcia Content to 0% and 100% Cubic Zirconia at Fixed Alumina Contents. . . . .	39
12. Cubic Zirconia Alkemade Lines at 20 and 40 Hours Firing at 1500 °C, Verifying Equilibrium by Reproducibility of Lines. . .	41
13. Alkemade Lines Bounding the Cubic + Monoclinic + $\text{CA}_2$ Region at 1500 °C . . . . .	42
14. Photomicrographs of Series 3, 1500 °C, 600x . . . . .	44
15. Extrapolation Of $\text{CA}_2$ Composition to 0% Alumina to Determine $\text{Al}_2\text{O}_3$ Solubility in Zirconia. . . . .	45
16. Calcia-Alumina-Zirconia Phase Diagram at 1500 °C. . . . .	47

## LIST OF ILLUSTRATIONS (Continued)

17. Alkemade Line at 1550 °C from $CA_2$ to Cubic Zirconia . . . . .	52
18. Change in Amount of Cubic Zirconia with Time at 900 °C. . . . .	54
19. Change in Amount of Cubic Zirconia with Time at 1300 °C . . . . .	55
20. Alkemade Line at 1300 °C from $CA_2$ to Cubic Zirconia . . . . .	56
21. Lattice Parameter Changes with Time . . . . .	59
22. Photomicrographs of Series 1, 1700 °C, 600x . . . . .	61



## SUMMARY

The phase diagram of the calcia-alumina-zirconia ternary system in the high zirconia region was determined by the disappearing phase method. Qualitative and quantitative X-ray analysis was used to determine the phases present in samples that had been fired to 1500 °C and 1700 °C. Optical analysis was used to determine the total calcium aluminates and zirconia phase contents by volume. Results indicated that  $CA_2$  may exhibit solid solution characteristics giving it a stoichiometry as high as  $C_3A_7$ . Solid solution was also observed in the cubic zirconia phase. A small portion of alumina entered the zirconia lattice, as well as 11.2 to 14.6 mole percent calcia in the completely stabilized zirconia phase. No quantitative determination could be made of the amount of calcia or alumina present in the monoclinic zirconia lattice. Considerable melting occurred in the samples fired at 1700 °C which led to a non-equilibrium state on cooling and thus made phase equilibria determinations questionable.

Samples were fired at 1550 °C to be used for the study of long term phase stability. When held at 1300 °C, cubic zirconia destabilization occurred with time and 800 to 1000 hours were required to reach equilibrium. However, at 900 °C destabilization occurred very slowly and was not nearly complete after 2000 hours. Lattice parameter measurements indicated approximately two mole percent more calcia in the cubic zirconia structure at equilibrium at 1300 °C than at 1550 °C.

## GLOSSARY OF ABBREVIATIONS

CA	$\text{CaO} \cdot \text{Al}_2\text{O}_3$
$\text{CA}_2$	$\text{CaO} \cdot 2\text{Al}_2\text{O}_3$
$\text{C}_3\text{A}_5$	$3\text{CaO} \cdot 5\text{Al}_2\text{O}_3$
$\text{CA}_6$	$\text{CaO} \cdot 6\text{Al}_2\text{O}_3$
CZ	$\text{CaO} \cdot \text{ZrO}_2$
$\text{C}_3\text{A}_7$	$3\text{CaO} \cdot 7\text{Al}_2\text{O}_3$
SS	Solid Solution
$\text{C}_7\text{A}_3\text{Z}$	$7\text{CaO} \cdot 3\text{Al}_2\text{O}_3 \cdot \text{ZrO}_2$

## CHAPTER I

### INTRODUCTION

A refractory of high zirconia content stabilized with both calcia and alumina may become useful in the coal gasification industry because of good corrosion resistant characteristics of the components. No complete phase diagram of this portion of the ternary system is available. In order to prepare such a phase diagram, samples of various compositions in the system were mixed and fired. X-ray and optical analysis of the resulting phases permitted determination of compatibility triangles. Because of the cubic zirconia solid solution phase and also because of the possibility of a solid solution of  $Ca_2$ , particular attention was required to determine the changing compositions as temperature of firing varied.

From a practical point of view, the quantity of phase change at different temperatures with long use must be determined if such a material were to be used as a refractory. Because of the thermal shock problems involved in the transition from tetragonal to monoclinic zirconia, it is especially important to know quantitatively the increase in the amount of monoclinic zirconia with time. This was studied by firing for up to 2000 hours at 900 °C and 1300 °C.

## CHAPTER II

## SURVEY OF LITERATURE

Little information has been published for the  $\text{CaO-Al}_2\text{O}_3\text{-ZrO}_2$  ternary system and no phase diagram of the high zirconia region has been published detailing the solid solution and polymorphic information. Only Berezhnoi<sup>1</sup> in Russia has published information directly relating to the ternary phase diagram.

In order to gain an understanding of the system from the literature one must study reports about the three binary systems that are involved:  $\text{ZrO}_2\text{-CaO}$ ,  $\text{Al}_2\text{O}_3\text{-CaO}$ , and  $\text{Al}_2\text{O}_3\text{-ZrO}_2$ . The first two of these systems have been well studied, although there remains much contradiction. The third system forms no binary compounds and is thus less complex.

$$\underline{\text{CaO-Al}_2\text{O}_3\text{-ZrO}_2}$$

Berezhnoi<sup>1</sup> has published the only available phase diagram of the ternary system  $\text{CaO-Al}_2\text{O}_3\text{-ZrO}_2$ , Figure 1. He was primarily interested in the new ternary compound which he had discovered,  $\text{Ca}_7\text{Al}_6\text{ZrO}_{18}$ , which is a potential hydraulic binder<sup>2</sup>, and thus he did not look at polymorphs of zirconia or at the solid solution structure of zirconia.

$\text{Ca}_7\text{Al}_6\text{ZrO}_{18}$  was found to be a useful binder in the hydrated state. It is the first known substance containing  $\text{ZrO}_2$  to exhibit such properties, according to Berezhnoi. The new compound was prepared from high purity silica chalk, technical grade alumina, and zirconia which were mixed and fired to a temperature of  $1400^\circ\text{C}$  to  $1460^\circ\text{C}$ . Synthesis required one

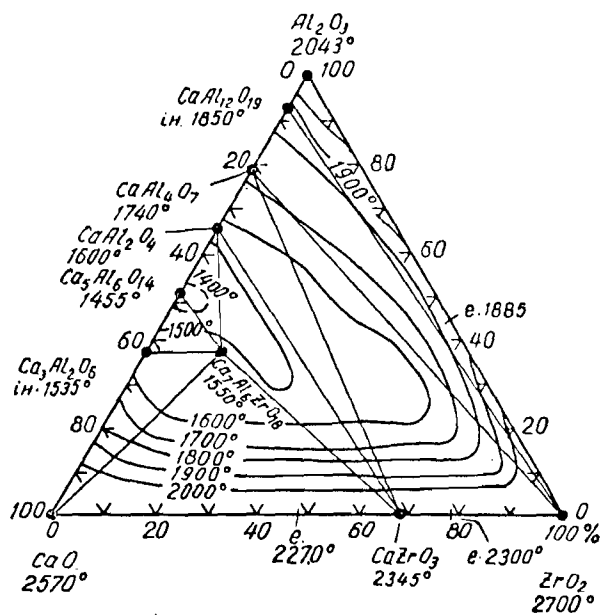


Figure 1. Phase Diagram of the CaO-Al<sub>2</sub>O<sub>3</sub>-ZrO<sub>2</sub> System as Determined by Berezhnoi<sup>1</sup>.

hour at 1450 °C. It melts incongruently at 1550 °C (with the formation of  $\text{CaZrO}_3$ ), has a density of 3.1 g/cc, and a linear thermal expansion coefficient of  $8.7 \times 10^{-6}/^\circ\text{C}$  (20-1000 °C). X-ray  $d$  spacing information is reproduced in Table 1.

Table 1. X-ray  $d$  Spacings<sup>2</sup> for  $\text{Ca}_7\text{Al}_6\text{ZrO}_{18}$

$d$ (Å)	I	$d$ (Å)	I	$d$ (Å)	I
7.61	10	2.218	6	1.829	12
4.10	10	2.177	6	1.669	5
3.42	29	2.114	4	1.647	6
3.36	10	2.081	5	1.628	5
2.758	10	1.945	5	1.565	19
2.696	100	1.918	16	1.555	10
2.647	26	1.889	22	1.537	11
2.305	5	1.863	12	1.507	5

Tarnopol'skaya and Gul'ko<sup>3</sup> have published some basic information concerning the quaternary system  $\text{CaO-SrO-Al}_2\text{O}_3\text{-ZrO}_2$ . Their investigation was limited to studying the compounds present in the system and possible uses of them as refractories. They confirmed the existence of  $\text{Ca}_7\text{Al}_6\text{ZrO}_{18}$  but presented no other information useful to the study of the ternary.

N. I. Voronin<sup>4</sup> commented that an alumina impurity in zirconia may improve the heat resistance of zirconia when it is stabilized with magnesia, but apparently he did not work with calcia stabilized zirconia.

Antonio Cocco<sup>5</sup> reported that up to three percent alumina could enter the structure of calcia stabilized zirconia without affecting that structure. His work was at temperatures from 1400 °C to 1700 °C but only compositions of more than 29 mole percent calcia were investigated, which limited his study to the phase region of cubic zirconia and  $\text{CaZrO}_3$ .

Takagi<sup>6</sup> investigated the effect of alumina on the sintering of

calcia stabilized zirconia. For raw materials he used zirconium oxychloride, calcium carbonate, and aluminum nitrate. Sixteen mole percent calcia was used to stabilize the zirconia phase. The samples were fired in air at 1700 °C for one hour. He discovered that the addition of from 0.5 to 4 weight percent of alumina enhanced the sintering of the zirconia. The zirconia grain size was about 50 microns for additions of from two to four weight percent alumina. At 1700 °C Takagi observed some liquid phase sintering. The only calcium aluminate phase observed was  $CA_6$  in both scanning electron microscope analysis and electron probe X-ray microanalysis.

#### ZrO<sub>2</sub>-CaO

Zirconia has a melting point of  $2680 \pm 20$  °C and therefore would appear to be very useful as a refractory,<sup>7</sup> especially since it has good corrosion resistance and high strength. Its density is 5.89 g/cc. It has low thermal conductivity and does not react with most metals nor is it easily wetted by molten glass. However, at 1000 °C there is a destructive transformation which makes zirconia a poor refractory in its pure state. Below 1000 °C zirconia has a monoclinic crystal structure. At 1000 °C it transforms rapidly into a tetragonal structure with a significant density change and thus destructive thermal expansion. Figure 2 shows the effect of heating zirconia through this transformation.

To combat this transformation in zirconia which causes destructive cracking, one of several different oxides may be added to stabilize zirconia. This eliminates, or at least reduces, the effects of the transformation from monoclinic to tetragonal zirconia. In commercial usage,

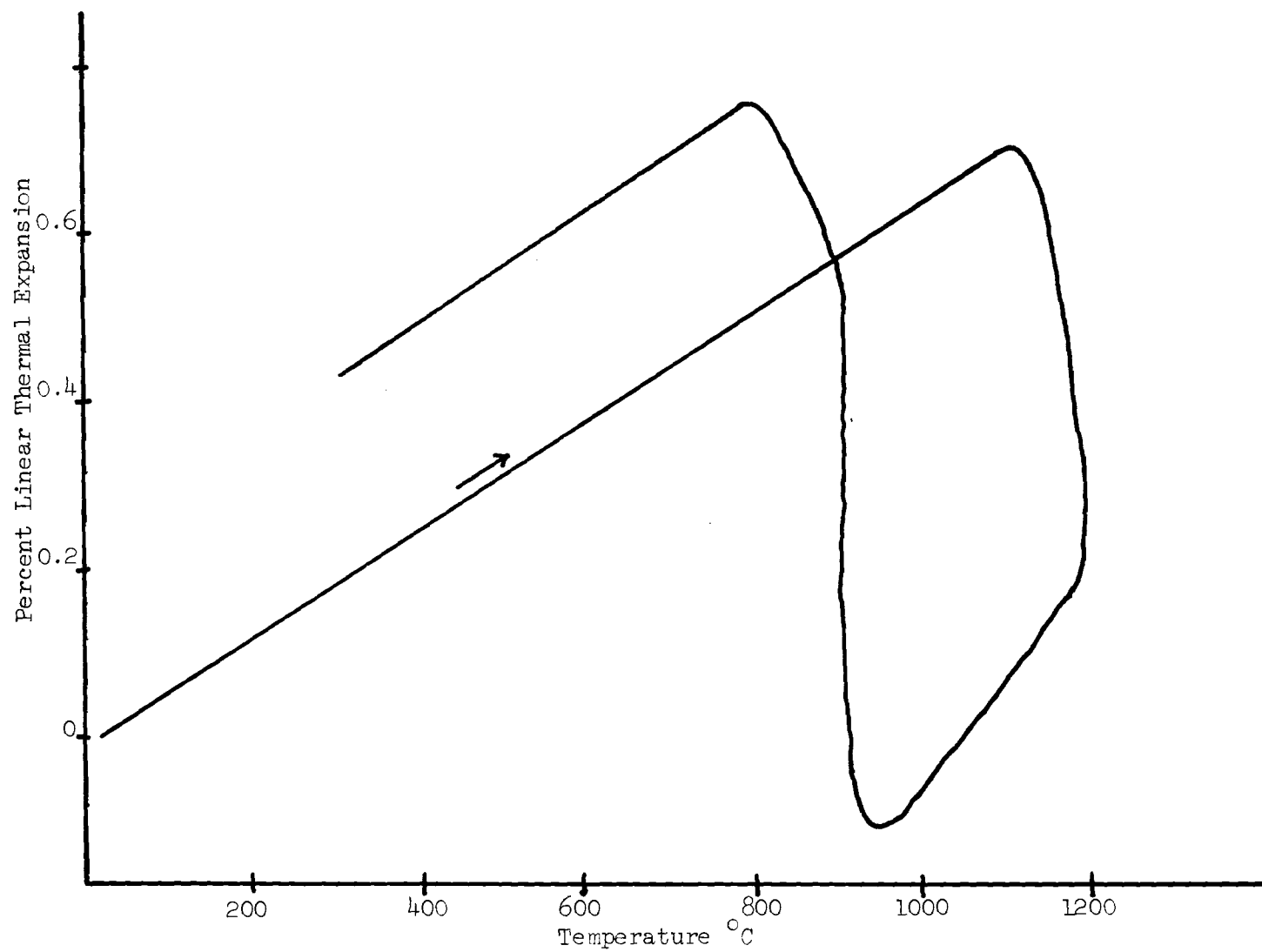


Figure 2. Linear Thermal Expansion of Monoclinic Zirconia<sup>8</sup>



the addition of calcia is most common. If between 16 and 29 mole percent of calcia is added to zirconia, the zirconia forms a cubic solid solution which is stable to room temperature. With the addition of less than 16 percent calcia the zirconia is called partially stabilized, i.e., there is some cubic solid solution but also some monoclinic phase in equilibrium; thus the monoclinic to tetragonal transformation can still be seen, but depending on the percentage of calcia, it is less destructive. The melting point is lowered by calcia additions, as shown in the phase diagram, Figure 3.

The stability of calcia stabilized zirconia is excellent. Isothermal tests<sup>9</sup> at 1375 °C for 336 hours, 1200 °C for 520 hours, 1100 °C for 812 hours, 980 °C for 1473 hours, and 815 °C for 2011 hours showed that there was no loss in stabilization, i.e., no decrease in the amount of cubic zirconia, with long term firing.

Duwez<sup>9</sup> found from differential thermal analysis that the transformation temperature from tetragonal to monoclinic zirconia was lowered as the amount of calcia (up to 16 mole percent) was increased, as shown in Figure 4. This transformation temperature depression was also found in the zirconia-magnesia and zirconia-ceria systems.

Lattice parameter variations as the amount of calcia was changed were also determined by Duwez, Figure 5. For his work the samples were fired at 2000 °C. Lattice parameters were determined from high angle reflections only and a 143.2 mm camera was used for diffraction analysis.

Garvie<sup>10</sup> criticized the phase diagram of Duwez and determined a much smaller region of cubic solid solution. He tentatively determined a second CZ compound,  $\text{CaZr}_4\text{O}_9$ , which exists in an alpha form from 1240 °C

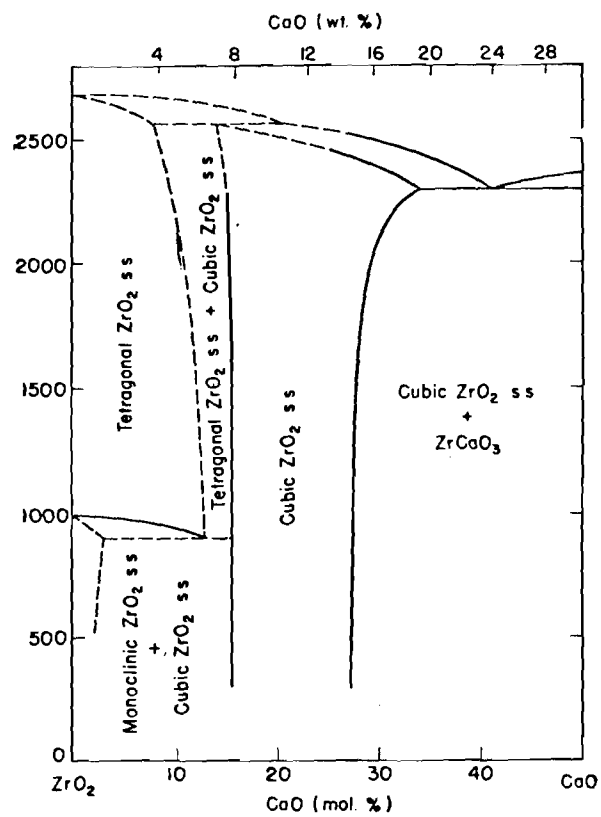


Figure 3. Phase Diagram of the CaO-ZrO<sub>2</sub> System  
as Determined by Duwez<sup>9</sup>

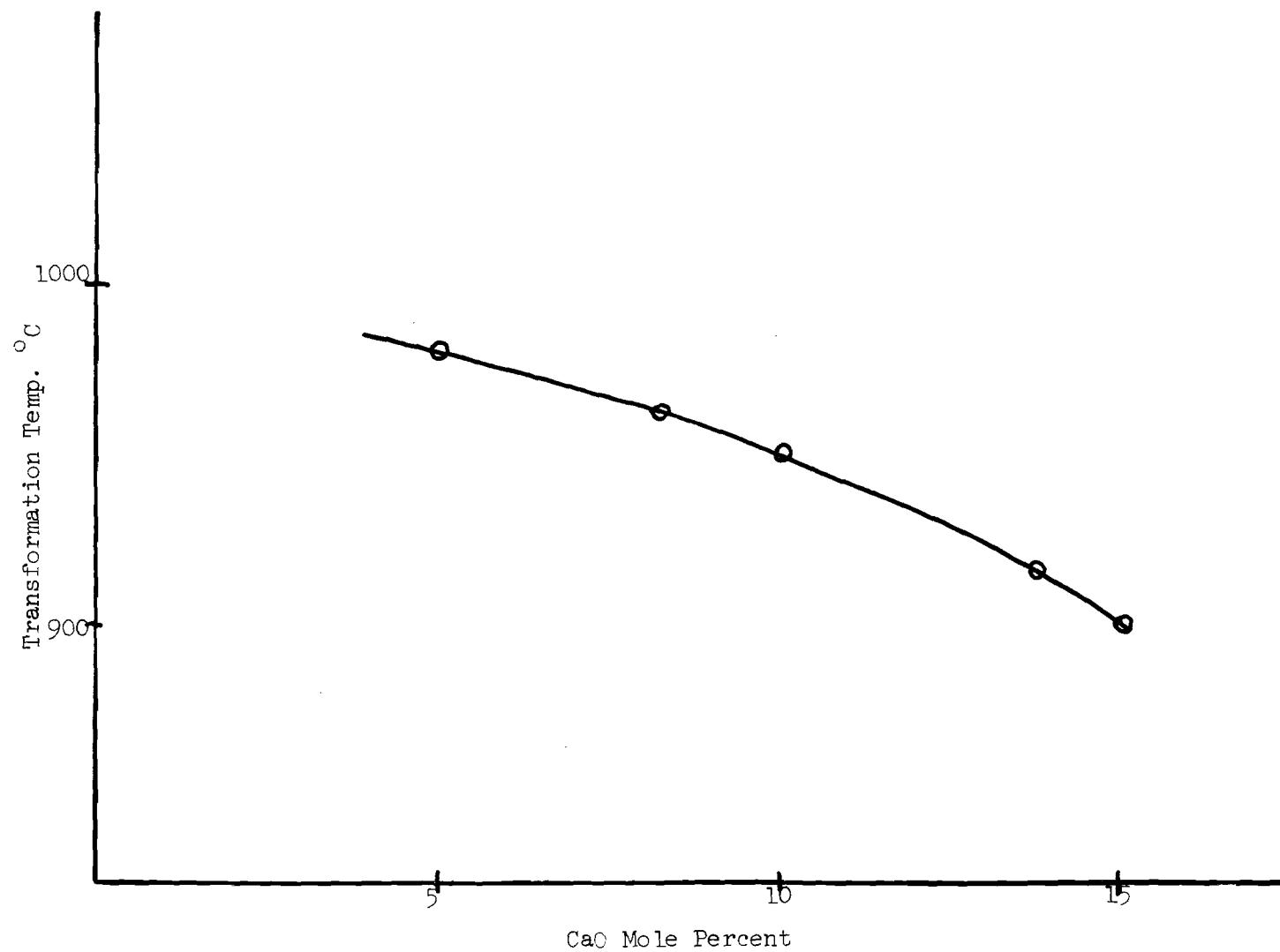


Figure 4. Effect of the Amount of Calcia on Transformation Temperature from Cubic to Monoclinic Zirconia<sup>9</sup>

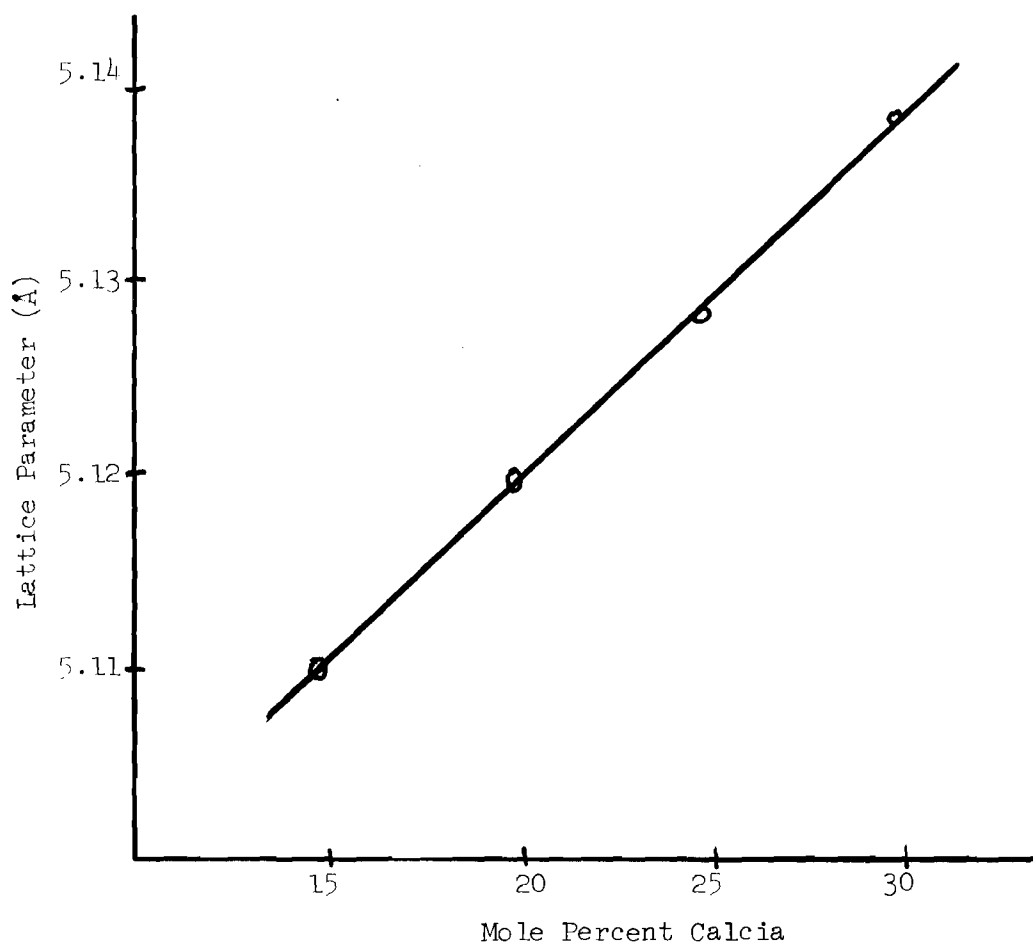


Figure 5. Lattice Parameter Variations with Solid Solution Changes in Cubic Zirconia<sup>9</sup>

to 1650 °C and above 1650 °C exists in a beta form. If the cubic phase is metastable, as he asserted from the work of Weber<sup>11</sup>, then there is great difficulty in determining the actual equilibrium phases. Garvie used lattice parameter determinations employing the Nelson-Riley extrapolation and a Debye-Scherrer camera of 114.6 mm diameter to determine changes in the structure of the solid solution. Figure 6 shows his lattice parameter determinations and the resulting phase diagram, both of which differ considerably from the information published by Duwez<sup>9</sup>.

Garvie discovered that the raw materials used may cause variations in the cubic solid solution. He showed that the use of  $\text{CaCO}_3$  as a reagent resulted in a larger cubic field than the use of  $\text{CaO}$ . He theorized that with  $\text{CaCO}_3$  as a reagent, as the salt decomposed, an active intermediate oxide formed which caused an irreversible, metastable formation of the cubic phase. This problem may also partially explain the discrepancies in different phase diagram information that has been published for the system. Garvie also stated that the strain energy involved in the transformation from tetragonal to monoclinic zirconia must be considered an additional degree of freedom. Such an explanation is necessary in order to draw the cubic boundaries as he did at 1200 °C and not violate the Gibbs Phase Rule.

Gavrish<sup>12</sup> has also studied the stability of calcia stabilized zirconia. His work indicated that the temperature of maximum destabilization is approximately 1400 °C. This, he determined, is also true for yttria stabilization, but for magnesia stabilization the temperature of maximum destabilization is only 1200 °C. He determined that yttria stabilized zirconia has the greatest stability and at the lowest mole

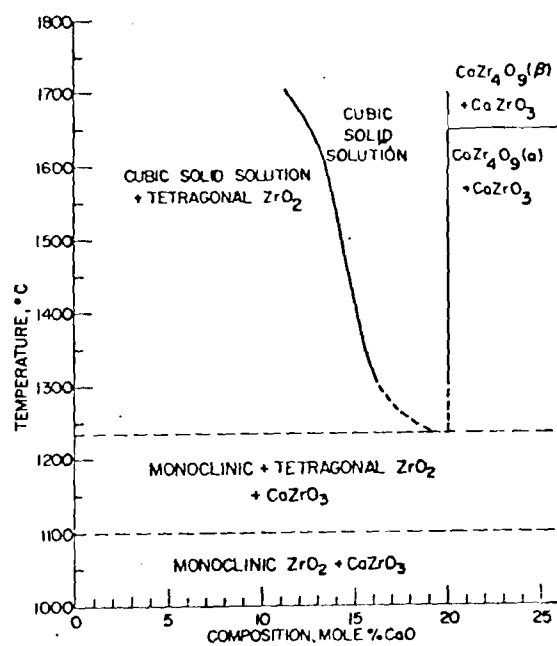
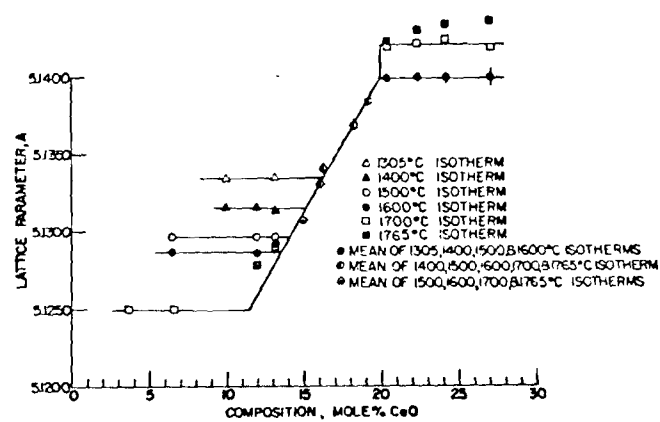


Figure 6. Phase Diagram and Lattice Parameter Data for the  $CaO-ZrO_2$  System after Garvie<sup>10</sup>

percent of the three additives, Table 2. Note that his studies extended only 60 hours. For raw materials he used a 99.7% pure zirconia and  $\text{CaZrO}_3$  which had been prepared from zirconia and calcium carbonate. Firing temperature was  $1750^\circ\text{C}$  for five hours and the samples were quenched. Phase analysis was by quantitative X-ray diffraction determination. Gavrish theorized that the reason for varying stability of different oxides is related to the size of the different ions, i.e., magnesium is the smallest and yttrium is the largest. The substitution of a small ion into the zirconia lattice increases the stresses more than the substitution of a larger ion more nearly the size of the zirconium ion. The activation energy of the diffusion process is thus decreased and the rate of decomposition is increased. Table 3 lists accepted values for various ionic radii.

Table 3. Ionic Crystal Radii<sup>13</sup>

Ion	$\text{Al}^{3+}$	$\text{Mg}^{2+}$	$\text{Zr}^{4+}$	$\text{Y}^{3+}$	$\text{Ce}^{4+}$	$\text{Ca}^{2+}$
Radius (A)	0.51	0.67	0.79	0.92	0.94	0.99

Gavrish also studied the stability of cubic zirconia heated in argon. With calcia and yttria stabilization he found no change in results from those samples heated in air. With magnesia he found that the lattice parameters changed, indicating a change in the structure of the solid solution. It indicated that some of the magnesia was vaporizing from the solid solution. At  $2300^\circ\text{C}$  the cubic structure remained only with a composition of 12 mole percent magnesia and the X-ray pattern indicated that there was considerable stress in the structure. The same

Table 2. Decomposition of the Solid Solutions during Heating in Air

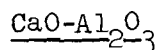
Concentration of the oxide additive in mole %		Destabilization at 1200 °C for 60 h.		Destabilization at 1400 °C for 60 h		Destabilization at 1600 °C for 60 h	
		Cubic ZrO <sub>2</sub> , in %	Monoclinic ZrO <sub>2</sub> in %	Cubic ZrO <sub>2</sub> , in %	Monoclinic ZrO <sub>2</sub> in %	Cubic ZrO <sub>2</sub> , in %	Monoclinic ZrO <sub>2</sub> in %
CaO	6	85	15	74	25	93	7
	12	100	0	98	2	100	0
	15	100	0	100	0	100	0
	20	100	0	100	0	100	0
MgO	12	20	80	45	55	100	0
	15	0	100	20	80	100	0
	20	0	100	10	90	100	0
Y <sub>2</sub> O <sub>3</sub>	8	98	2	88	12	91	9
	12	100	0	100	0	100	0
	15	100	0	100	0	100	0



samples were thermally cycled from 2000 °C and 2300 °C to room temperature to study destabilization. As in the other experiments, calcia and yttria stabilization proved to be completely stable but the magnesia stabilization was lost, particularly at 2300 °C, in a short period of time.

Magnesia has been used commercially to stabilize zirconia. However, at equilibrium the cubic solid solution was found not to exist below approximately 1375 °C. Thus, although magnesia stabilized zirconia may be prepared, it reverts to its unstabilized form with time above 1000 °C. Therefore, magnesia stabilization is not generally as useful as calcia stabilization.

The stabilization of zirconia by several other oxides has been studied.<sup>8, 12</sup> Many of the rare earths have been used, although on a commercial basis the cost is usually too high. Yttria and ceria are two oxides that may be used successfully. With ceria a different mechanism of stabilization is found. With the addition of greater than 15 mole percent ceria to zirconia the temperature of the monoclinic to tetragonal transformation is lowered below room temperature. There is still a cubic solid solution structure above 1000 °C to 2000 °C, depending on the composition, but it is not relevant to the stabilization problem, since the destructive transformation does not appear in normal usage.



The calcia-alumina binary has had much investigation. However, there has been considerable discrepancy about the actual phases that exist at equilibrium. Of particular importance to this study is the compound originally called  $\text{C}_3\text{A}_5$  and more recently determined to be  $\text{CA}_2$ . It

is apparent that earlier researchers obtained the same compound but incorrectly determined the stoichiometry. The calcium aluminates are of primary importance to the study of cements and therefore much work has been done with the various hydrated forms. This is generally not relevant to the calcia-alumina-zirconia ternary system.

As determined by Nurse, et.al.,<sup>14</sup> there are four binary compounds in the  $\text{CaO-Al}_2\text{O}_3$  system:  $\text{C}_3\text{A}$ ,  $\text{CA}$ ,  $\text{CA}_2$ , and  $\text{CA}_6$ . Lea and Desch<sup>15</sup> add  $\text{C}_{12}\text{A}_7$ , which Nurse stated is not an anhydrous compound and thus not properly part of the binary system. Nurse determined that thermodynamically a mixture of  $\text{CA}$  and  $\text{C}_3\text{A}$  is more stable than  $\text{C}_{12}\text{A}_7$  up to the melting point of  $\text{C}_{12}\text{A}_7$ , which is  $1392^\circ\text{C}$ . He was not able to prepare completely anhydrous  $\text{C}_{12}\text{A}_7$  and found that the formula is most accurately, at  $950^\circ\text{C}$ ,  $\text{C}_{12}\text{A}_7 \cdot \text{H}_2\text{O}$ . Thus it is most probable that  $\text{C}_{12}\text{A}_7$  is metastable.  $\text{C}_5\text{A}_3$  has also been suggested, possibly as a polymorph of  $\text{C}_{12}\text{A}_7$ . Nurse says that it is metastable. Berezhnoi<sup>1</sup> did show  $\text{C}_5\text{A}_3$  in his ternary diagram. Brooksbank<sup>16</sup> also considered  $\text{C}_{12}\text{A}_7$  to be a part of the binary system.  $\text{CA}_6$  has also been called  $\text{C}_3\text{A}_{16}$  as published by the American Ceramic Society<sup>17</sup>, but generally it has been accepted to have the formula  $\text{CA}_6$ . Figure 7 shows the complete phase diagram as determined by Lea and Desch.<sup>15</sup>

Nurse showed that the four calcium aluminates,  $\text{C}_3\text{A}$ ,  $\text{CA}$ ,  $\text{CA}_2$  and  $\text{CA}_6$ , melt incongruently, although  $\text{CA}$  and  $\text{CA}_2$  are only very slightly incongruent. If  $\text{CA}_2$  were considered to be  $\text{C}_3\text{A}_5$ , then it would have to be shown as a congruently melting compound.

An examination of X-ray data published by JCPDS<sup>18</sup> shows that  $\text{CA}_2$

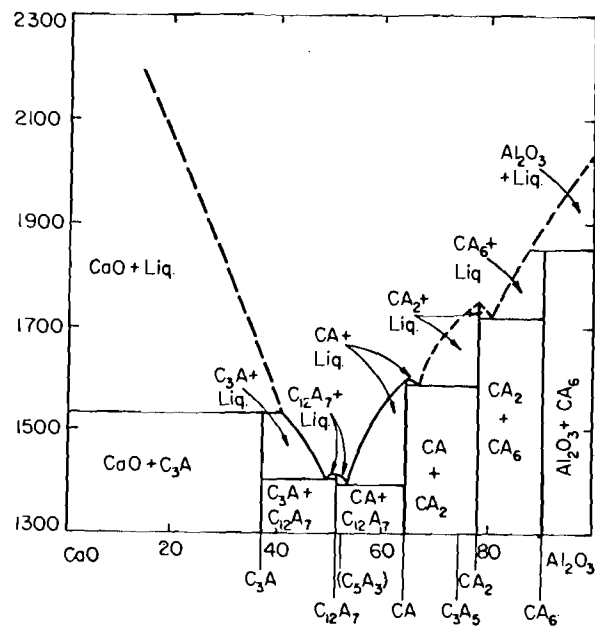


Figure 7. Phase Diagram of the CaO-Al<sub>2</sub>O<sub>3</sub> System  
as determined by Lea and Desch <sup>15</sup>

and  $C_3A_5$  have been listed with almost identical patterns. This could be understood if one accepted that the real compound is either one or the other, and the remaining stoichiometric formulation is really a solid solution. Brooksbank showed that the linear coefficient of thermal expansion is approximately the same, as determined by authors who claimed to have  $C_3A_5$  and as he determined for what he called  $CA_2$ . His value for thermal expansion was  $5.0 \times 10^{-6}/^{\circ}C$  from  $0^{\circ}C$  to  $800^{\circ}C$ . Rigby and Green<sup>19</sup> determined a value of  $3.5 \times 10^{-6}/^{\circ}C$  from  $100^{\circ}C$  to  $800^{\circ}C$ . They attempted to prepare  $CA_2$  from a stoichiometric mixture, but after heating to  $1530^{\circ}C$  they found the resultant mixture to be  $C_3A_5$  and free alumina, from an optical thin section examination. In their observation  $CA$  is the most easily prepared of the calcium aluminates and it is for that reason, they explained, that one could obtain excess  $CA$  when starting from a  $CA_2$  stoichiometry. They stated very strongly that the equilibrium state is  $C_3A_5$ .

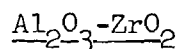
Goldsmith<sup>20</sup> prepared samples from the melt and found that when  $CA_2$  stoichiometry was used as the starting mixture, that he saw optically only a single phase. When  $C_3A_5$  stoichiometry was used, he saw two phases. Firing was done at  $1500^{\circ}C$ . Goldsmith's work was done to confirm earlier work of Tavisci<sup>21</sup> and came to similar conclusions. Wisnyi<sup>22</sup> did considerable work studying  $CA_2$  and it is his X-ray information that is published by JCPDS. Wisnyi determined that the density of  $CA_2$  is  $2.86 \text{ g/cc}$ . Table 4 shows a comparison between the results of X-ray indexing obtained by Wisnyi and later research done by Baldock.<sup>23</sup> There are no significant disagreements, but enough minor discrepancies to question if the structure

Table 4. Powder Diffraction Data for  $\text{CaO} \cdot 2\text{Al}_2\text{O}_3$ <sup>23</sup>

WIGNYI	(ASTM 7-0012)	PRESENT WORK				
d	$1/I_{100}$	h k l	$d_{\text{obs}}$	$d_{\text{calc}}$	$1/I_{100}$	
6.193	20	1 1 0	7.196	7.2091	$\frac{1}{2}$ B	
		2 0 0	6.161	6.1642	7	
		1 1 -1	4.607	4.6101	3	
4.439	75	0 2 0	4.4416	4.4437	54	
		1 1 1	3.913	3.9164	1	
		3 1 0	3.727	3.7302	$\frac{1}{2}$	
3.609	20	2 2 0	3.604	3.6046	20	
3.520	100	3 1 -1	3.503	3.5020	100	
3.372	5	0 2 1	3.379	3.3801	2	
3.239	20	2 2 -1	3.234	3.2326	7	
3.079	55	4 0 0	3.0840	3.0823	29	
2.882	50	1 3 0	2.882	2.8806	20	
2.760	60	2 2 1	2.753	2.7526	27	
2.717	55	3 1 1	2.712	2.7120	23	
		0 0 2		2.6033		
2.607	85	1 1 -2	2.5989	2.5939	60	
		1 3 -1		2.5965		
2.531	25	4 2 0	2.534	2.5327	13	
		3 1 -2	2.462	2.4621	4	
		1 3 1	2.452	2.4509	3	
2.436	35	5 1 -1	2.436	2.4351	17	
		3 3 0	2.404	2.4032	3	
		4 0 -2	2.350	2.3556	$\frac{1}{2}$ B	
2.350	35	1 1 2	2.325	2.3255	10	
		0 4 0	2.222	2.2212	1	
2.208	40	2 0 2	2.181	2.1815	7	
		2 4 0		2.0703		
		4 2 1	2.0807	2.0894	2	
		4 2 -2	2.0827	2.0813	2	
		5 1 -2	2.0678	2.0676	6	
2.059	55	6 0 0	2.0539	2.0519	14	
		3 3 1		2.0531		
		0 4 1	2.044	2.0437	4	
		2 4 -1	2.0035	2.0097	2	
2.003	40	1 3 -2	2.0001	2.0004	7	
		5 1 1	1.9634	1.9636	5	
1.960	25	2 2 2	1.9592	1.9593	5	
1.941	30	3 3 -2	1.9379	1.9381	3	
		6 2 -1		1.9251		
		5 3 -1		1.9218		
1.904	25	6 0 -2	1.9049	1.9052	7	
		5 3 0	1.8956	1.8953	5	
1.875	40	1 3 2	1.8683	1.8693	5	
1.801	30	4 4 -1	1.8007	1.8007	11	
1.760	20	3 1 -3	1.7615	1.7619	10	
		6 2 -2	1.7502	1.7511	$\frac{1}{2}$	
		7 1 0		1.7277		
		5 3 -2	1.7277	1.7272	$\frac{1}{2}$	
		2 4 -2	1.7140	1.7147	$\frac{1}{2}$	
		1 5 -1	1.6680	1.6682	5	
		7 1 -2	1.6760	1.6771	$\frac{1}{2}$	
		5 3 1	1.6646	1.6652	1	
		1 5 1	1.6461	1.6462	$\frac{1}{2}$	
		5 1 -3	1.6372	1.6374	1	
		4 2 2	1.6306	1.6309	4	
1.628	30	6 2 1	1.6247	1.6249	5B	
		4 2 -3		1.6244		
		4 4 1	1.6204	1.6202	6	
		3 5 -1	1.6112	1.6109	2	
		7 3 -1	1.5623	1.5624	2B	
1.556	20	2 4 2	1.5570	1.5567	3	
		5 1 2	1.5523	1.5516	5	
		8 0 0		1.5405		
		6 4 -1		1.5397		
1.537	30	3 3 -3	1.5364	1.5368	12	
		1 3 -3	1.5334	1.5335	12	
		7 1 1		1.5155		
1.511	25	8 2 -1	1.5145	1.5144	4	
		7 3 0		1.5140		
		6 4 0	1.5021	1.5027	1	
		0 6 0		1.4813		
1.475	5	6 2 -3	1.4808	1.4807	4	
		2 2 3	1.4651	1.4692	1	
		3 5 -2	1.4603	1.4606	1	
		8 2 0	1.4561	1.4561	1	
		8 2 -2	1.4521	1.4524	2	
		5 3 -3		1.4521		
		1 3 3	1.4445	1.4439	$\frac{1}{2}$	
		2 6 0	1.4401	1.4403	2	
		1 5 2	1.4305	1.4314	1	
		0 6 1	1.4248	1.4248	2	
		9 1 -1		1.4133		
		2 6 -1		1.4131		
1.403	5	2 4 -3	1.4054	1.4054	2	
1.372	45	6 4 1	1.3729	1.3727	9B	
		4 4 -3		1.3725		
		7 3 1	1.3648	1.3651	1	
		2 6 1		1.3646		
		2 0 -4	1.3560	1.3560	1	
		6 2 2		1.3560		
		9 1 0	1.3539	1.3540	2	
		4 0 -4	1.3479	1.3482	$\frac{1}{2}$	
1.337	25	4 6 0	1.3350	1.3352	5	
1.319	20					

of  $CA_2$  is fixed. In preparing  $CA_2$  with a CA impurity of only 0.5 weight percent Baldock used dried analar calcite and gibbsite mixed stoichiometrically and fired for five hours at  $1400^\circ\text{C}$  to  $1450^\circ\text{C}$ . He used a Phillips diffractometer for X-ray analysis, whereas Wisnyi used a powder camera.

No one has suggested that both  $CA_2$  and  $C_3A_5$  exist in equilibrium or that the structure exists as a solid solution. Since the published X-ray patterns are similar, perhaps this possibility should be considered. The possibility of hydrated products should also be considered, since in other calcium aluminates, hydrates are important phases. The preparation of pure samples is apparently a problem which may also hinder an accurate understanding of the structure and properties of  $CA_2$ .



The  $Al_2O_3$ - $ZrO_2$  binary system has no compounds. If Dietzel's rules concerning cation field strength are considered, this is to be expected. By Dietzel's calculations<sup>24</sup> the field strength of Al is 0.96 and that of Zr is 0.77. Since the difference is only 0.19, less than the 0.3 difference required for compound formation, it is predicted that no stable compound can be formed between the oxides of zirconium and aluminum.

Hennicke<sup>25</sup> found that alumina can be used to partially stabilize zirconia. He mixed  $Zr(OH)_4$  and  $Al(OH)_3$  together and fired at temperatures from  $1200^\circ\text{C}$  to  $1600^\circ\text{C}$ . He also experimented with oxide powders sintered at  $1600^\circ\text{C}$ . Approximately one mole percent of alumina entered the zirconia lattice. This solution caused part of the zirconia to remain in the tetragonal form at room temperature. After several of his samples

were ground, they contained more monoclinic zirconia than before grinding, which indicated that there was also a mechanical stabilization. Of practical importance was his discovery that on repeated thermal cycling, mixtures of more than ten mole percent  $\text{Al}_2\text{O}_3$  became brittle. Another important observation was that the corundum structure absorbed part of the stress that was caused by the density change when the transition from tetragonal to monoclinic zirconia occurred. Hennicke also observed that the temperature at which the tetragonal to monoclinic transition occurred was lowered as the percentage of alumina was increased, when a cooling rate of  $10^\circ\text{C}$  per minute was maintained.

#### The Disappearing Phase Method of Phase Diagram Determination

The disappearing phase method<sup>26</sup> uses quantitative X-ray diffraction analysis to determine phase boundaries on a phase diagram. Several samples of differing phase compositions are analyzed by X-ray diffraction and a weight ratio or a mole ratio of two phases for each composition is determined. The relationship between weight ratio or mole ratio of two phases and the phase composition is linear so that an extrapolation may be made to determine at what composition the phase ratio becomes zero. This determines the position of the phase boundary. The method can be used in a ternary system if the amount of one component is held constant and the variation of the remaining two components is observed. For solid solution endpoints which vary in composition with temperature, the composition at constant temperatures may be evaluated by this technique.

## CHAPTER III

### PROCEDURE

Forty-six samples were prepared with a minimum of 55 mole percent zirconia for determining the phase diagram of the high zirconia region of the calcia-alumina-zirconia ternary system. Using quantitative and qualitative phase analysis and lattice parameter information determined from X-ray diffraction, the phase diagram was determined by the disappearing phase technique. The raw materials used were TAM CP zirconia of greater than 99.0% purity and 1.4 micron particle size, Alcoa A-16 Superground alumina, and Fisher Scientific Certified calcium carbonate, 99.9% pure. Optical analysis was made with a metallographic microscope to confirm the X-ray results. Three compositions were chosen to be fired for up to 2000 hours to determine stability of the phases. X-ray analysis was used to determine the phase stability.

#### Sample Preparation

Compositions for four separate series of firings were chosen in the high zirconia region of the ternary system. Tables 5, 6, 7, and 8 show the compositions which were chosen for the four series of samples. For series 1, series 2, and series 4, all three components were weighed out for each composition and each was mixed thoroughly in an alumina automatic mortar and pestle for 30 minutes in acetone. Several pellets of each composition were pressed using a Carver hydraulic laboratory press to 5000 psi. in a stainless steel die 0.75 inches in diameter lubricated



Table 5. Composition of Series 1

Sample Number	ZrO <sub>2</sub> mole %	Al <sub>2</sub> O <sub>3</sub> mole %	CaO mole %
1-1	64.0	20.0	16.0
1-2	68.0	20.0	12.0
1-3	72.0	20.0	8.0
1-4	69.6	13.0	17.4
1-5	74.0	13.0	13.0
1-6	78.3	13.0	8.7
1-7	76.2	4.8	19.0
1-8	80.9	4.8	14.3
1-9	85.7	4.8	9.5

Table 6. Composition of Series 2

Sample Number	ZrO <sub>2</sub> mole %	Al <sub>2</sub> O <sub>3</sub> mole %	CaO mole %
2-1	55.0	25.0	20.0
2-2	57.5	25.0	17.5
2-3	60.0	25.0	15.0
2-4	62.5	25.0	12.5
2-5	65.0	25.0	10.0
2-6	60.0	20.0	20.0
2-7	62.5	20.0	17.5
2-8	65.0	20.0	15.0
2-9	67.5	20.0	12.5
2-10	70.0	20.0	10.0
2-11	65.0	15.0	20.0
2-12	67.5	15.0	17.5
2-13	70.0	15.0	15.0
2-14	72.5	15.0	12.5
2-15	75.0	15.0	10.0
2-16	70.0	10.0	20.0
2-17	72.5	10.0	17.5
2-18	75.0	10.0	15.0
2-19	77.5	10.0	12.5
2-20	80.0	10.0	10.0
2-21	75.0	5.0	20.0
2-22	77.5	5.0	17.5
2-23	80.0	5.0	15.0
2-24	82.5	5.0	12.5
2-25	85.0	5.0	10.0

Table 7. Composition of Series 3

Sample Number	ZrO <sub>2</sub> mole %	Al <sub>2</sub> O <sub>3</sub> mole %	CaO mole %
3-1	64.0	20.0	16.0
3-2	68.0	20.0	12.0
3-3	72.0	20.0	8.0
3-4	69.6	13.0	17.4
3-5	74.0	13.0	13.0
3-6	78.3	13.0	8.7
3-7	76.2	4.8	19.0
3-8	80.9	4.8	14.3
3-9	85.7	4.8	9.5
3-10	80.0	0	20.0
3-11	85.0	0	15.0
3-12	90.0	0	10.0

Table 8. Composition of Series 4

Sample Number	ZrO <sub>2</sub> mole %	Al <sub>2</sub> O <sub>3</sub> mole %	CaO mole %
4-1	22.0	33.0	45.0
4-2	40.0	20.0	40.0
4-3	50.0	12.0	38.0
4-4	60.0	12.0	28.0

with stearic acid in acetone. No binder was found to be required since the pellets held together and no laminations appeared. The thickness of the pellets was approximately 0.25 inches.

Series 1 pellets were calcined at  $1200^{\circ}\text{C}$  in a silicon carbide resistance furnace for 3.5 hours and fired to  $1700^{\circ}\text{C}$  in a gas fired furnace for three hours. The pellets were allowed to slow cool in the furnace before being removed.

Series 2 and series 4 samples were calcined as powders at  $1300^{\circ}\text{C}$  for 16 hours. The calcined powders were remixed in the automatic mortar and pestle and pressed as pellets. The pellets were sintered at  $1500^{\circ}\text{C}$  in a silicon carbide resistance furnace for 20 hours. Cooling was controlled at a rate of one degree per minute. After the series 2 samples had been analyzed as described below, they were all reloaded into the furnace and refired to  $1500^{\circ}\text{C}$  for 20 hours. After 20 hours at  $1500^{\circ}\text{C}$  they were rapidly removed and quenched in water.

For series 3 a different method of preparation was used. The correct proportions of calcia and zirconia were mixed in the automatic mortar and pestle for one hour. These mixtures were calcined as powders at  $1400^{\circ}\text{C}$  for 16 hours. After this stabilized zirconia was prepared, alumina of the required proportions was added, mixed, and the powder pressed into pellets as described above. These pellets were fired at  $1500^{\circ}\text{C}$  for 25 hours and slow cooled at one degree per minute.

For the determination of the long term phase stability, three compositions were chosen as shown in Table 9. Four kilograms of each composition was prepared. Each batch was mixed in a polyethylene jar with

alumina balls for 24 hours and the powder was calcined at 1200 °C for 20 hours. The calcined powder was examined by X-ray diffraction to determine if a stable ratio of cubic to monoclinic zirconia had been achieved. The batches were reground in the polyethylene jars and recalcined twice before a constant cubic to monoclinic zirconia ratio was obtained. One hundred pellets of each composition were prepared and fired to 1550 °C for 24 hours. Fifty were placed in an electric resistance furnace and brought up to 900 °C and 50 were placed in a second furnace and brought up to 1300 °C. All of the pellets were placed on stabilized zirconia plates which were stacked for maximum use of the furnace space. At 200 hours two pellets of each composition at each temperature were removed. The furnace door was opened and the required pellets removed as quickly as possible and thus air cooled, without affecting the remaining pellets. This procedure was followed successively at each 200 hours up to 2000 hours. At 1000 hours both furnaces were cooled to room temperature at one degree per minute to examine the contents and to remove other samples not involved with the phase stability work. Both furnaces were reheated at the same one degree per minute to 900 °C and 1300 °C respectively for the second one thousand hours.

Table 9. Composition of Batches for Long Term Firing

Batch Designation	ZrO <sub>2</sub> mole %	Al <sub>2</sub> O <sub>3</sub> mole %	CaO mole %
A	77.5	10.0	12.5
B	68.0	17.5	14.5
C	57.5	25.0	17.5

### Qualitative X-Ray Analysis

For all of the X-ray work a Philips Electronics diffractometer with a solid state scintillation detector and Ortec single channel amplifier, rate meter, and associated electronics with output displayed on a Bristol ten millivolt recorder was used. This unit employed nickel filtered Cu K $\alpha$  radiation and the X-ray tube was operated at 45 kv and 25 ma. Geometrically the X-ray beam had a 4 $^{\circ}$  take off angle, a 1 $^{\circ}$  divergence slit, a 1 $^{\circ}$  scatter slit, and a 0.003 inch receiving slit. All scans were run at one degree per minute unless otherwise noted. Powder samples were back loaded into an aluminum holder and packed onto a frosted glass slide to give a random surface for scanning. For identification of phases, scans were made from  $2\theta = 14^{\circ}$  to  $2\theta = 70^{\circ}$ . Comparison was made to the Joint Committee on Powder Diffraction Standards Powder Diffraction File to determine exactly which phases were present as each line in the X-ray scan was accounted for.

One pellet of each of the series 1 compositions was crushed and ground to approximately -325 mesh in the automatic mortar and pestle for X-ray analysis. For the remaining series of samples it was determined that X-raying the surface of the pellets was satisfactory and less time consuming than crushing the pellets, which were very difficult to grind. The surface of each pellet was ground slightly with silicon carbide paper of 180 and 320 grit to insure a flat surface which would fit reproducibly into the sample holder clip of the goniometer.

### Quantitative X-Ray Analysis

Azaroff<sup>27</sup> showed that for polymorphic modifications of the same

composition (such as cubic zirconia and monoclinic zirconia) the weight ratio of the two polymorphs in a mixture is directly proportional to the ratio of the two peak heights, one generated by each crystalline structure. He recommended preparing a graph to relate intensity ratios to composition. In order to follow this procedure, samples of pure cubic zirconia (15 mole percent CaO) and of pure monoclinic zirconia were mixed together in the automatic mortar and pestle to have weight ratios (cubic: monoclinic) of 4:1, 1:1, and 1:4. An X-ray scan was made of each composition from  $2\theta = 27^\circ$  to  $2\theta = 32^\circ$ . For the cubic phase the major peak of 100% intensity corresponding to the  $111$  plane at a  $d$  spacing of 2.92 Å was chosen. Two peaks from the monoclinic phase were chosen to compare to the cubic peak in order that two separate weight ratios might be determined. The values reported are an average of the two weight ratios. Both monoclinic peaks were close to the cubic peak: one corresponded to the  $11\bar{1}$  plane at  $d$  spacing 3.16 Å and the other to the  $111$  plane at  $d$  spacing 2.834 Å. Ratios of peak intensity for the three standard samples were determined and a graph was constructed to be used for determining weight ratios for all of the samples, Figure 8. The equations for the two lines are as follows:

$$Y_1 = 2.027 X_1 + 0.054 \qquad Y_2 = 3.082 X_1 + 0.105 \qquad (1)$$

where  $Y_1$  is  $\frac{\text{intensity of cubic } 111 \text{ peak}}{\text{intensity of mono } 111 \text{ peak}}$

$X_1$  is  $\frac{\text{weight cubic}}{\text{weight mono}}$

$Y_2$  is  $\frac{\text{intensity of cubic } 111 \text{ peak}}{\text{intensity of mono } 11\bar{1} \text{ peak}}$  .

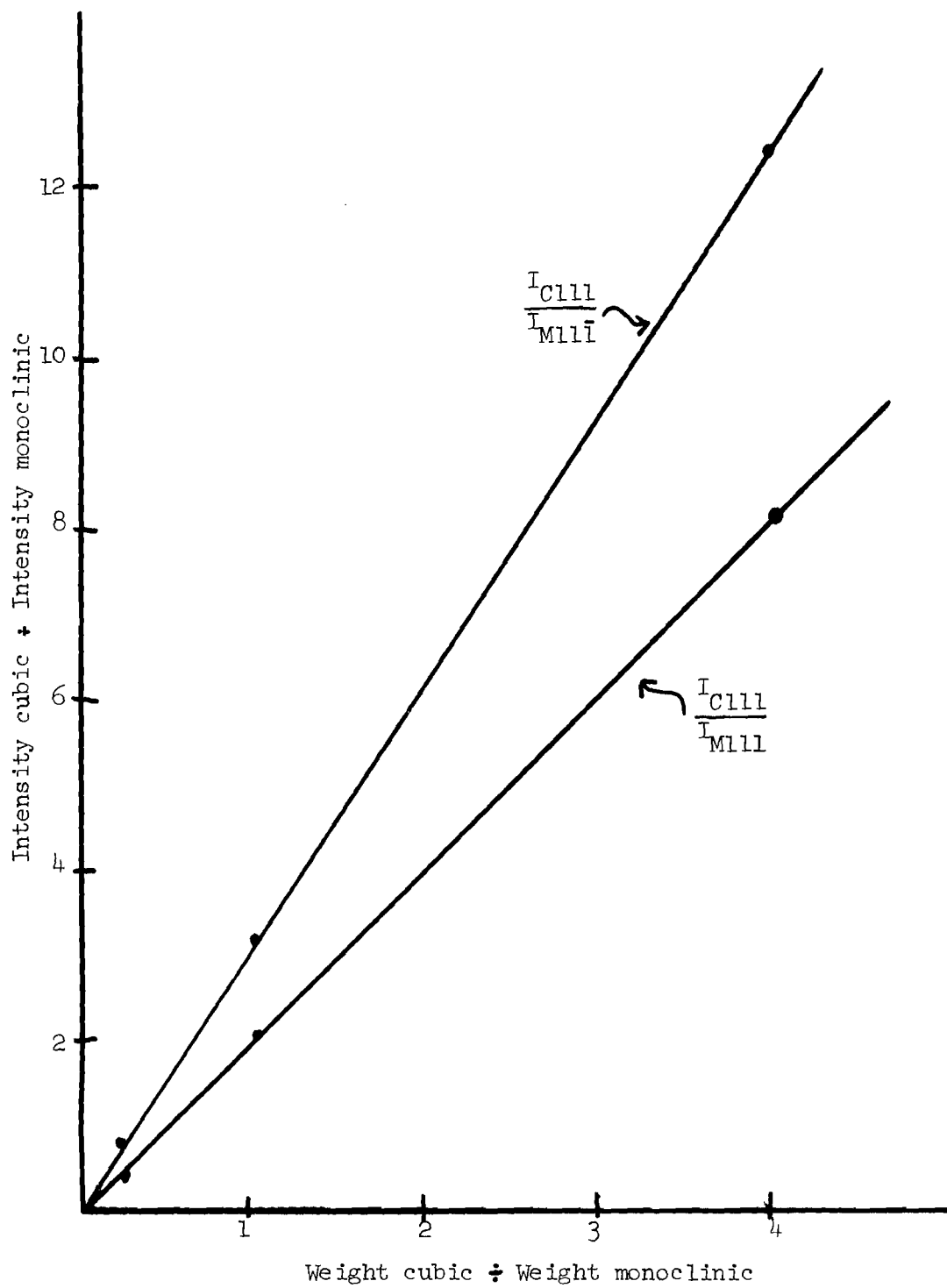


Figure 8. Relationship between Peak Intensities and Weight Ratios of Cubic to Monoclinic Zirconia



For each of the samples which had both cubic zirconia and monoclinic zirconia, a determination of the weight ratio was made from these equations. The average value determined from the two ratios was calculated.

### Lattice Parameter Measurement

Lattice parameter values were determined for the cubic zirconia phase in samples A, B, and C at 0, 200, 1000, and 2000 hours at 900 °C and 1300 °C, and also at 400 hours for the 1300 °C samples. X-ray scans were made at one half degree per minute from  $2\theta = 13^\circ$  to  $2\theta = 135^\circ$ . From information in the JCPDS files relating to  $\underline{d}$  spacing in crystalline planes accurate values for the  $\underline{a}$  parameter were determined by using the following formula:

$$\frac{1}{\underline{d}^2} = \frac{h^2}{a^2} + \frac{k^2}{a^2} + \frac{l^2}{a^2} \quad (2)$$

where h, k, l are the indices of the plane

$\underline{a}$  is the lattice parameter (in a cubic structure all three dimensions are the same)

$\underline{d}$  is the interplanar spacing.

Bragg's Law gives the relationship between  $\underline{d}$  and  $\theta$ , the angle of diffraction in terms of  $\lambda$ , the wavelength of radiation used, in this case 1.5418 Å for Cu K $\alpha$ :

$$n\lambda = 2d \sin\theta \quad (3)$$

where n is an integer.

In order to determine the actual lattice parameter  $\underline{a}$  for any particular sample, an extrapolation must be made. For this  $\underline{a}$  was plotted versus  $\cos\theta\cot\theta$  and this curve was extrapolated to the point where

$\cos\theta\cot\theta$  is zero. This value of  $\underline{a}$  at  $\cos\theta\cot\theta = 0$  is the true lattice parameter for the sample. For actually determining this intercept a PDP 8 computer which had been programmed to do a least squares regression was used to give an accurate estimate of the lattice parameter. The program also gave a value for the correlation coefficient of the estimate, an indication of the closeness of all of the points to the line. Figure 9 gives an example of one extrapolation that was made.

An attempt at extrapolation by relating  $\underline{a}$  to  $\cos^2\theta$  was also made, but this was not accurate compared to the extrapolation of the  $\underline{a}$  versus  $\cos\theta\cot\theta$  graph. Generally the  $\underline{a}$  versus  $\cos\theta\cot\theta$  extrapolation works better than the  $\underline{a}$  versus  $\cos^2\theta$  extrapolation when the X-ray beam is aligned so that it is not exactly aimed at the plane of the surface of the sample. This misalignment does not particularly affect the accuracy of lattice parameter determinations when the  $\cos\theta\cot\theta$  extrapolation is used.

#### Quantitative Optical Determination

One pellet of each sample was prepared for optical examination by mounting in Quickmount, a self-setting resin type of translucent plastic commonly used for metallographic work. Each pellet was wet polished successively on 180, 320, and 600 grit silicon carbide grinding paper. Final polishing was done with a Syntron automatic vibrating polisher. One micron diamond paste with water as a lubricant was used on a nylon cloth surface. Twenty-four hours of polishing on this device was required to obtain a satisfactory surface on each sample. Each sample was

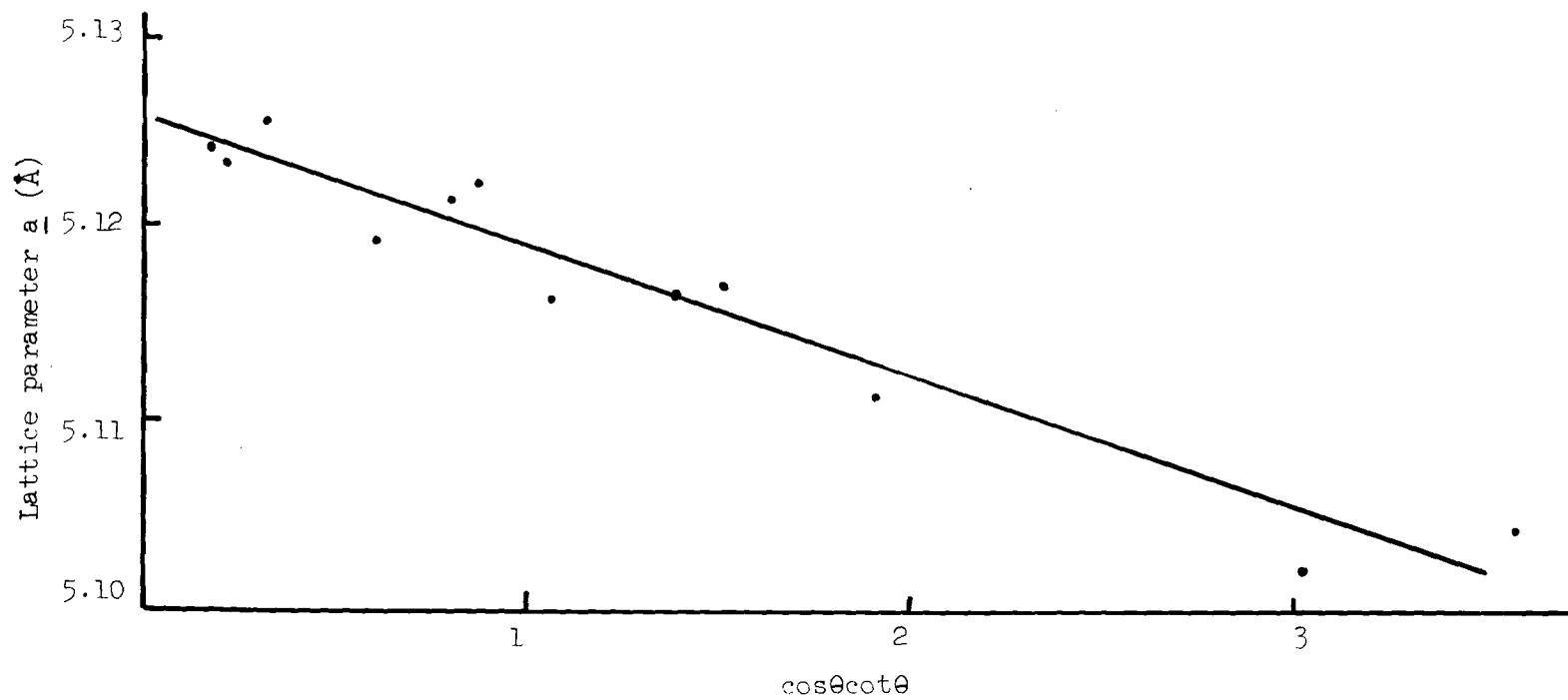


Figure 9. Lattice Parameter Extrapolation for Composition A before Heat Treatment

photographed using a Polaroid attachment on a Reichert Metallographic Microscope at 600x in reflected light and bright field. From these photographs the volume fraction of each phase was determined by a systematic point counting technique, which is described in Appendix A.

#### Density Determination

The bulk density of each sample was determined by a technique involving immersion in kerosene. Each sample was weighed on an accurate balance. For 24 hours all of the samples were soaked in kerosene in order to fill all of the pores. After soaking, each sample was weighed again while suspended on a wire mesh hanger in a beaker of kerosene, insuring that no air bubbles remained attached to the pellet. Density was calculated from the following formula:

$$\text{density} = \frac{\text{d.w.}}{\text{d.w.} - \text{s.w.}} \times \text{s.g.} \quad (4)$$

where d.w. is the dry weight

s.w. is the suspended weight

s.g. is the specific gravity of the kerosene.

## CHAPTER IV

## RESULTS AND DISCUSSION OF RESULTS

From qualitative and quantitative X-ray analysis of fired samples, a phase diagram was determined for the zirconia rich corner of the  $\text{CaO-Al}_2\text{O}_3\text{-ZrO}_2$  ternary system. Comparison of the analysis of samples fired at  $1500^\circ\text{C}$  for 20 hours and for an additional 20 hours was made to prove that the derived diagram was indeed an equilibrium diagram. From optical analysis of the samples, it was determined that there was less than 0.5 mole percent alumina solubility in zirconia. Optical and X-ray analysis indicated the possibility of solid solution of the compound known as  $\text{CA}_2$  since the stoichiometry at  $1500^\circ\text{C}$  was more nearly  $\text{C}_3\text{A}_7$ . Long term changes in calcia solubility in cubic zirconia were studied for up to 2000 hours in samples which had been sintered at  $1550^\circ\text{C}$ . These studies were made at  $900^\circ\text{C}$  and  $1300^\circ\text{C}$ . Solubility changes were measured by quantitative X-ray analysis and by measuring changes in lattice parameter dimensions of cubic zirconia. Evaluation of several samples fired at  $1700^\circ\text{C}$  indicated that melting had occurred and that equilibrium was not attained.

Qualitative Phase Diagram at  $1500^\circ\text{C}$ 

Using the phases present as obtained from qualitative X-ray diffraction analysis of series 2 and series 3 samples, Appendix B, estimated Alkemade lines were drawn to divide the three phase regions which were obtained, Figure 10. The crystalline phases found in each sample after

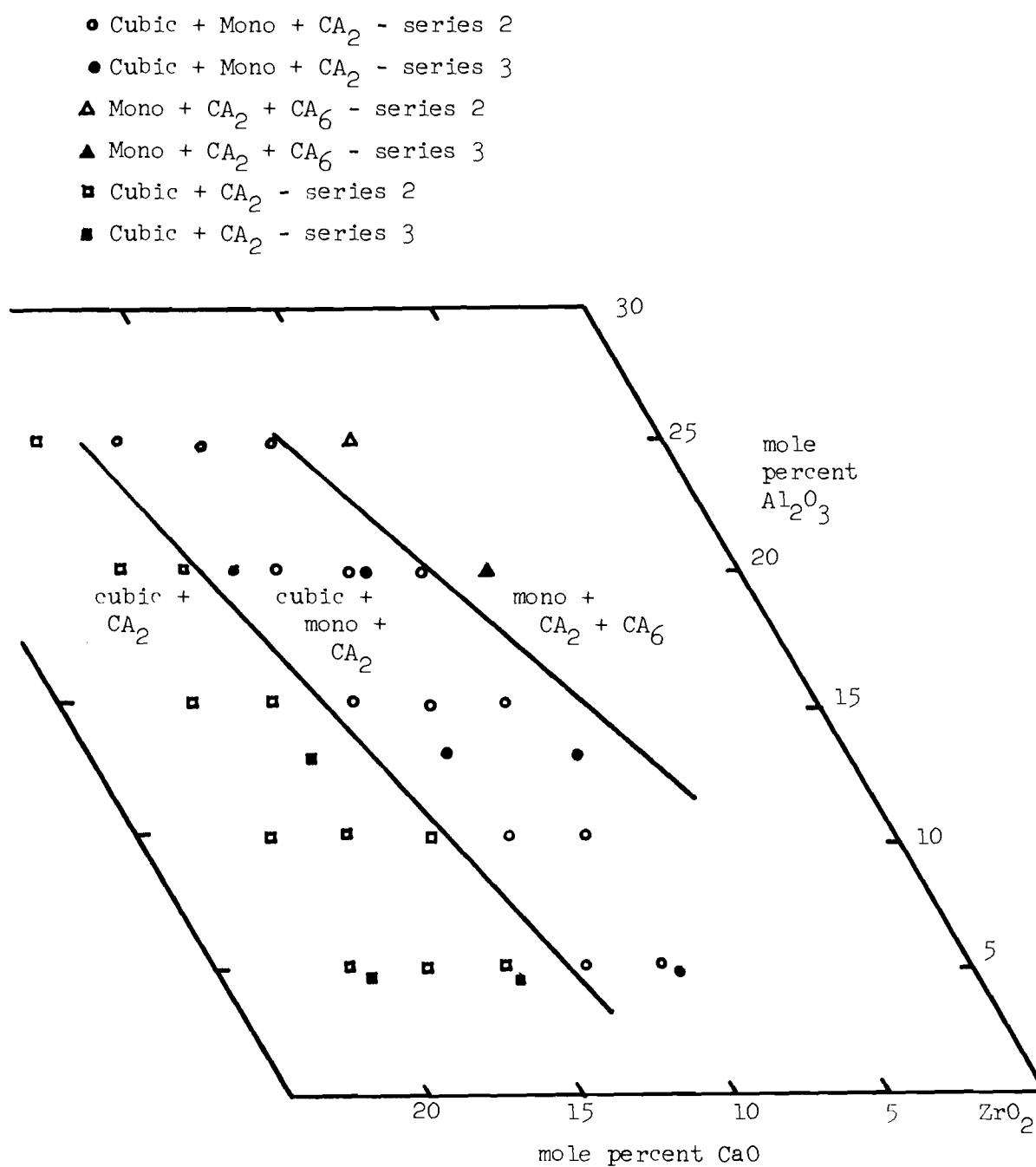


Figure 10. Phase Analysis of Samples Slow-Cooled from 1500 °C

firing for 20 hours and slow cooling were identical to those found in the samples after firing for 40 hours and water quenching. From these qualitative results at 1500 °C, equilibrium appeared to have been obtained, but the question was approached more rigorously in the following section. From phase equilibria theory, a two phase region should divide the  $CA_2 + CA_6 + \text{monoclinic zirconia}$  area from the  $CA_2 + \text{cubic zirconia} + \text{monoclinic zirconia}$  area. No sample with only  $CA_2 + \text{monoclinic zirconia}$  was found, but it is certainly reasonable that the region is almost the width of a line and that no composition was chosen for analysis that fell exactly on that line.

#### Calculation of Alkemade Lines and Verification of Equilibrium at 1500 °C

In order to calculate the exact position of the  $CA_2$  - cubic and  $CA_2$  - monoclinic Alkemade lines, the cubic and monoclinic zirconia peak heights from the X-ray scan for each sample were used to determine quantitatively the weight ratio of cubic zirconia to monoclinic zirconia in each sample that contained both phases. These weight ratio values were converted to a mole basis to be compatible with the remaining quantitative information which was in mole percent. For conversion the composition of cubic zirconia was assumed to be 13 mole percent CaO and 87 mole percent zirconia. No significant variation in the values would have been obtained if a composition for cubic zirconia of 16 mole percent calcia, which is also suggested in the literature, had been used. The assumption was also made that monoclinic zirconia was 100 percent zirconia. This assumption is justified since no more than one mole percent calcia exists in monoclinic zirconia, from published phase diagrams. The cubic zirconia

to monoclinic zirconia Alkemade line must also be assumed to lie at a constant mole percent alumina. With these assumptions made, it may be stated that the ratio of cubic zirconia to cubic plus monoclinic zirconia varies linearly from 0 to 1 on any constant mole percent alumina line across the compatibility triangle. Thus the exact position of the Alkemade lines may be determined from quantitative X-ray data.

To predict the two Alkemade lines intersecting at  $CA_2$  and bounding the cubic + monoclinic +  $CA_2$  phase region, the cubic : (cubic + monoclinic) ratio was plotted versus the mole percent calcia of samples containing a constant mole percent of alumina, Figure 11. These relationships were then extrapolated using a linear regression program to determine the endpoints, which are points on the Alkemade lines. The calcia contents at 0 percent and 100 percent cubic at various alumina contents were used to calculate, again by the linear regression method, the equations of the two Alkemade lines. Appendix C contains the data from measuring cubic to monoclinic ratios and the calculated mole basis.

Initially, equations for the lines for the slow cooled series 2 samples were determined as follows:

$$\% \text{ CaO at 100 \% cubic} = 0.29 (\text{Al}_2\text{O}_3) + 11.09 \quad (5)$$

$$\% \text{ CaO at 0 \% cubic} = 0.56 (\text{Al}_2\text{O}_3) + 2.58. \quad (6)$$

In order to prove that equilibrium had been reached, the same procedure for calculating the two Alkemade lines was performed for the series 2 samples after they had been refired for a second 20 hours and quenched. The equations determined for these two lines were as follows:



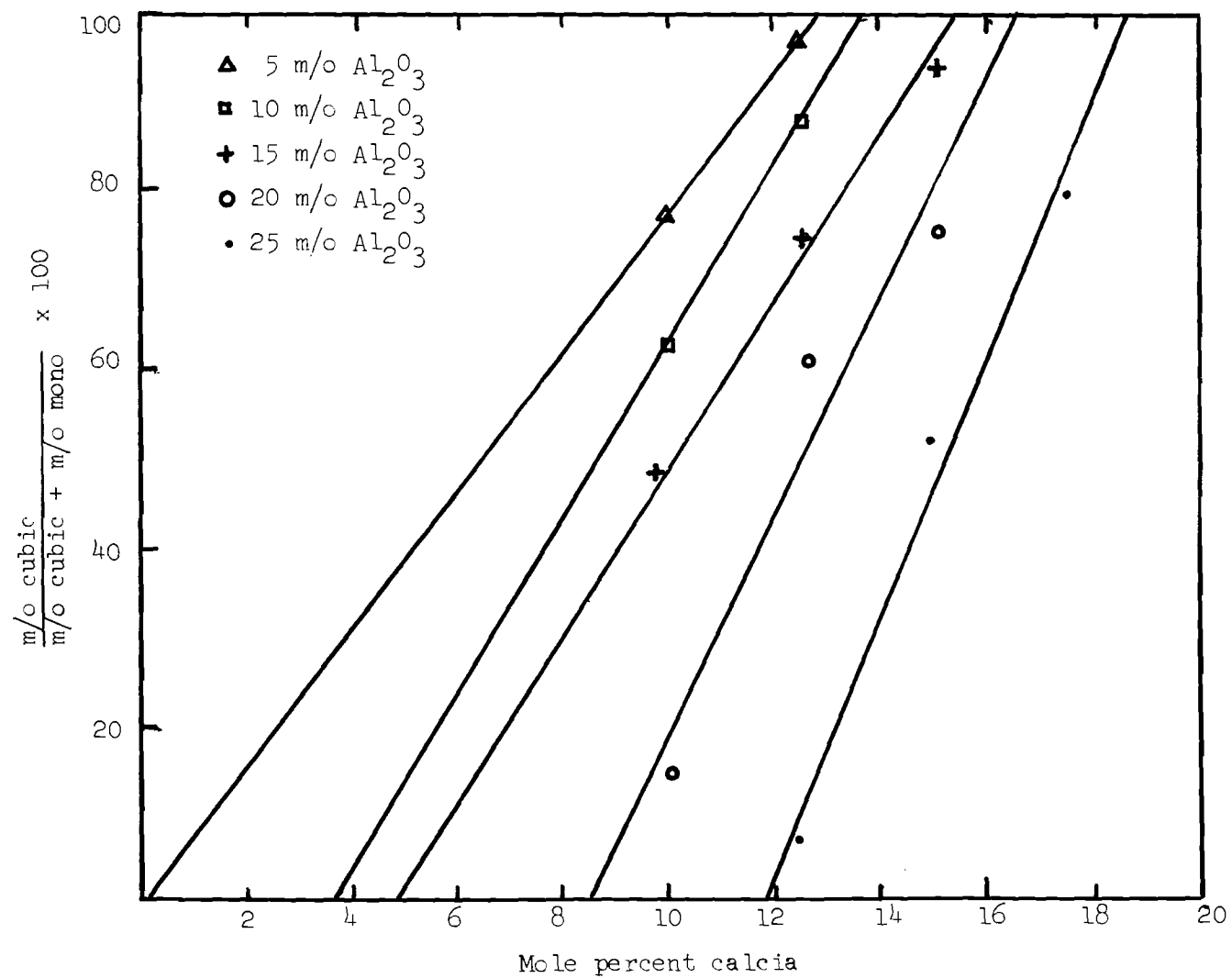


Figure 11. Extrapolation of Calcia Content to 0% and 100 % Cubic Zirconia at Fixed Alumina Contents

$$\% \text{ CaO at 100 \% cubic} = 0.26 (\text{Al}_2\text{O}_3) + 11.8 \quad (7)$$

$$\% \text{ CaO at 0 \% cubic} = 0.53 (\text{Al}_2\text{O}_3) - 2.25 . \quad (8)$$

As can be seen in Figure 12, within the limits of experimental error, a close agreement exists between the Alkemade lines determined at 20 and 40 hours. This agreement demonstrates that the slow cooled series 2 samples had reached equilibrium after being fired for 20 hours, since there was no change after a second 20 hour firing and quenching.

Examination of the series 3 quantitative results indicated that there was good agreement with the series 2 results. This observation indicated that the method of preparation did not affect the resulting phases, as should be expected if equilibrium had been reached. Thus alumina may be added to stabilized zirconia with the same results as mixing calcia, alumina, and monoclinic zirconia in one operation.

In order to obtain the most accurate lines, since all three sets of data (series 2 slow cooled, series 2 quenched, and series 3) were in agreement, the cubic to monoclinic ratio for all of the samples was used to calculate the two Alkemade lines, Figure 13. The equation of the  $\text{CA}_2$ -cubic zirconia line was as follows:

$$\% \text{ CaO at 100 \% cubic} = 0.28 (\text{Al}_2\text{O}_3) + 11.58, \quad (9)$$

and the equation of the  $\text{CA}_2$  - monoclinic zirconia line was as follows:

$$\% \text{ CaO at 0 \% cubic} = 0.48 (\text{Al}_2\text{O}_3) - 0.89 . \quad (10)$$

#### Alumina Solubility in Cubic and Monoclinic Zirconia

The solid solution region along the calcia-zirconia binary line

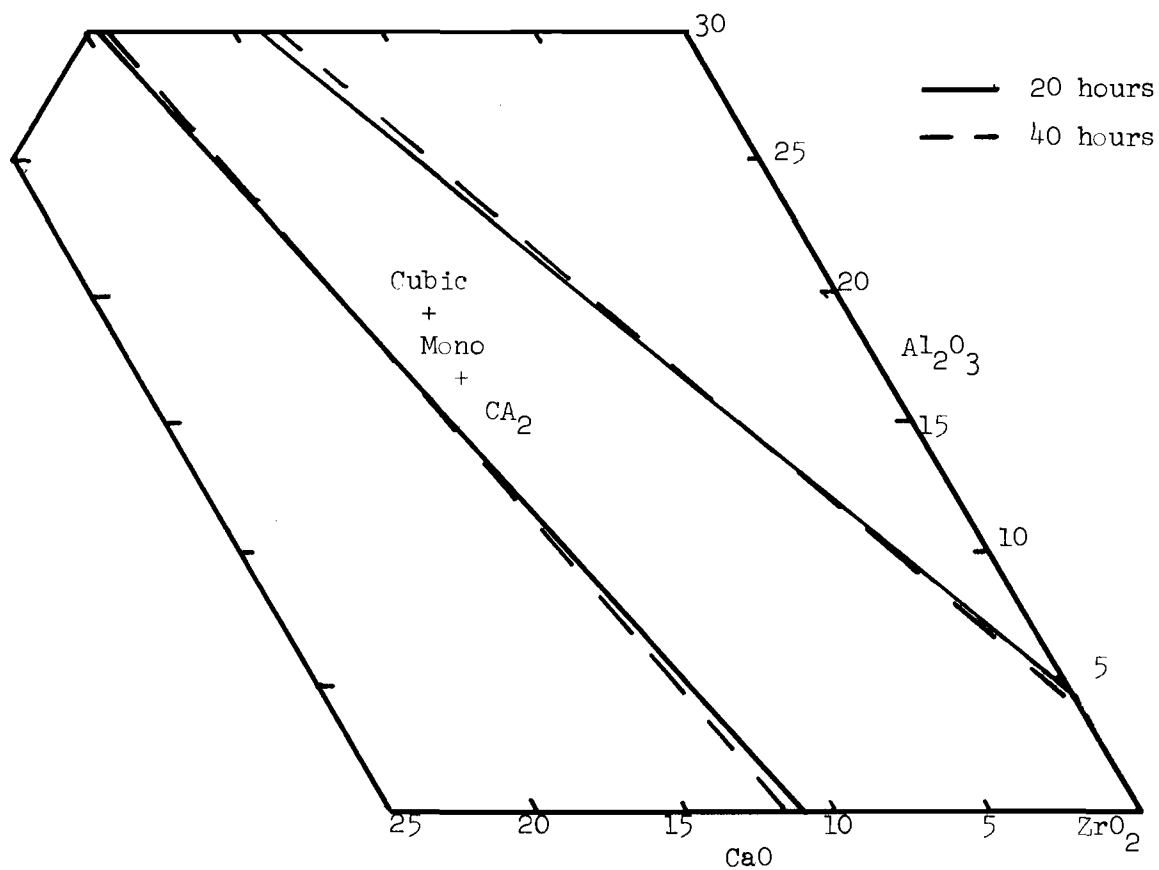


Figure 12. Cubic Zirconia Alkemade Lines at 20 and 40 Hours Firing at 1500 °C, Verifying Equilibrium by Reproducibility of Lines

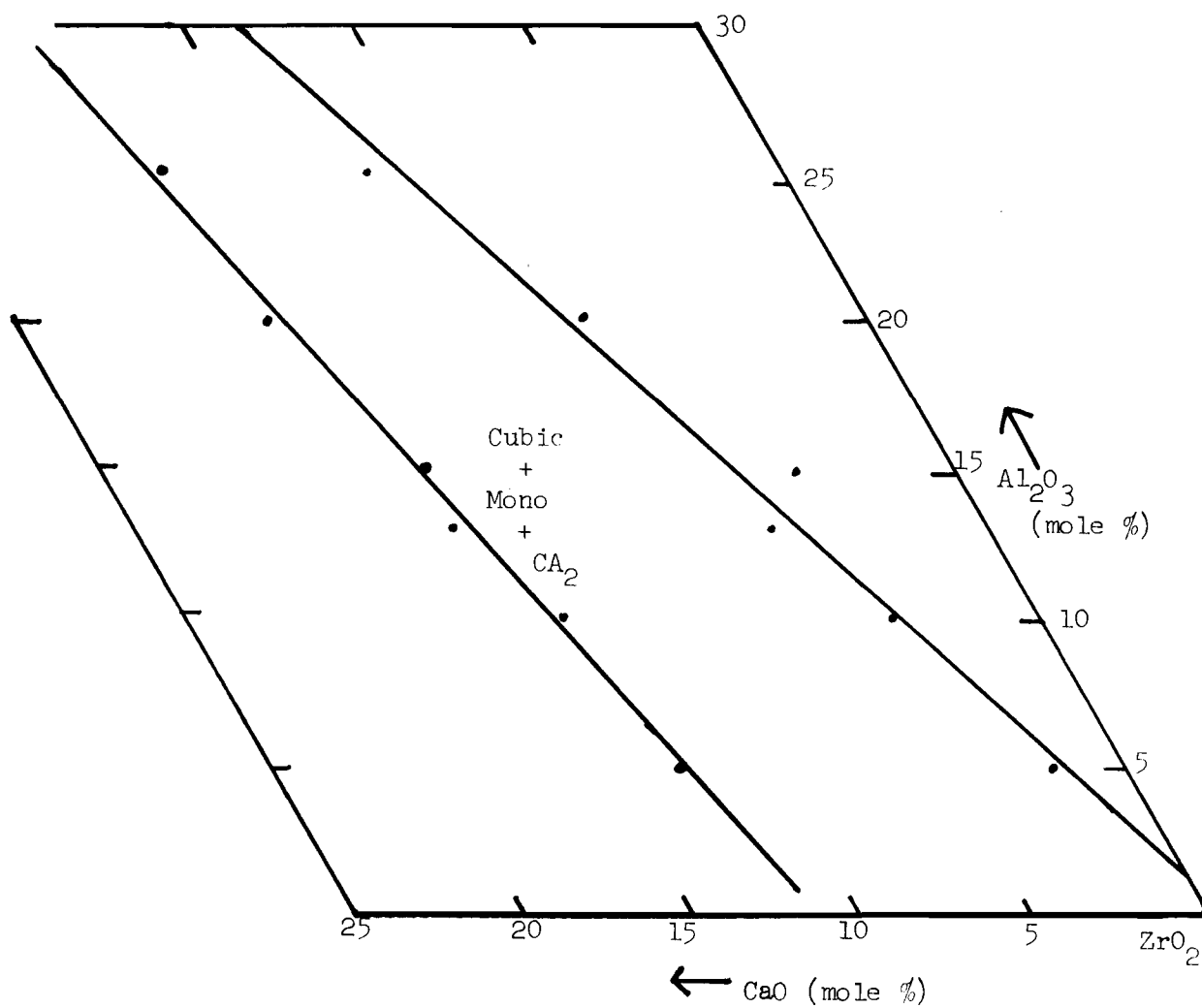
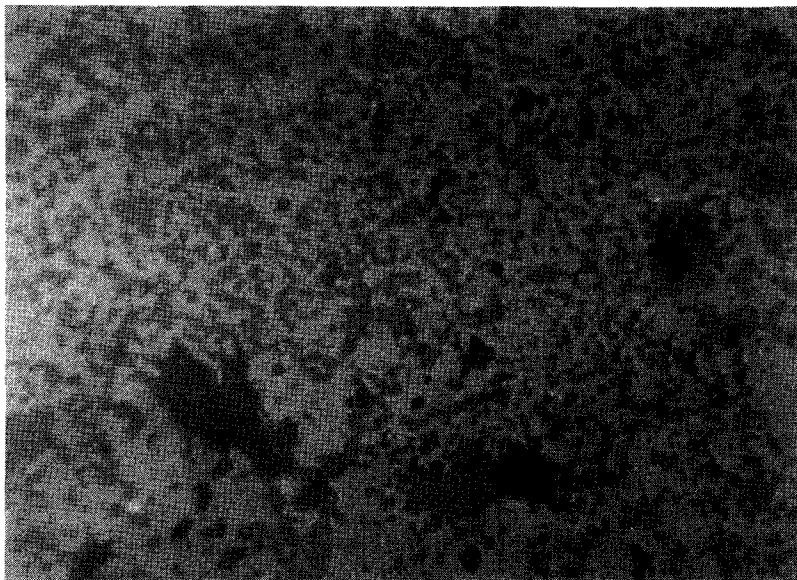


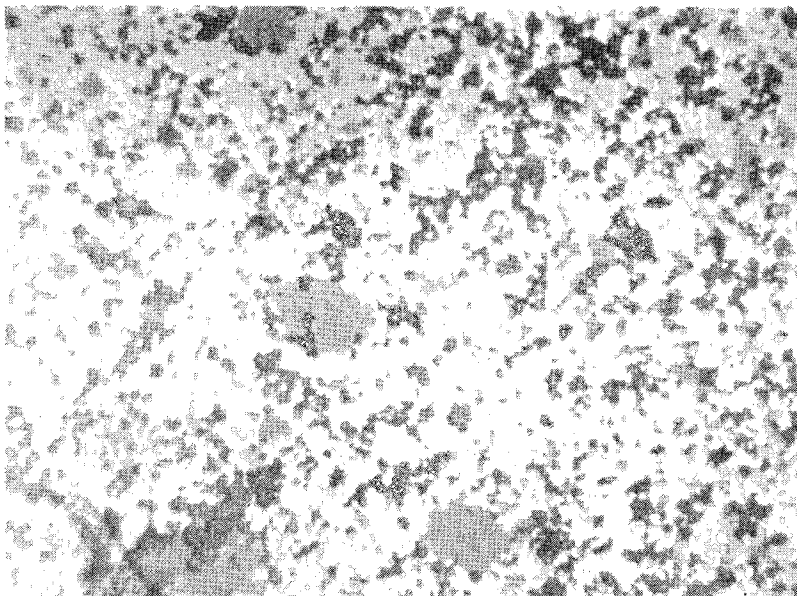
Figure 13. Alkemade Lines Bounding the Cubic + Monoclinic +  $\text{CA}_2$  Region at  $1500^\circ\text{C}$

for alumina has been estimated from information in the literature and from optically determined  $CA_2$  volume contents. Takagi<sup>6</sup> indicated that at 0.5 weight percent alumina he saw a calcium aluminate phase when samples were fired at 1700 °C. This observation suggests that the region of alumina solubility does not extend as much as 0.55 mole percent above the line. Quantitative X-ray analysis could not be used to determine the amount of  $CA_2$  present in each sample because a sufficiently pure sample of  $CA_2$  was not available.

From the optical data, an estimate was made of the compositions at which the  $CA_2$  phase disappeared and reached 100 %. Samples 2-2, 3-1, 3-5, 2-25, and 3-9 were chosen since they lay on a line drawn from  $CA_2$  to a composition of eight mole percent calcia and 92 mole percent zirconia. The photographs of two samples, 3-1 and 3-9 are shown in Figure 14 as examples of the microstructures which were observed. A method similar to that used for determining the position of the Alkemade lines was used. The volume percents of the  $CA_2$  phase were converted to weight percents, assuming a 2:1 weight ratio of cubic to monoclinic zirconia and densities of 6.15 g/cc for cubic zirconia, 5.83 g/cc for monoclinic zirconia, and 2.89 g/cc for  $CA_2$ . Weight percents were converted to mole percents assuming that  $CA_2$  was exactly a 1:2 ratio and that the other end point of the tie line was at eight mole percent calcia and 92 mole percent zirconia. Table 10 shows the data as converted. Mole percent  $CA_2$  was plotted versus mole percent  $Al_2O_3$  and with a linear regression program the best line fit was determined, Figure 15. Extrapolation to 100 %  $CA_2$  gave a stoichiometry for  $CA_2$  of 69.2 mole percent alumina and 30.8 mole percent calcia,



Sample 3-1

 $\text{ZrO}_2$  64 m/o $\text{CaO}$  16 m/o $\text{Al}_2\text{O}_3$  20 m/o

Sample 3-9

 $\text{ZrO}_2$  85.7 m/o $\text{CaO}$  9.5 m/o $\text{Al}_2\text{O}_3$  4.8 m/o

Figure 14. Photomicrographs of Series 3, 1500 °C, 600x

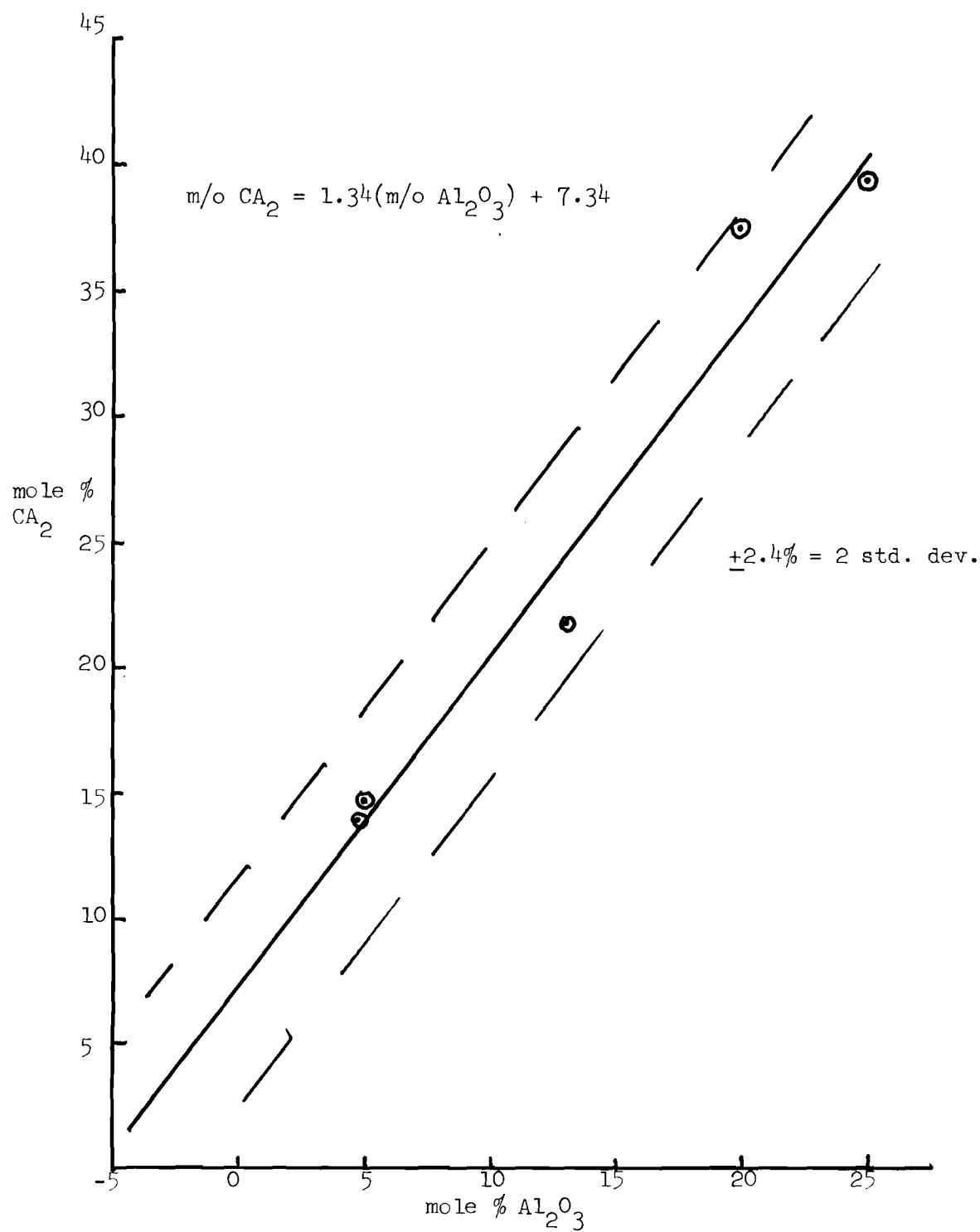


Figure 15. Extrapolation of  $\text{CA}_2$  Composition to 0% Alumina to Determine  $\text{Al}_2\text{O}_3$  Solubility in Zirconia

Table 10. Optical data for  $CA_2$  Stoichiometry Determination

Sample Number	m/o CaO	m/o $Al_2O_3$	vol % $CA_2$	wt % $CA_2$	m/o $CA_2$
2-2	17.5	25.0	50	32.35	39.4
3-1	16.0	20.0	48	30.63	37.5
3-5	13.0	13.0	30	17.01	21.8
2-25	10.0	5.0	21	11.28	14.7
3-9	9.5	4.8	20	10.68	14.0

which is closer to  $C_3A_7$  than  $CA_2$ . Extrapolation to 0 %  $CA_2$  resulted in a negative alumina value, which is obviously erroneous, but does suggest that very little alumina exists in solid solution in either zirconia phase, as noted by Takagi.<sup>6</sup>

#### $CaO-Al_2O_3-ZrO_2$ Phase Equilibria at 1500 °C

From the data presented above plus information obtained from the literature, it is possible to construct a phase diagram of the high zirconia region of the calcia-alumina-zirconia ternary system at 1500 °C, Figure 16. The  $CA_2$  - cubic zirconia and  $CA_2$  - monoclinic zirconia Alkemade lines determined above are shown solid because they have been accurately determined. From equation 9, the Alkemade line extrapolation to 0 % alumina, the boundary between the cubic +  $CA_2$  region and the cubic + monoclinic +  $CA_2$  region is placed at 11.6 mole percent CaO, rather than the 13 to 16 mole percent reported by other investigators. The cubic zirconia - monoclinic zirconia Alkemade line is drawn at 0.5 mole percent alumina, as described above.



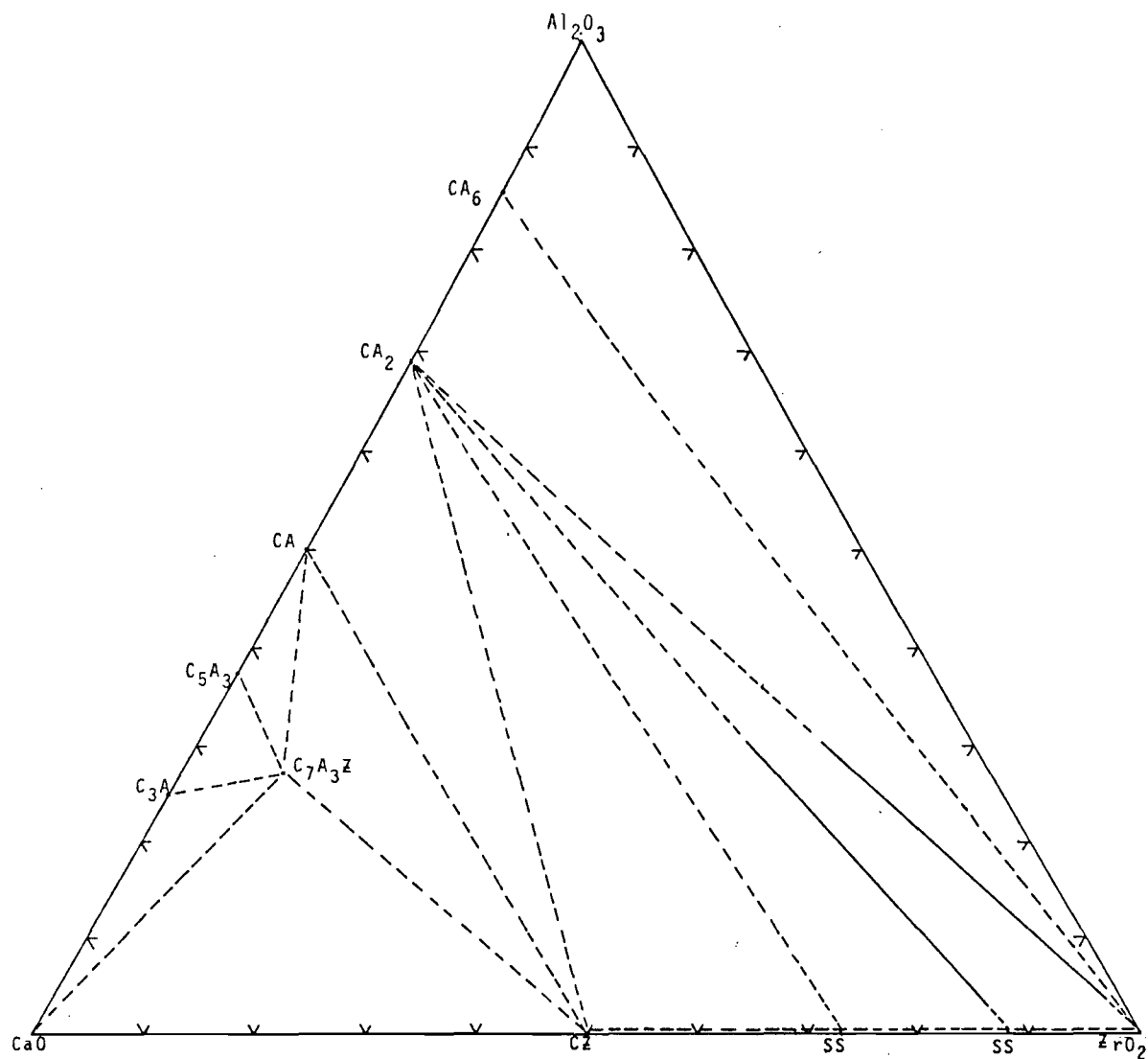


Figure 16. Calcia-Alumina-Zirconia Phase Diagram  
at 1500 °C

The fact that the Alkemade lines from  $\text{CA}_2$  to cubic zirconia and from  $\text{CA}_2$  to monoclinic zirconia intersected the  $\text{Al}_2\text{O}_3$  -  $\text{CaO}$  binary at 69 mole percent  $\text{Al}_2\text{O}_3$  and 31 mole percent  $\text{CaO}$  and also that the  $\text{CA}_2$  volumes extrapolated to 100% resulted in the same  $\text{Al}_2\text{O}_3$  -  $\text{CaO}$  composition for  $\text{CA}_2$  may prove to be significant. Because the extrapolations were made from the high zirconia region to the low zirconia region, experimental error may have produced the indicated deviation from  $\text{CA}_2$  stoichiometry. However, if these results were accepted, then  $\text{CA}_2$  must exist as a solid solution. From the data obtained, the stoichiometry was closer to  $\text{C}_{3/7}\text{A}_2$ , but nowhere in the literature was any suggestion of this possibility made. Determination of the  $\text{CA}_2$  lattice parameters at various temperatures would show if the  $\text{CA}_2$  stoichiometry were changing, but because the  $\text{CA}_2$  crystal structure is monoclinic, accurate calculation is very difficult. An attempt at determining the lattice parameters of  $\text{CA}_2$  was made by assuming that the lattice angles remained unchanged, but the results were extremely scattered, indicating that only a low degree of accuracy was possible. Because of the lack of agreement in the literature about the structure of  $\text{CA}_2$ , different investigators may have arrived at different solid solution compositions of the same compound, depending on their method of preparation or the raw materials used. A small amount of zirconia may possibly have entered the  $\text{CA}_2$  lattice, which would alter the results of quantitative X-ray analysis as calculated from the data. More investigation needs to be done concerning the structure of  $\text{CA}_2$  in the presence of zirconia.

The Alkemade line from the high calcia cubic zirconia to  $\text{CA}_2$  was

estimated from the calcia-zirconia binary diagram by Duwez<sup>9</sup> as was the line from CZ to  $CA_2$ . To confirm qualitatively that the regions were labeled correctly, three samples in the cubic + CZ +  $CA_2$  triangle and one in the  $CA_2$  + CZ + CA triangle, series 4 samples, were fired and analyzed by X-ray. No quantitative or other exhaustive analysis was performed. Phase analysis by X-ray did confirm that the two triangles were drawn properly. The Alkemade line from monoclinic zirconia to  $CA_6$  is also drawn from literature data.<sup>1</sup> Samples 2-5 and 2-10 did confirm the composition of the region to be monoclinic +  $CA_2$  +  $CA_6$ . The phase diagram at greater than 50 mole percent calcia is drawn from the investigation of Berezhnoi<sup>1</sup>.

Upon original x-ray examination of samples 2-11, 2-12, 2-16, 2-21, and 2-22, an additional phase was found to be present in small amounts. Identification from JCPDS File Cards indicated that the phase was  $4CaO \cdot 3Al_2O_3 \cdot SO_3$ . The chemical analysis of the TAM zirconia which was used as a raw material showed an  $SO_2$  content of 0.1%, which was apparently enough for this additional phase to appear on the surface of the samples. When the surface of the pellets was ground off with silicon carbide grinding paper, this phase disappeared in the X-ray scans. Since the phase appeared only on the surface and was caused by an impurity, further consideration was omitted and the surface of each sample was ground sufficiently to eliminate what was considered to be a contaminant.

#### Long Term Phase Equilibria Stability

Changes in the amount of solubility of calcia in cubic zirconia were studied for up to 2000 hours at 900 °C and 1300 °C. Quantitative

X-ray analysis was used to study the destabilization of cubic zirconia. Lattice parameter measurements were made to confirm the indicated amount of destabilization.

#### Quantitative X-Ray Analysis

Three compositions were chosen in the cubic zirconia + monoclinic zirconia +  $\text{Ca}_2$  compatibility triangle for determining the stability of the phases over periods of time up to 2000 hours of firing. Two temperatures,  $900^\circ\text{C}$  and  $1300^\circ\text{C}$ , were chosen for experimentation since these seemed to be temperatures at which industry might use these compositions as refractories. The three compositions were chosen at points where the cubic to monoclinic zirconia weight ratio was approximately 3:1 as determined from the results of the  $1500^\circ\text{C}$  analysis. Sample A was 10.0 mole percent alumina and 12.5 mole percent calcia, sample B was 17.5 mole percent alumina and 14.5 mole percent calcia, and sample C was 25 mole percent alumina and 17.5 mole percent calcia.

The three compositions were initially fired at  $1550^\circ\text{C}$  in order to densify the pellets more completely than at  $1500^\circ\text{C}$ . X-ray analysis of the fired pellets showed that even a  $50^\circ\text{C}$  increase in temperature had significantly increased the weight ratio of cubic to monoclinic zirconia compared to the contents at  $1500^\circ\text{C}$ . This change in weight ratio indicated that one of the solid solution endpoints changed considerably. The analysis of sample C showed no monoclinic zirconia at  $1550^\circ\text{C}$ , which meant that the Alkemade line had moved to a  $\text{CaO}$  content lower than this composition point. In order to calculate the position of the  $\text{Ca}_2$  - cubic zirconia Alkemade line, it was assumed that the Alkemade line joining

$\text{Ca}_2$  and monoclinic zirconia did not move, since Duwez<sup>9</sup> and Hennicke<sup>25</sup> both indicated that there was very limited solid solution in monoclinic zirconia. From the equation for the  $\text{Ca}_2$  - monoclinic zirconia line at 1500 °C, the CaO content at 10, 17.5, and 25 mole percent alumina (compositions A, B, and C respectively) was determined. Using the calcia contents at 0% cubic zirconia and the ratio of cubic to cubic plus monoclinic zirconia at the three compositions, the 100 % cubic line was calculated as described for 1500 °C, Figure 17. Since there was only one data point at each alumina composition, the location of the line could not be determined as accurately as the 1500 °C line was established. The implication from the position of the 1550 °C line is that the composition of  $\text{Ca}_2$  was varying more than the composition of the cubic zirconia. Because only three data points were available, this conclusion is open to question. It must also be stated that if the  $\text{Ca}_2$  composition were changing with temperature increase, then the  $\text{Ca}_2$  - monoclinic zirconia Alkemade line would also be changing; thus the 1500 °C line equation would not be valid for determining the second data point at each alumina composition. However, from lattice parameter measurements for cubic zirconia, to be presented below, it will be shown that CaO solid solution changes in zirconia resulted in the Alkemade line movement.

Quantitative X-ray results of the surface scans of the long term fired samples after firing at 900 °C and 1300 °C were inconsistent, particularly for the samples being held at 900 °C. The pellet surfaces were ground to remove approximately 1 mm and consistency was obtained. Further grinding showed no changes in the weight ratios of cubic to monoclinic

At 1550 °C for 100% cubic zirconia: %CaO = 0.26 ( $\text{Al}_2\text{O}_3$ ) + 11.14

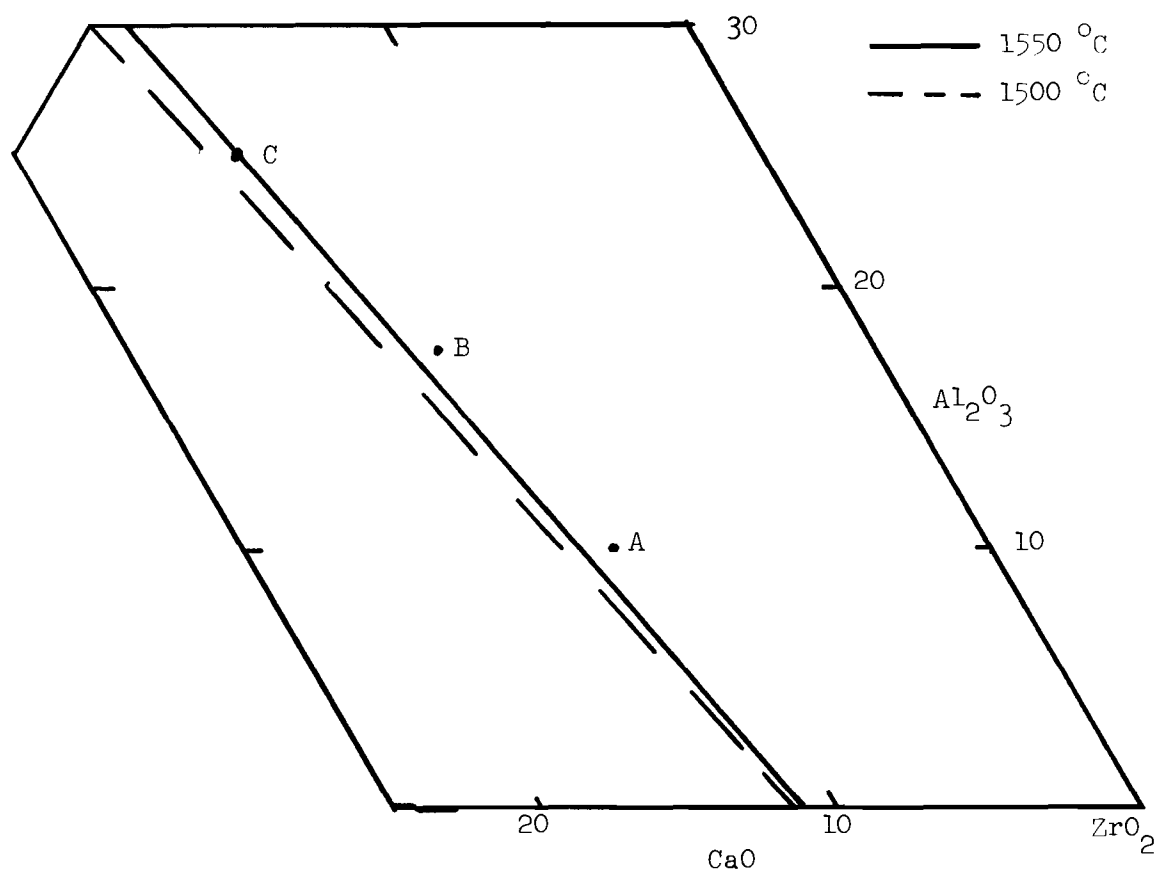


Figure 17. Alkemade Line at 1550 °C from  $\text{CA}_2$  to Cubic Zirconia

zirconia. The quantitative X-ray results for the long term fired samples are presented in Appendix D. Changes in the ratio of cubic zirconia to cubic plus monoclinic zirconia, Figures 18 and 19, give a clear indication of phase changes with respect to time.

At 1300 °C little problem existed with surface inconsistencies, as results obtained from a lightly ground surface agreed well with a 1 mm surface removal. A considerable decrease in the amount of cubic zirconia with firing time can be seen. By 1000 hours equilibrium had been reached, as indicated by a constant cubic to cubic plus monoclinic ratio from 1000 to 2000 hours. It may be noted that sample C must be very close to the boundary because its composition changed radically in the first 400 hours. Samples A and B changed in the same direction but to a lesser extent.

The Alkemade line from  $Ca_2$  to cubic zirconia at 1300 °C was determined by the same method as was used at 1550 °C, and thus not too great an accuracy could be implied. The calculated position, Figure 20, indicates that approximately a three mole percent increase occurred in the calcia content of cubic zirconia from 1500 °C to 1300 °C. The increase was slightly more than expected from results reported by Duwez<sup>9</sup>, but the data is limited, and therefore not conclusive.

At 900 °C the destabilization Process took place very slowly. Sample C showed this process most clearly, in that the X-ray data indicated no monoclinic zirconia for 1000 hours and only a slow increase from 1000 to 2000 hours. Changes in samples A and B are almost imperceptible. After about 1400 hours sample A appeared to begin to destabilize. In sample B there was no perceptible change in the weight ratio of cubic to

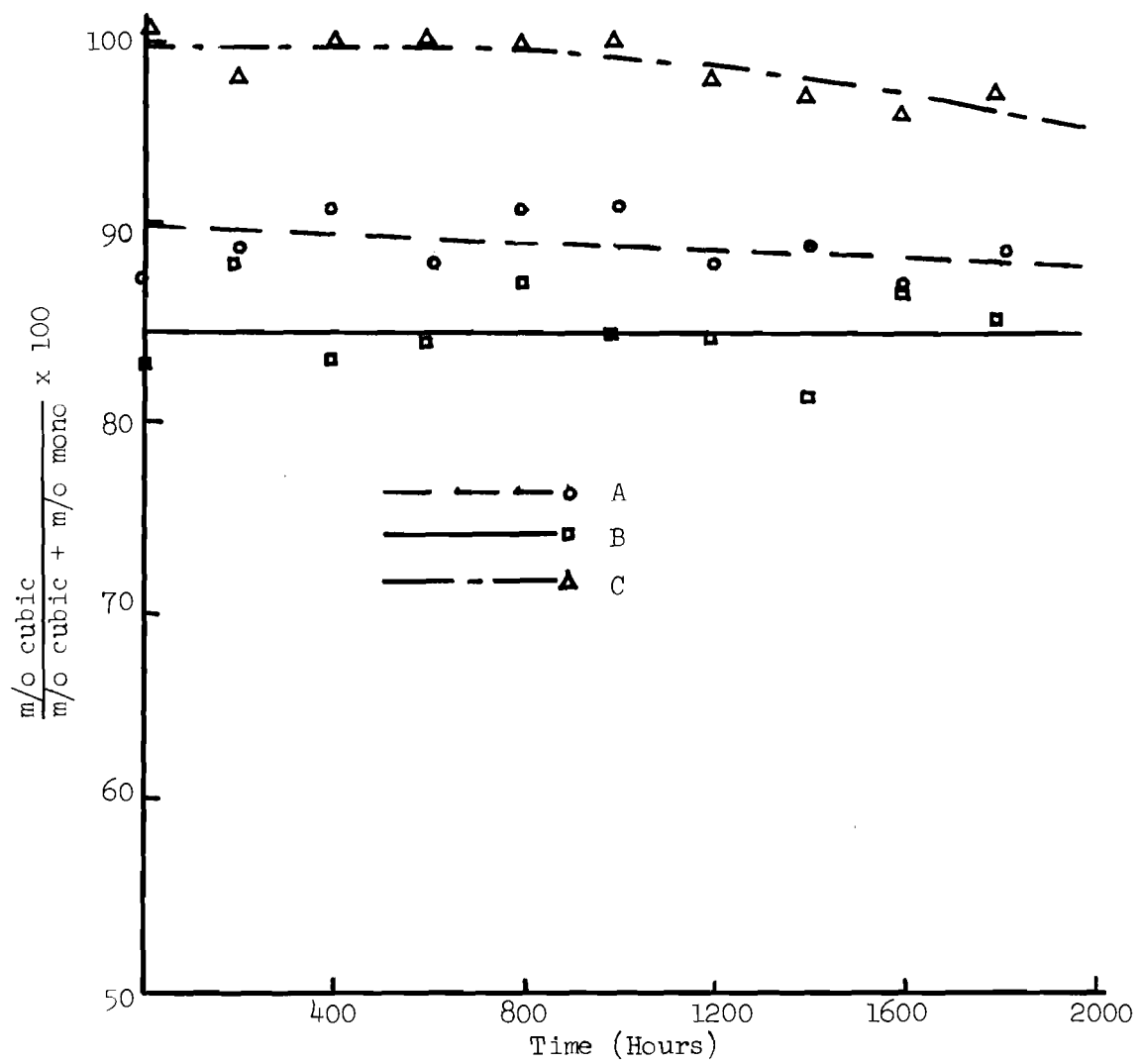


Figure 18. Change in Amount of Cubic Zirconia with Time at 900 °C



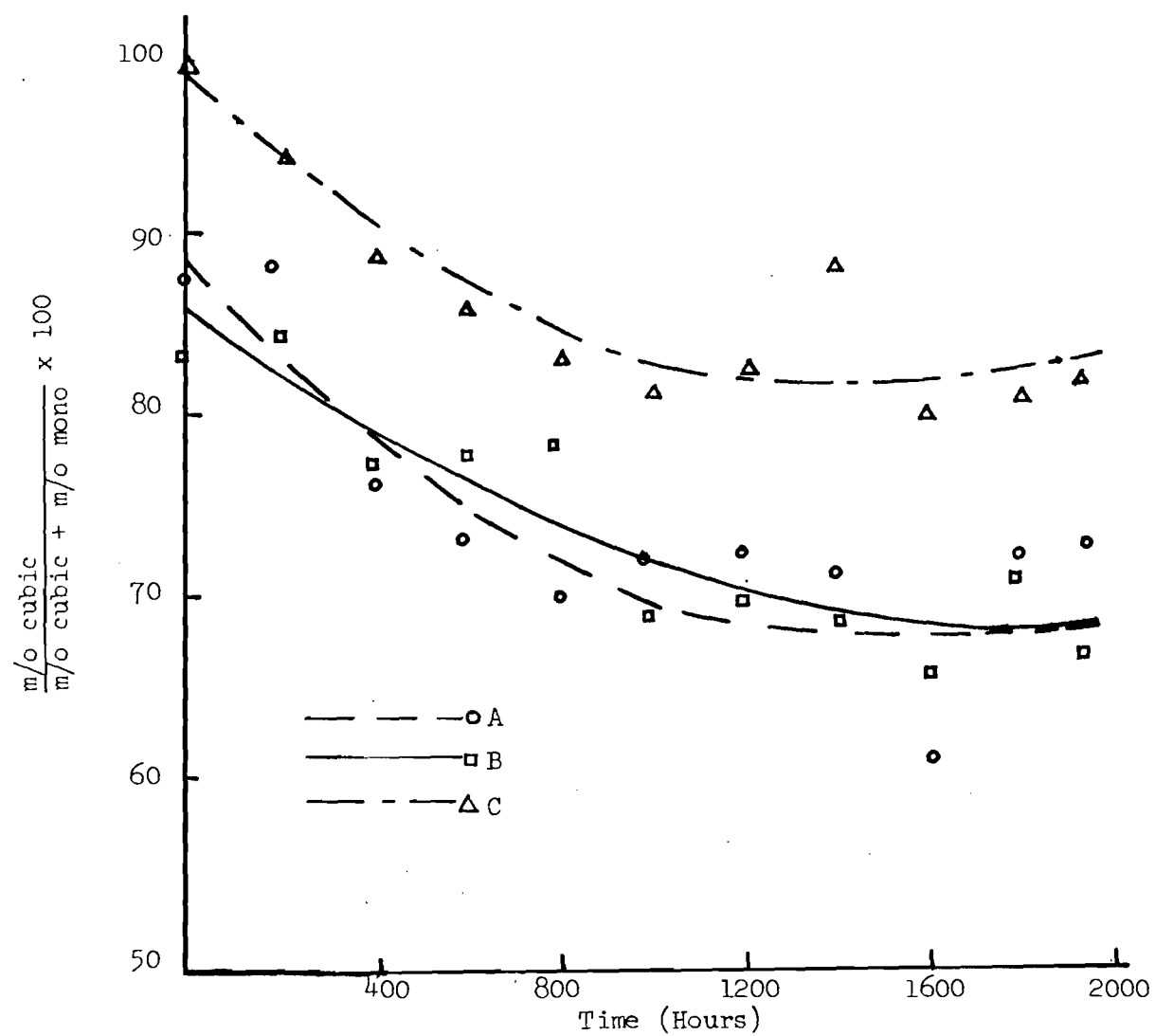


Figure 19. Change in Amount of Cubic Zirconia with Time at 1300 °C

At 1300 °C for 100% cubic zirconia:  $\%CaO = 0.17 (Al_2O_3) + 14.6$

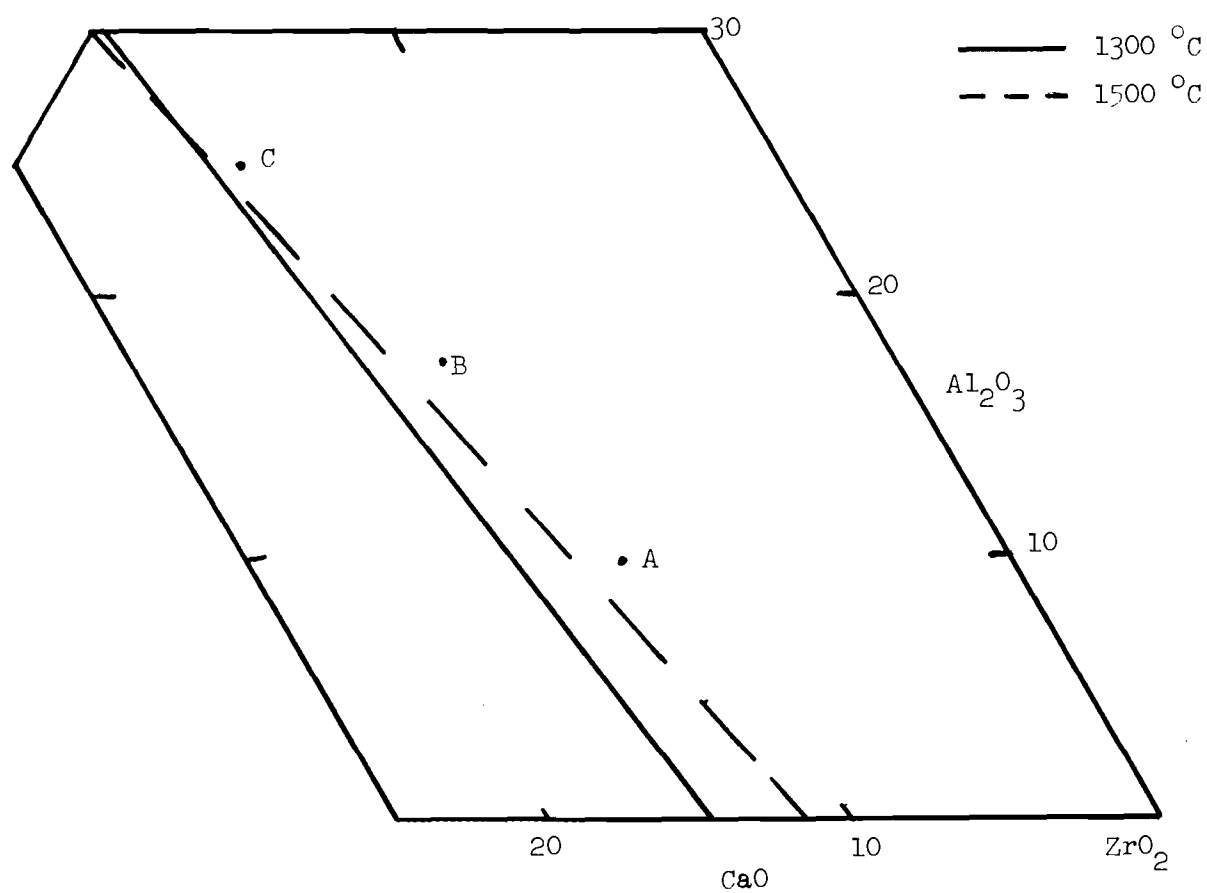


Figure 20. Alkemade Line at 1300 °C from CA<sub>2</sub> to Cubic Zirconia

monoclinic zirconia. Thus with the cubic to monoclinic ratios showing little change from 1550 °C, the samples are not near equilibrium, even after 2000 hours. From thermal expansion measurements made on these samples in related work<sup>28</sup>, the monoclinic zirconia content was found to be increasing even at 200 and 400 hours for each of the samples at 900 °C, but the change was small, indicating that only a slight amount of destabilization was occurring in samples fired to 1550 °C. Because equilibrium was not attained at 900 °C, no estimation of the tie line at this temperature could be made.

At 900 °C the above data agrees well with the results obtained by Duwez<sup>9</sup> for long term stability of a pure calcia stabilized zirconia. At 1300 °C, though, he found much better stability of calcia stabilized zirconia than was indicated for calcia stabilized zirconia with alumina additions. For samples A and B the actual amount of destabilization at 1300 °C may not be enough to cause a practical problem. For instance, sample A changed from a composition that was 11.0 weight percent monoclinic zirconia at 1550 °C to one that was 25.0 weight percent monoclinic zirconia at 1300 °C. Measurements of the coefficients of linear thermal expansion might show a small enough change that the thermal shock characteristics would not be adversely affected. Even the change in sample C from a cubic zirconia composition to one that was 10.8 weight percent monoclinic might not be enough of a change to cause a problem in actual use. This particular area is one in which more work must be done.

#### Lattice Parameter Determinations for Cubic Zirconia

In order to study changes in the structure of the zirconia cubic solid solution, the lattice parameter was determined for samples at 0,

200, 1000, and 2000 hours at both 900 °C and 1300 °C and for the 1300 °C samples also at 400 hours. A lattice parameter value of 5.126 for the samples as fired at 1550 °C agrees better with the data published by Garvie<sup>10</sup> than with that of Duwez<sup>9</sup>. Figure 21 shows the averaged lattice parameters of samples A, B, and C versus time and includes the variations which were observed. The 1300 °C data is as expected. Both Duwez and Garvie indicated that a variation in  $\underline{a}$  of 0.003 Å represents approximately a change in composition of two mole percent calcia. Thus the change in lattice parameter from 1550 °C to 1300 °C agrees well with the calculated measurement of the Alkemade line. The phase diagram of the calcia-zirconia binary by Duwez also confirms the results. The samples fired at 1550 °C have about two mole percent less calcia than those that have reached equilibrium at 1300 °C.

The lattice parameter results for the 900 °C samples cannot be understood strictly from a crystal structure point of view. With the cubic zirconia being the highest thermal expansion phase present, cooling the samples from 1550 °C apparently resulted in enough tension in the lattice to expand it slightly. On reheating, annealing at 900 °C, and cooling, the lattice expansion due to tension is less, because the temperature change is smaller. Thus annealing at 900 °C with no composition change could result in a decrease of the cubic zirconia lattice parameter. From quantitative X-ray measurements equilibrium was shown not to have been attained at 900 °C even after firing for 2000 hours. If equilibrium at 900 °C were obtained, a larger lattice would have been expected than that found at 1300 °C, due to increasing calcia content. The tension in the lattice is apparently masking the increase in size, and since the

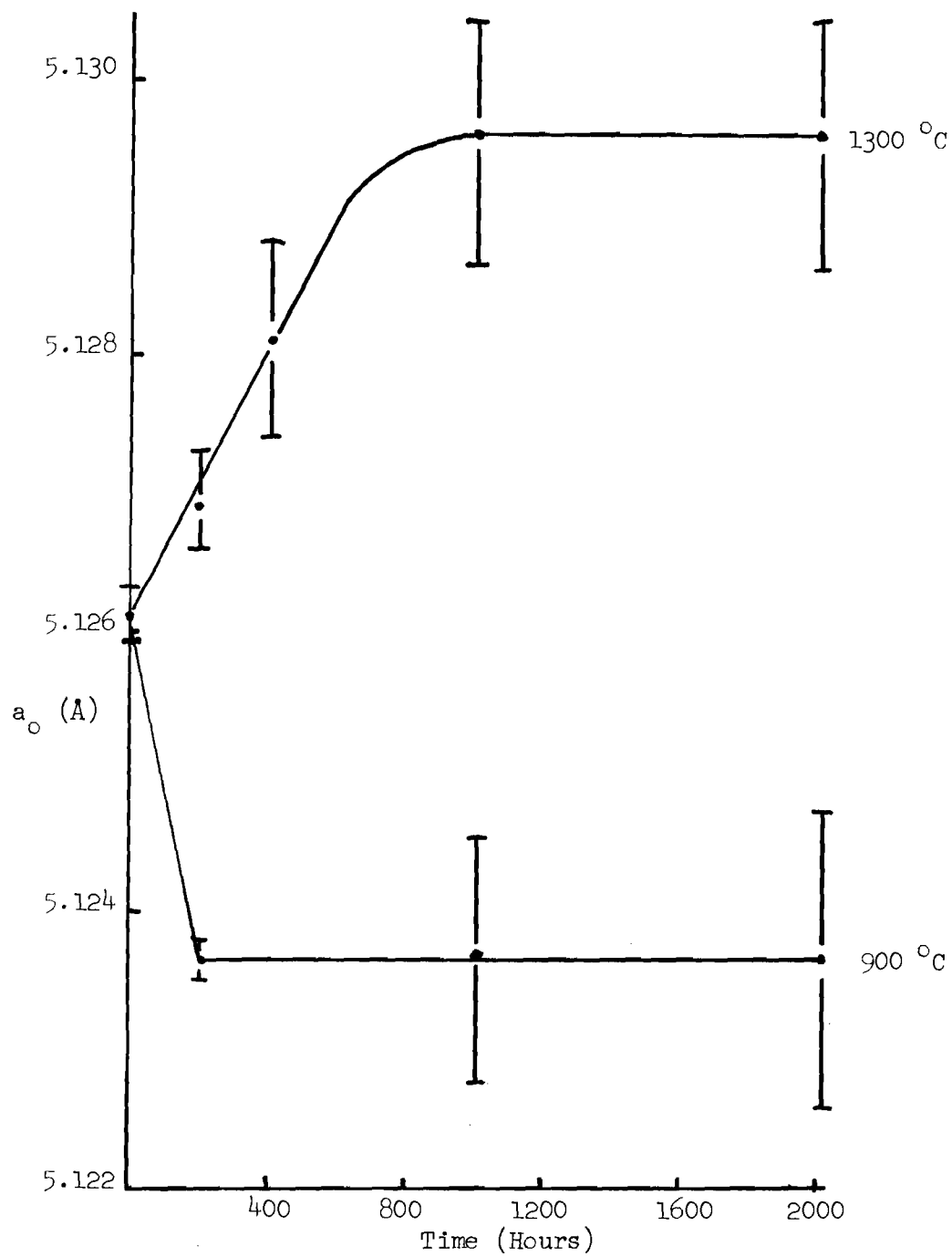


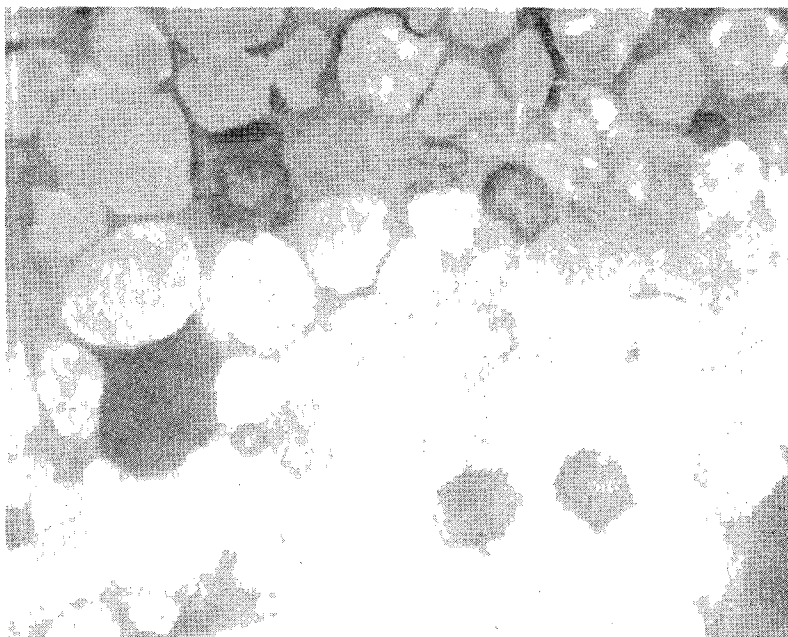
Figure 21. Lattice Parameter Changes with Time

samples were not even near equilibrium, the lattice might not in reality be as large as the 1300 °C lattice at 2000 hours. An effect that cannot be evaluated is the presence of alumina ions, which are half the size of calcia ions. If there were indeed an amount of alumina in the cubic zirconia lattice, then as the amount varied with temperature changes, the alumina could cause the lattice to become smaller, reversing the effect of the addition of calcia. Evaluation of this effect was not possible from the data and equipment available.

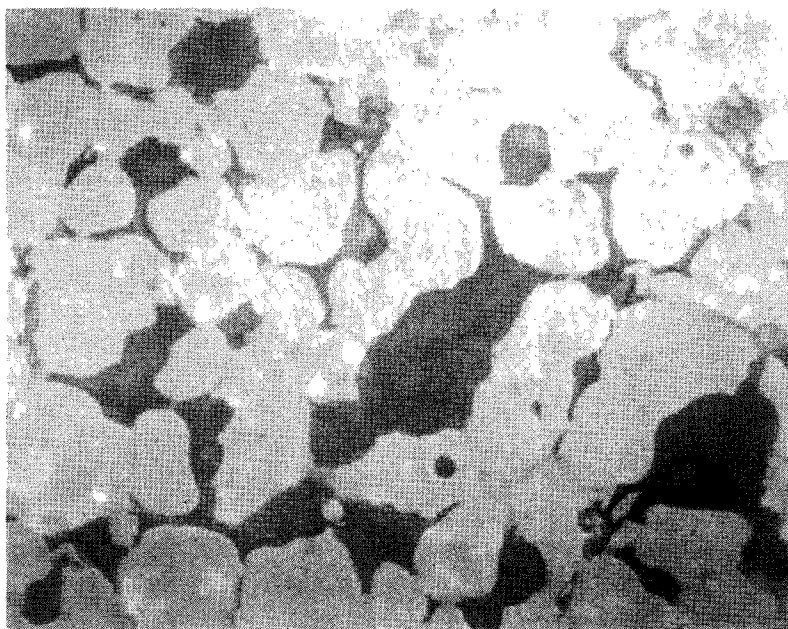
#### Analysis of Series 1 Fired at 1700 °C

When the nine samples 1-1 through 1-9 were removed from the furnace, it was observed that 1-1, 1-2, and 1-4 had definitely undergone partial melting because the edges of the pellets were rounded and slumped. Photographs of samples 1-1 and 1-9 are included, Figure 22, showing large uniformly rounded grains surrounded by the secondary gray phase, which is a clear indication that melting occurred. Table 11 shows the results of the qualitative X-ray analysis and the optical analysis. It is clear from the phase analysis that the samples were not at equilibrium. The phases present do not correspond to the equilibrium phases at 1500 °C and sample 1-1 has four phases present, an impossibility in equilibrium unless the composition was exactly at the eutectic point. Thus no phase diagram information may be taken from these results.

The presence of  $CA_6$  is important. First of all, it corroborates the work of Takagi<sup>6</sup>, who also found melting of the samples at 1700 °C, with the formation of  $CA_6$ . From the literature it has not been clear if  $CA_2$  melted congruently or incongruently. The presence of  $CA_6$  in several



Sample 1-1

 $\text{ZrO}_2$  64 m/o $\text{CaO}$  16 m/o $\text{Al}_2\text{O}_3$  20 m/o

Sample 1-9

 $\text{ZrO}_2$  85.7 m/o $\text{CaO}$  9.5 m/o $\text{Al}_2\text{O}_3$  4.8 m/o

Figure 22. Photomicrographs of Series 1, 1700 °C, 600x

Table 11. Phase Composition and Optically Determined Phase Volume of Series 1, 1700 °C

Sample Number	Crystalline Phases	Percent Porosity	Optical	
			% White	% Gray
1-1	Cubic, $CA_6$ , $CA_2$ , Mono	13	61	39
1-2	Cubic, Mono, $CA_2$	25	79	21
1-3	Cubic, Mono, $CA_6$	13	62	38
1-4	Cubic, $CA_2$ , Mono	21	76	24
1-5	Cubic, $CA_2$	7	69	31
1-6	Cubic, Mono, $CA_6$	11	78	22
1-7	Cubic, $CA_2$ , CZ	10	84	16
1-8	Cubic, Mono	10	89	11
1-9	Cubic, Mono, $CA_6$	16	94	6



of the samples, where from previous phase diagram results  $CA_2$  should have been the only calcium aluminate phase, indicates that  $CA_2$  melts incongruently forming  $CA_6$  and a liquid. Thus if the samples did not attain equilibrium on cooling (which was at the relatively fast cool down rate of the gas-fired furnace), it would be reasonable for  $CA_6$  to be present. Much more work must be done to clarify the understanding about  $CA_2$ .

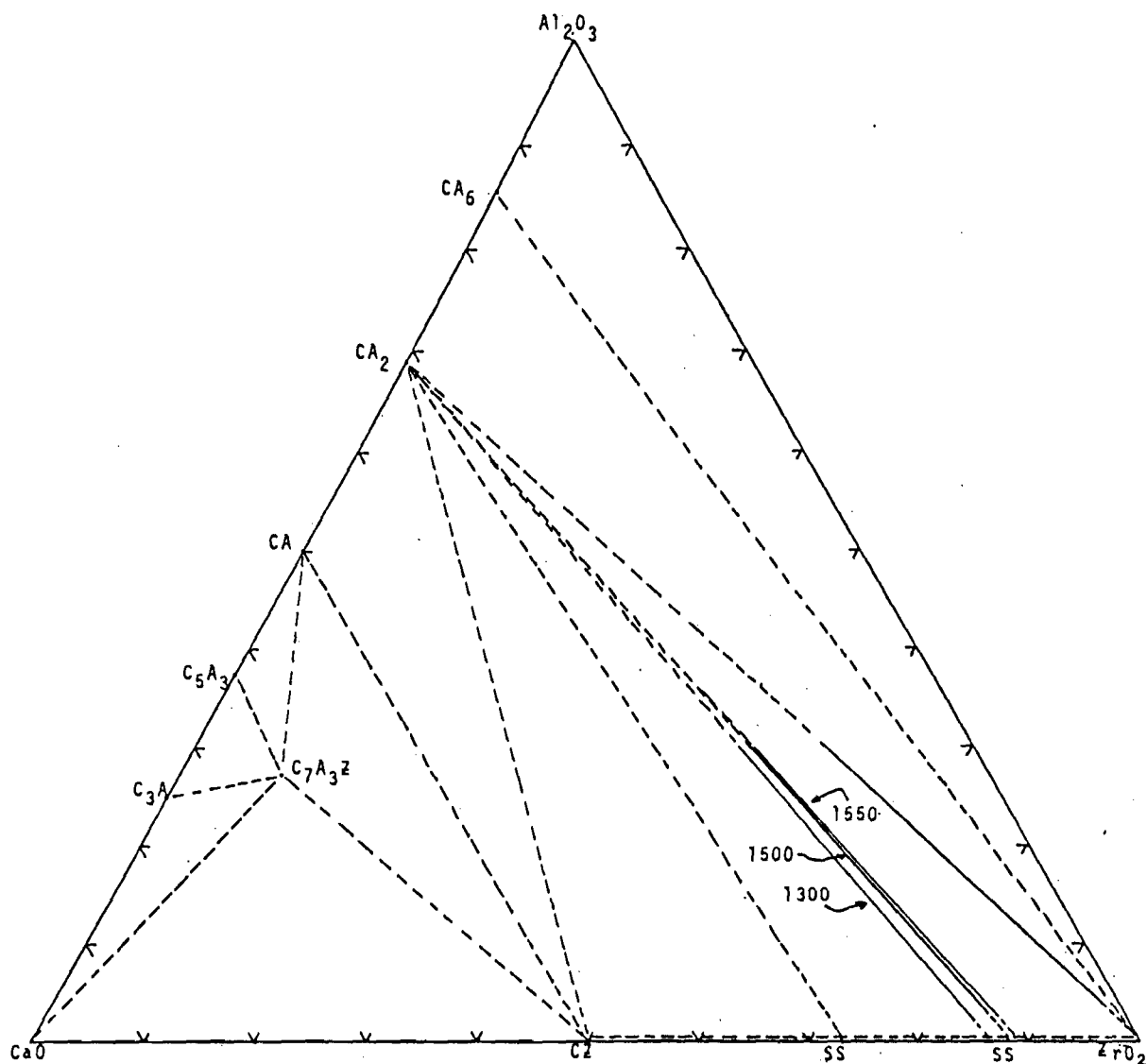
The X-ray phase analysis from sample 1-8 would suggest considerable solid solution of alumina in zirconia. However, the optical information showed that there was still a considerable amount of calcium aluminate in this sample, but that it was below the detection limits of the X-ray diffractometer.

Because equilibrium was not attained because of partial melting of the samples, it was not possible to make any determination about solid solution phenomena for either cubic zirconia or  $CA_2$  at 1700 °C. The incongruent melting of  $CA_2$  was, however, more definitely established.

## CHAPTER V

## CONCLUSIONS

1. The phase diagram for the high zirconia region of the calcia-alumina-zirconia system was determined at 1500 °C and combined with available information to prepare a complete phase diagram of the calcia-alumina-zirconia system as shown:



2. The equation of the  $CA_2$  - monoclinic zirconia Alkemade line is

$$\%CaO = 0.48 (Al_2O_3) - 0.89 .$$

The equation of the  $CA_2$  - cubic zirconia Alkemade line is

$$\%CaO = 0.28 (Al_2O_3) + 11.68 .$$

3. Solution of  $Al_2O_3$  in cubic and monoclinic zirconia is extremely limited and probably less than one mole percent.

4. The lower limit of calcia solid solution in cubic zirconia varies from 14.6 mole percent at 1300 °C to 11.1 mole percent at 1550 °C.

5. After firing to 1550 °C, the composition of the solid solution cubic zirconia in the  $CA_2$  - cubic  $ZrO_2$  - monoclinic  $ZrO_2$  compatibility triangle required 800 to 1000 hours to reach equilibrium at 1300 °C and changed so slowly at 900 °C that after 2000 hours, equilibrium was not obtained.

6. Calcium di-aluminate,  $CA_2$ , melts incongruently to  $CA_6$  plus a liquid.

## CHAPTER VI

## RECOMMENDATIONS

The behavior of  $CA_2$  should be studied to determine if it really exists as a solid solution and if it changes composition with temperature changes. It should be studied with a small zirconia content in an attempt to ascertain the phase relations of the three component system. A liquidus diagram of the ternary system should also be prepared as a continuation of the phase diagram study. Physical property studies of the samples which were prepared for long term firing would be useful in determining if such compositions might have practical industrial application. In a general sense different areas of the ternary should be studied. The existence of the ternary compound  $C_{7/3}A_3Z$  claimed by Berezhnoi should be confirmed.

## APPENDIX A

## SYSTEMATIC POINT COUNTING TECHNIQUE

The systematic point counting technique was used for determining the volume fraction of calcium aluminates, porosity, and zirconia phases from optical micrographs of polished sections of the samples. Accuracy is directly related to the number of points used in the count and the method depends on the fact that the following relationship is true:<sup>29</sup>

$$P_p = V_v \quad (11)$$

where  $P_p$  is the fraction of points falling on a phase of interest, and  $V_v$  is the volume fraction of the phase of interest. Standard deviation is given by the following formula:

$$\sigma V_v = \frac{V_v}{(N)^{\frac{1}{2}}} \quad (12)$$

where  $N$  is the number of points falling on the phase. For a confidence factor of 95%, two standard deviations from the average value are allowed. Table 12 shows the accuracy that can be expected statistically when a total of three hundred points are counted.

Table 12. Accuracy of Systematic Point Counting Technique

$V_v$	0.01	0.05	0.1	0.2	0.4	0.6	0.8
$\sigma V_v$	0.006	0.013	0.018	0.026	0.037	0.045	0.052
$\pm$ % accuracy	120	52	36	26	18.5	15	13

Percent accuracy in Table 12 is written in terms of the volume fraction. Accuracy increases as the inverse square of the number of points counted so that, for instance, quadrupling the number of points would only halve the uncertainty. Thus 300 points were determined to be sufficient as a good balance between the time required and the accuracy obtained. A square grid of 25 points spaced on 0.25" centers was dropped randomly without bias on each photograph 12 times as a tally of the points in each phase was made. Randomness was required for accuracy and it was necessary that a representative sector of the sample be photographed, rather than an area with some outstanding feature. The actual numbers determined for volume fractions of the three phases in each pellet were reasonably accurate, within  $\pm 30\%$  for most cases.

## APPENDIX B

## PHASE ANALYSIS OF COMPOSITIONS FIRED AT 1500 °C

The phases present were determined qualitatively by X-ray diffraction. Qualitative analysis of series 2 was performed on samples fired for 20 and 40 hours. The results were the same, as listed in the table.

Several of the samples were polished after being fired to 1500 °C and slow cooled. A small amount of porosity, which appeared as very dark areas, was observed. The major phase was white in color and was apparently, as confirmed by quantitative information, the sum of the two zirconia phases. The gray phase was the sum of the calcium aluminate phases,  $CA_2$  and  $CA_6$ . The total white and gray phases were expressed in terms of 100%, mathematically eliminating the amount of porosity.

Table 13. Phase Analysis of Series 2

Sample Number	Porosity vol %	White vol %	Gray vol %	Phases Present
2-1	6	49	51	Cubic, $CA_2$
2-2				Cubic, Mono, $CA_2$
2-3				Cubic, Mono, $CA_2$
2-4	8	52	48	Mono, Cubic, $CA_2$
2-5				Mono, $CA_2$ , $CA_6$
2-6				Cubic, $CA_2$
2-7	11	49	51	Cubic, $CA_2$
2-8				Cubic, Mono, $CA_2$
2-9				Cubic, Mono, $CA_2$
2-10	4	54	46	Mono, Cubic, $CA_2$
2-11				Cubic, $CA_2$
2-12				Cubic, $CA_2$
2-13	4	65	35	Cubic, Mono, $CA_2$
2-14				Cubic, Mono, $CA_2$
2-15				Cubic, Mono, $CA_2$
2-16	4	65	35	Cubic, $CA_2$
2-17				Cubic, $CA_2$
2-18				Cubic, $CA_2$
2-19	10	79	21	Cubic, Mono, $CA_2$
2-20				Cubic, Mono, $CA_2$
2-21				Cubic, $CA_2$
2-22	20	79	21	Cubic, $CA_2$
2-23				Cubic, $CA_2$
2-24				Cubic, Mono, $CA_2$
2-25				Cubic, Mono, $CA_2$



Table 14. Phase Analysis of Series 3

Sample Number	Porosity vol %	White vol %	Gray vol %	Phases Present
3-1	7	52	48	Cubic, $CA_2$ , Mono
3-2	6	56	44	Cubic, $CA_2$ , Mono
3-3	38	65	35	Mono, $CA_2$ , $CA_6$
3-4	7	67	33	Cubic, $CA_2$
3-5	24	70	30	Cubic, Mono, $CA_2$
3-6	24	71	29	Cubic, Mono, $CA_2$
3-7	9	81	19	Cubic, $CA_2$
3-8	33	87	13	Cubic, $CA_2$
3-9	26	80	20	Cubic, Mono, $CA_2$
3-10				Cubic
3-11				Cubic
3-12				Cubic, Mono

## APPENDIX C

DATA FOR CALCULATING  $\text{Ca}_2$  - CUBIC  $\text{ZrO}_2$  AND  $\text{Ca}_2$  - MONOCLINIC  $\text{ZrO}_2$   
 ALKEMADE LINES

In Tables 15 - 18 are presented the data necessary to calculate the  $\text{Ca}_2$  - Cubic  $\text{ZrO}_2$  and  $\text{Ca}_2$  - Monoclinic  $\text{ZrO}_2$  Alkemade lines. Columns two and three list the  $\text{Al}_2\text{O}_3$  and CaO composition of each sample on a mole percent basis. The monoclinic to cubic zirconia weight ratio as measured by quantitative X-ray diffraction is in column four. The weight ratio of column four was converted to a mole percent ratio of cubic to cubic plus monoclinic zirconia and is shown in column five. As discussed earlier, at a constant  $\text{Al}_2\text{O}_3$  mole content, the mole percent ratio of cubic zirconia varies linearly with mole percent CaO from 0 at the  $\text{Ca}_2$  - Monoclinic zirconia Alkemade line to 100 at the  $\text{Ca}_2$  - cubic zirconia Alkemade line. Therefore the least squares line fit of mole percent CaO (x) versus mole percent ratio of cubic to cubic plus monoclinic zirconia (y) at constant  $\text{Al}_2\text{O}_3$  content could be calculated (column six). At each  $\text{Al}_2\text{O}_3$  content the least squares line was extrapolated to give the mole percent CaO at 100% cubic (column seven) and at 0% cubic (column eight), which are the CaO compositions at that  $\text{Al}_2\text{O}_3$  composition for the  $\text{Ca}_2$  - cubic zirconia Alkemade line and the  $\text{Ca}_2$  - monoclinic zirconia Alkemade line respectively. Linear regression analysis of mole percent CaO versus mole percent  $\text{Al}_2\text{O}_3$  for the respective lines was used to determine the best fit equations for those two lines, which are presented in Chapter IV.

Table 15. Quantitative X-Ray Data for Series 2 and 3, Slow-Cooled

Sample Number	m/o $Al_2O_3$	m/o CaO (x)	wt. mono wt. cubic	m/o cubic (y)	Equation of line	m/o CaO 100 % cubic	m/o CaO 0 % cubic
2-2	25	17.5	0.267	80.1	$y = 14.43x - 169.57$	18.68	11.75
2-3	25	15	0.962	52.8			
2-4	25	12.5	12.5	7.93			
2-8	20	15	0.345	75.7	$y = 10.83x - 90.82$	17.62	8.39
2-9	20	12.5	0.684	61.1			
2-10	20	10	6.25	14.7			
3-1	20	16	0.340	76.0			
3-2	20	12	2.78	27.9			
2-13	15	15	0.0558	95.1	$y = 9.34x - 43.95$	15.41	4.71
2-14	15	12.5	0.361	74.9			
2-15	15	10	1.149	48.4			
3-5	13	13	0.469	69.6	$y = 10.23x - 63.42$	15.97	6.20
3-6	13	8.7	3.125	25.6			
2-19	10	12.5	0.138	88.6	$y = 10.2x - 38.9$	13.62	3.81
2-20	10	10	0.629	63.1			
2-24	5	12.5	0.034	96.9	$y = 9.96x - 26.82$	12.73	2.69
2-25	5	10	0.316	77.3			
3-9	5	9.5	0.606	64.0			

Table 16. Quantitative X-Ray Data for Series 2, Quenched

Sample Number	m/o $Al_2O_3$	m/o CaO (x)	wt. mono wt. cubic	m/o cubic (y)	Equation of line	m/o CaO 100 % cubic	m/o CaO 0 % cubic
2-2	25	17.5	0.0236	97.9	$y = 18.81x - 233.77$	17.74	12.43
2-3	25	15	1.39	43.6			
2-4	25	12.5	27.03	3.83			
2-8	20	15	0.392	73.3	$y = 8.8x - 58.7$	18.03	6.67
2-9	20	12.5	1.02	51.3			
2-13	15	15	0.0554	95.1	$y = 8.7x - 37.62$	15.82	4.32
2-14	15	12.5	0.538	66.7			
2-15	15	10	1.01	51.6			
2-19	10	12.5	0.183	85.5	$y = 10.52x - 46.0$	13.88	4.37
2-20	10	10	0.741	59.3			
2-24	5	12.5	0.0658	94.2	$y = 7.8x - 3.3$	13.24	0.42
2-25	5	10	0.365	74.7			

Table 17. Quantitative X-Ray Data for Long-Term Samples at 1550 °C

Sample	m/o $\text{Al}_2\text{O}_3$	m/o CaO (x)	wt. mono wt. cubic	m/o cubic (y)	Equation of line	m/o CaO 100 % cubic	m/o CaO 0 % cubic
A*	10	3.91	infinite	0	} $y = 10.28x - 40.19$	13.64	3.91
A	10	12.5	0.143	88.3			
B*	17.5	7.51	infinite	0	} $y = 12.06x - 90.57$	15.80	7.51
B	17.5	14.5	14.5	0.2			
C*	25	11.11	infinite	0	} $y = 15.6x - 173.3$	17.5	11.11
C	25	17.5	0	100			

Table 18. Quantitative X-Ray Data for Long-Term Samples at 1300 °C

Sample	m/o $\text{Al}_2\text{O}_3$	m/o CaO (x)	wt. mono wt. cubic	m/o cubic (y)	Equation of line	m/o CaO 100 % cubic	m/o 0 % cubic
A*	10	3.91	infinite	0	} $y = 8.49x - 33.18$	15.7	3.91
A	10	12.5	0.47	72.9			
B*	17.5	7.51	infinite	0	} $y = 10.43x - 78.32$	17.10	7.51
B	17.5	14.5	0.47	72.9			
C*	25	11.11	infinite	0	} $y = 13.38x - 148.7$	18.6	11.11
C	25	17.5	0.235	85.5			

\* Mole percent CaO at 0 mole percent cubic  $\text{ZrO}_2$  was calculated from Equation (10).

## APPENDIX D

QUANTITATIVE CHANGES IN CUBIC TO MONOCLINIC ZIRCONIA CONTENTS  
FOR LONG TERM FIRINGS

The weight ratio of cubic to cubic plus monoclinic zirconia contained in each of the long term fired samples was determined by X-ray diffraction and is recorded in Table 19.

Table 19. Ratios of Cubic to Cubic plus Monoclinic Zirconia for Compositions A, B, and C Fired at 900 °C and 1300 °C for up to 2000 Hours

Time (Hours)	900 °C			1300 °C		
	A	B	C	A	B	C
0	0.88	0.83	1.0	0.88	0.83	1.0
200	0.89	0.88	0.98	0.88	0.84	0.94
400	0.91	0.83	1.0	0.76	0.77	0.89
600	0.88	0.84	1.0	0.73	0.78	0.86
800	0.91	0.87	1.0	0.70	0.78	0.83
1000	0.91	0.84	1.0	0.72	0.69	0.81
1200	0.88	0.84	0.98	0.72	0.70	0.82
1400	0.89	0.81	0.97	0.71	0.69	0.88
1600	0.87	0.87	0.96	0.61	0.66	0.80
1800	0.89	0.85	0.97	0.72	0.71	0.81
2000	0.85	0.84	0.95	0.73	0.69	0.83

## REFERENCES

1. A. S. Berezhnoi and R. A. Kordyuk, "Melting Diagram of the System  $\text{CaO-Al}_2\text{O}_3\text{-ZrO}_2$ ," Dopovidi Akademii Nauk Ukrainskoi RSR, No. 10, 1344 - 1347 (1963).
2. A. S. Berezhnoi and R. A. (Kordyuk) Tarnopol'skaya, "Calcium Alumino-zirconate - A New Hydraulic Binder," Izvestiya Akademii Nauk SSSR Neorganicheskie Materialy, 4 (12) 2151-2154 (1968).
3. R. A. Tarnopol'skaya and N. V. Gul'ko, "The  $\text{CaO-SrO-Al}_2\text{O}_3\text{-ZrO}_2$  System and Its Importance for Refractories Technology," Ogneupory, No. 12, 38-42 (1967).
4. N. I. Voronin, V. S. Gorodetskii, and E. P. Fedorova, "Effect of Impurities on Stabilization of Zirconium Dioxide with Magnesium Dioxide and the Technical Properties of Zirconium Products," Trudy Vsesoyuznyi Inst. Nauch-Issled. Proekt. Rab. Ogneupory Prom., No. 37, 81 (1965). In Chemical Abstracts (66-98068p).
5. Antonio Cocco, "Sull'azione Esercitata da Piccole Percentuali de  $\text{Al}_2\text{O}_3$  sui Limiti di Composizione della Fase con Struttura Cubica Costituata da  $\text{CaO}$  e  $\text{ZrO}_2$ ," La Chimica e L'Industria, 42 (2) 142- 145 (1960).
6. Hiroyoshi Takagi, et al., Effects of Alumina on Sintering of Zirconia Stabilized with Calcia," Sprechsaal fuer Keramik, Glas, Baustoffe, 107 (13) 584-588 (1974).
7. Kenneth Shaw, Refractories and Their Uses. John Wiley & Sons, New York, 1972, p. 151.
8. Pol Duwez and Francis Odell, "Phase Relationships in the System Zirconia-Ceria," Journal of the American Ceramic Society, 33 (9) 274-283 (1950).
9. Pol Duwez, Francis Odell, and Frank H. Brown, Jr., "Stabilization of Zirconia with Calcia and Magnesia," Journal of the American Ceramic Society, 51 (10) 553-556 (1968).
10. Ronald C. Garvie, "The Cubic Field in the System  $\text{CaO-ZrO}_2$ ," Journal of the American Ceramic Society, 51 (10) 553-556 (1968).
11. B. C. Weber, et al., "Observations on the Stabilization of Zirconia," Journal of the American Ceramic Society, 39 (6) 197-207 (1956).

12. A. M. Gavrish, et al., "X-Ray Diffraction Investigation of the Decomposition Solid Solutions Based on Zirconium Dioxide," Izvestiya Akademii Nauk SSSR Neorganicheskie Materialy, 5 (9) 1584-1588 (1969).
13. W. D. Kingery, Introduction to Ceramics. John Wiley & Sons, New York, 1960, p. 151.
14. R. W. Nurse, J. H. Welch, and A. J. Mujumdar, "The  $\text{CaO-Al}_2\text{O}_3$  System in a Moisture Free Atmosphere," Transactions of the British Ceramic Society, 64 409-418 (1965).
15. F. M. Lea and C. H. Desch, The Chemistry of Cement and Concrete, 2d ed. Edward Arnold & Co., London, 1956, p. 52.
16. D. Brooksbank, "Thermal Expansion of Calcium-Aluminate Inclusions and Relation to Tessellated Stresses," Journal of the Iron and Steel Institute, 208 495-499 (1970).
17. A. Auriol, Phase Diagrams for Ceramists, American Ceramic Society, Columbus, Ohio, 1964, p. 102, fig. 232.
18. Powder Diffraction File, Joint Committee on Powder Diffraction Standards, Philadelphia, 1960, cards 7-82 and 1-572.
19. G. R. Rigby and A. T. Green, "The Thermal Expansion Characteristics of the Calcium Aluminates and Calcium Ferrites," Transactions of the British Ceramic Society, 42 (5) 95-103 (1943).
20. Julian R. Goldsmith, "The Compound  $\text{CaO} \cdot 2\text{Al}_2\text{O}_3$ ," Journal of Geology, 56 80-81 (1948).
21. B. Tavisci, "Constitution of Portland Cement Clinker," Tonindustrie-Zeitung 61 717-719 (1937).
22. E. R. Boyko and L. G. Wisnyi, "The Optical Properties and Structures of  $\text{CaO} \cdot 2\text{Al}_2\text{O}_3$  and  $\text{SrO} \cdot 2\text{Al}_2\text{O}_3$ ," Acta Crystallographica 11 444-445 (1958).
23. P. J. Baldock, et al., "X-Ray Powder Diffraction Data for Calcium Monoaluminate and Calcium Dialuminate," Journal of Applied Crystallography, 3 188-191 (1970).
24. Woldemar A. Weyl and Evelyn C. Marboe, The Constitution of Glasses, Interscience Publishers, New York, 1962, p. 30.
25. Hans W. Hennicke and Horst Vaupel, "The Stabilization of Zirconium Dioxide with Aluminum Dioxide," Tonindustrie-Zeitung, 94 45-50 (1970).
26. R. E. Thoma, "Determination of Phase Diagrams," Handbook of X-rays E. F. Kaeble, McGraw Hill, New York, 1964, chapter 20.



27. Leonid V. Azaroff, Elements of X-Ray Crystallography, McGraw-Hill, New York, 1968. p. 517.
28. J. K. Cochran, Private Communication, Georgia Institute of Technology, Atlanta, Ga., March, 1976.
29. S. W. Freiman, "Applied Stereology," c. 19 in Characterization of Ceramics, ed. L. L. Hench, Marcel Dekker, Inc., New York, 1971, p. 569.

E-18-612

INVESTIGATION OF LONG TERM,  
HIGH-TEMPERATURE CHANGES IN THE  
CALCIA-STABILIZED ZIRCONIA-ALUMINA SYSTEM

QUARTERLY PROGRESS REPORT NO.7  
JANUARY 1, 1977 THROUGH MARCH 31, 1977

SUBMITTED TO:  
U.S. BUREAU OF MINES -- METALLURGY  
WASHINGTON, D.C. 20240

GRANT NUMBER G0155189

SUBMITTED BY:  
JAMES F. BENZEL  
SCHOOL OF CERAMIC ENGINEERING  
GEORGIA INSTITUTE OF TECHNOLOGY  
ATLANTA, GEORGIA 30032

INVESTIGATION OF LONG TERM,  
HIGH-TEMPERATURE CHANGES IN THE  
CALCIA-STABILIZED ZIRCONIA-ALUMINA SYSTEM

Quarterly Progress Report #7  
January 1, 1977 through March 31, 1977

INTRODUCTION

The purpose of this investigation is to measure microstructural and phase changes in the CaO-stabilized  $\text{ZrO}_2\text{-Al}_2\text{O}_3$  system after heat treatment as high as  $1300^\circ\text{C}$  for up to 2000 hours. In addition, high temperature flexural strength, thermal expansion, and room temperature microhardness has been investigated in an attempt to correlate these properties to microstructure and phase changes.

The original intent of this work was to investigate compositions of high stabilized zirconia content plus  $\text{Al}_2\text{O}_3$ . Phase relations for the  $\text{CaO-Al}_2\text{O}_3\text{-ZrO}_2$  ternary were not available. Thus, prior to selection of compositions for long term heat treatment, the phase relations in the high zirconia (greater than or equal to 55 w/o) portion of the ternary were established and were reported in Quarterlies 1-4.

Based on the results from the phase diagram study, three compositions (identified as A, B and C) in the  $\text{CA}_2$ -cubic

prepared as thermal expansion samples. This was accomplished by making two parallel cuts one-half inch apart across the flat face of each pellet with a diamond wafering machine. The pellet was then rotated  $90^{\circ}$  and sliced in half so that two one-half inch long pieces with flat and parallel ends were produced.

These two pieces were then carefully placed end to end, in an Orton Automatic Recording Dilatometer, to produce the required one inch specimen. The percent elongation and contraction of each sample was then determined by heating and cooling them to  $1200^{\circ}\text{C}$  at a controlled rate of  $\approx 4^{\circ}\text{C}/\text{minute}$ .

## RESULTS AND DISCUSSION

Typical dilatometer traces for as-fired pellets of compositions A, B and C are shown in Figures 1-3. No monoclinic  $\text{ZrO}_2$  was detected by x-ray diffraction for composition C. The "as-fired" expansion curves confirmed the absence of monoclinic  $\text{ZrO}_2$  in the C pellet and the presence of appreciable monoclinic  $\text{ZrO}_2$  in the A and B pellets.

The results obtained from the as-fired, heat treated at  $900^{\circ}\text{C}$  and heat treated at  $1300^{\circ}$  thermal expansion runs are summarized in Tables I and II respectively. X-ray results (Reported in Quarterly No. 5) indicated that the amount of monoclinic  $\text{ZrO}_2$  present in composition A and B pellets increased slowly with heat treatment time at  $900^{\circ}\text{C}$ . The size of the

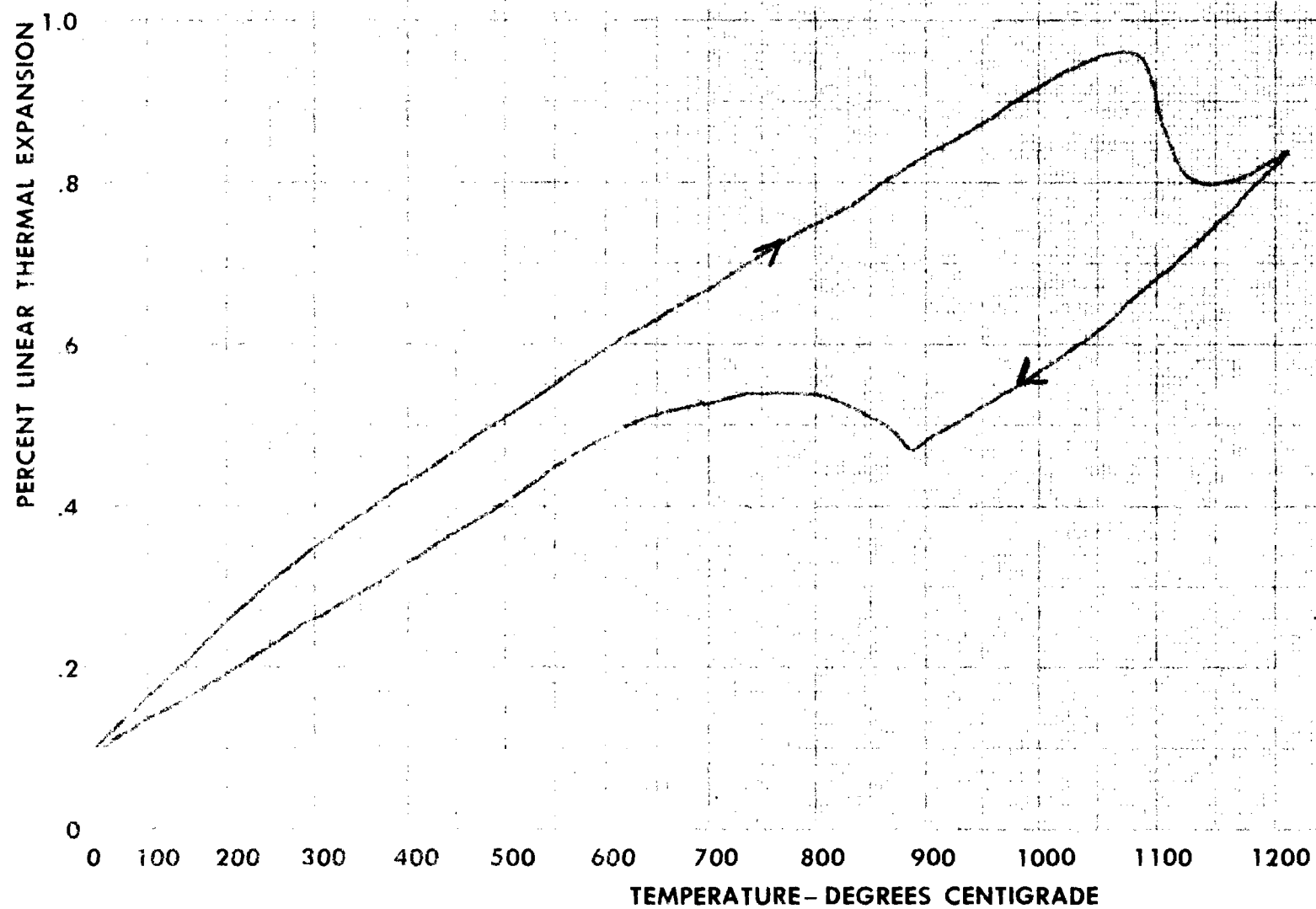


Figure 1. Thermal Expansion and Contraction Curve for As-Fired Composition A Sample.

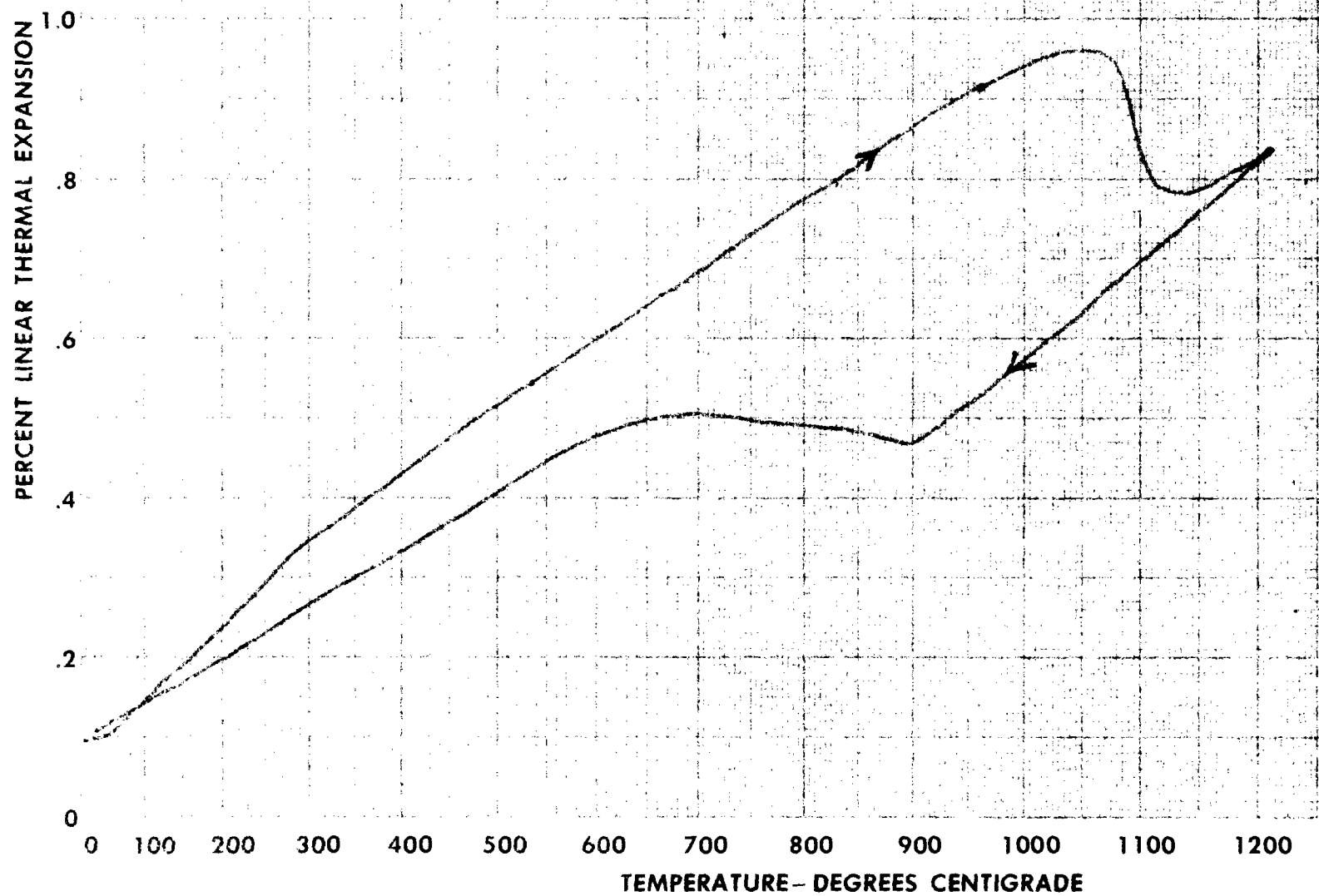


Figure 2. Thermal Expansion and Contraction Curve for As-Fired Composition B Sample

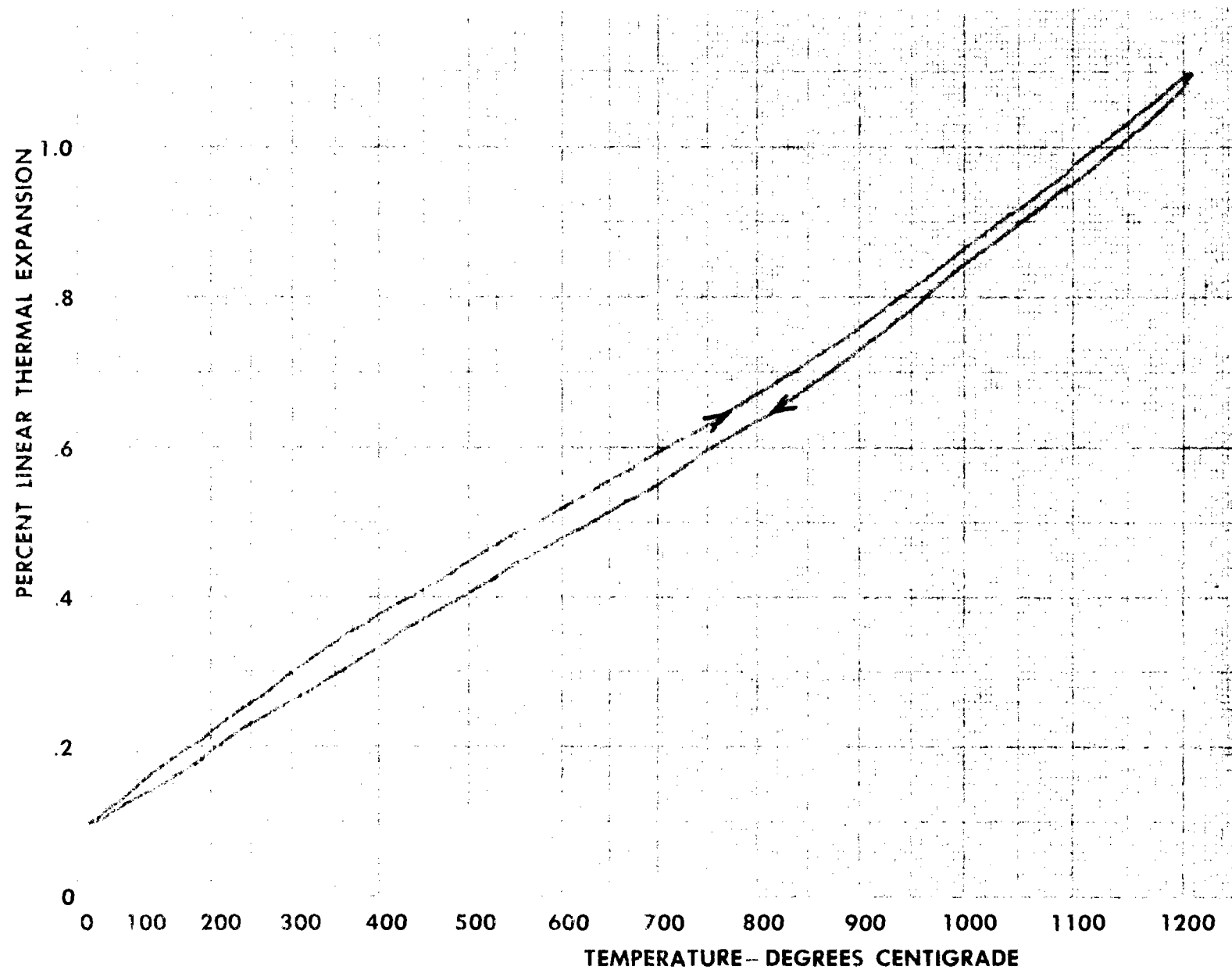


Figure 3. Thermal Expansion and Contraction Curve for As-Fired Composition C Sample.

Table I. Thermal Expansion Results of Samples  
Heat Treated at 900°C

Composition	Time (Hrs)	ZrO <sub>2</sub> Temperature	Inversion (°C)	Size (Linear %)	Thermal Expansion (20°C - 1020°C) (10 <sup>-6</sup> cm/cm/°C)
		On Heating	On Cooling		
A	0*	1055	855	-0.166	8.34
	200	1065	897	-0.149	9.27
	1000	1075	900	-0.155	8.99
	2000	1090	881	-0.181	8.33
B	0*	1043	894	-0.172	8.56
	200	1056	890	-0.076	8.82
	1000	1065	905	-0.097	9.80
	2000	1077	895	-0.197	9.80
C	0*	N/A	N/A	0	7.81
	200	N/A	N/A	0	9.79
	1000	N/A	N/A	0	9.30
	2000	N/A	N/A	0	9.06

\* As-Fired



Table II. Thermal Expansion Results of Samples  
Heat Treated at 1300°C

Composition	Time	ZrO <sub>2</sub> Inversion		Size (Linear%)	Thermal Expansion (20°C - 1020°C) (10 <sup>-6</sup> cm/cm/°C)
		Temperature On Heating	(°C) On Cooling		
A	0*	1055	855	-0.166	8.34
	200	1078	-	-0.218	8.83
	400	1088	925	-0.292	7.30
	1000	1095	943	-0.286	7.59
	1400	1089	935	-0.325	8.21
B	0*	1043	894	-0.172	8.56
	200	1074	923	-0.248	7.98
	400	1078	917	-0.289	7.57
	1000	1079	930	-0.203	7.29
	1400	1078	922	-0.329	8.22
C	0*	N/A	N/A	0	7.81
	200	N/A	N/A	0	8.11
	400	1040	730	-0.008	7.46
	1000	1065	805	-0.022	7.33
	1400	1085	785	-0.041	8.23

\*As-Fired

inversion contraction measured on heat-up also shows this trend but the two low values observed for the B pellets heat treated for 200 and 1000 hours can not be explained. There also appears to be an increase in the heat-up inversion temperature for these two compositions as heat treatment time at 900°C is increased. No monoclinic inversion was detected on composition C expansion curves even after 2000 hours at 900°C. X-ray data indicated that the amount of monoclinic  $\text{ZrO}_2$  in composition C pellets increased from 0 at about 1000<sup>o</sup> hours to 3.5 w/o after 2000 hours. It appears that more than 3.5 w/o monoclinic  $\text{ZrO}_2$  must be present to be detected by dilatometry.

The thermal expansion curves for the samples of all three compositions heat treated at 1300°C also appear to indicate the inversion temperature on heating slowly increased as the length of the heat treatment increased. This trend may be due to the loss of CaO from the  $\text{ZrO}_2$  portion of the samples, since it has been reported in the literature (Ref. 1) that the transformation temperature decreased as the CaO content was increased up to 16 m/o.

The amount of monoclinic  $\text{ZrO}_2$  present as evidenced by increasing contraction (due to the inversion) on the expansion curves indicates that cubic  $\text{ZrO}_2$  is being converted to monoclinic  $\text{ZrO}_2$  more rapidly at 1300°C than at 900°C (See Tables I and II). The x-ray analysis of composition C samples indicated

that there was 8 w/o monoclinic  $\text{ZrO}_2$  present in the C samples after they had been heat treated at  $1300^\circ\text{C}$  for 400 hours. The inversion reported for these conditions in Table II (-0.008%) was just detectable on the expansion curve. Thus the threshold for detecting monoclinic  $\text{ZrO}_2$  by dilatometry must be about 8 w/o.

No well defined trends between the linear thermal expansion coefficient ( $20$ - $1020^\circ\text{C}$ ) and heat treatment cycles were detected. A possible explanation for the apparent randomness of the thermal expansion coefficients could be the presence of strains in the samples. The presence of strain was demonstrated in Quarterly No. 4, where the cubic  $\text{ZrO}_2$  lattice parameters decreased in size on grinding as-fired pellets of A, B and C.

#### REFERENCE

1. P. Duwey, F. Odell and F.H. Brown, Jr., "Stabilization of Zirconia with Calcia and Magnesia," J. Am. Ceram. Soc., (51) 553-56 (1968).

*Corrected  
Copy*

# INVESTIGATION OF LONG TERM HIGH-TEMPERATURE CHANGES IN THE CALCIA-STABILIZED ZIRCONIA- ALUMINA SYSTEM

## FINAL TECHNICAL REPORT

June 15, 1975 through June 15, 1977

### Project Director

J. K. Cochran

### Principal Investigators

J. F. Benzel

J. Day

J. D. Lee

B. H. Kim

### Sponsored by

U. S. Department of Interior, Washington, D. C.

Grant Number G0155189

August 1977

1977



School of Ceramic Engineering  
Georgia Institute of Technology  
Atlanta, Georgia 30332

INVESTIGATION OF LONG TERM HIGH-TEMPERATURE CHANGES  
IN THE CALCIA-STABILIZED ZIRCONIA-ALUMINA SYSTEM

FINAL TECHNICAL REPORT

June 15, 1975 through June 15, 1977

Project Director

J.K. Cochran

Principal Investigators

J.F. Benzel

J. Day

J.D. Lee

B.H. Kim

Sponsored by

U.S. Department of Interior,  
Bureau of Mines, Washington, D.C.

Grant Number G0155189

August 1977

School of Ceramic Engineering  
Georgia Institute of Technology  
Atlanta, Georgia 30332

### Foreword

This research was supported by the U.S. Department of Interior, Bureau of Mines, Washington, D.C., under Grant Number G0155189 and was monitored by the Bureau of Mines - Tuscaloosa, Metallurgy Research Center, Tuscaloosa, Alabama.

The views and conclusions contained in this document are those of the authors and should not be interpreted as necessarily representing the official policies or recommendations of the Interior Departments' Bureau of Mines or of the U.S. Government.

### Abstract

A  $\text{CaO-Al}_2\text{O}_3\text{-ZrO}_2$  refractory of high zirconia content may become useful in new **pyrometallurgical** applications because of the good corrosion resistant characteristics of the components. No complete phase diagram has been available for this system and information on long term high temperature stability has been lacking for these compositions. In this study, the ternary phase diagram was developed and long term high temperature stability was investigated.

To develop the phase diagram, compositions were fired to  $1500^\circ\text{C}$  and compatibility triangles were drawn from qualitative and quantitative x-ray diffraction analysis. Solubility of  $\text{Al}_2\text{O}_3$  in  $\text{CaO}$  stabilized  $\text{ZrO}_2$  and  $\text{ZrO}_2$  in calcium dialuminate,  $\text{CA}_2$ , was observed optically to be less than 0.5 m/o.  $\text{CA}_2$  was shown to be one of the equilibrium phases over most of the high  $\text{ZrO}_2$  region of the ternary.

Heat treatments of selected high  $\text{ZrO}_2$  compositions for up to 2000 hours at 900 and  $1300^\circ\text{C}$  showed that the minimum  $\text{CaO}$  necessary to stabilize cubic  $\text{ZrO}_2$  was a

function of temperature. The changing CaO solubility resulted in changing cubic and monoclinic  $\text{ZrO}_2$  contents with temperature. At  $1300^\circ\text{C}$ , 1000 hours was required for the cubic and monoclinic  $\text{ZrO}_2$  contents to stabilize. This was shown with quantitative x-ray diffraction and lattice parameter measurements on the cubic  $\text{ZrO}_2$ .

Room temperature and high temperature flexure strength, Knoop's microhardness, and microstructure were shown to be independent of the long term heat treatments. Thermal expansion characteristics did vary with heat treatment and correlated to the changing quantities of cubic and monoclinic  $\text{ZrO}_2$ .

Properties of  $\text{CA}_2$  were measured and the microstructure was observed.  $\text{CA}_2$  was shown not to be detrimental to the properties of high  $\text{ZrO}_2$  compositions except for a reduction in the useful temperature of the material. The solidus temperature of CaO stabilized  $\text{ZrO}_2$  was below  $1700^\circ\text{C}$  in the presence of  $\text{CA}_2$ .



TABLE OF CONTENTS	<u>Page</u>
FORWORD	i
ABSTRACT	ii
LIST OF TABLES	vii
LIST OF ILLUSTRATIONS	ix
SECTION	
I.    INTRODUCTION	1
II.   BACKGROUND LITERATURE	3
A.   CaO-Al <sub>2</sub> O <sub>3</sub> -ZrO <sub>2</sub>	3
B.   ZrO <sub>2</sub> -CaO	7
C.   CaO-Al <sub>2</sub> O <sub>3</sub>	18
D.   Al <sub>2</sub> O <sub>3</sub> -ZrO <sub>2</sub>	22
E.   The Disappearing Phase Method of Phase Diagram Determination	25
III.  EXPERIMENTAL PROCEDURES	26
A.   Sample Preparation	27
1.   High ZrO <sub>2</sub> Phase Diagram Samples	27
2.   Compositions Surrounding CaO·2Al <sub>2</sub> O <sub>3</sub>	32
3.   Long Term, Heat Treatment Samples	34
4.   CA <sub>2</sub> Physical Property Samples	35
B.   X-ray Diffraction Analysis	36
1.   Qualitative X-ray Analysis	36
2.   Quantitative X-ray Analysis	37
3.   Lattice Parameter Measurement	38

## TABLE OF CONTENTS (Continued)

	<u>Page</u>
C. Quantitative Optical Determination	42
D. Density Determination	42
E. Thermal Expansion Measurements	43
F. Flexure Strength Measurements	43
G. Knoop's Microhardness Measurements	44
IV. RESULTS AND DISCUSSION	46
A. CaO-Al <sub>2</sub> O <sub>3</sub> -ZrO <sub>2</sub> Phase Diagram at 1500°C	47
1. Qualitative Phase Diagram for High ZrO <sub>2</sub> Portion of Ternary	47
2. Quantitative Verification of Equilibrium at 1500°C	49
3. Alumina Solubility in Cubic and Monoclinic Zirconia	54
4. Phase Diagram Surrounding CA <sub>2</sub>	59
5. Complete CaO-Al <sub>2</sub> O <sub>3</sub> -ZrO <sub>2</sub> Phase Diagram at 1500°C	62
B. Long Term, High Temperature Phase Stability	65
1. Quantitative X-ray Analysis	65
2. Lattice Parameter Determinations for Cubic Zirconia	73
C. Long Term, High Temperature Property Changes	76
1. Properties of Calcium Dialuminate, CA <sub>2</sub>	76
2. Flexure Strength of High ZrO <sub>2</sub> Compositions	79
3. Microhardness of High ZrO <sub>2</sub> Compositions	94
4. Microstructure of High ZrO <sub>2</sub> Compositions	99
5. Thermal Expansion of High ZrO <sub>2</sub> Composition	103
D. Liquid Formation in CaO-Al <sub>2</sub> O <sub>3</sub> -ZrO <sub>2</sub> at 1700°C	106

## TABLE OF CONTENTS (Continued)

	<u>Page</u>
V. SUMMARY	110
APPENDICES	113
A. SYSTEMATIC POINT COUNTING TECHNIQUE	113
B. PHASE ANALYSIS OF COMPOSITIONS FIRED AT 1500°C	115
C. DATA FOR CALCULATING CA <sub>2</sub> -CUBIC ZrO <sub>2</sub> AND CA <sub>2</sub> - MONOCLINIC ZrO <sub>2</sub> ALKEMADE LINES	119
D. QUANTITATIVE CHANGES IN CUBIC TO MONOCLINIC ZIRCONIA CONTENTS FOR LONG TERM FIRINGS	127
E. FLEXURE STRENGTH OF HIGH ZrO <sub>2</sub> COMPOSITIONS	128
F. KNOOP'S MICROHARDNESS OF HIGH ZrO <sub>2</sub> COMPOSITIONS	133
REFERENCES	137

LIST OF TABLES

<u>Table</u>	<u>Title</u>	<u>Page</u>
1	X-ray <u>d</u> Spacings <sup>2</sup> for $\text{Ca}_7\text{Al}_6\text{ZrO}_{18}$ .	5
2	Decomposition of the Solid Solutions During Heating in Air.	16
3	Ionic Crystal Radii <sup>13</sup> .	17
4	Powder Diffraction Data for $\text{CaO} \cdot 2\text{Al}_2\text{O}_3$ <sup>23</sup> .	23
5	Composition of Series 1.	28
6	Composition of Series 2.	29
7	Composition of Series 3.	30
8	Composition of Series 4.	30
9	Composition of Series 5.	31
10	Composition of Series 6.	33
11	Composition of Batches for Long Term Firing.	34
12	Optical Data for $\text{CA}_2$ Stoichiometry Determination.	56
14	Flexure Strength of $\text{CaO} \cdot 2\text{Al}_2\text{O}_3$ as a Function of Temperature.	80
15	Room Temperature Microhardness of $\text{CaO} \cdot 2\text{Al}_2\text{O}_3$ .	80
16	Thermal Expansion of $\text{CA}_2$ .	81
17	Compositions of $\text{CaO} \cdot \text{Al}_2\text{O}_3 \cdot \text{ZrO}_2$ . Samples A, B, and C.	84
18	Phase Composition and Optically Determined Phase Volume of Series 1, 1700°C.	108
19	Accuracy of Systematic Point Counting Technique.	114
20	Phase Analysis of Series 2.	116

LIST OF TABLES (Continued)

<u>Table</u>	<u>Title</u>	<u>Page</u>
21	Phase Analysis of Series 3.	117
22	Phase Analysis of Series 5.	117
23	Phase Analysis of Series 6.	118
24	Quantitative X-ray Data for Series 2 and 3, Slow-Cooled.	120
24	Quantitative X-ray Data for Series 2 and 3, Slow-Cooled (Contd).	121
25	Quantitative X-ray Data for Series 2, Quenched.	122
26	Quantitative X-ray Data for Long-Term Samples at 1550°C.	123
27	Quantitative X-ray Data for Long-Term Samples at 1300°C.	124
28	Weight Ratio of Cubic to Cubic + Monoclinic ZrO <sub>2</sub> , Compositions A, B, and C.	127
29	Flexure Strength of As-Fired CaO-Al <sub>2</sub> O <sub>3</sub> -ZrO <sub>2</sub> Compositions A, B, and C, As a Function of Breaking Temperature.	129
30	Flexure Strength of Composition A as a Function of Breaking Temperature For Various Heat Treatment Conditions.	130
31	Flexure Strength of Composition B as a Function of Breaking Temperature for Various Heat Treatment Conditions.	131
32	Flexure Strength of Composition C as a Function of Breaking Temperature for Various Heat Treatment Conditions.	132
33	Room Temperature Microhardness of Composition C After Various Heat Treatments.	134
34	Room Temperature Microhardness of Composition B After Various Heat Treatments.	135
35	Room Temperature Microhardness of Composition A After Various Heat Treatments.	136

LIST OF ILLUSTRATIONS

<u>Figure</u>	<u>Title</u>	<u>Page</u>
1	Phase Diagram of the $\text{CaO-Al}_2\text{O}_3\text{-ZrO}_2$ System as Determined by Berezhnoi <sup>12</sup> .	4
2	Linear Thermal Expansion of Monoclinic Zirconia <sup>8</sup> .	8
3	Phase Diagram of the $\text{CaO-ZrO}_2$ System as Determined by Duwez <sup>9</sup> .	10
4	Effect of the Amount of Calcia on Transformation Temperature from Cubic to Monoclinic Zirconia <sup>9</sup> .	11
5	Lattice Parameter Variations with Solid Solution Changes in Cubic Zirconia <sup>9</sup> .	12
6	Phase Diagram and Lattice Parameter Data for the $\text{CaO-ZrO}_2$ System After Garvie <sup>10</sup> .	14
7	Phase Diagram of the $\text{CaO-Al}_2\text{O}_3$ System as Determined by Lea and Desch <sup>15</sup> .	20
8	Relationship Between Peak Intensities and Weight Ratios of Cubic to Monoclinic Zirconia.	39
9	Lattice Parameter Extrapolation for Composition A Before Heat Treatment.	41
10	Phase Analysis of Samples Fired at $1500^\circ\text{C}$ .	48
11	Extrapolation of Calcia Content to 0% and 100% Cubic Zirconia at Fixed Alumina Contents.	51
12	Cubic Zirconia Alkemade Lines at 20 and 40 Hours Firing at $1500^\circ\text{C}$ , Verifying Equilibrium by Reproducibility of Lines.	53
13	Alkemade Lines Bounding the Cubic + Monoclinic + $\text{CA}_2$ Region at $1500^\circ\text{C}$ .	55
14	Photomicrographs of Series 3, $1500^\circ\text{C}$ , 600x.	57

LIST OF ILLUSTRATIONS (Continued)

<u>Figure</u>	<u>Title</u>	<u>Page</u>
15	Extrapolation of $CA_2$ Composition to 0% Alumina to Determine $Al_2O_3$ Solubility in Zirconia.	58
16	Phase Diagram of the $CaO-Al_2O_3-ZrO_2$ System for Compositions Surrounding $CA_2$ .	60
17	Relative Z-ray Intensity of $CA_6/CA_2$ and $CA/CA_2$ for $CaO-Al_2O_3$ Composition. Note: Lines Should Extrapolate to Zero at $CA_2$ Composition.	61
18	Calcium-Alumina-Zirconia Phase Diagram at $1500^\circ C$ .	63
19	Alkemade Line at $1550^\circ C$ from $CA_2$ to Cubic Zirconia.	67
20	Change in Amount of Cubic Zirconia with Time at $900^\circ C$ .	69
21	Change in Amount of Cubic Zirconia with Time at $1300^\circ C$ .	70
22	Alkemade Line at $1300^\circ C$ from $CA_2$ to Cubic Zirconia.	72
23	Lattice Parameter Changes with Time.	75
24	X-ray Diffraction Trace of $CA_2$ Bars Showing Peaks for $CA_2$ and a Trace of CA (Marked Peaks).	77
25	Reflected Light Micrographs of CA Bars, (a) Polished Structure, (b) Thermally Etched to Show Grain Boundaries, 600X.	78
26	Thermal Expansion of $CA_2$ Containing a Trace of CA ( $CA_2$ Bar) and $CA_2$ Containing a Trace of $CA_6$ (Composition 6-7).	82
27	Change in Monoclinic $ZrO_2$ Content with Time at $900^\circ C$ for $CaO-Al_2O_3-ZrO_2$ Compositions A, B, and C.	85

LIST OF ILLUSTRATIONS (Continued)

<u>Figure</u>	<u>Title</u>	<u>Page</u>
28	Change in Monoclinic $\text{ZrO}_2$ Content with Time at $1300^\circ\text{C}$ for $\text{CaO-Al}_2\text{O}_3\text{-ZrO}_2$ Compositions A, B, and C.	86
29	Effect of Temperature on Flexure Strength of $\text{CaO-Al}_2\text{O}_3\text{-ZrO}_2$ Compositions A, B, and C. Each Point Represents the Average of All Heat Treatment Conditions.	87
30	Effect of Temperature on Flexure Strength of $\text{CaO-Al}_2\text{O}_3\text{-ZrO}_2$ Composition A After Heat Treatments.	89
31	Effect of Temperature on Flexure Strength of $\text{CaO-Al}_2\text{O}_3\text{-ZrO}_2$ Composition B for Various Heat Treatment Conditions.	90
32.	Effect of Temperature on Flexure Strength of $\text{CaO-Al}_2\text{O}_3\text{-ZrO}_2$ Composition C for Various Heat Treatment Conditions.	91
33	Flexure Strength of $\text{CA}_2$ Compared to "As-Fired" Compositions A, B, and C.	93
34	Room Temperature Microhardness of "As-Fired" $\text{CaO-Al}_2\text{O}_3$ Compositions A, B, and C and Compound $\text{CA}_2$ .	95
35	Room Temperature of $\text{CaO-Al}_2\text{O}_3\text{-ZrO}_2$ Composition A After Various Heat Treatments.	96
36	Room Temperature Microhardness of $\text{CaO-Al}_2\text{O}_3\text{-ZrO}_2$ Composition B After Various Heat Treatments.	97
37	Room Temperature Microhardness of $\text{CaO-Al}_2\text{O}_3\text{-ZrO}_2$ Composition C After Various Heat Treatments.	98
38	Reflected Light Micrograph of Microstructure of Composition A (a) "As-Fired" at $1550^\circ\text{C}$ and (b) After Heat Treatment at $1300^\circ\text{C}$ for 2000 Hours; 600X.	100
39	Reflected Light Micrograph of Microstructure of Composition B (a) "As-Fired" at $1550^\circ\text{C}$ and (b) After Heat Treatment at $1300^\circ\text{C}$ for 2000 Hours; 600X.	101



LIST OF ILLUSTRATIONS (Continued)

<u>Figure</u>	<u>Title</u>	<u>Page</u>
40	Reflected Light Micrograph of Microstructure of Composition C (a) "As-Fired" at 1550°C and (b) After Heat Treatment at 1300°C for 2000 Hours; 600X.	102
41	Comparison of Linear Thermal Expansion of Compositions A, B, and C "As-Fired" at 1550°C and After Heat Treatment at 1300°C for 1400 Hours.	104
42	Length Change for Monoclinic to Tetragonal Inversion as a Function of Monoclinic ZrO <sub>2</sub> Content for Samples Shown in Figure 41.	105
43	Expansion of Compositions A, B, and C as a Function of Cubic ZrO <sub>2</sub> Content for Samples Shown in Figure 41.	105
44	Photomicrographs of Series 1, 1700°C, 600X.	107

## SECTION I

### Introduction

One of the major efforts of the U.S. Bureau of Mines has been in the area of developing new pyrometallurgical materials to serve future needs. There are several areas that may require refractory materials with the corrosion resistance of zirconia but at reduced  $\text{ZrO}_2$  contents in a system such as  $\text{CaO-Al}_2\text{O}_3\text{-ZrO}_2$ . Thus, the Department of Interior through the Bureau of Mines initiated a project at Georgia Tech to investigate high  $\text{ZrO}_2$  compositions in the  $\text{CaO-Al}_2\text{O}_3\text{-ZrO}_2$ .

When the program was initiated no phase diagram was available for the  $\text{CaO-Al}_2\text{O}_3\text{-ZrO}_2$  system, therefore most of the first year of the project was devoted to developing the phase diagram in the high  $\text{ZrO}_2$  end of the ternary at  $1500^\circ\text{C}$ . Crystallographic and physical stability of selected high  $\text{ZrO}_2$  compositions were determined for long term, high temperature heat treatments at 900 and  $1300^\circ\text{C}$  for up to 2000 hours. Property changes investigated were room temperature and high

temperature flexure strength, room temperature Knoop's microhardness, and linear thermal expansion. Microstructure of the selected compositions were observed for any changes created by the long term heat treatments.

The phase diagram results indicated that calcium dialuminate  $CA_2$ , was one of the subliquidus equilibrium phases in most of the high  $ZrO_2$  end of the  $CaO-Al_2O_3-ZrO_2$  ternary. Only meager data was available in the literature on the physical properties of  $CA_2$  and such information was needed to evaluate the characteristics of the high  $ZrO_2$  compositions. Therefore quantities of  $CA_2$  were synthesized and the same physical properties were measured as for the selected compositions.

Near the end of the program, an investigation was initiated to determine the liquidus phase diagram for the high  $ZrO_2$  end of the  $CaO-Al_2O_3-ZrO_2$  system. This work is still in progress and has not been reported here. The results will be reported in a Master's degree thesis by Mr. Baek Hee Kim in early 1978. These results will be forwarded to the Bureau of Mines when available because knowledge of the temperature limitations in the system will be required if compositions of this type develop as prime material candidates for coal gasification.

## SECTION II

### Background Literature

Little information has been published for the CaO- $\text{Al}_2\text{O}_3$ - $\text{ZrO}_2$  ternary system and no phase diagram of the high zirconia region has been published detailing the solid solution and polymorphic information. Only Berezhnoi<sup>1</sup> in Russia has published information directly relating to the ternary phase diagram.

In order to gain an understanding of the system from the literature one must study reports about the three binary systems that are involved:  $\text{ZrO}_2$ -CaO,  $\text{Al}_2\text{O}_3$ -CaO, and  $\text{Al}_2\text{O}_3$ - $\text{ZrO}_2$ . The first two of these systems have been well studied, although there remains much contradiction. The third system forms no binary compounds and is thus less complex.

#### A. CaO- $\text{Al}_2\text{O}_3$ - $\text{ZrO}_2$

Berezhnoi<sup>1</sup> has published the only available phase diagram of the ternary system CaO- $\text{Al}_2\text{O}_3$ - $\text{ZrO}_2$ , Figure 1. He was primarily interested in the new ternary compound which he had discovered,  $\text{Ca}_7\text{Al}_6\text{ZrO}_{18}$ , which is a potential hydraulic binder<sup>2</sup>, and thus he did not look at polymorphs of

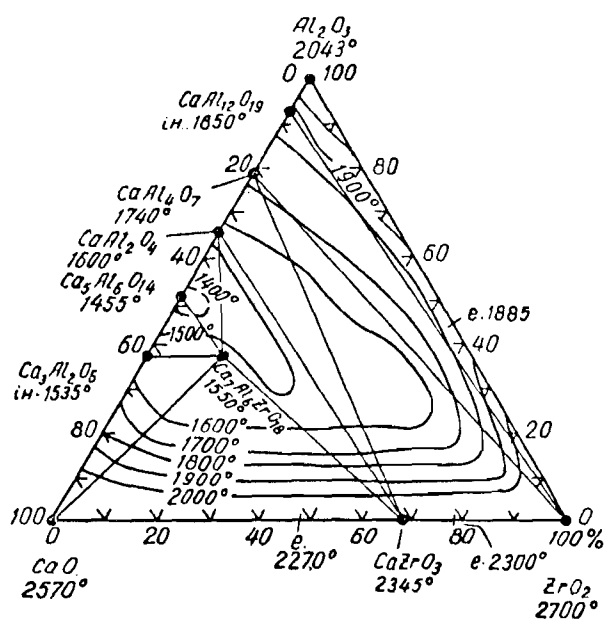


Figure 1. Phase Diagram of the CaO-Al<sub>2</sub>O<sub>3</sub>-ZrO<sub>2</sub> System as Determined by Berezhnoi<sup>1</sup>

zirconia or at the solid solution structure of zirconia.

$\text{Ca}_7\text{Al}_6\text{ZrO}_{18}$  was found to be a useful binder in the hydrated state. It is the first known substance containing  $\text{ZrO}_2$  to exhibit such properties, according to Berezhnoi. The new compound was prepared from high purity silica chalk, technical grade alumina, and zirconia which were mixed and fired to a temperature of  $1400^\circ\text{C}$  to  $1460^\circ\text{C}$ . Synthesis required one hour at  $1450^\circ\text{C}$ . It melts incongruently at  $1550^\circ\text{C}$  (with the formation of  $\text{CaZrO}_3$ ), has a density of 3.1 g/cc, and a linear thermal expansion coefficient of  $8.7 \times 10^{-6}$  ( $20$ - $1000^\circ\text{C}$ ). X-ray  $d$  spacing information is reproduced in Table I.

Table 1. X-ray  $d$  Spacings<sup>2</sup> for  $\text{Ca}_7\text{Al}_6\text{ZrO}_{18}$ .

$d$ (Å)	I	$d$ (Å)	I	$d$ (Å)	I
7.61	10	2.218	6	1.829	12
4.10	10	2.177	6	1.669	5
3.42	29	2.114	4	1.647	6
3.36	10	2.081	5	1.628	5
2.758	10	1.945	5	1.565	19
2.696	100	1.918	16	1.555	10
2.647	26	1.889	22	1.537	11
2.305	5	1.863	12	1.507	5

Tarnopol'skaya and Gul'ko<sup>3</sup> have published some basic information concerning the quaternary system  $\text{CaO-SrO-Al}_2\text{O}_3\text{-ZrO}_2$ . Their investigation was limited to studying the compounds present in the system and possible uses of them as refractories. They confirmed the existence of  $\text{Ca}_7\text{Al}_6\text{ZrO}_{18}$

but presented no other information useful to the study of the ternary.

N.I. Voronin<sup>4</sup> commented that an alumina impurity in zirconia may improve the heat resistance of zirconia when it is stabilized with magnesia, but apparently he did not work with calcia stabilized zirconia.

Antonio Cocco<sup>5</sup> reported that up to three percent alumina could enter the structure of calcia stabilized zirconia without affecting that structure. His work was at temperatures from 1400°C to 1700°C but only compositions of more than 29 mole percent calcia were investigated, which limited his study to the phase region of cubic zirconia and  $\text{CaZrO}_3$ .

Takagi<sup>6</sup> investigated the effect of alumina on the sintering of calcia stabilized zirconia. For raw materials he used zirconium oxychloride, calcium carbonate, and aluminum nitrate. Sixteen mole percent calcia was used to stabilize the zirconia phase. The samples were fired in air at 1700°C for one hour. He discovered that the addition of from 0.5 to 4 weight percent of alumina enhanced the sintering of the zirconia. The zirconia grain size was about 50 microns for additions of from two to four weight percent alumina. The only calcium aluminate phase observed was  $\text{CA}_6$  in both scanning electron microscope analysis and electron probe x-ray microanalysis.

### B. $\text{ZrO}_2\text{-CaO}$

Zirconia has a melting point of  $2680 \pm 20^\circ\text{C}$  and therefore would appear to be very useful as a refractory,<sup>7</sup> especially since it has good corrosion resistance and high strength. Its density is 5.89 g/cc. It has low thermal conductivity and does not react with most metals nor is it easily wetted by molten glass. However, at  $1000^\circ\text{C}$  there is a destructive transformation which makes zirconia a poor refractory in its pure state. Below  $1000^\circ\text{C}$  zirconia has a monoclinic crystal structure. At  $1000^\circ\text{C}$  it transforms rapidly into a tetragonal structure with a significant density change and thus destructive thermal expansion. Figure 2 shows the effect of heating zirconia through this transformation.

To combat this transformation in zirconia which causes destructive cracking, one of several different oxides may be added to stabilize zirconia. This eliminates, or at least reduces, the effects of the transformation from monoclinic to tetragonal zirconia. In commercial usage, the addition of calcia is most common. If between 16 and 29 mole percent of calcia is added to zirconia, the zirconia forms a cubic solid solution which is stable to room temperature. With the addition of less than 16 percent calcia the zirconia is called partially stabilized, i.e., there



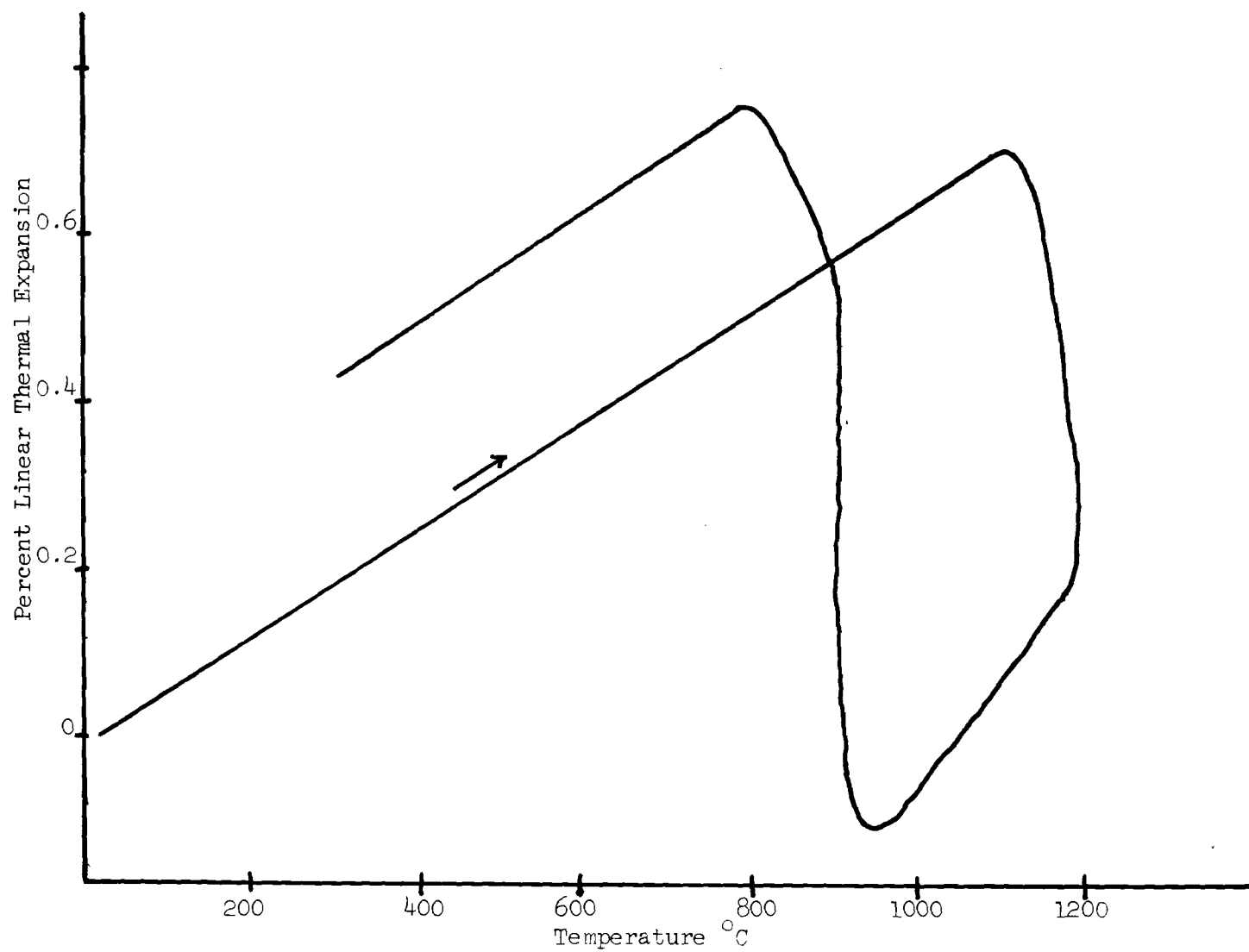


Figure 2. Linear Thermal Expansion of Monoclinic Zirconia<sup>8</sup>

is some cubic solution but also some monoclinic phase in equilibrium; thus the monoclinic to tetragonal transformation can still be seen, but depending on the percentage of calcia, it is less destructive. The melting point is lowered by calcia additions, as shown in the phase diagram, Figure 3.

The stability of calcia stabilized zirconia is excellent. Isothermal tests<sup>9</sup> at 1375°C for 336 hours, 1200°C for 520 hours, 1100°C for 812 hours, 980°C for 1473 hours, and 815°C for 2011 hours showed that there was no loss in stabilization, i.e., no decrease in the amount of cubic zirconia, with long term firing.

Duwez<sup>9</sup> found from differential thermal analysis that the transformation temperature from tetragonal to monoclinic zirconia was lowered as the amount of calcia (up to 16 mole percent) was increased, as shown in Figure 4. This transformation temperature depression was also found in the zirconia-magnesia and zirconia-ceria systems.

Lattice parameter variations as the amount of calcia was changed were also determined by Duwez, Figure 5. For his work the samples were fired at 2000°C. Lattice parameters were determined from high angle reflections only and a 143.2 mm camera was used for diffraction analysis.

Garvie<sup>10</sup> criticized the phase diagram of Duwez and determined a much smaller region of cubic solid solution.

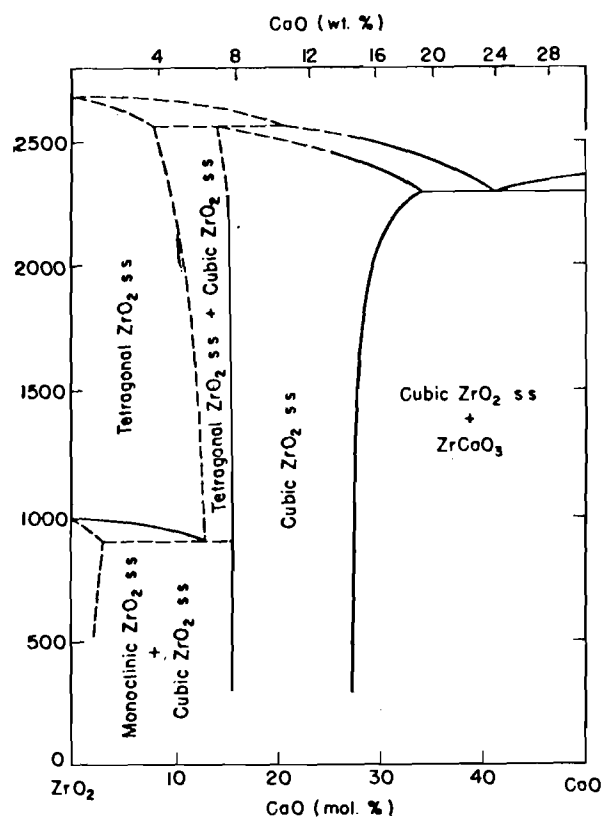


Figure 3. Phase Diagram of the CaO-ZrO<sub>2</sub> System  
as Determined by Duwez<sup>9</sup>

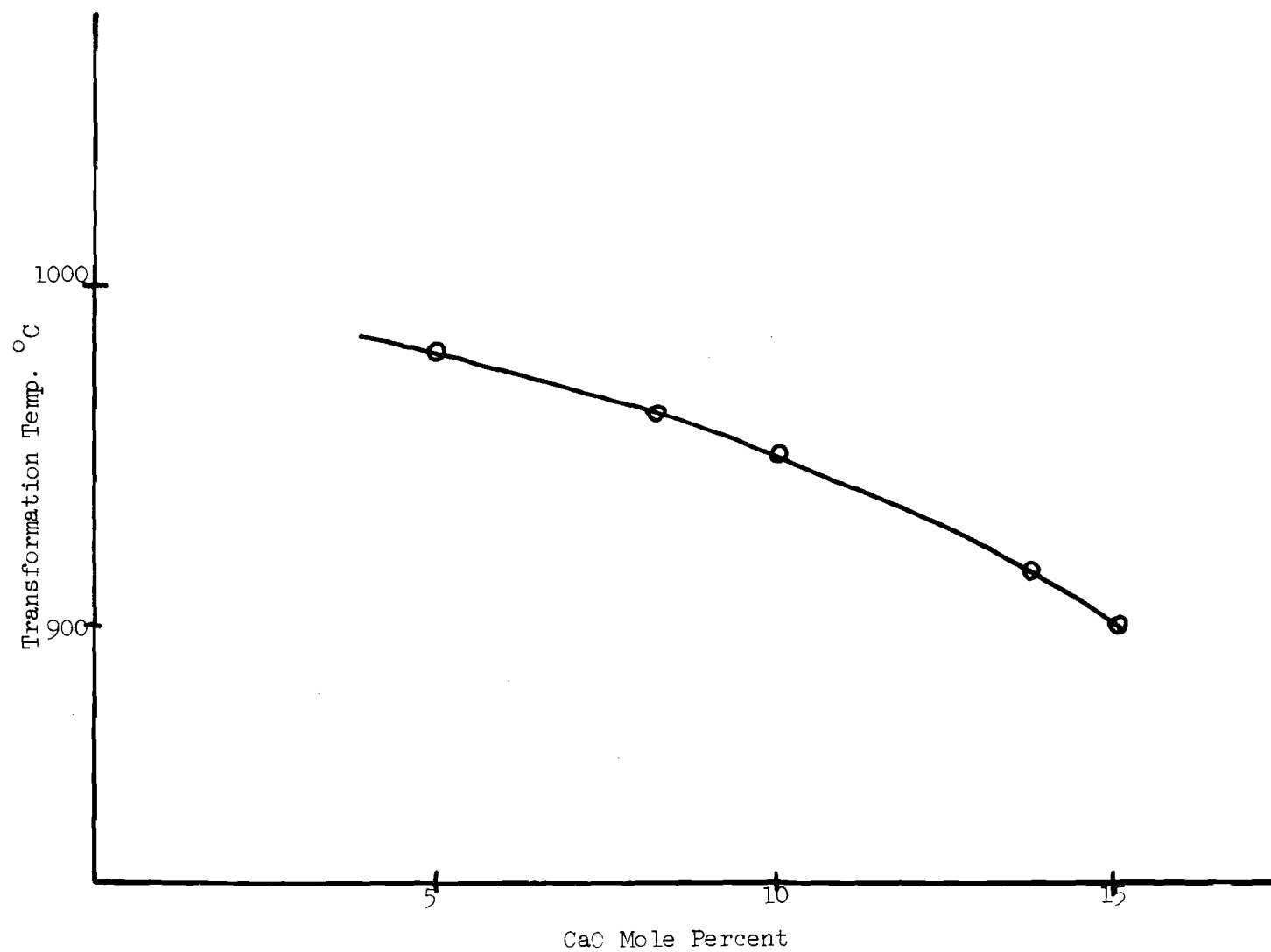


Figure 4. Effect of the Amount of Calcia on Transformation Temperature from Cubic to Monoclinic Zirconia<sup>9</sup>

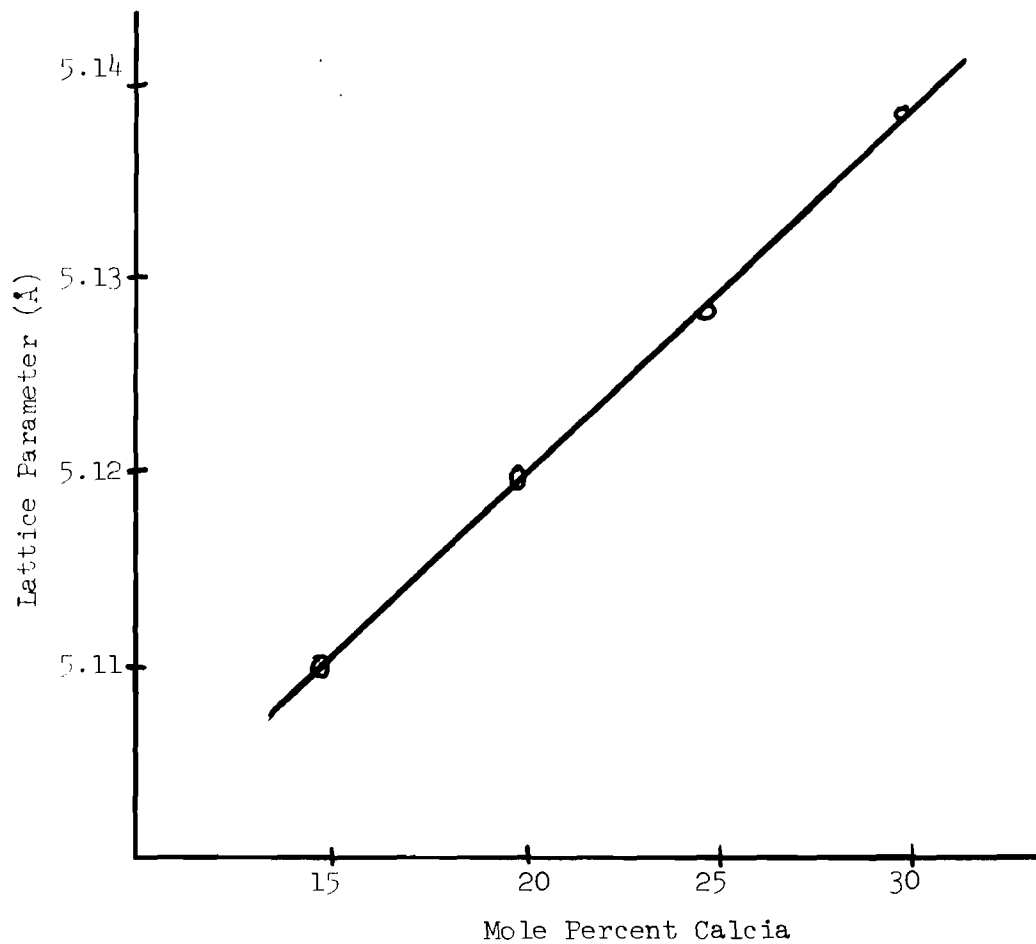


Figure 5. Lattice Parameter Variations with Solid Solution Changes in Cubic Zirconia<sup>9</sup>

He tentatively determined a second CZ compound,  $\text{CaZr}_4\text{O}_9$ , which exists in an alpha form from  $1240^\circ\text{C}$  to  $1650^\circ\text{C}$  and above  $1650^\circ\text{C}$  exists in a beta form. If the cubic phase is metastable, as he asserted from the work of Weber<sup>11</sup>, then there is great difficulty in determining the actual equilibrium phases. Garvie used lattice parameter determinations employing the Nelson-Riley extrapolation and a Debye-Scherrer camera of 114.6 mm diameter to determine changes in the structure of the solid solution. Figure 6 shows his lattice parameter determinations and the resulting phase diagrams, both of which differ considerably from the information published by Duwez<sup>9</sup>.

Garvie discovered that the raw materials used may cause variations in the cubic solid solution. He showed that the use of  $\text{CaCO}_3$  as a reagent resulted in a larger cubic field than the use of  $\text{CaO}$ . He theorized that with  $\text{CaCO}_3$  as a reagent, as the salt decomposed, an active intermediate oxide formed which caused an irreversible metastable formation of the cubic phase. This problem may also partially explain the discrepancies in different phase diagram information that has been published for the system. Garvie also stated that the strain energy involved in the transformation from tetragonal to monoclinic zirconia must be considered an additional degree of freedom. Such an explanation is necessary in order to draw the cubic

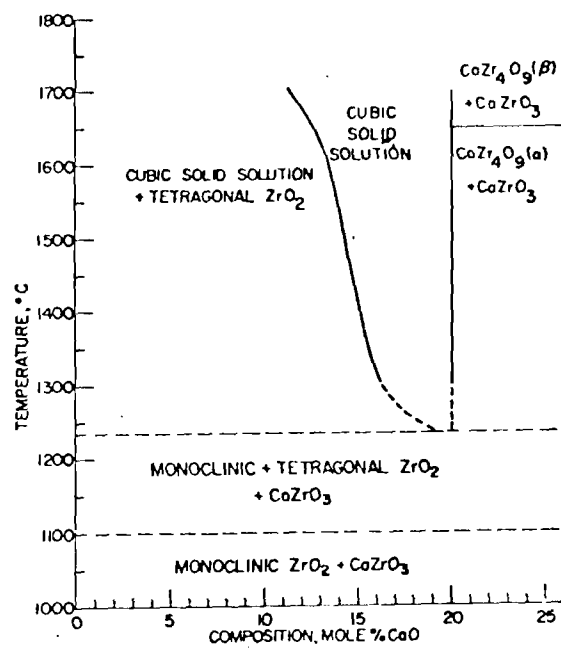
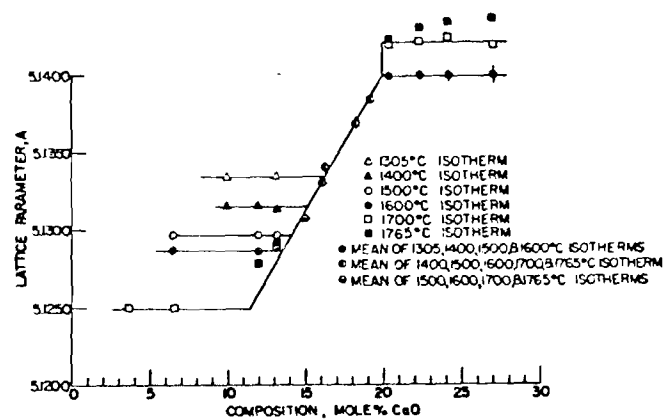


Figure 6. Phase Diagram and Lattice Parameter Data for the CaO- $ZrO_2$  System after Garvie<sup>10</sup>

boundaries as he did at 1200°C and not violate the Gibbs Phase Rule.

Gavrish<sup>12</sup> has also studied the stability of calcia stabilized zirconia. His work indicated that the temperature of maximum destabilization is approximately 1400°C. This, he determined, is also true for yttria stabilization, but for magnesia stabilization the temperature of maximum destabilization is only 1200°C. He determined that yttria stabilized zirconia has the greatest stability and at the lowest mole percent of the three additives, Table 2. Note that his studies extended only 60 hours. For raw materials he used a 99.7% pure zirconia and  $\text{CaZrO}_3$  which had been prepared from zirconia and calcium carbonate. Firing temperature was 1750°C for five hours and the samples were quenched. Phase analysis was by quantitative x-ray diffraction determination. Gavrish theorized that the reason for varying stability of different oxides is related to the size of the different ions, i.e., magnesium is the smallest and yttrium is the largest. The substitution of a small ion into the zirconia lattice increases the stresses more than the substitution of a larger ion more nearly the size of the zirconium ion. The activation energy of the diffusion process is thus decreased and the rate of decomposition is increased. Table 3 lists accepted



Table 2. Decomposition of the Solid Solutions during Heating in Air

Concentration of the oxide additive in mole %		Destabilization at 1200 °C for 60 h.		Destabilization at 1400 °C for 60 h		Destabilization at 1600 °C for 60 h	
		Cubic ZrO <sub>2</sub> , in %	Monoclinic ZrO <sub>2</sub> in %	Cubic ZrO <sub>2</sub> , in %	Monoclinic ZrO <sub>2</sub> in %	Cubic ZrO <sub>2</sub> , in %	Monoclinic ZrO <sub>2</sub> in %
CaO	6	85	15	74	25	93	7
	12	100	0	98	2	100	0
	15	100	0	100	0	100	0
	20	100	0	100	0	100	0
MgO	12	20	80	45	55	100	0
	15	0	100	20	80	100	0
	20	0	100	10	90	100	0
Y <sub>2</sub> O <sub>3</sub>	8	98	2	88	12	91	9
	12	100	0	100	0	100	0
	15	100	0	100	0	100	0

values for various ionic radii.

Table 3. Ionic Crystal Radii<sup>13</sup>

Ion	Al <sup>3+</sup>	Mg <sup>2+</sup>	Zr <sup>4+</sup>	Y <sup>3+</sup>	Ce <sup>4+</sup>	Ca <sup>2+</sup>
Radius (A)	0.51	0.67	0.79	0.92	0.94	0.99

Gavrish also studied the stability of cubic zirconia heated in argon. With calcia and yttria stabilization he found no change in results from those samples heated in air. With magnesia he found that the lattice parameters changed, indicating a change in the structure of the solid solution. It indicated that some of the magnesia was vaporizing from the solid solution. At 2300°C the cubic structure remained only with a composition of 12 mole percent magnesia and the x-ray pattern indicated that there was considerable stress in the structure. The same samples were thermally cycled from 2000°C and 2300°C to room temperature to study destabilization. As in the other experiments, calcia and yttria stabilization proved to be completely stable but the magnesia stabilization was lost, particularly at 2300°C, in a short period of time.

Magnesia has been used commercially to stabilize zirconia. However, at equilibrium the cubic solid solution was found not to exist below approximately 1375°C. Thus, although magnesia stabilized zirconia may be prepared, it

reverts to its unstabilized form with time above  $1000^{\circ}\text{C}$ . Therefore, magnesia stabilization is not generally as useful as calcia stabilization.

The stabilization of zirconia by several other oxides has been studied <sup>8,12</sup>. Many of the rare earths have been used, although on a commercial basis the cost is usually too high. Yttria and ceria are two oxides that may be used successfully. With ceria a different mechanism of stabilization is found. With the addition of greater than 15 mole percent ceria to zirconia the temperature of the monoclinic to tetragonal transformation is lowered below room temperature. There is still a cubic solid solution structure above  $1000^{\circ}\text{C}$  to  $2000^{\circ}\text{C}$ , depending on the composition, but it is not relevant to the stabilization problem, since the destructive transformation does not appear in normal usage.

### C. $\text{CaO-Al}_2\text{O}_3$

The calcia-alumina binary has had much investigation. However, there has been considerable discrepancy about the actual phases that exist at equilibrium. Of particular importance to this study is the compound originally called  $\text{C}_3\text{A}_5$  and more recently determined to be  $\text{CA}_2$ . It is apparent that earlier researchers obtained the same compound but incorrectly determined the stoichiometry. The calcium aluminates are of primary importance to the study of cements and therefore much work has been done with the various hydrated forms. This is generally not relevant to the

calcia-alumina-zirconia ternary system.

As determined by Nurse, et.al.,<sup>14</sup> there are four binary compounds in the  $\text{CaO-Al}_2\text{O}_3$  system:  $\text{C}_3\text{A}$ ,  $\text{CA}$ ,  $\text{CA}_2$ , and  $\text{CA}_6$ . Lea and Desch<sup>15</sup> proposed  $\text{C}_{12}\text{A}_7$ , which Nurse stated is not an anhydrous compound and thus not properly part of the binary system. Nurse determined that thermodynamically a mixture of  $\text{CA}$  and  $\text{C}_3\text{A}$  is more stable than  $\text{C}_{12}\text{A}_7$  up to the melting point of  $\text{C}_{12}\text{A}_7$ , which is  $1392^\circ\text{C}$ . He was not able to prepare completely anhydrous  $\text{C}_{12}\text{A}_7$  and found that the formula is most accurately, at  $950^\circ\text{C}$ ,  $\text{C}_{12}\text{A}_7 \cdot \text{H}_2\text{O}$ . Thus it is most probably that  $\text{C}_{12}\text{A}_7$  is metastable.  $\text{C}_5\text{A}_3$  has also been suggested, possibly as a polymorph of  $\text{C}_{12}\text{A}_7$ . Nurse says that it is metastable. Berezhnoi<sup>1</sup> did show  $\text{C}_5\text{A}_3$  in his ternary diagram. Brooksbank<sup>16</sup> also considered  $\text{C}_{12}\text{A}_7$  to be a part of the binary system.  $\text{CA}_6$  has also been called  $\text{C}_3\text{A}_{16}$  as published by the American Ceramic Society<sup>17</sup>, but generally it has been accepted to have the formula  $\text{CA}_6$ . Figure 7 shows the complete phase diagram as determined by Lea and Desch.<sup>15</sup>

Nurse showed that the four calcium aluminates,  $\text{C}_3\text{A}$ ,  $\text{CA}$ ,  $\text{CA}_2$  and  $\text{CA}_6$ , melt incongruently, although  $\text{CA}$  and  $\text{CA}_2$  are only very slightly incongruent. If  $\text{CA}_2$  were considered to be  $\text{C}_3\text{A}_5$ , then it would have to be shown as a congruently melting compound.

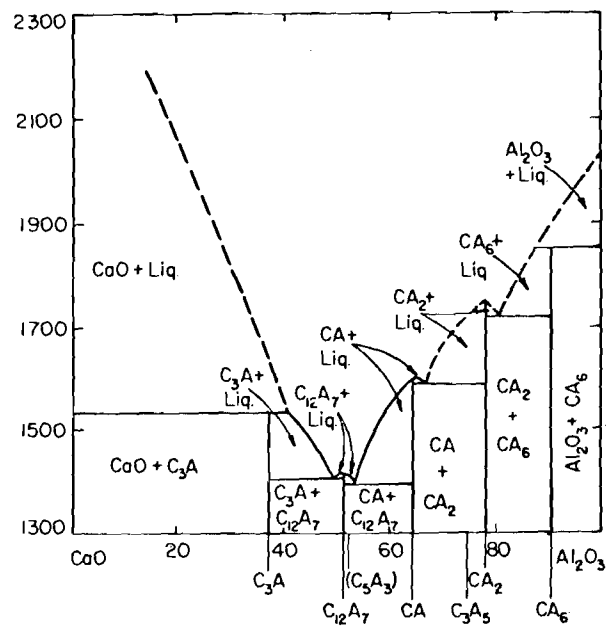


Figure 7. Phase Diagram of the CaO-Al<sub>2</sub>O<sub>3</sub> System as determined by Lea and Desch <sup>15</sup>

An examination of x-ray data published by JCPDS<sup>18</sup> shows that  $CA_2$  and  $C_3A_5$  have been listed with almost identical patterns. This could be understood if one accepted that the real compound is either one or the other, and the remaining stoichiometric formulation is really a solid solution. Brooksbank showed that the linear coefficient of thermal expansion is approximately the same, as determined by authors who claimed to have  $C_3A_5$  and as he determined for what he called  $CA_2$ . His value for thermal expansion was  $5.0 \times 10^{-6}/^{\circ}C$  from  $0^{\circ}C$  to  $800^{\circ}C$ . Rigby and Green<sup>19</sup> determined a value of  $3.5 \times 10^{-6}/^{\circ}C$  from  $100^{\circ}C$  to  $800^{\circ}C$ . They attempted to prepare  $CA_2$  from a stoichiometric mixture, but after heating to  $1530^{\circ}C$  they found the resultant mixture to be  $C_3A_5$  and free alumina, from an optical thin section examination. In their observation CA is the most easily prepared of the calcium aluminates and it is for that reason, they explained, that one could obtain excess CA when starting from a  $CA_2$  stoichiometry. They stated very strongly that their equilibrium state is  $C_3A_5$ .

Goldsmith<sup>20</sup> prepared samples from the melt and found that when  $CA_2$  stoichiometry was used as the starting mixture, only a single phase was observed optically. When  $C_3A_5$  stoichiometry was used, he was two phases. Firing was done at  $1500^{\circ}C$ . Goldsmith's work was done to confirm earlier work of Tavisci<sup>21</sup> and led to similar conclusions.

Wisnyi<sup>22</sup> did considerably work studying  $CA_2$  and it is his x-ray information that is published by JCPDS. Wisnyi determined that the density of  $CA_2$  is 2.86 g/cc. Table 4 shows a comparison between the results of x-ray indexing obtained by Wisnyi and later research done by Baldock.<sup>23</sup> There are no significant disagreements, but enough minor discrepancies to question if the structure of  $CA_2$  is fixed. In preparing  $CA_2$  with a CA impurity of only 0.5 weight percent Baldock used dried analar calcite and gibbsite mixed stoichiometrically and fired for five hours at 1400°C to 1450°C. He used a Phillips diffractometer for x-ray analysis, whereas Wisnyi used a powder camera.

No one has suggested that both  $CA_2$  and  $C_3A_5$  exist in equilibrium or that the structure exists as a solid solution. Since the published x-ray patterns are similar, perhaps this possibility should be considered. The possibility of hydrated products should also be considered, since in other calcium aluminates, hydrates are important phases. The preparation of pure samples is apparently a problem which may also hinder an accurate understanding of the structure and properties of  $CA_2$ .

#### D. $Al_2O_3$ - $ZrO_2$

The  $Al_2O_3$ - $ZrO_2$  binary system has no compounds. If Dietzel's rules concerning cation field strength are considered, this is to be expected. By Dietzel's calculations<sup>24</sup>

Table 4. Powder Diffraction Data for  $\text{CaO} \cdot 2\text{Al}_2\text{O}_3$ 

WICNY1	(ASTM 7-00012)	PRESENT WORK				
d	$1/\lambda_{100}$	h k l	d <sub>obs</sub>	d <sub>calc</sub>	$1/\lambda_{100}$	
6.193	20	1 1 0	7.196	7.2091	$\frac{1}{2}$ B	
		2 0 0	6.161	6.1642	7	
		1 1 -1	4.607	4.6101	3	
4.439	75	0 2 0	4.4416	4.4437	54	
		1 1 1	3.913	3.9164	1	
		3 1 0	3.727	3.7302	$\frac{1}{2}$	
3.609	20	2 2 0	3.604	3.6046	20	
3.520	100	3 1 -1	3.503	3.5020	100	
3.372	5	0 2 1	3.379	3.3801	2	
3.239	20	2 2 -1	3.234	3.2326	7	
3.079	55	4 0 0	3.0340	3.0823	29	
2.882	50	1 3 0	2.882	2.8806	20	
2.760	60	2 2 1	2.753	2.7526	27	
2.717	55	3 1 1	2.712	2.7120	23	
		0 0 2		2.6033		
2.607	85	1 1 -2	2.5989	2.5939	60	
		1 3 -1		2.5965		
2.531	25	4 2 0	2.534	2.5327	13	
		3 1 -2	2.462	2.4621	4	
		1 3 1	2.452	2.4509	3	
2.436	35	5 1 -1	2.436	2.4351	17	
		3 3 0	2.404	2.4032	3	
		4 0 -2	2.350	2.3556	$\frac{1}{2}$ B	
2.350	35	1 1 2	2.325	2.3255	10	
		0 4 0	2.222	2.2219	1	
2.208	40	2 0 2	2.181	2.1815	7	
		2 4 0		2.0903		
		4 2 1		2.0894	2	
		4 2 -2	2.0827	2.0813	2	
		5 1 -2	2.0678	2.0676	6	
2.059	55	6 0 0		2.0549		
		3 3 1	2.0539	2.0531	14	
		0 4 1	2.044	2.0437	4	
		2 4 -1	2.0055	2.0097	2	
2.003	40	1 3 -2	2.0001	2.0004	7	
		5 1 1	1.9634	1.9636	5	
1.960	25	2 2 2	1.9592	1.9593	5	
1.941	30	3 3 -2	1.9379	1.9381	3	
		6 2 -1		1.9251		
		5 3 -1		1.9248	1	
1.904	25	6 0 -2	1.9049	1.9052	7	
		5 3 0	1.8956	1.8953	5	
1.875	40	1 3 2	1.8683	1.8693	5	
1.801	30	4 4 -1	1.8007	1.8007	11	
1.760	20	3 1 -3	1.7615	1.7619	10	
		6 2 -2	1.7502	1.7511	$\frac{1}{2}$	
		7 1 0		1.7277		
		5 3 -2	1.7277	1.7272	$\frac{1}{2}$	

WICNY1	(ASTM 7-00012)	PRESENT WORK				
d	$1/\lambda_{100}$	h k l	d <sub>obs</sub>	d <sub>calc</sub>	$1/\lambda_{100}$	
		2 4 -2	1.7140	1.7147	$\frac{1}{2}$	
		1 5 -1	1.6680	1.6682	5	
		7 1 -2	1.6760	1.6771	$\frac{1}{2}$	
		5 3 1	1.6646	1.6652	1	
		1 5 1	1.6461	1.6462	$\frac{1}{2}$	
		5 1 -3	1.6372	1.6374	1	
		4 2 2	1.6306	1.6309	4	
1.628	30	6 2 1		1.6247		
		4 2 -3		1.6244	5B	
		4 4 1	1.6204	1.6202	6	
		3 5 -1	1.6112	1.6109	2	
		7 3 -1	1.5623	1.5624	2B	
1.556	20	2 4 2	1.5570	1.5567	3	
		5 1 2	1.5523	1.5516	5	
		8 0 0		1.5405		
		6 4 -1		1.5397		
1.537	30	3 3 -3	1.5364	1.5368	12	
		1 3 -3	1.5334	1.5335	12	
		7 1 1		1.5155		
1.511	25	8 2 -1	1.5145	1.5144	4	
		7 3 0		1.5140		
		6 4 0	1.5021	1.5017	1	
1.475	5	0 6 0		1.4813		
		6 2 -3	1.4808	1.4807	4	
		2 2 3	1.4621	1.4622	1	
		3 5 -2	1.4603	1.4606	1	
		8 2 0	1.4561	1.4561	1	
		8 2 -2		1.4524		
		5 3 -3	1.4521	1.4521	2	
		1 3 3	1.4445	1.4439	$\frac{1}{2}$	
		2 6 0	1.4401	1.4403	2	
		1 5 2	1.4305	1.4304	1	
		0 6 1	1.4248	1.4248	2	
		9 1 -1		1.4132		
		2 6 -1	1.4133	1.4131	$\frac{1}{2}$	
1.403	5	2 4 -3	1.4054	1.4054	2	
1.372	45	6 4 1		1.3729		
		4 4 -3		1.3725	9B	
		7 3 1		1.3651		
		7 6 1	1.3648	1.3646	1	
		2 0 -4	1.3560	1.3560	1	
		6 2 2		1.3539		
		9 1 0	1.3539	1.3540	2	
		4 0 -4	1.3472	1.3462	$\frac{1}{2}$	
1.337	25	4 6 0	1.3350	1.3352	5	
1.319	20					



the field strength of Al is 0.96 and that of Zr is 0.77. Since the difference is only 0.19, less than the 0.3 difference required for compound formation, it is predicted that no stable compound will be formed between the oxides of zirconium and aluminum.

Hennicke<sup>25</sup> found that alumina can be used to partially stabilize zirconia. He mixed  $\text{Zr}(\text{OH})_4$  and  $\text{Al}(\text{OH})_3$  together and fired them at temperatures from  $1200^\circ\text{C}$  to  $1600^\circ\text{C}$ . He also experimented with oxide powders sintered at  $1600^\circ\text{C}$ . Approximately one mole percent of alumina entered the zirconia lattice. This solution caused part of the zirconia to remain in the tetragonal form at room temperature. After several of his samples were ground, they contained more monoclinic zirconia than before grinding, which indicated that there was also a mechanical stabilization. Of practical importance was his discovery that on repeated thermal cycling, mixtures of more than ten mole percent  $\text{Al}_2\text{O}_3$  became brittle. Another important observation was that the corundum structure absorbed part of the stress that was caused by the density change when the transition from tetragonal to monoclinic zirconia occurred. Hennicke also observed that the temperature at which the tetragonal to monoclinic transition occurred was lowered as the percentage of alumina was increased, when a cooling rate of  $10^\circ\text{C}$  per minute was maintained.

E. The Disappearing Phase Method of Phase Diagram Determination.

The disappearing phase method<sup>26</sup> uses quantitative x-ray diffraction analysis to determine phase boundaries on a phase diagram. Several samples of differing phase compositions are analyzed by x-ray diffraction and a weight ratio or a mole ratio of two phases for each composition is determined. The relationship between weight ratio or mole ratio of two phases and the phase composition is linear so that an extrapolation may be made to determine at what composition the phase ratio becomes zero. This determines the position of the phase boundary. The method can be used in a ternary system if the amount of one component is held constant and the variation of the remaining two components is observed. For solid solution endpoints which vary in composition with temperature, the composition at constant temperatures may be evaluated by this technique.

## CHAPTER III

Experimental Procedure

Sixty-six samples were prepared for determining the phase diagram of the calcia-alumina-zirconia ternary system. Using quantitative and qualitative phase analysis and lattice parameter information determined from x-ray diffraction, part of the phase diagram was determined by the disappearing phase technique. The raw materials used were TAM CP zirconia of greater than 99.0% purity and 1.4 micron particle size, Alcoa A-16 Superground alumina, and Fisher Scientific Certified calcium carbonate, 99.9% pure. Optical analysis was made with a metallographic microscope to confirm the x-ray results.

Three compositions in the high  $ZrO_2$  end of the ternary were chosen for long term heat treatment at 900 and 1300°C for 2000 hours. Crystallographic phase stability and physical property stability were determined for the long term heat treatment conditions. Physical properties measured were room temperature and high temperature flexure strength, Knoop's microhardness, and linear thermal expansion.

## A. Sample Preparation

### 1. High ZrO<sub>2</sub> Phase Diagram Samples

Compositions for five separate series of firings were chosen in the high zirconia region of the ternary system. Tables 5-9 show the compositions which were chosen for the five series of samples. For series 1, 2, 4, and 5, all three components were weighed out for each composition and each was mixed thoroughly in an alumina automatic mortar and pestle for 30 minutes in acetone. Several pellets of each composition were pressed using a Carver hydraulic laboratory press to 5000 psi. in a stainless steel die 0.75 inches in diameter lubricated with stearic acid in acetone. No binder was found to be required since the pellets held together and no laminations appeared. The thickness of the pellets was approximately 0.25 inches.

Series 1 pellets were calcined at 1200°C in a silicon carbide resistance furnace for 3.5 hours and fired to 1700°C in a gas fired furnace for three hours. The pellets were allowed to slow cool in the furnace before being removed.

Series 2, 4, and 5 samples were calcined as powders at 1300°C for 16 hours. The calcined powders were remixed in the automatic mortar and pestle and pressed as pellets. Series 2 and 4 pellets were sintered at 1500°C in a silicon carbide resistance furnace for 20 hours. Cooling was controlled at a rate of one degree per minute. After the

Table 5. Composition of Series 1

Sample Number	ZrO <sub>2</sub> mole %	Al <sub>2</sub> O <sub>3</sub> mole %	CaO mole %
1-1	64.0	20.0	16.0
1-2	68.0	20.0	12.0
1-3	72.0	20.0	8.0
1-4	69.6	13.0	17.4
1-5	74.0	13.0	13.0
1-6	78.3	13.0	8.7
1-7	76.2	4.8	19.0
1-8	80.9	4.8	14.3
1-9	85.7	4.8	9.5

Table 6. Composition of Series 2

Sample Number	ZrO <sub>2</sub> mole %	Al <sub>2</sub> O <sub>3</sub> mole %	CaO mole %
2-1	55.0	25.0	20.0
2-2	57.5	25.0	17.5
2-3	60.0	25.0	15.0
2-4	62.5	25.0	12.5
2-5	65.0	25.0	10.0
2-6	60.0	20.0	20.0
2-7	62.5	20.0	17.5
2-8	65.0	20.0	15.0
2-9	67.5	20.0	12.5
2-10	70.0	20.0	10.0
2-11	65.0	15.0	20.0
2-12	67.5	15.0	17.5
2-13	70.0	15.0	15.0
2-14	72.5	15.0	12.5
2-15	75.0	15.0	10.0
2-16	70.0	10.0	20.0
2-17	72.5	10.0	17.5
2-18	75.0	10.0	15.0
2-19	77.5	10.0	12.5
2-20	80.0	10.0	10.0
2-21	75.0	5.0	20.0
2-22	77.5	5.0	17.5
2-23	80.0	5.0	15.0
2-24	82.5	5.0	12.5
2-25	85.0	5.0	10.0

Table 7. Composition of Series 3

Sample Number	ZrO <sub>2</sub> mole %	Al <sub>2</sub> O <sub>3</sub> mole %	CaO mole %
3-1	64.0	20.0	16.0
3-2	68.0	20.0	12.0
3-3	72.0	20.0	8.0
3-4	69.6	13.0	17.4
3-5	74.0	13.0	13.0
3-6	78.3	13.0	8.7
3-7	76.2	4.8	19.0
3-8	80.9	4.8	14.3
3-9	85.7	4.8	9.5
3-10	80.0	0	20.0
3-11	85.0	0	15.0
3-12	90.0	0	10.0

Table 8. Composition of Series 4

Sample Number	ZrO <sub>2</sub> mole %	Al <sub>2</sub> O <sub>3</sub> mole %	CaO mole %
4-1	22.0	33.0	45.0
4-2	40.0	20.0	40.0
4-3	50.0	12.0	38.0
4-4	60.0	12.0	28.0

Table 9. Composition of Series 5

Sample Number	ZrO <sub>2</sub> mole%	Al <sub>2</sub> O <sub>3</sub> mole%	CaO mole%
5-1	70	5	25
5-2	65	10	25
5-3	60	15	25
5-4	55	20	25
5-5	50	25	25



series 2 samples had been analyzed as described below, they were all reloaded into the furnace and refired to  $1500^{\circ}\text{C}$  for 20 hours. After 20 hours at  $1500^{\circ}\text{C}$  they were rapidly removed and quenched in water. Series 5 pellets were fired in a vacuum furnace for two hours and cooled as rapidly as possible.

For series 3 a different method of preparation was used. The correct proportions of calcia and zirconia were mixed in the automatic mortar and pestle for one hour. These mixtures were calcined as powders at  $1400^{\circ}\text{C}$  for 16 hours. After this stabilized zirconia was prepared, alumina of the required proportions was added, mixed, and the powder pressed into pellets as described above. These pellets were fired at  $1500^{\circ}\text{C}$  for 25 hours and slow cooled at one degree per minute.

## 2. Compositions Surrounding $\text{CaO} \cdot 2\text{Al}_2\text{O}_3$

Fifteen  $\text{CaO}-\text{Al}_2\text{O}_3-\text{ZrO}_2$  samples, series 6, Table 10, surrounding the composition  $\text{CaO} \cdot 2\text{Al}_2\text{O}_3$ ,  $\text{CA}_2$ , were prepared from the identical raw materials used for the high  $\text{ZrO}_2$  samples. The compositions were pressed into pellets, fired to  $1500^{\circ}\text{C}$  for four hours, ground after cooling, repressed and fired again to  $1500^{\circ}\text{C}$  for 20 hours. Both firings were conducted in a silicon carbide resistance furnace and samples were cooled to room temperature at  $1^{\circ}\text{C}/\text{min}$ .

Table 10. Composition of Series 6

Sample Number	CaO mole%	Al <sub>2</sub> O <sub>3</sub> mole%	ZrO <sub>2</sub> mole%
6-1	29	71	0
6-2	28.4	69.6	2
6-3	27.9	68.3	3.8
6-4	31	69	0
6-5	30.4	67.6	2
6-6	29.8	66.3	3.8
6-7	33.3	66.7	0
6-8	32.6	65.4	2
6-9	32.0	64.1	3.8
6-10	35.3	64.7	0.
6-11	34.6	63.4	2
6-12	33.9	62.2	3.8
6-13	37.5	62.5	0
6-14	36.8	61.3	2
6-15	36.1	60.1	3.8

### 3. Long Term, Heat Treatment Samples

For the determination of the long term high temperature stability, three compositions were chosen as shown in Table 11. Four kilogram batches of each composition were prepared. Each batch was mixed in a polyethylene jar with alumina balls for 24 hours and the powder was calcined at  $1200^{\circ}\text{C}$  for 20 hours. The calcined powder was examined by x-ray diffraction to determine if a stable ratio of cubic to monoclinic zirconia had been achieved. The batches were reground in the polyethylene jars and recalcined twice before a constant cubic to monoclinic zirconia ratio was obtained. Batches were lightly ground after the final calcining prior to sample fabrication. One hundred pellets of (0.75 in diameter and 0.25 inches thick) each composition were dry pressed in a Stokes Model F tablet press and 50 (0.25 x 0.25 x 4 inches) bars were dry pressed at 5000 psi. Three weight percent kerosene was added to both the bars and pellets as a lubricant. Both the bars and pellets were fired at  $1550^{\circ}\text{C}$  for 24 hours on stabilized  $\text{ZrO}_2$  setter plates. Both heating and cooling was carried out at  $1^{\circ}\text{C}/\text{min}$ . After firing, the bars were cut with a diamond saw to 1.5 inch lengths.

Table 11. Composition of Batches for Long Term Firing

Batch Designation	$\text{ZrO}_2$ mole %	$\text{Al}_2\text{O}_3$ mole %	$\text{CaO}$ mole %
A	77.5	10.0	12.5
B	68.0	17.5	14.5
C	57.5	25.0	17.5

Samples were subjected to long term heat treatment at 900 and 1300°C. Thirty-two bars and 18 pellets of each composition were placed in covered alumina saggars and 12 pellets of each composition were placed on top of the saggars. The samples were heated to temperature at 1°C/min. After 200, 400, 600 and 800 hours, three pellets of each composition were withdrawn from the furnace and air quenched. Samples inside the sagger thus were not thermal shocked by removal of the pellets. At 1000 hours, the furnaces were cooled at 1°C/min., 16 bars and 3 pellets of each composition were removed, 12 pellets from inside the saggars were placed on top, and the furnaces were reheated to temperature at 1°C/min. Pellets were withdrawn 1200, 1400, 1600, and 1800 hours and after 2000 hours, the furnaces were cooled at 1°C/min.

#### 4. CA<sub>2</sub> Physical Property Samples

After analyzing the CA<sub>2</sub> stoichiometry results, a composition, 67.5 m/o Al<sub>2</sub>O<sub>3</sub>-32.0 m/o CaO-0.5 m/o ZrO<sub>2</sub>, was selected for physical property determination.

A 200 gram batch was prepared by pressing into pellets, firing to 1200°C for four hours, grinding to a powder after cooling and repressing into bars 4" x 0.25" x 0.25". The bars were fired to 1500°C for 50 hours on ZrO<sub>2</sub> sleds and slow cooled. Flexure strength (room temperature and high temperature), microhardness, and thermal expansion were

measured for the  $\text{CA}_2$  bars.

## B. X-ray Diffraction Analysis

### 1. Qualitative X-ray Analysis

For all of the x-ray work a Philips Electronics diffractometer with a solid state scintillation detector and Ortec single channel amplifier, rate meter, and associated electronics with output displayed on a Bristol ten millivolt recorder was used. This unit employed nickel filtered  $\text{Cu K}\alpha$  radiation and the x-ray tube was operated at 45 kv and 25 ma. Geometrically the x-ray beam had a  $4^\circ$  take off angle, a  $1^\circ$  divergence slit, a  $1^\circ$  scatter slit, and a 0.003 inch receiving slit. All scans were run at one degree per minute unless otherwise noted. Powder samples were back loaded into an aluminum holder and packed onto a frosted glass slide to give a random surface for scanning. For identification of phases, scans were made from  $2\theta = 14^\circ$  to  $2\theta = 70^\circ$ . Comparison was made to the Joint Committee on Powder Diffraction Standards Powder Diffraction File to determine exactly which phases were present as each line in the x-ray scan was accounted for.

One pellet of each of the series 1 and series 6 compositions was crushed and ground to approximately -325 mesh in the automatic mortar and pestle for x-ray analysis. For the remaining series of samples it was determined that x-raying the surface of the pellets was satisfactory and

less time consuming than crushing the pellets, which were very difficult to grind. The surface of each pellet was ground slightly with silicon carbide paper of 180 and 320 grit to insure a flat surface which would fit reproducibly into the sample holder clip of the goniometer.

## 2. Quantitative X-ray Analysis

Azaroff<sup>27</sup> showed that for polymorphic modifications of the same composition (such as cubic zirconia and monoclinic zirconia) the weight ratio of the two polymorphs in a mixture is directly proportional to the ratio of the two peak heights, one generated by each crystalline structure. He recommended preparing a graph to relate intensity ratios to composition. In order to follow this procedure, samples of pure cubic zirconia (15 mole percent CaO) and of pure monoclinic zirconia were mixed together in the automatic mortar and pestle to have weight ratios (cubic:monoclinic) of 4:1, 1:1, and 1:4. An x-ray scan was made of each composition from  $2\theta = 27^\circ$  to  $2\theta = 32^\circ$ . For the cubic phase the major peak of 100% intensity corresponding to the 111 plane at a  $d$  spacing of 2.92 Å was chosen. Two peaks from the monoclinic phase were chosen to compare to the cubic peak in order that two separate weight ratios might be determined. The values reported are an average of the two weight ratios. Both monoclinic

peaks were close to the cubic peak: one corresponded to the  $11\bar{1}$  plane at  $\underline{d}$  spacing 3.16 Å and the other to the  $111$  plane at  $\underline{d}$  spacing 2.834 Å. Ratios of peak intensity for the three standard samples were determined and a graph was constructed to be used for determining weight ratios for all of the samples, Figure 8. The equations for the two lines are as follows:

$$Y_1 = 2.027 X_1 + 0.054 \quad Y_2 = 3.082 X_1 + 0.105 \quad (1)$$

where  $Y_1$  is  $\frac{\text{intensity of cubic } 111 \text{ peak}}{\text{intensity of mono } 111 \text{ peak}}$

$X_1$  is  $\frac{\text{weight cubic}}{\text{weight mono}}$

$Y_2$  is  $\frac{\text{intensity of cubic } 11\bar{1} \text{ peak}}{\text{intensity of mono } 11\bar{1} \text{ peak}}$

For each of the samples which had both cubic zirconia and monoclinic zirconia, a determination of the weight ratio was made from these equations. The average value determined from the two ratios was calculated.

### 3. Lattice Parameter Measurement

Lattice parameter values were determined for the cubic zirconia phase in long term, heat treatment samples A, B, and C at 0, 200, 1000, and 2000 hours at 900°C and 1300°C, and also at 400 hours for the 1300°C samples. X-ray scans were made at one half degree per minute from  $2\theta = 13^\circ$  to  $2\theta = 135^\circ$ . From information in the JCPDS files relating to  $\underline{d}$  spacing in crystalline planes accurate values for the

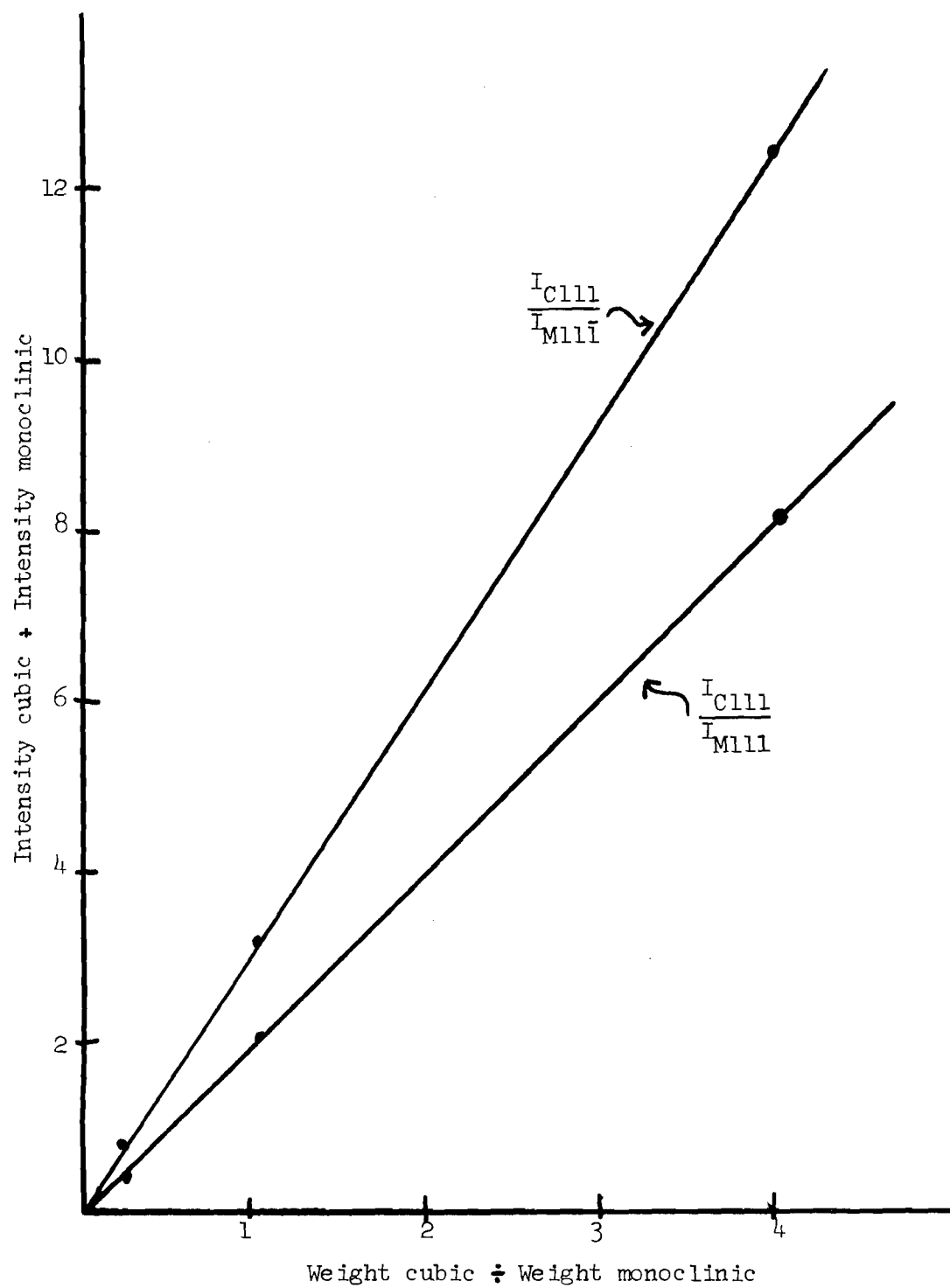


Figure 8. Relationship between Peak Intensities and Weight Ratios of Cubic to Monoclinic Zirconia



a parameter were determined by using the following formula:

$$\frac{1}{d^2} = \frac{h^2}{a^2} + \frac{k^2}{a^2} + \frac{l^2}{a^2} \quad (2)$$

where h, k, l are the indices of the plane

a is the lattice parameter (in a cubic structure all three dimensions are the same)

d is the interplanar spacing.

Bragg's Law gives the relationship between d and  $\theta$ , the angle of diffraction in terms of  $\lambda$ , the wavelength of radiation used, in this case 1.5418 Å for Cu K $\alpha$ :

$$n\lambda = 2d \sin\theta \quad (3)$$

where n is an integer.

In order to determine the actual lattice parameter a for any particular sample, and extrapolation must be made. For this a was plotted versus  $\cos\theta\cot\theta$  and this curve was extrapolated to the point where  $\cos\theta\cot\theta$  is zero. This value of a at  $\cos\theta\cot\theta = 0$  is the true lattice parameter for the sample. For actually determining this intercept a PDP 8 computer which had been programmed to do a least squares regression was used to give an accurate estimate of the lattice parameter. The program also gave a value for the correlation coefficient of the estimate, an indication of the closeness of all of the points to the line. Figure 9 gives an example of one extrapolation that was made.

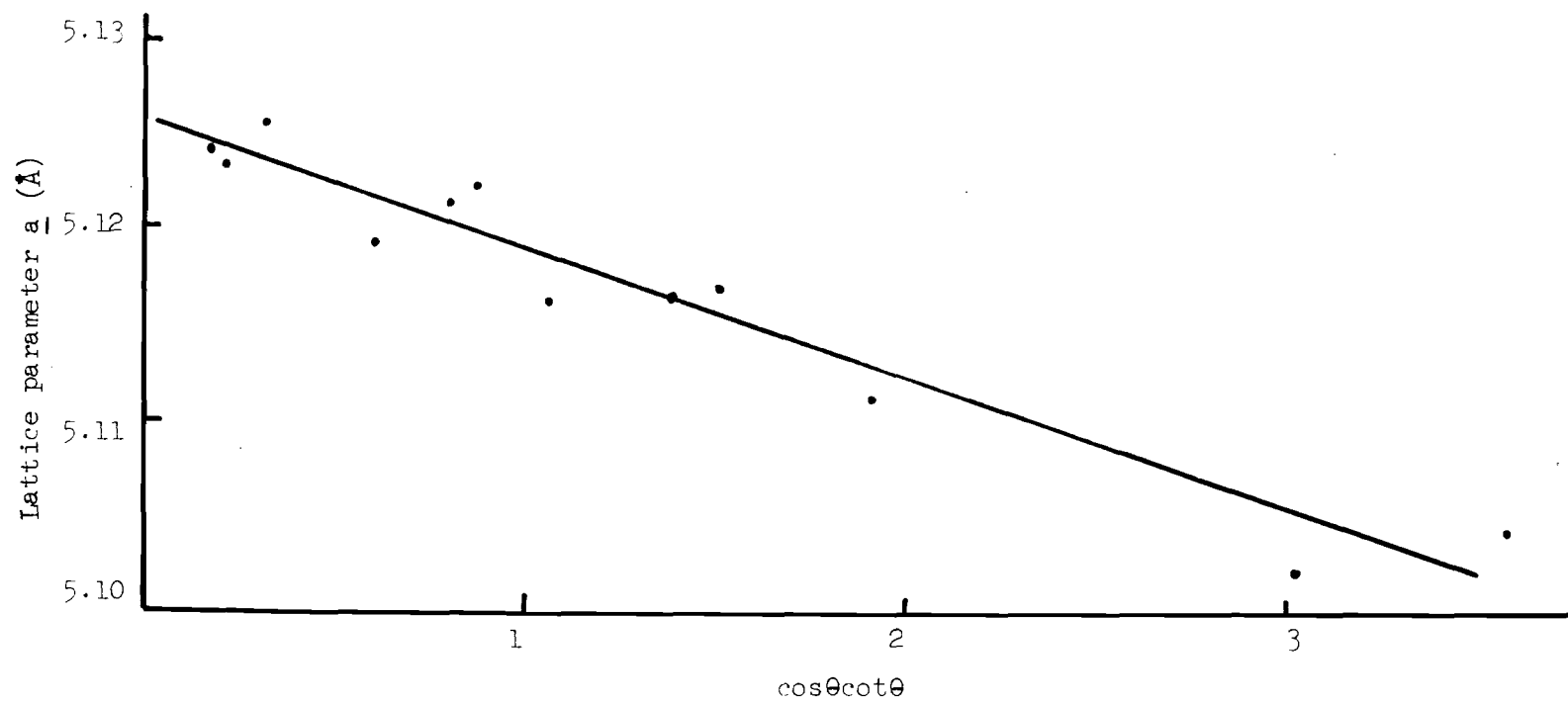


Figure 9. Lattice Parameter Extrapolation for Composition A before Heat Treatment

### C. Quantitative Optical Determination

One pellet of selected compositions was prepared for optical examination by mounting in Quickmount, a self-setting resin type of translucent plastic commonly used for metallographic work. Each pellet was wet polished successively on 180, 320, and 600 grit silicon carbide grinding paper. Final polishing was done with a Syntron automatic vibrating polisher. One micron diamond paste with water as a lubricant was used on a nylon cloth surface. Twenty-four hours of polishing on this device was required to obtain a satisfactory surface on each sample. Each sample was photographed using a Polaroid attachment on a Reichert Metallographic Microscope at 600x in reflected light and bright field. From these photographs the volume fraction of each phase was determined by a systematic point counting technique, which is described in Appendix A.

### D. Density Determination

The bulk density of each sample was determined by a technique involving immersion in kerosene. Each sample was weighed on an accurate balance. For 24 hours all of the samples were soaked in kerosene in order to fill all of the pores. After soaking, each sample was weighed again while suspended on a wire mesh hanger in a beaker of kerosene, insuring that no air bubbles remained attached to the pellet. Density was calculated from the following formula:

$$\text{density} = \frac{\text{d.w.}}{\text{d.w.} - \text{s.w.}} \times \text{s.g.} \quad (4)$$

where d.w. is the dry weight

s.w. is the suspended weight

s.g. is the specific gravity of the kerosene.

#### E. Thermal Expansion Measurements

Thermal expansion measurements were made on an Orton Automatic Recording Dilatometer using an  $\text{Al}_2\text{O}_3$  sample tube and push rod. Maximum temperature was limited to  $1200^\circ\text{C}$  which was sufficient to observe the monoclinic to tetragonal inversion in  $\text{ZrO}_2$ . The thermal expansion on both heating and cooling was recorded.

#### F. Flexure Strength Measurements

Flexure strength was measured for long term, heat treatment compositions A, B, and C for the following heat treatment conditions; "as-fired" at  $1550^\circ\text{C}$ ,  $900^\circ\text{C}$ -1000 hours,  $900^\circ\text{C}$ -2000 hours,  $1300^\circ\text{C}$ -1000 hours, and  $1300^\circ\text{C}$ -2000 hours. In addition, samples of calcium dialuminate,  $\text{CA}_2$ , were flexure strength tested. Four samples were broken for each of the above compositions, heat treatment conditions, and breaking temperatures. Breaking temperatures were  $20^\circ\text{C}$ ,  $900^\circ\text{C}$ ,  $1100^\circ\text{C}$  and  $1300^\circ\text{C}$ . The average flexure strength, standard deviation, and percent standard deviation [(standard deviation/flexure strength) x 100] were recorded.

The final sample geometry for flexure strength was bars 0.20 x 0.20 x 1.50 inches. Measurement of flexure strength was made in three point loading on an Instron Universal Tester using a span 1.25 inches and a head speed of 0.01 cm/min. Samples were broken as fired with no surface treatment.

For high temperature flexure strength measurements a furnace was constructed using molybdenum disilicide heating elements and temperature control was accomplished using a proportional band controller with rate and reset.

Temperature during flexure strength measurement was maintained  $\pm 5^{\circ}\text{C}$ . The furnace was a pusher type design with high  $\text{Al}_2\text{O}_3$  sample sleds pushed in tandem through the furnace on 0.5 inch diameter  $\text{Al}_2\text{O}_3$  tubes. Each sample sled had slots for five samples and 0.125 inch diameter sapphire rods served as the knife edges on which the samples were broken. The load was applied via a 0.5 inch diameter  $\text{Al}_2\text{O}_3$  tube that had been ground to a knife edge with an approximately 0.05 inch radius on the knife edge. The samples were broken at five minute intervals and each sample was at the breaking temperature for a minimum of 20 minutes prior to loading.

#### G. Knoop's Microhardness Measurements

Room temperature microhardness measurements were made on samples of the same conditions as were flexure strength tested.

Samples were mounted in clear resin and ground for twenty minutes utilizing 180, 320, and 600 grit grinding paper. The samples were polished for 48 hours on a vibratory grinder incorporating one micron diamond paste.

A Reichart metalograph was set up with a Knoop micro-hardness tester under a power of 480x. Three indentations measurements were made at each of the following loads: 30.5, 34, 39, 42.5, 46, 51, and 59 grams. Fracturing occurred after the higher loads, requiring re-indentation and measurement. The testing device determines the indentation length in drum divisions each of which is equal to 0.167 microns.

The three values for length were averaged for each load and sample and the Knoop hardness was determined by a computer using the following equation:

$$KHN = \frac{P}{0.07028 L^2}$$

where KHN = Knoop Hardness Number

P = load in kilograms

L = indentation length in millimeters

The average microhardness values as a function of load was recorded.

## SECTION IV

Results and Discussion

The purpose of this investigation was to measure microstructural and phase changes in the CaO-stabilized  $\text{ZrO}_2\text{-Al}_2\text{O}_3$  system after heat treatment as high as  $1300^\circ\text{C}$  for up to 2000 hours. In addition, high temperature flexural strength, thermal expansion, and room temperature microhardness was to be investigated in an attempt to correlate these properties to microstructure and crystal changes.

The original intent of this work was to investigate compositions of high stabilized zirconia content plus  $\text{Al}_2\text{O}_3$ . Phase relations for the  $\text{CaO-Al}_2\text{O}_3\text{-ZrO}_2$  ternary were not available. Thus, prior to selection of compositions for long term heat treatment, the phase relations in the high zirconia (greater than or equal to 50%) portion of the ternary were established at  $1500^\circ\text{C}$ . During the phase diagram investigation a question as to the stoichiometry of the compound  $\text{CA}_2$  arose. Thus, the phase regions around the composition  $\text{CA}_2$  were also studied.

Based on the results of the phase diagram study, three compositions in the  $\text{CA}_2$ -cubic  $\text{ZrO}_2$ -monoclinic  $\text{ZrO}_2$ , compatibility triangle were selected for long term firing studies. The phase changes found on heat treating these compositions at 900 and 1300°C for 2000 hours were determined and compared to flexural strength, microhardness and thermal expansion results. Only a few of the properties of  $\text{CA}_2$  have been investigated with only the x-ray pattern, density, and thermal expansion having been reported in the literature. Therefore in an effort to characterized  $\text{CA}_2$  more fully, the flexure strength, microhardness and thermal expansion of  $\text{CA}_2$  was measured for comparison to results compiled on the high  $\text{ZrO}_2$  compositions.

#### A. $\text{CaO-Al}_2\text{O}_3\text{-ZrO}_2$ Phase Diagram at 1500°C

##### 1. Qualitative Phase Diagram for High $\text{ZrO}_2$ Portion of Ternary

Using the phases present as obtained from qualitative x-ray diffraction analysis of series 2, 3, and 5 samples, Appendix B, estimated Alkemade lines were drawn to divide the compatibility triangle regions which were obtained, Figure 10. The crystalline phases found in each sample of series 2 and 3 after firing for 20 hours and slow cooling were identical to those found in the samples after firing for 40 hours and water quenching. From these qualitative results at 1500°C, equilibrium appeared to have been obtained,



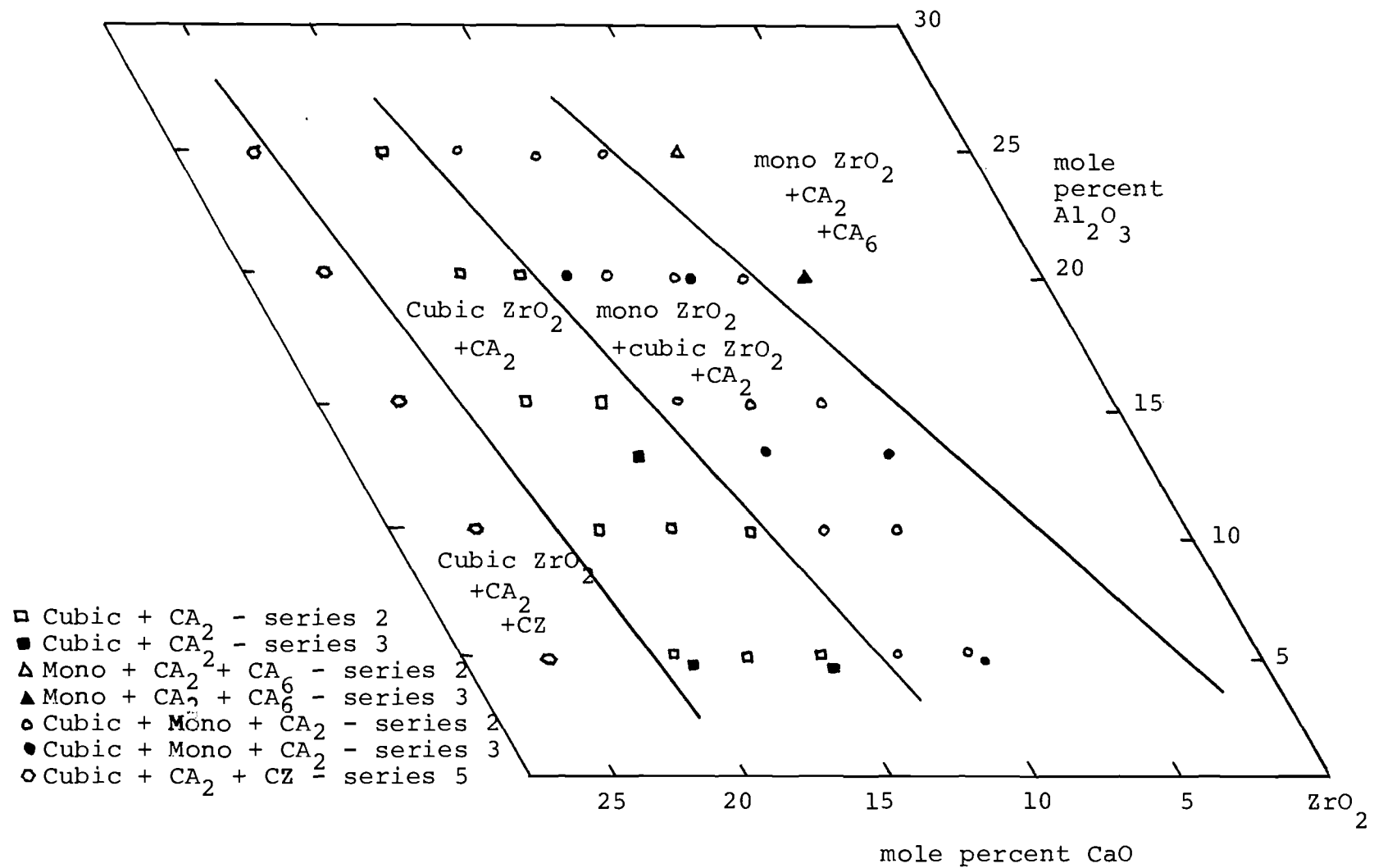


Figure 10. Phase Analysis of Samples Fired at 1500°C.

but the question was approached more rigorously in the following section. From phase equilibria theory, a two phase region should divide the  $CA_2 + CA_6 + \text{monoclinic zirconia}$  area from the  $CA_2 + \text{cubic zirconia} + \text{monoclinic zirconia}$  area. No sample with only  $CA_2 + \text{monoclinic zirconia}$  was found, but it is certainly reasonable that the region is almost the width of a line and that no composition was chosen for analysis that fell exactly on that line.

## 2. Quantitative Verification of Equilibrium at 1500°C

In order to calculate the exact position of the  $CA_2$ -cubic and  $CA_2$ -monoclinic Alkemade lines, the cubic and monoclinic zirconia peak heights from the x-ray scan for each sample were used to determine quantitatively the weight ratio of cubic zirconia to monoclinic zirconia in each sample that contained both phases. These weight ratio values were converted to a mole basis to be compatible with the remaining quantitative information which was in mole percent. For conversion the composition of cubic zirconia was assumed to be 13 mole percent  $CaO$  and 87 mole percent zirconia. No significant variation in the values would have been obtained if a composition for cubic zirconia of 16 mole percent calcia, which is also suggested in the literature, had been used. The assumption was also made that monoclinic zirconia was 100 percent zirconia. This assump-

tion is justified since no more than one mole percent calcia exists in monoclinic zirconia, from published phase diagrams. The cubic zirconia to monoclinic zirconia Alkemade line must also be assumed to lie at a constant mole percent alumina. With these assumptions made, it may be stated that the ratio of cubic zirconia to cubic plus monoclinic zirconia varies linearly from 0 to 1 on any constant mole percent alumina line across the compatibility triangle. Thus the exact position of the Alkemade lines may be determined from quantitative x-ray data.

To predict the two Alkemade lines intersecting at  $CA_2$  and bounding the cubic + monoclinic +  $CA_2$  phase region, the cubic/(cubic + monoclinic) ratio was plotted versus the mole percent calcia of samples containing a constant mole percent of alumina, Figure 11. These relationships were then extrapolated using a linear regression program to determine the endpoints, which are points on the Alkemade lines. The calcia contents at 0 percent and 100 percent cubic at various alumina contents were used to calculate, again by the linear regression method, the equations of the two Alkemade lines. Appendix C contains the data from measuring cubic to monoclinic ratios and the calculated mole basis.

Initially, equations for the two Alkemade lines for the slow cooled series 2 samples were determined as follows:

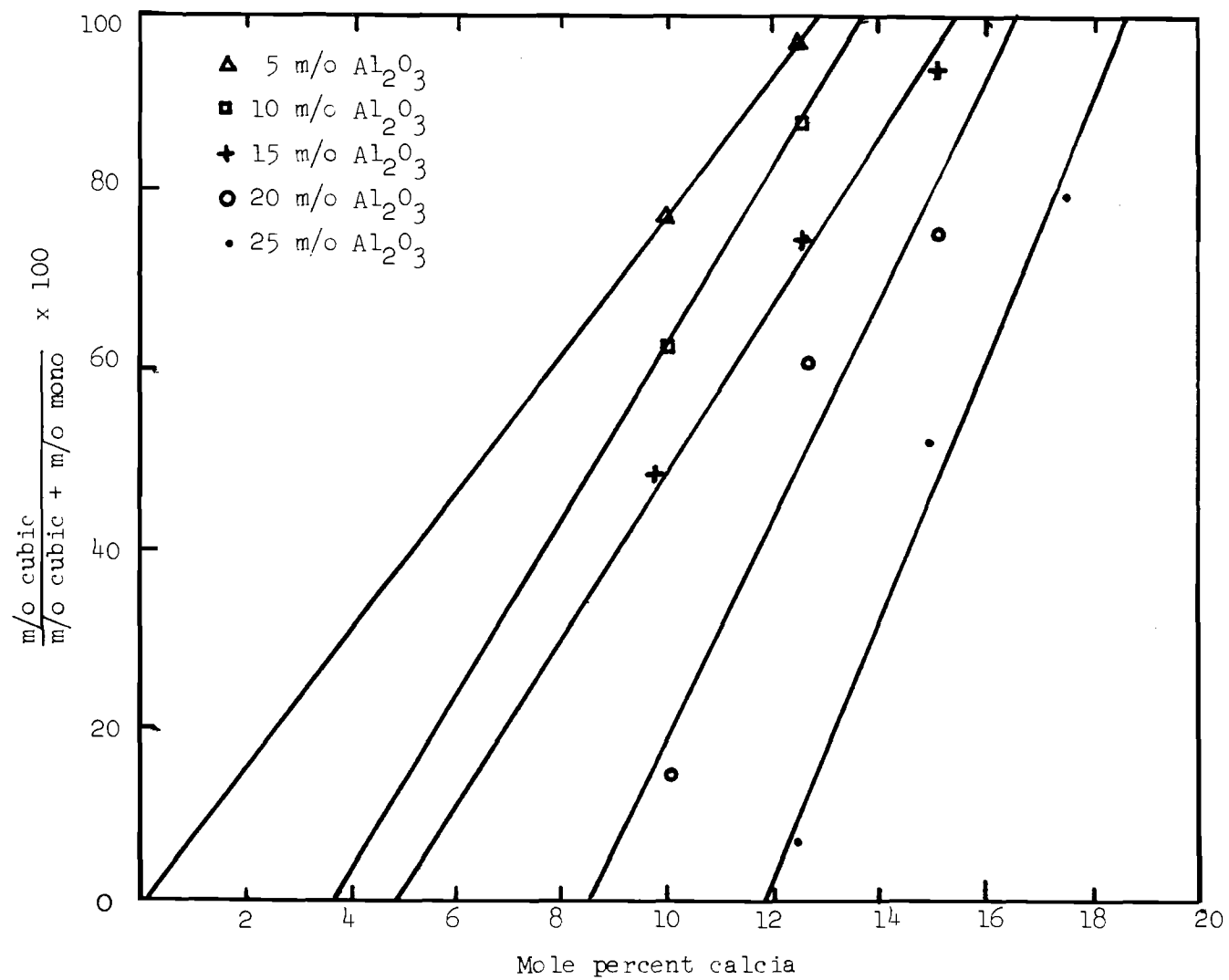


Figure 11. Extrapolation of Calcia Content to 0% and 100 % Cubic Zirconia at Fixed Alumina Contents

$$\% \text{ CaO at 100 \% cubic} = 0.29 (\text{Al}_2\text{O}_3) + 11.09 \quad (5)$$

$$\% \text{ CaO at 0 \% cubic} = 0.56 (\text{Al}_2\text{O}_3) + 2.58 \quad (6)$$

In order to prove that equilibrium had been reached, the same procedure for calculating the two Alkemade lines was performed for the series 2 samples after they had been refired for a second 20 hours and quenched. The equations determined for these two lines were as follows:

$$\% \text{ CaO at 100 \% cubic} = 0.26 (\text{Al}_2\text{O}_3) + 11.8 \quad (7)$$

$$\% \text{ CaO at 0 \% cubic} = 0.53 (\text{Al}_2\text{O}_3) + 2.25 \quad (8)$$

As can be seen in Figure 12, within the limits of experimental error, a close agreement exists between the Alkemade lines determined at 20 and 40 hours. This agreement demonstrates that the slow cooled series 2 samples had reached equilibrium after being fired for 20 hours, since there was no change after a second 20 hours firing and quenching.

Examination of the series 3 quantitative results indicated that there was good agreement with the series 2 results. This observation indicated that the method of preparation did not affect the resulting phases, as should be expected if equilibrium had been reached. Thus alumina may be added to stabilized zirconia with the same results as mixing calcia, alumina, and monoclinic zirconia in one operation.

In order to obtain the most accurate lines, since all three sets of data (series 2 slow cooled, series 2 quenched,

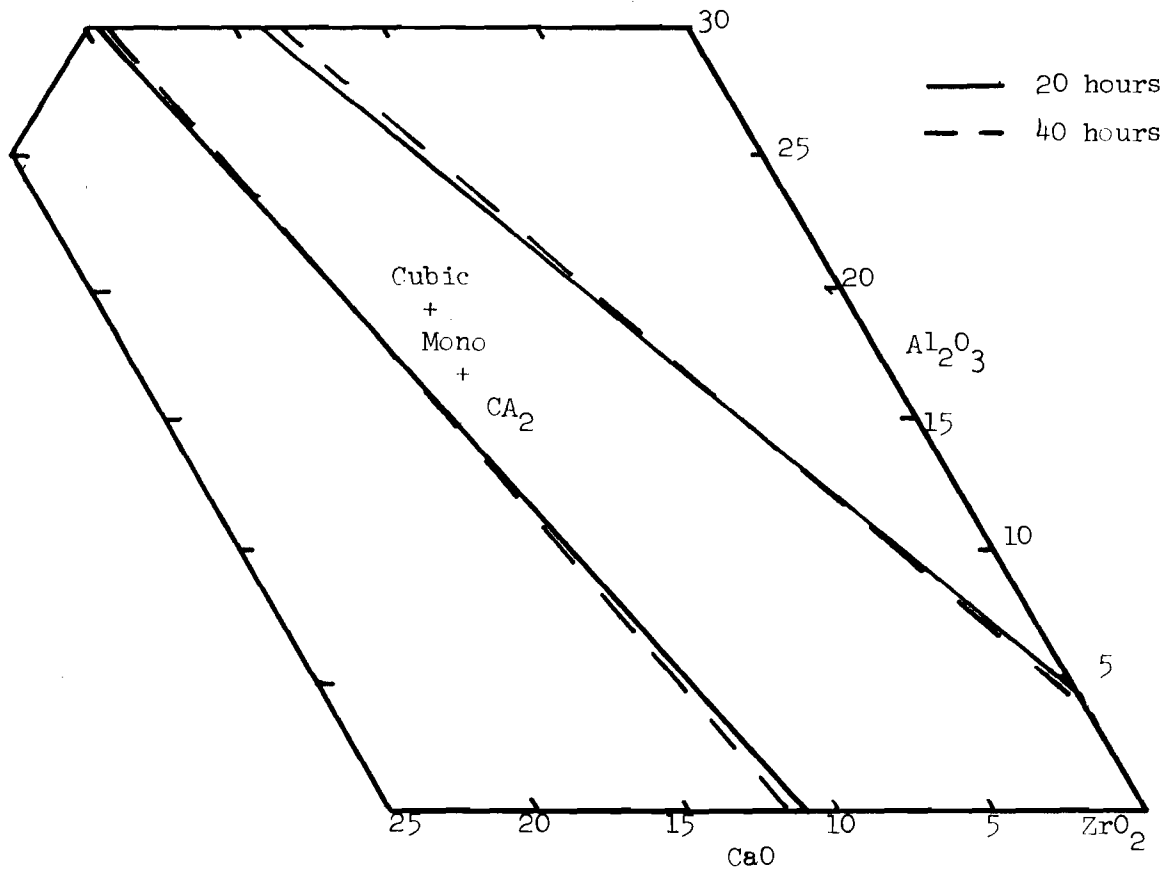


Figure 12. Cubic Zirconia Alkemade Lines at 20 and 40 Hours Firing at 1500 °C, Verifying Equilibrium by Reproducibility of Lines

and series 3) were in agreement, the cubic to monoclinic ratio for all of the samples was used to calculate the two Alkemade lines, Figure 13. The equation of the  $CA_2$ -cubic zirconia line was as follows:

$$\% \text{ CaO at 100 \% cubic} = 0.28 (\text{Al}_2\text{O}_3) + 11.58 \quad (9)$$

and the equation of the  $CA_2$ -monoclinic zirconia line was as follows:

$$\% \text{ CaO at 0 \% cubic} = 0.48 (\text{Al}_2\text{O}_3) - 0.89 \quad (10)$$

### 3. Alumina Solubility in Cubic and Monoclinic Zirconia

The solid solution region along the calcia-zirconia binary line for alumina has been estimated from information in the literature and from optically determined  $CA_2$  volume contents. Takagi<sup>6</sup> indicated that at 0.5 weight percent alumina he saw a calcium aluminate phase when samples were fired at 1700°C. This observation suggests that the region of alumina solubility does not extend as much as 0.50 mole percent above the line. Quantitative x-ray analysis could not be used to determine the amount of  $CA_2$  present in each sample because a sufficiently pure sample of  $CA_2$  was not available.

From the quantitative optical data, an estimate was made of the compositions at which the  $CA_2$  phase disappeared and reached 100%. Samples 2-2, 3-1, 3-5, 2-25, and 3-9 were chosen since they lay on a line drawn from  $CA_2$  to a composition of 8 m/o CaO-92 m/o  $ZrO_2$ . The photographs of

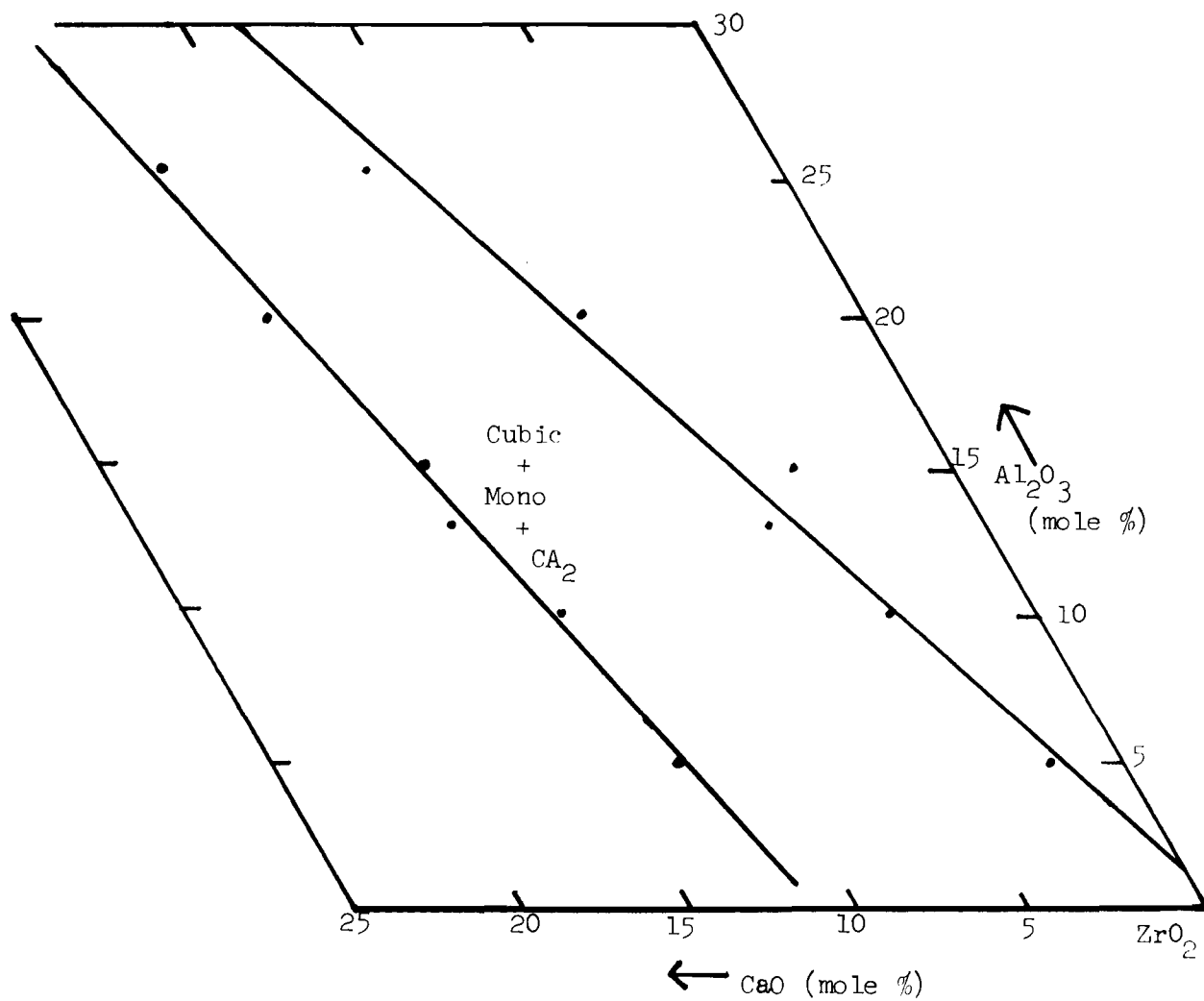


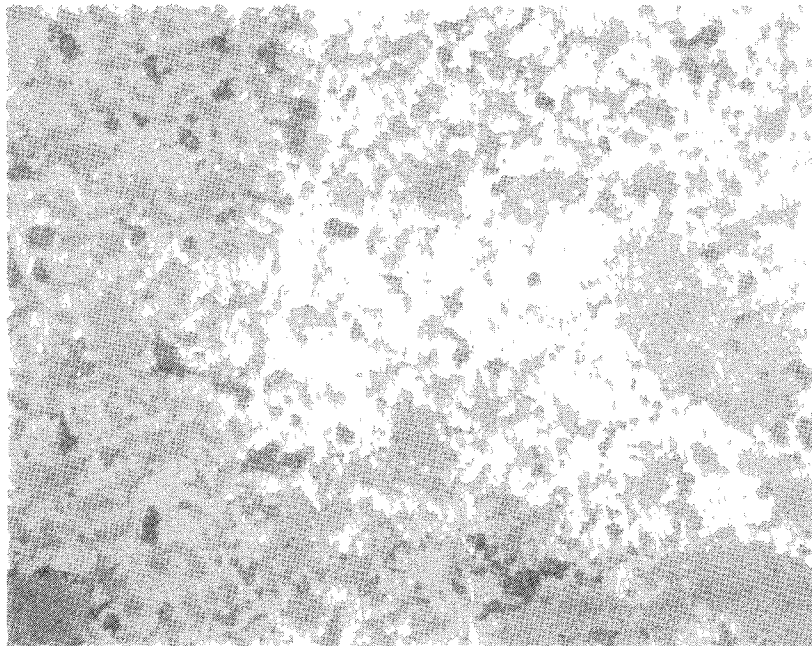
Figure 13. Alkemade Lines Bounding the Cubic + Monoclinic + CA<sub>2</sub> Region at 1500 °C



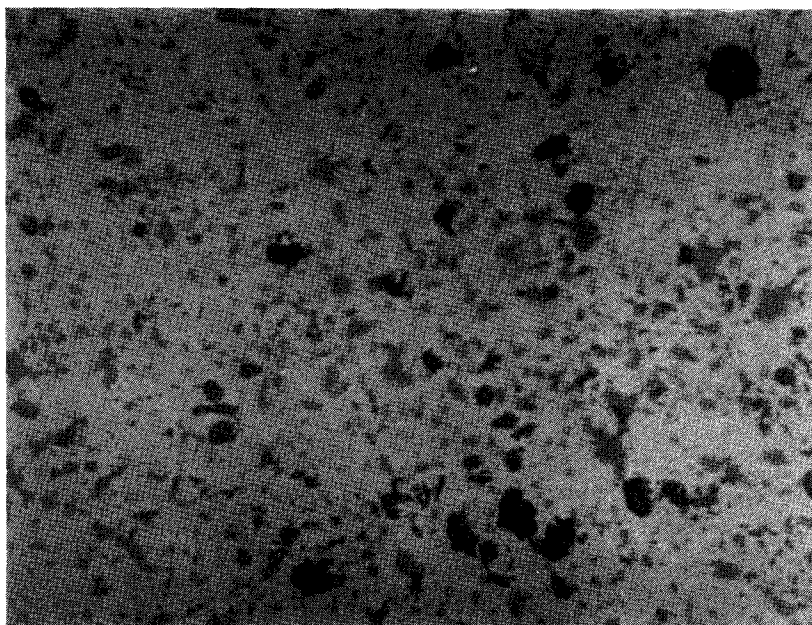
two samples, 3-1 and 3-9 are shown in Figure 14 as examples of the microstructures which were observed. A method similar to that used for determining the position of the Alkemade lines was used. The volume percents of the  $CA_2$  phase were converted to weight percents, assuming a 2:1 weight ratio of cubic to monoclinic zirconia and densities of 6.15 g/cc for cubic zirconia, 5.83 g/cc for monoclinic zirconia, and 2.89 g/cc for  $CA_2$ . Weight percents were converted to mole percents assuming that  $CA_2$  was exactly a 1:2 ratio and that the other end point of the tie line was at 8 m/o CaO-92 m/o  $ZrO_2$ . Table 12 shows the data as converted. Mole percent  $CA_2$  was plotted versus mole percent  $Al_2O_3$  and with a linear regression program the best line fit was determined, Figure 15. Extrapolation to 100%  $CA_2$  gave a stoichiometry for  $CA_2$  of 69.2 mole percent alumina and 30.8 mole percent calcia, which is closer to  $C_3A_7$  than  $CA_2$ .

Table 12. Optical Data for  $CA_2$  Stoichiometry Determination

Sample Number	m/o CaO	m/o $Al_2O_3$	vol% $CA_2$	wt% $CA_2$	m/o $CA_2$
2-2	17.5	25.0	50	32.35	39.4
3-1	16.0	20.0	48	30.63	37.5
3-5	13.0	13.0	30	17.01	21.8
2-25	10.0	5.0	21	11.28	14.7
3-9	9.5	4.8	20	10.68	14.0



Sample 3-1

 $\text{ZrO}_2$  64 m/o $\text{CaO}$  16 m/o $\text{Al}_2\text{O}_3$  20 m/o

Sample 3-9

 $\text{ZrO}_2$  85.7 m/o $\text{CaO}$  9.5 m/o $\text{Al}_2\text{O}_3$  4.8 m/o

Figure 14. Photomicrographs of Series 3, 1500 °C, 600x

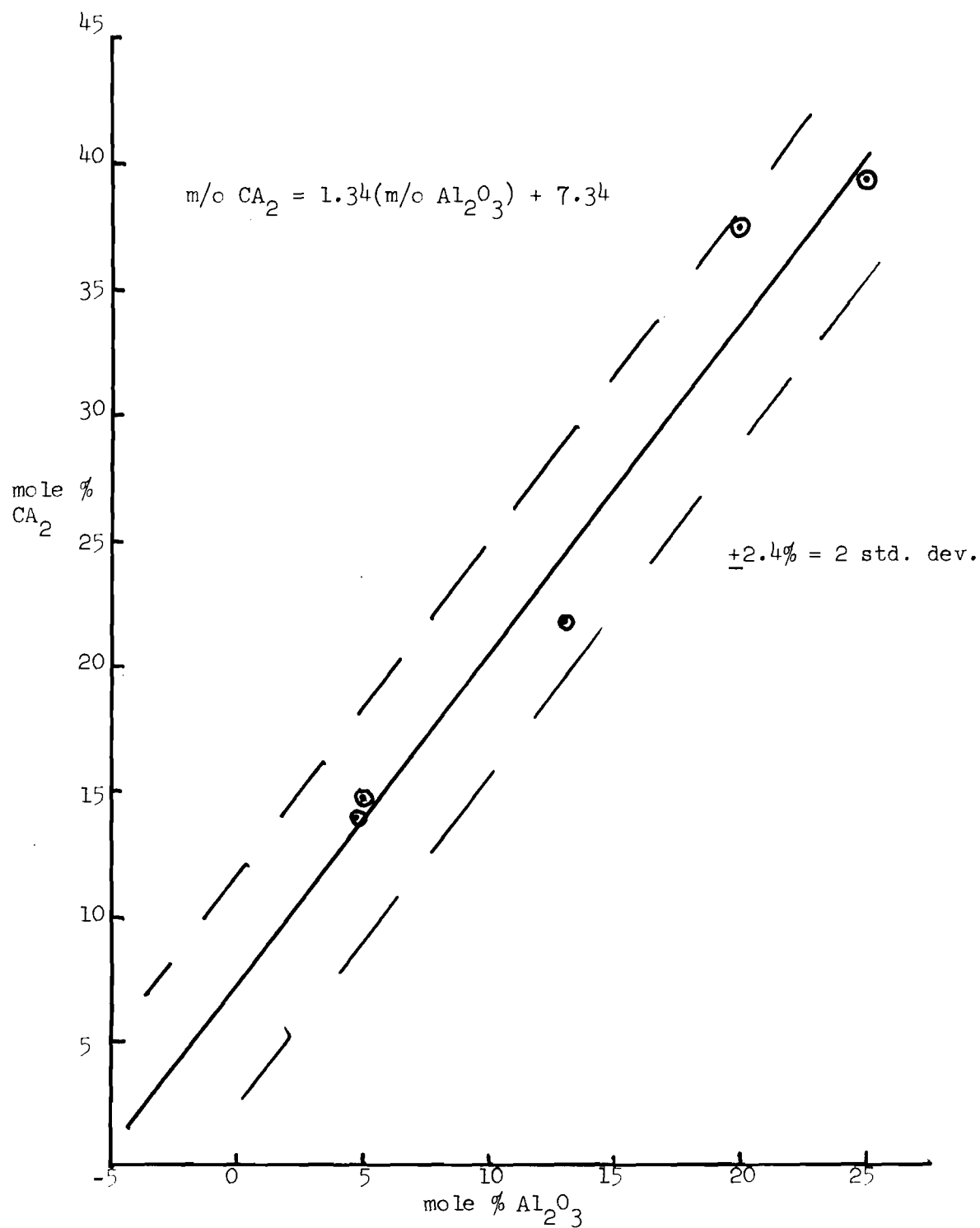


Figure 15. Extrapolation of  $\text{CA}_2$  Composition to 0% Alumina to Determine  $\text{Al}_2\text{O}_3$  Solubility in Zirconia

Extrapolation to 0%  $CA_2$  resulted in a negative alumina value, which is obviously erroneous, but does suggest that very little alumina exists in solid solution in either zirconia phase, as noted by Takagi.<sup>6</sup>

#### 4. Phase Diagram Surrounding $CA_2$

The phases detected in the  $CA_2$  stoichiometry samples, series 6, are reported in Appendix B and the compatability triangles near  $CA_2$  were constructed from the determined phases, Figure 16.  $CA_2$  was the major phase in all compositions and the x-ray intensity of the major peak of the remaining phases ( $CA$ ,  $CA_6$ , Cubic  $ZrO_2$ , Monoclinic  $ZrO_2$ , and calcium zirconate, relative to  $CA_2$  were noted to confirm that the quantity of the phases were changing in the correct order. The phases detected were as expected except for compositions 2, 3, 5, 6 and 9 where  $CA$  was present (see Figure 16). Apparently these compositions are difficult to take to equilibrium.

For the raw materials used in this study, the composition of  $CA_2$  appears to occur at 68 m/o  $Al_2O_3$ , 32 m/o  $CaO$ . To show this, the relative intensity of  $CA_6/CA_2$  for compositions 6-1 and 6-3 and  $CA/CA_2$  for compositions 6-7, 6-10 and 6-13 was plotted vs  $Al_2O_3$  content, Figure 17. The relative intensities of  $CA$  and  $CA_6$  were extrapolated to zero in an effort to pinpoint the composition of  $CA_2$ .  $CA$  extrapolated to zero at 67%  $Al_2O_3$  and  $CA_6$  at 68.7% for

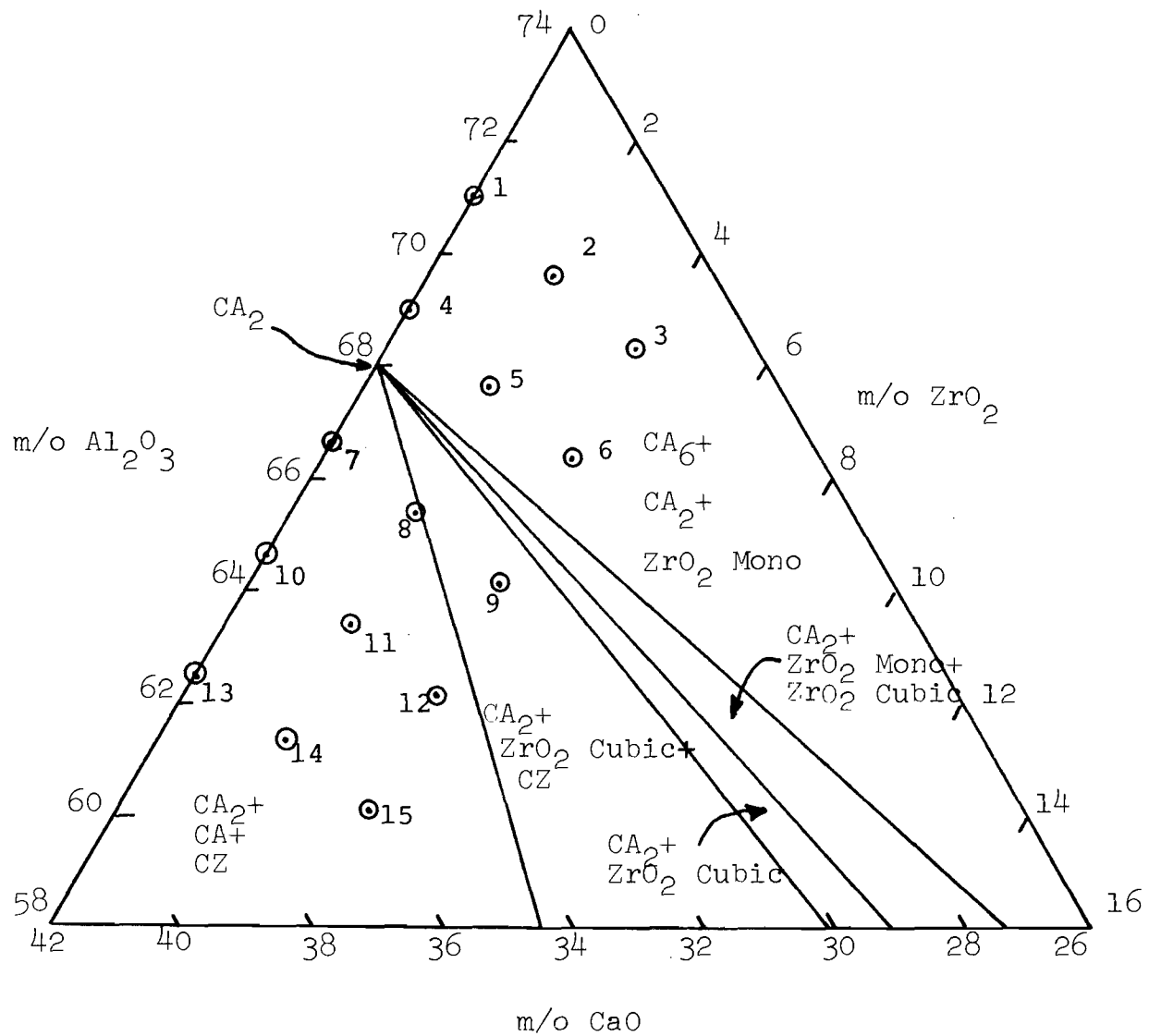


Figure 16. Phase Diagram of the CaO-Al<sub>2</sub>O<sub>3</sub>-ZrO<sub>2</sub> System for Compositions Surrounding CA<sub>2.3</sub>

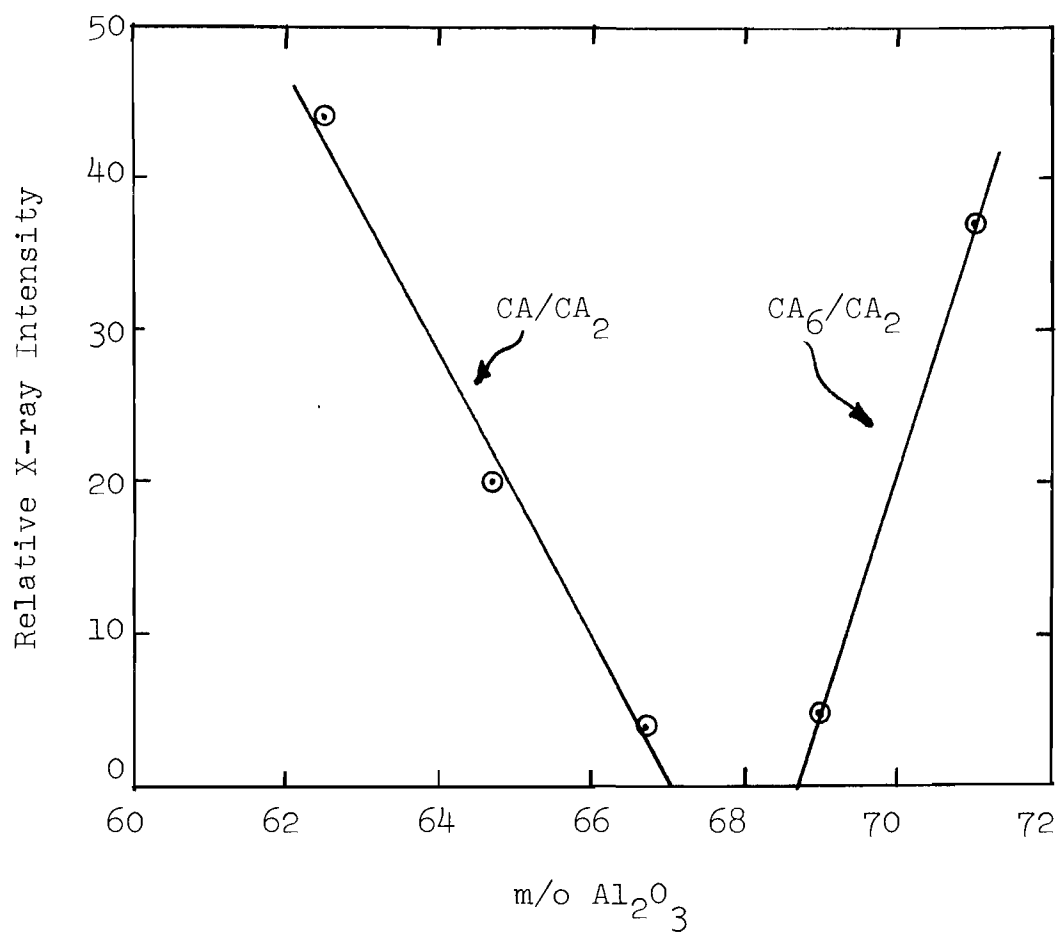


Figure 17. Relative X-ray Intensity of  $\text{CA}_6/\text{CA}_2$  and  $\text{CA}/\text{CA}_2$  for  $\text{CaO-Al}_2\text{O}_3$  Composition. Note: Lines Should Extrapolate to Zero at  $\text{CA}_2$  Composition.

an average of 67.9%  $\text{Al}_2\text{O}_3$ . In addition, composition 6-8 contained CA and no cubic  $\text{ZrO}_2$ . Thus the join between  $\text{CA}_2$  and calcium zirconate must be drawn to 68%  $\text{Al}_2\text{O}_3$ , 32% CaO.

In summary, the data reported here and that extrapolated from high  $\text{ZrO}_2$  compositions reported above indicated that the composition of  $\text{CA}_2$  is 68%  $\text{Al}_2\text{O}_3$  and 32% CaO for our raw materials.

#### 5. Complete CaO- $\text{Al}_2\text{O}_3$ - $\text{ZrO}_2$ Phase Diagram at 1500°C

From the data presented above plus information obtained from the literature, it is possible to construct a phase diagram of the high zirconia region of the calcia-alumina-zirconia ternary system at 1500°C, Figure 18. The two  $\text{CA}_2$ -cubic zirconia SS and  $\text{CA}_2$ -monoclinic zirconia Alkemade lines determined above are shown solid because they have been accurately determined. From equation 9, the Alkemade line extrapolation to 0% alumina, the boundary between the cubic +  $\text{CA}_2$  region and the cubic + monoclinic +  $\text{CA}_2$  region is placed at 11.6 mole percent CaO, rather than the 13 to 16 mole percent reported by other investigators. The cubic zirconia-monoclinic zirconia Alkemade line is drawn at 0.5 mole percent alumina, as described above.

The Alkemade line from the high calcia cubic zirconia SS to  $\text{CA}_2$  was drawn from 20 m/o CaO-80 m/o  $\text{ZrO}_2$  to 32 m/o CaO-68 m/o  $\text{Al}_2\text{O}_3$ . To confirm qualitatively that the following regions were labeled correctly, three samples in

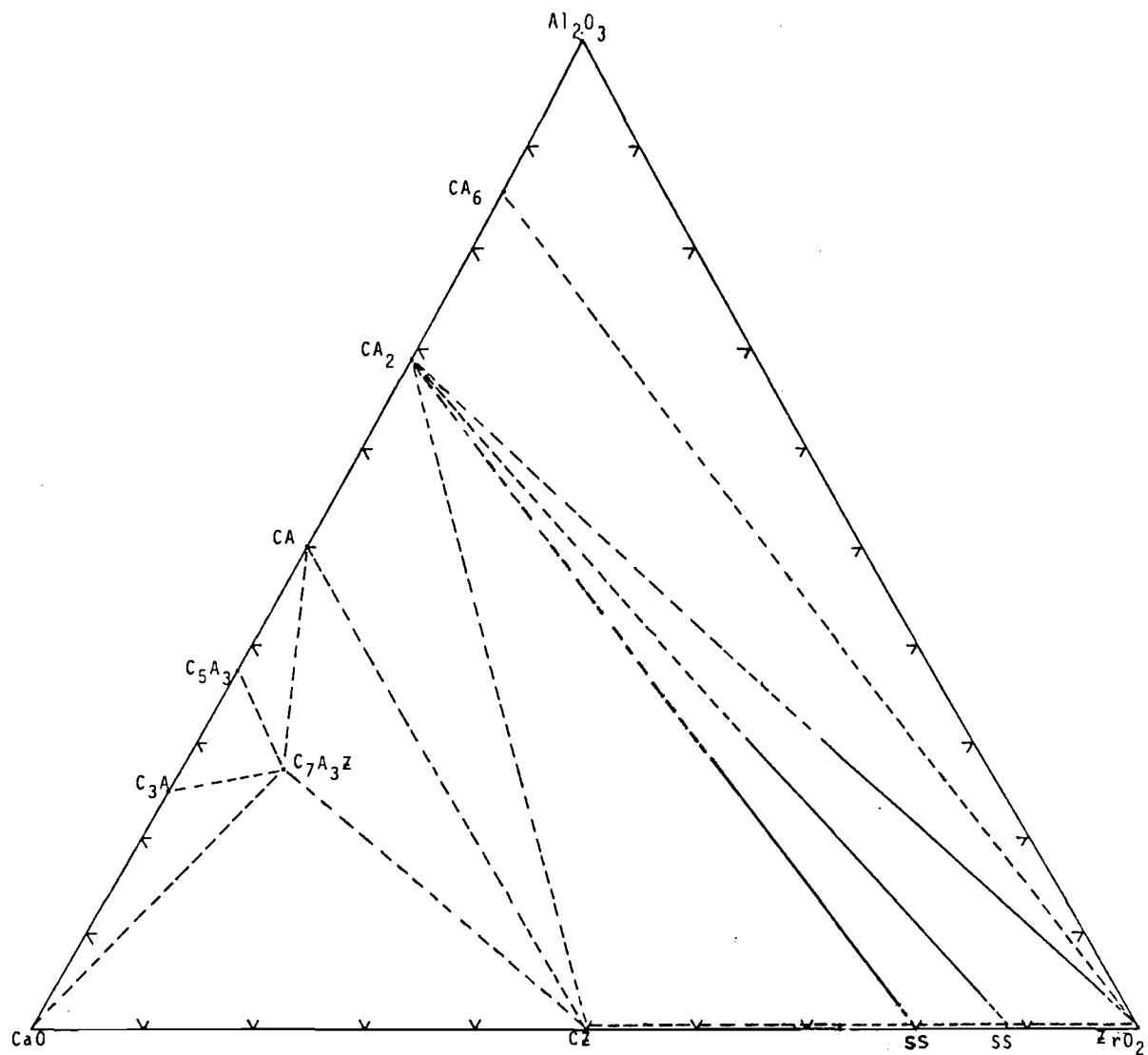


Figure 18. Calcia-Alumina-Zirconia Phase Diagram  
at 1500 °C



the cubic + CZ +  $CA_2$  triangle and one in the  $CA_2$  + CZ + CA triangle, series 4 samples, were fired and analyzed by x-ray. No quantitative or other exhaustive analysis was performed. Phase analysis by x-ray did confirm that the two triangles were drawn properly. The Alkemade line from monoclinic zirconia to  $CA_6$  is also drawn from literature data.<sup>1</sup> Samples 2-5 and 2-10 did confirm the composition of the region to be monoclinic +  $CA_2$  +  $CA_6$ . The phase diagram at greater than 50 mole percent calcia is drawn from the investigation of Berezhnoi.<sup>1</sup>

Upon original x-ray examination of samples 2-11, 2-12, 2-16, 2-21, and 2-22, an additional phase was found to be present in small amounts. Identification from JCPDS File Cards indicated that the phase was  $4CaO \cdot 3Al_2O_3 \cdot SO_3$ . The chemical analysis of the TAM zirconia which was used as a raw material showed an  $SO_2$  content of 0.1%, which was apparently enough for this additional phase to appear on the surface of the samples. When the surface of the pellets was ground off with silicon carbide grinding paper, this phase disappeared in the x-ray scans. Since the phase appeared only on the surface and was caused by an impurity, further consideration was omitted and the surface of each sample was ground sufficiently to eliminate what was considered to be a contaminant.

## B. Long Term, High Temperature Phase Stability

Changes in the amount of solubility of calcia in cubic zirconia were studied for up to 2000 hours at 900°C and 1300°C using compositions A, B, and C. Quantitative x-ray analysis was used to study the destabilization of cubic zirconia. Lattice parameter measurements were made to confirm the indicated amount of destabilization.

### 1. Quantitative X-ray Analysis

The three compositions were chosen in the cubic zirconia + monoclinic zirconia +  $CA_2$  compatibility triangle for determining the stability of the phases over periods of time up to 2000 hours of firing. Two temperatures, 900°C and 1300°C, were chosen for experimentation since these temperatures bracketed the range over which industry might use these compositions as refractories. The three compositions were chosen at points where the cubic to monoclinic zirconia weight ratio was approximately 3:1 as determined from the results of the 1500°C analysis. Sample A was 10.0 mole percent alumina and 12.5 mole percent calcia, sample B was 17.5 mole percent alumina and 14.5 mole percent calcia, and sample C was 25 mole percent alumina and 17.5 mole percent calcia.

The three compositions were initially fired at 1550°C in order to densify the pellets more completely than at 1500°C. X-ray analysis of the fired pellets showed that

even a 50°C increase in temperature had significantly increased the weight ratio of cubic to monoclinic zirconia compared to the contents at 1500°C. This change in weight ratio indicated that one of the solid solution endpoints changed considerably. The analysis of sample C showed no monoclinic zirconia at 1550°C, which meant that the Alkemade line had moved to a CaO content lower than this composition point. In order to calculate the position of the  $\text{Ca}_2$ -cubic zirconia SS Alkemade line, it was assumed that the Alkemade line joining  $\text{Ca}_2$  and monoclinic zirconia did not move, since Duwez<sup>9</sup> and Hennicke<sup>25</sup> both indicated that there was very limited solid solution in monoclinic zirconia. From the equation for the  $\text{Ca}_2$ -monoclinic zirconia line at 1500°C, the CaO content on the  $\text{Ca}_2$ -monoclinic zirconia line at 10, 17.5, and 25 mole percent alumina (compositions A, B, and C respectively) was determined. Using these calcia contents at 0% cubic zirconia and the ratio of cubic to cubic plus monoclinic zirconia at the three compositions, the 100% cubic line was calculated for the 1550°C firing as described for 1500°C, Figure 19. Since there was only one data point at each alumina composition, the location of the line could not be determined as accurately as the 1500°C line was established. The implication from the position of the 1550°C line is

At 1550 °C for 100% cubic zirconia:  $\%CaO = 0.26 (Al_2O_3) + 11.14$

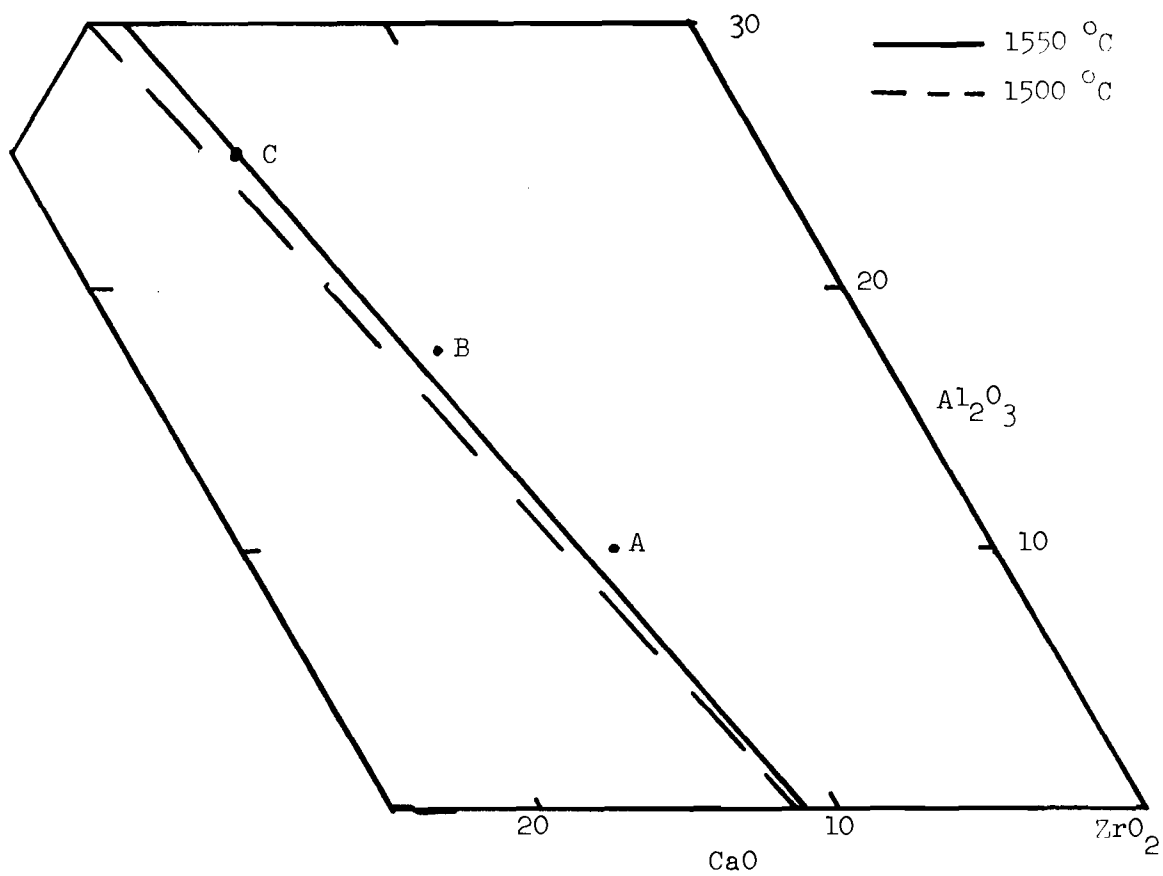


Figure 19. Alkemade Line at 1550 °C from  $CA_2$  to Cubic Zirconia

that the composition of  $\text{CA}_2$  was varying more than the composition of the cubic zirconia. Because only three data points were available, this conclusion is open to question. It must also be stated that if the  $\text{CA}_2$  composition were changing with temperature increase, then the  $\text{CA}_2$ -monoclinic zirconia Alkemade line would also be changing; thus the  $1500^\circ\text{C}$  line equation would not be valid for determining the second data point at each alumina composition. However, from lattice parameter measurements for cubic zirconia, to be presented below, it will be shown that CaO solid solution changes in zirconia resulted in the Alkemade line movement.

Quantitative x-ray results of the surface scans of the long term fired samples after firing at  $900^\circ\text{C}$  and  $1300^\circ\text{C}$  were inconsistent, particularly for the samples being held at  $900^\circ\text{C}$ . The pellet surfaces were ground to remove approximately 1mm and consistency was obtained. Further grinding showed no changes in the weight ratios of cubic to monoclinic zirconia. The quantitative x-ray results for the long term fired samples are presented in Appendix D. Changes in the ratio of cubic zirconia to cubic plus monoclinic zirconia, Figures 20 and 21, give a clear indication of phase changes with respect to time.

At  $1300^\circ\text{C}$  little problem existed with surface inconsistencies, as results obtained from a lightly ground

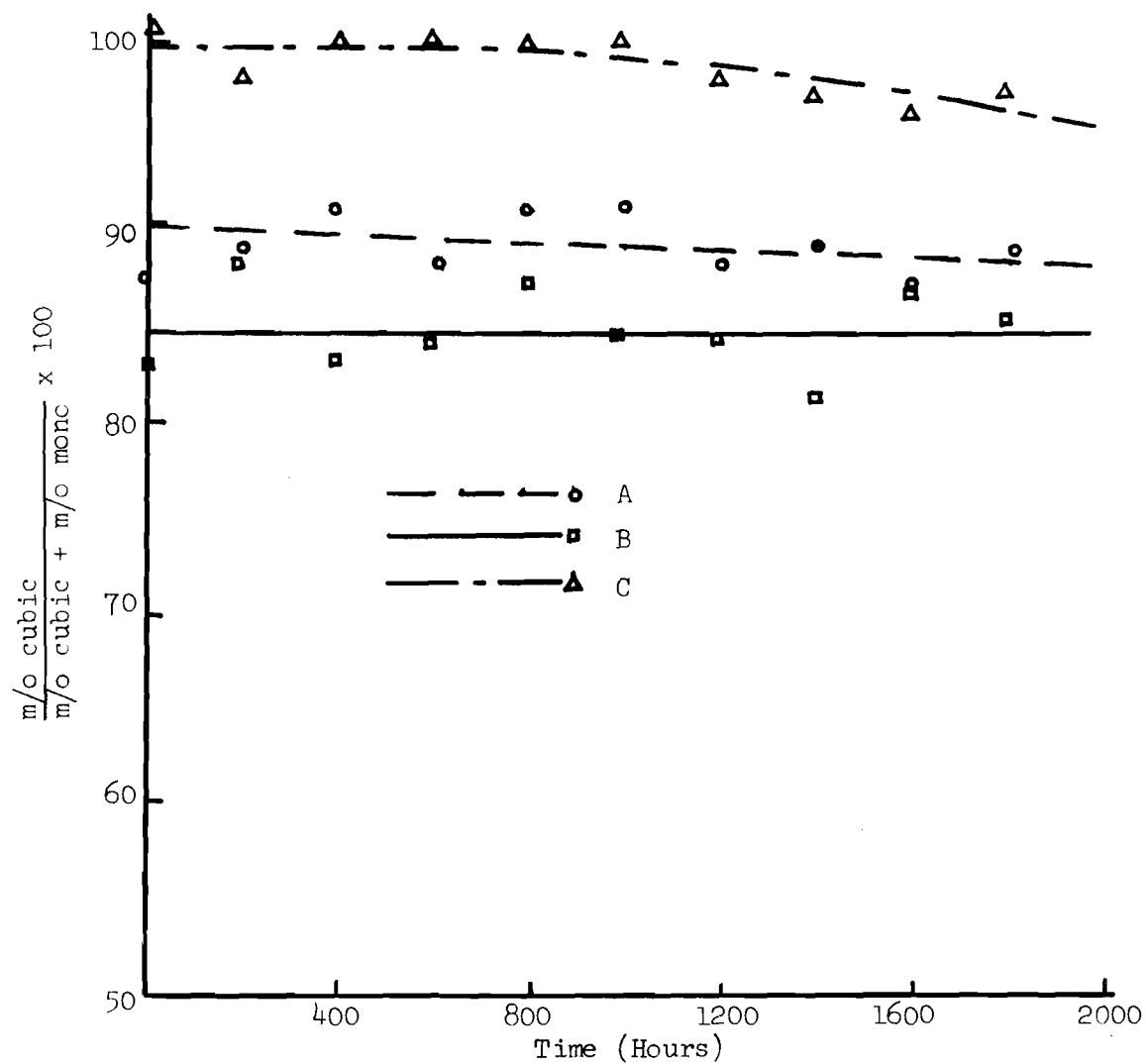


Figure 20. Change in Amount of Cubic Zirconia with Time at 900 °C

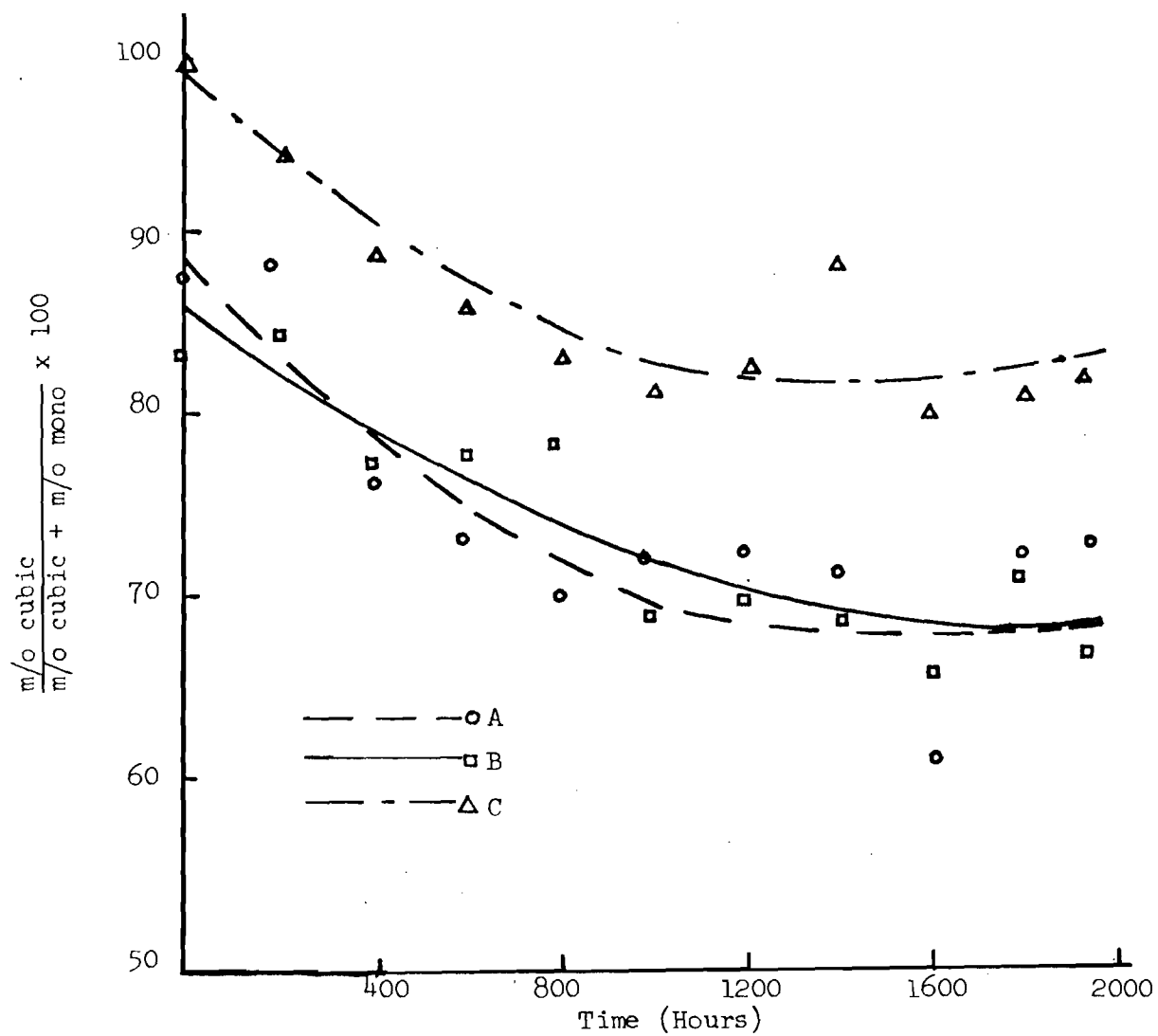


Figure 21. Change in Amount of Cubic Zirconia with Time at 1300 °C

surface agreed well with a 1mm surface removal. A considerable decrease in the amount of cubic zirconia with firing time can be seen. By 1000 hours equilibrium had been reached, as indicated by a constant cubic to cubic plus monoclinic ratio from 1000 to 2000 hours. It may be noted that sample C must be very close to the boundary because its composition changed radically in the first 400 hours. Samples A and B changes in the same direction but to a lesser extent.

The Alkemade line from  $CA_2$  to cubic zirconia at  $1300^{\circ}C$  was determined by the same method as was used at  $1550^{\circ}C$ , and thus not too great an accuracy could be implied. The calculated position, Figure 22, indicates that approximately a three mole percent increase occurred in the calcia content of cubic zirconia from  $1500^{\circ}C$  to  $1300^{\circ}C$ . The increase was slightly more than expected from results reported by Duwez<sup>9</sup>, but the data is limited, and therefore not conclusive.

At  $900^{\circ}C$  the destabilization process took place very slowly. Sample C showed this process most clearly, in that the x-ray data indicated no monoclinic zirconia for 1000 hours and only a slow increase from 1000 to 2000 hours. Changes in samples A and B are almost imperceptible. After about 1400 hours sample A appeared to begin to destabilize. In sample B there was no perceptible change in the weight



At 1300 °C for 100% cubic zirconia:  $\%CaO = 0.17 (Al_2O_3) + 14.6$

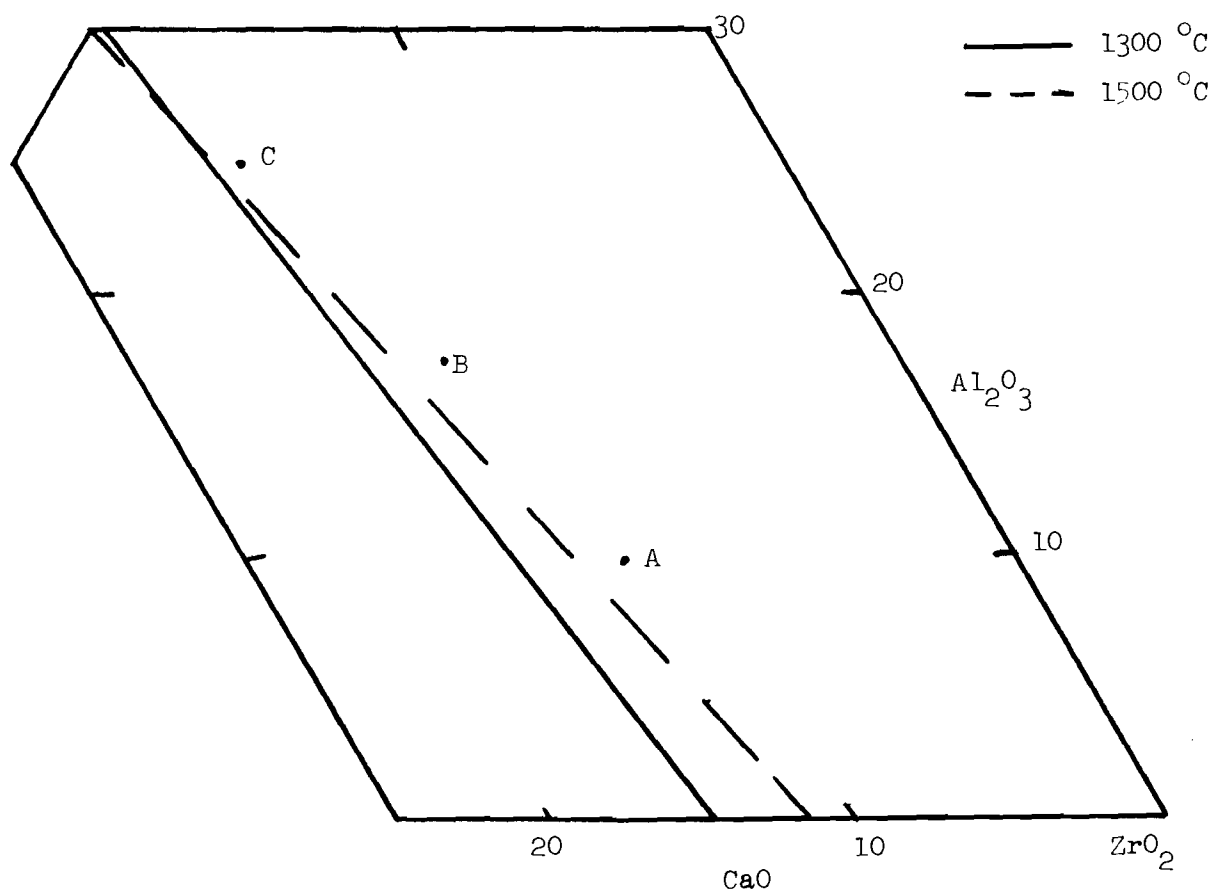


Figure 22. Alkemade Line at 1300 °C from  $CA_2$  to Cubic Zirconia

ratio of cubic to monoclinic zirconia. Thus with the cubic to monoclinic ratios showing little change from 1550°C, the 900°C samples are not near equilibrium, even after 2000 hours. From thermal expansion measurements made on these samples to be presented later, the monoclinic zirconia content was found to be increasing even at 200 and 400 hours for each of the samples at 900°C, but the change was small, indicating that only a slight amount of destabilization was occurring in samples fired to 1550°C. Because equilibrium was not attained at 900°C, no estimation of the tie line at this temperature could be made.

At 900°C the above data agrees well with the results obtained by Duwez<sup>9</sup> for long term stability of a pure calcia stabilized zirconia. At 1300°C, though, he found much better stability of calcia stabilized zirconia than was indicated for calcia stabilized zirconia with alumina additions.

## 2. Lattice Parameter Determinations for Cubic Zirconia

In order to show that the calcia content of the zirconia cubic solid solution was changing, the lattice parameter was determined for samples at 0, 200, 1000, and 2000 hours at both 900°C and 1300°C and for the 1300°C samples also at 400 hours. A lattice parameter value of 5.126 for the samples as fired at 1550°C agrees better with the data published by Garvie<sup>10</sup> than with that of Duwez<sup>9</sup>.

Figure 23 shows the averaged lattice parameters of samples A, B, and C versus time and includes the variations which were observed. The  $1300^{\circ}\text{C}$  data is as expected. Both Duwez and Garvie indicated that a variation in  $a$  of 0.003 Å represents approximately a change in composition of two mole percent calcia. Thus the change in lattice parameter from  $1550^{\circ}\text{C}$  to  $1300^{\circ}\text{C}$  agrees well with the calculated measurement of the Alkemade lines. The phase diagram of the calcia-zirconia binary by Duwez also confirms the results. The samples fired at  $1550^{\circ}\text{C}$  have about two mole percent less calcia than those that have reached equilibrium at  $1300^{\circ}\text{C}$ .

The lattice parameter results for the  $900^{\circ}\text{C}$  samples cannot be understood strictly from a crystal structure point of view. With the cubic zirconia being the highest thermal expansion phase present, cooling the samples from  $1550^{\circ}\text{C}$  apparently resulted in enough tension in the lattice to expand it slightly. On reheating, annealing at  $900^{\circ}\text{C}$ , and cooling, the lattice strain due to tension was less, because the temperature change was smaller. Thus annealing at  $900^{\circ}\text{C}$  with no composition change could result in a decrease of the cubic zirconia lattice parameter. From quantitative x-ray measurements, equilibrium was shown not to have been attained at  $900^{\circ}\text{C}$  even after firing for 2000 hours. If equilibrium at  $900^{\circ}\text{C}$  were obtained, a larger lattice would have been expected than that found at  $1300^{\circ}\text{C}$ ,

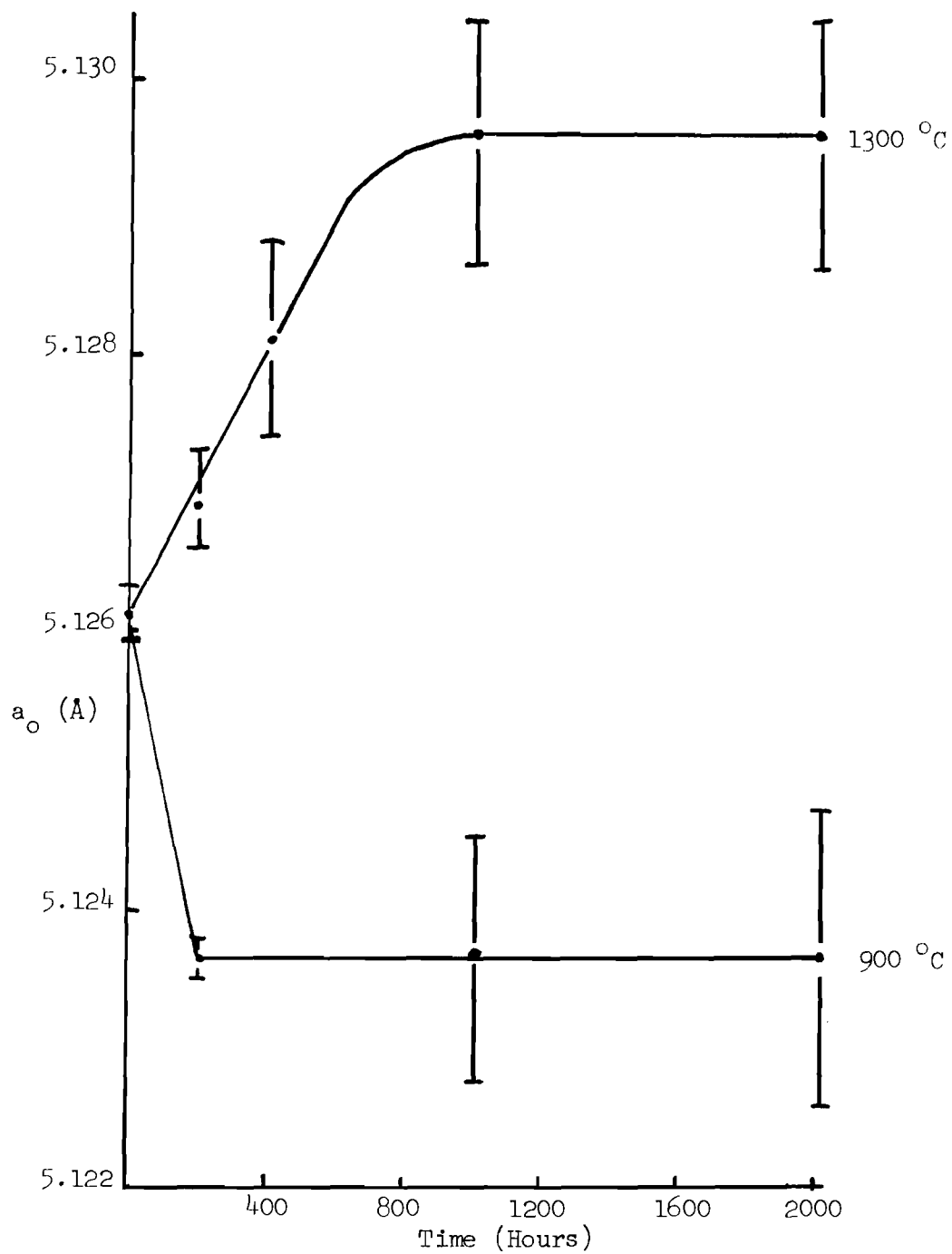


Figure 23. Lattice Parameter Changes with Time

due to increasing calcia content. The tension in the lattice was apparently masking the increase in size, and since the samples were not even near equilibrium, the lattice might not in reality be as large as the 1300°C lattice at 2000 hours. An effect that cannot be evaluated is the presence of alumina ions, which are half the size of calcia ions. If there were indeed an amount of alumina in the cubic zirconia lattice, then as the amount varied with temperature changes, the alumina could cause the lattice to become smaller, reversing the effect of the addition of calcia. Evaluation of this effect was not possible from the data and equipment available.

### C. Long Term, High Temperature Property Changes

#### 1. Properties of Calcium Dialuminate, $CA_2$

Prior to a discussion of the long term high temperature property changes in the high  $ZrO_2$  compositions A, B, and C, the properties determined for calcium dialuminate will be presented. The composition 67.5 m/o  $Al_2O_3$ -32.0 m/o  $CaO$ -0.5 m/o  $ZrO_2$  was selected for physical property determination of  $CA_2$ . X-ray diffraction analysis of the fired  $CA_2$  bars, Figure 24, indicated a trace of CA as the only other crystalline phase. However, a zirconia phase was observed optically, Figure 25a, therefore the solubility of  $ZrO_2$  in  $CA_2$  was less than 0.5%. The bulk density of the  $CA_2$  bars was  $2.40 \pm 0.02$  g/cc<sup>0</sup> which calculates to a

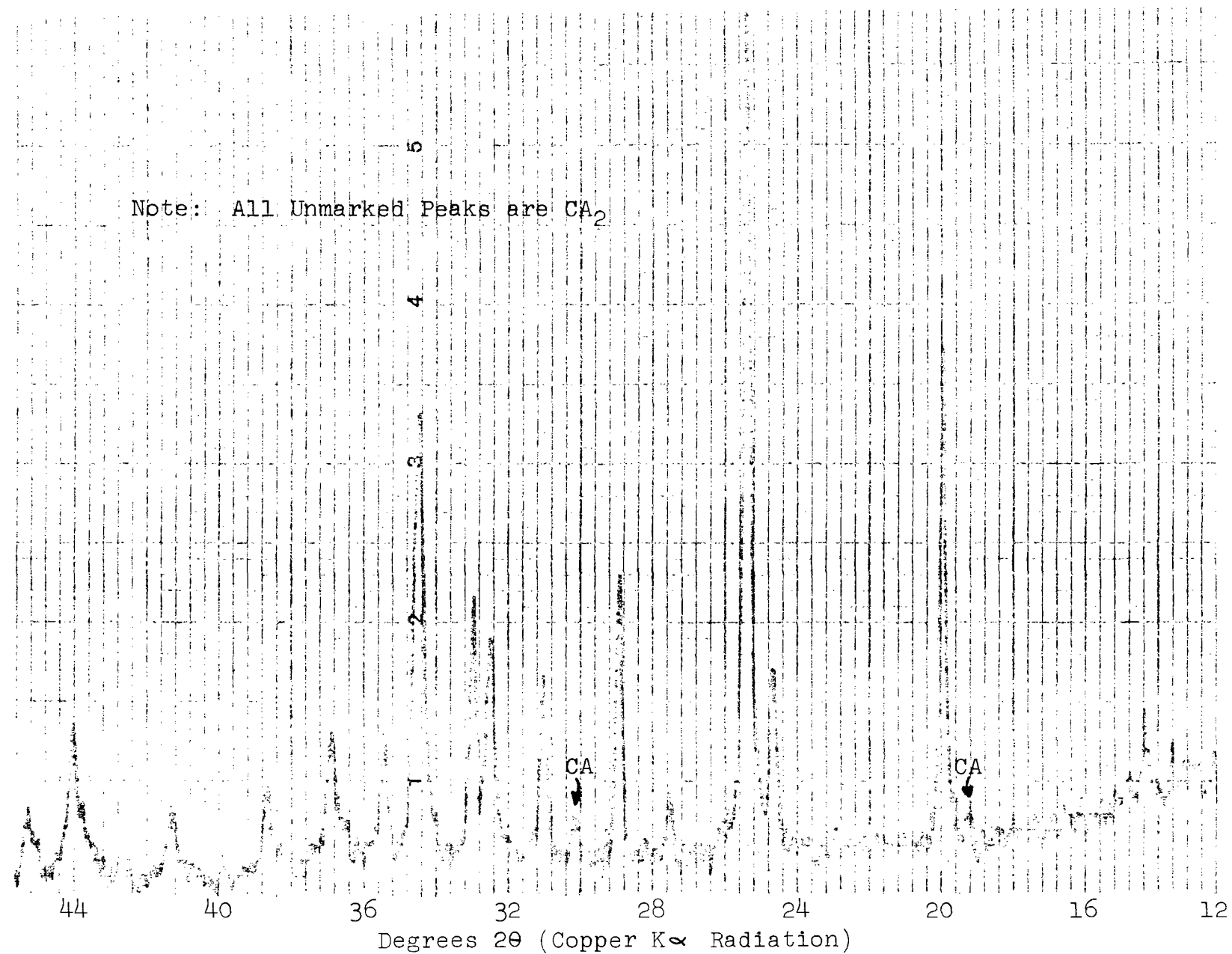
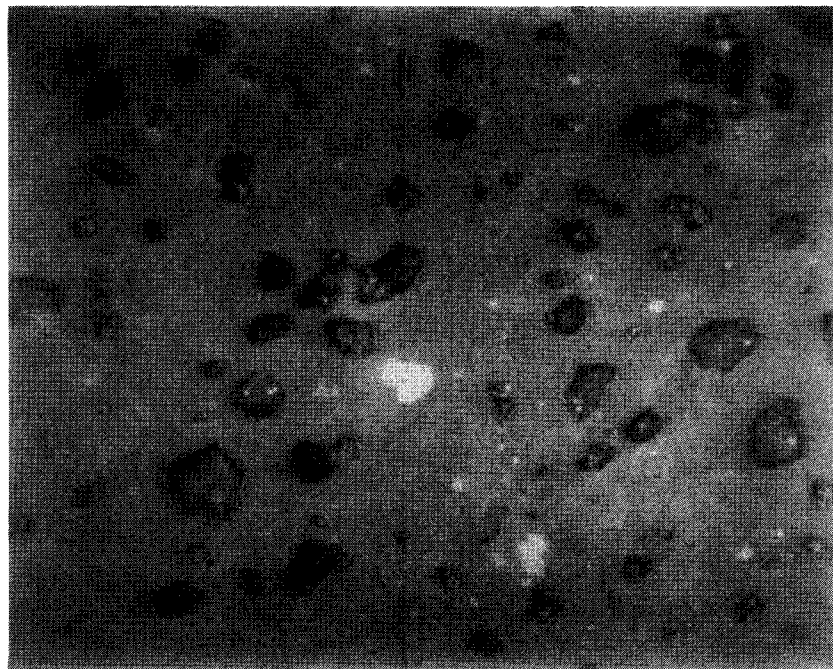
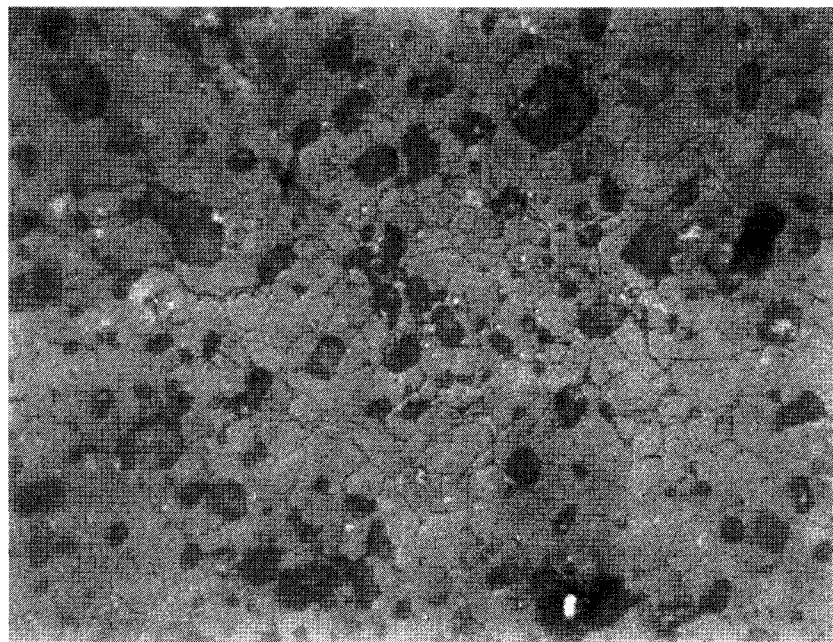


Figure 24. X-ray Diffraction Trace of  $\text{CA}_2$  Bars Showing Peaks for  $\text{CA}_2$  and a Trace of CA (Marked Peaks).



(a)



(b)

Figure 25. Reflected Light Micrographs of CA<sub>2</sub> Bars,  
(a) Polished Section, (b) Thermally Etched  
to Show Grain Boundaries, 600X.

porosity of 16.9%. Porosity calculated from optical micrographs was 17.4%. The average grain size of the  $CA_2$  as determined from thermally etched polished sections, Figure 25b, was approximately 6 to 7  $\mu m$ .

Flexure strength and microhardness of the  $CA_2$  samples has been reported in Tables 14 and 15. These data will be discussed in conjunction with the high  $ZrO_2$  compositions.

Thermal expansions measurements on the  $CA_2$  bars and composition 6-7 is reported in Table 16 and Figure 26. Composition 6-7 contained a trace of  $CA_6$  and the  $CA_2$  bars contained a trace of CA. The expansion of the two compositions agreed well with each other and with values reported in literature being approximately  $5.0 \times 10^{-6}/^{\circ}C$  at  $1200^{\circ}C$ .

## 2. Flexure Strength of High $ZrO_2$ Compositions

Results of room temperature and high temperature flexure strengths of compositions A, B, and C from the  $CA_2$ -Cubic  $ZrO_2$ -Monoclinic  $ZrO_2$  compatibility triangle are summarized in this section and tabulated in Appendix E. Prior to a discussion of the flexure strength data, a review of the chemical and crystallographic compositions of A, B, and C will help to provide an explanation of the changing compositions of A, B, and C with time.



Table 14. Flexure Strength of  $\text{CaO} \cdot 2\text{Al}_2\text{O}_3$  as a Function of Temperature

Temperature (°C)	Flexure Strength (psi)	Standard Deviations (psi)	Percent Standard Deviations
20	5040	1010	20.0
900	5780	800	13.8
1100	5770	910	15.8
1300	6340	920	14.5

Table 15. Room Temperature Microhardness of  $\text{CaO} \cdot 2\text{Al}_2\text{O}_3$

Load (grams)	Knoop Hardness ( $\text{kg/mm}^2$ )
30.5	1006
34.0	984
39.0	917
42.5	906
46.0	770
51.0	651
59.0	528

Table 16. Thermal Expansion of  $CA_2$ 

Temperature	$CA_2$ Bars*		Composition 6-7!	
$^{\circ}C$	Expansion	$\overset{a}{Eng}$ $\times 10^{-6}/^{\circ}C$	Expansion	$\overset{a}{Eng}$ $\times 10^{-6}/^{\circ}C$
200	0.058	3.22	0.058	3.22
400	0.148	3.90	0.130	3.42
600	0.240	4.14	0.230	3.96
800	0.360	4.61	0.335	4.30
1000	0.490	5.00	0.460	4.69
1200	0.610	5.16	0.565	4.79

\* $CA_2$  Bars - Composition (m/o), 67.5  $Al_2O_3$ , 32.0 CaO,  
0.5  $ZrO_2$  Phases,  $CA_2$ , and trace of CA.

! Composition 6-7 - Composition (m/o), 69.0  $Al_2O_3$ ,  
31.0 CaO Phases,  $CA_2$  and trace of  
 $CA_6$ .

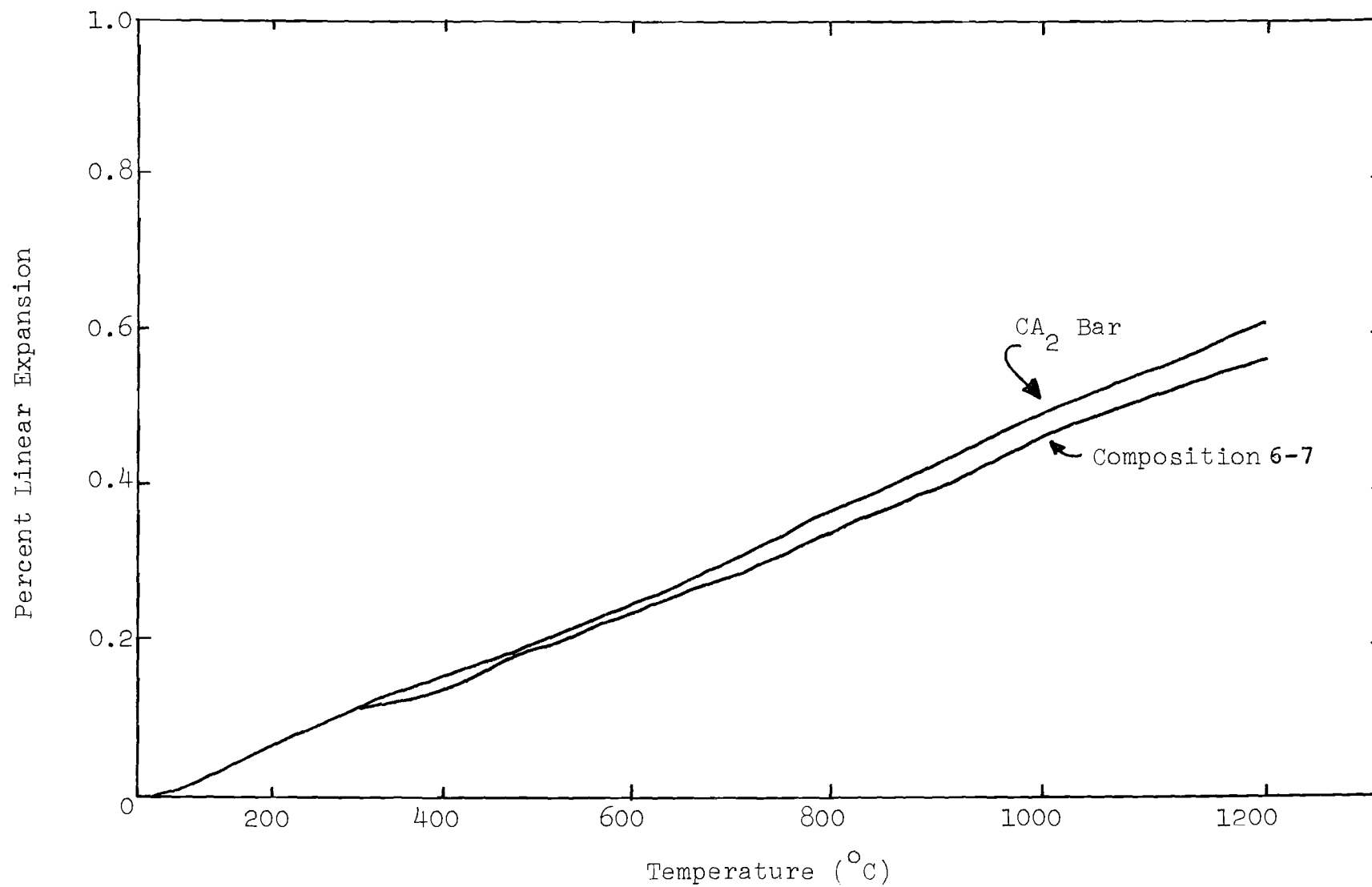


Figure 26 Thermal Expansion of CA<sub>2</sub> Containing a Trace of CA (CA<sub>2</sub> Bar) and CA<sub>2</sub> Containing a Trace of CA<sub>6</sub> (Composition 6-7 ).

The change in chemical composition from A to B to C, Table 17, was to larger CaO and  $\text{Al}_2\text{O}_3$  contents and to smaller  $\text{ZrO}_2$  contents. These compositions are near the tie line between  $\text{CA}_2$  and the lower CaO content Cubic  $\text{ZrO}_2$  SS composition. Crystallographic contents "as fired" at  $1550^\circ\text{C}$  for A, B, and C on a weight basis, Table 17, shows increases in  $\text{CA}_2$  quantity from A to B to C. Composition A contained the most cubic  $\text{ZrO}_2$  at 78.6 w/o and composition B the least cubic  $\text{ZrO}_2$  at 65.9 w/o. On heat treatment at 900 and  $1300^\circ\text{C}$ , the monoclinic  $\text{ZrO}_2$  content of all compositions increased with time and the cubic  $\text{ZrO}_2$  content decreased correspondingly. At  $900^\circ\text{C}$ , Figure 27, the change in monoclinic  $\text{ZrO}_2$  content was small (2-3 w/o) and probably would not affect flexure strength. However, the increase in monoclinic  $\text{ZrO}_2$  at  $1300^\circ\text{C}$ , Figure 28, was approximately 12-16 w/o for all three compositions and if this quantity change in monoclinic  $\text{ZrO}_2$  content significantly affects flexure strength it should be detectable between "as fired" samples and samples heat treated at  $1300^\circ\text{C}$  for 1000 for 2000 hours.

Comparisons of the flexure strength of compositions A, B, and C may be seen in Figure 29 where each data point represents the average strength of all heat treatment conditions. Significant strength increases occurred as the  $\text{CA}_2$  content increased from A to B to C. The strength

Table 17. Compositions of  $\text{CaO-Al}_2\text{O}_3\text{-ZrO}_2$   
Samples A, B, and C.

Oxide	Mole%		
	A	B	C
CaO	12.5	14.5	17.5
$\text{Al}_2\text{O}_3$	10.0	17.5	25.0
$\text{ZrO}_2$	77.5	68.0	57.5

Phase	Weight% "As Fired"		
	A	B	C
Cubic $\text{ZrO}_2$	78.6	65.9	67.7
Monoclinic $\text{ZrO}_2$	8.0	12.0	0
$\text{CaO-2Al}_2\text{O}_3$	12.4	22.1	32.4

Phase	Wt.% After 2000 hrs. at 1300°C		
	A	B	C
Cubic $\text{ZrO}_2$	62.6	54.4	55.1
Monoclinic $\text{ZrO}_2$	25.0	23.5	12.5
$\text{CaO-2Al}_2\text{O}_3$	12.4	22.1	32.4

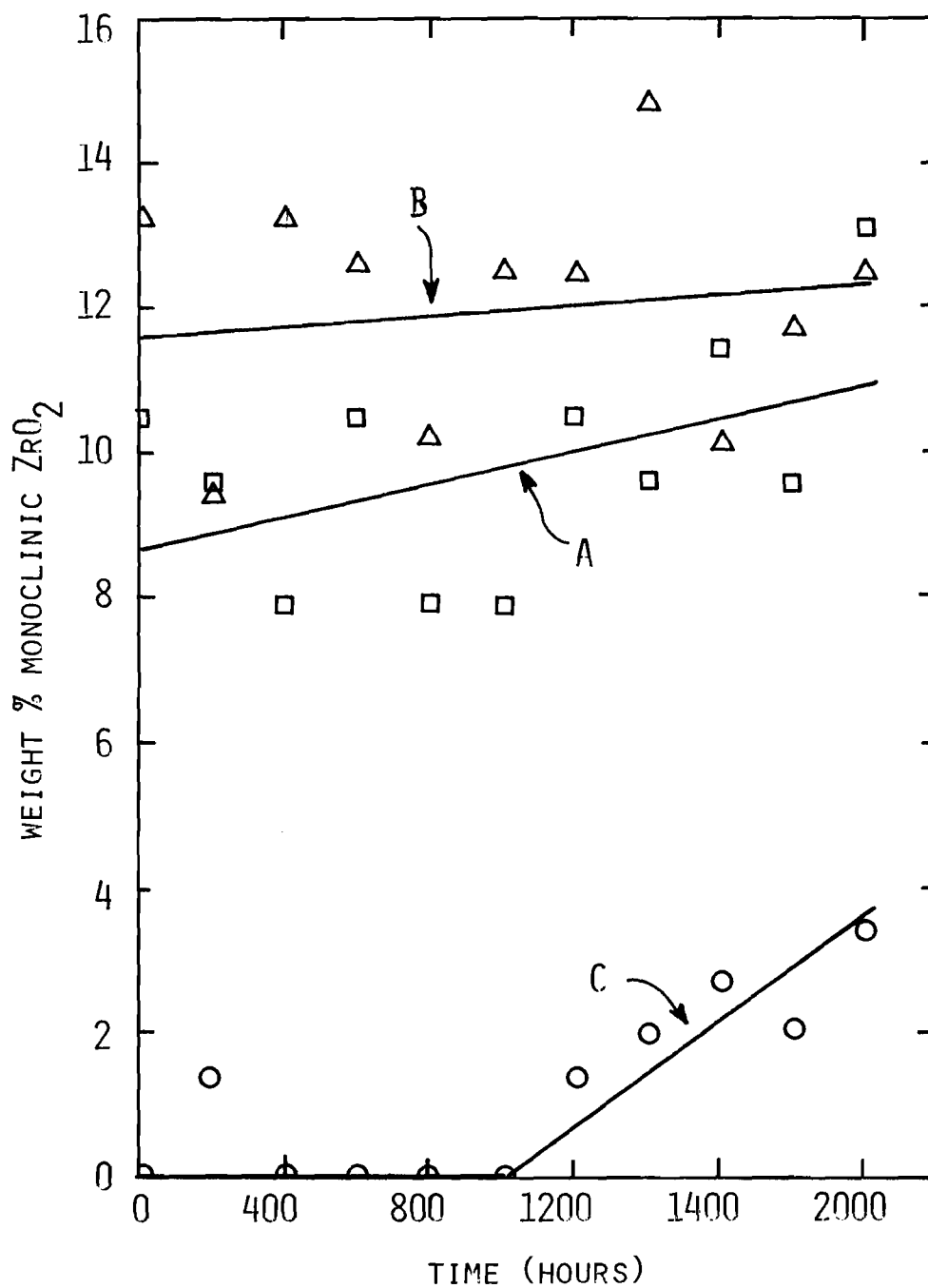


FIGURE 27. CHANGE IN MONOCLINIC  $ZrO_2$  CONTENT WITH TIME AT 900°C FOR  $CaO-Al_2O_3-ZrO_2$  COMPOSITIONS A, B, AND C.

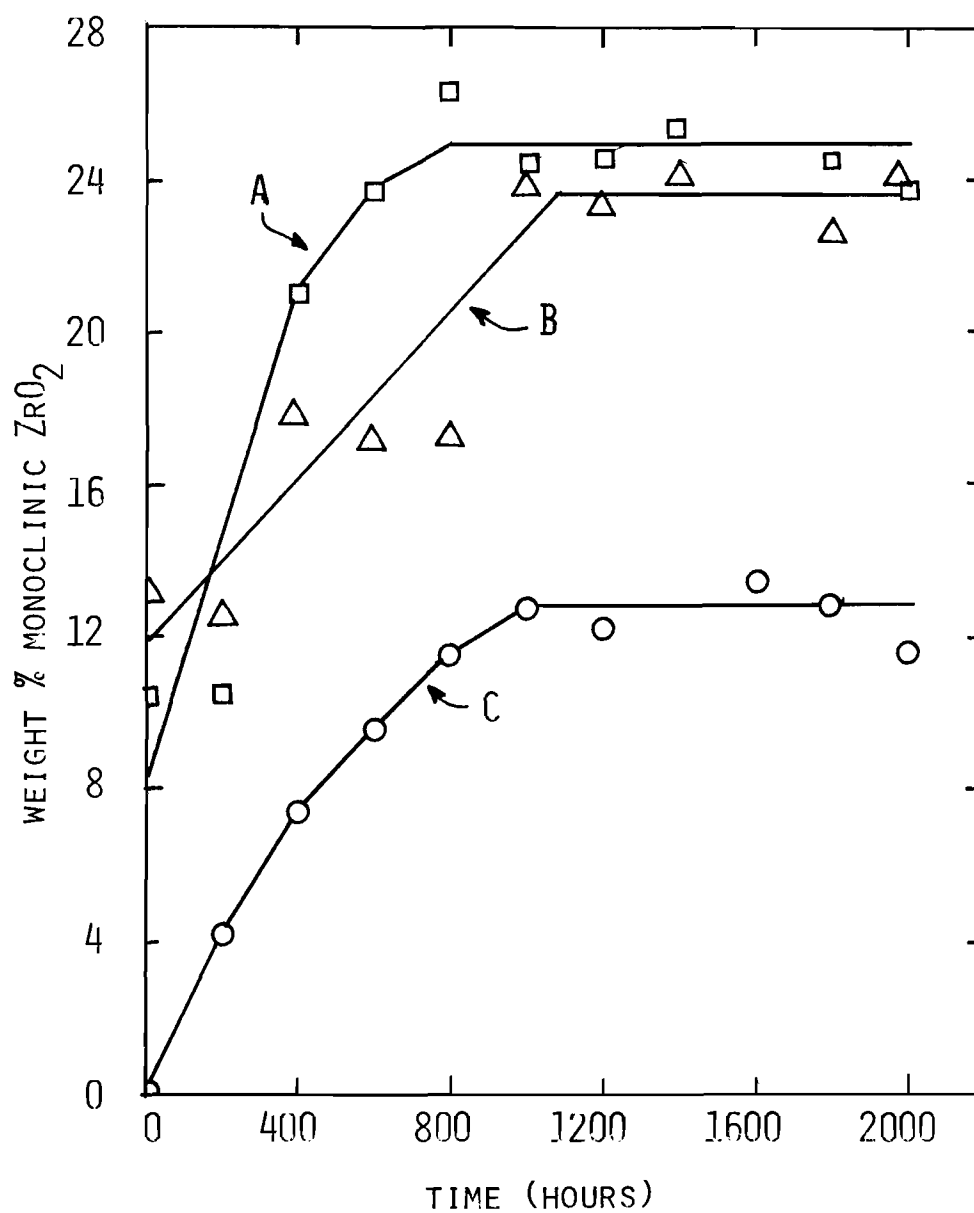


FIGURE 28. CHANGE IN MONOCLINIC  $ZrO_2$  CONTENT WITH TIME AT 1300°C FOR  $CaO-Al_2O_3-ZrO_2$  COMPOSITIONS A, B, AND C.

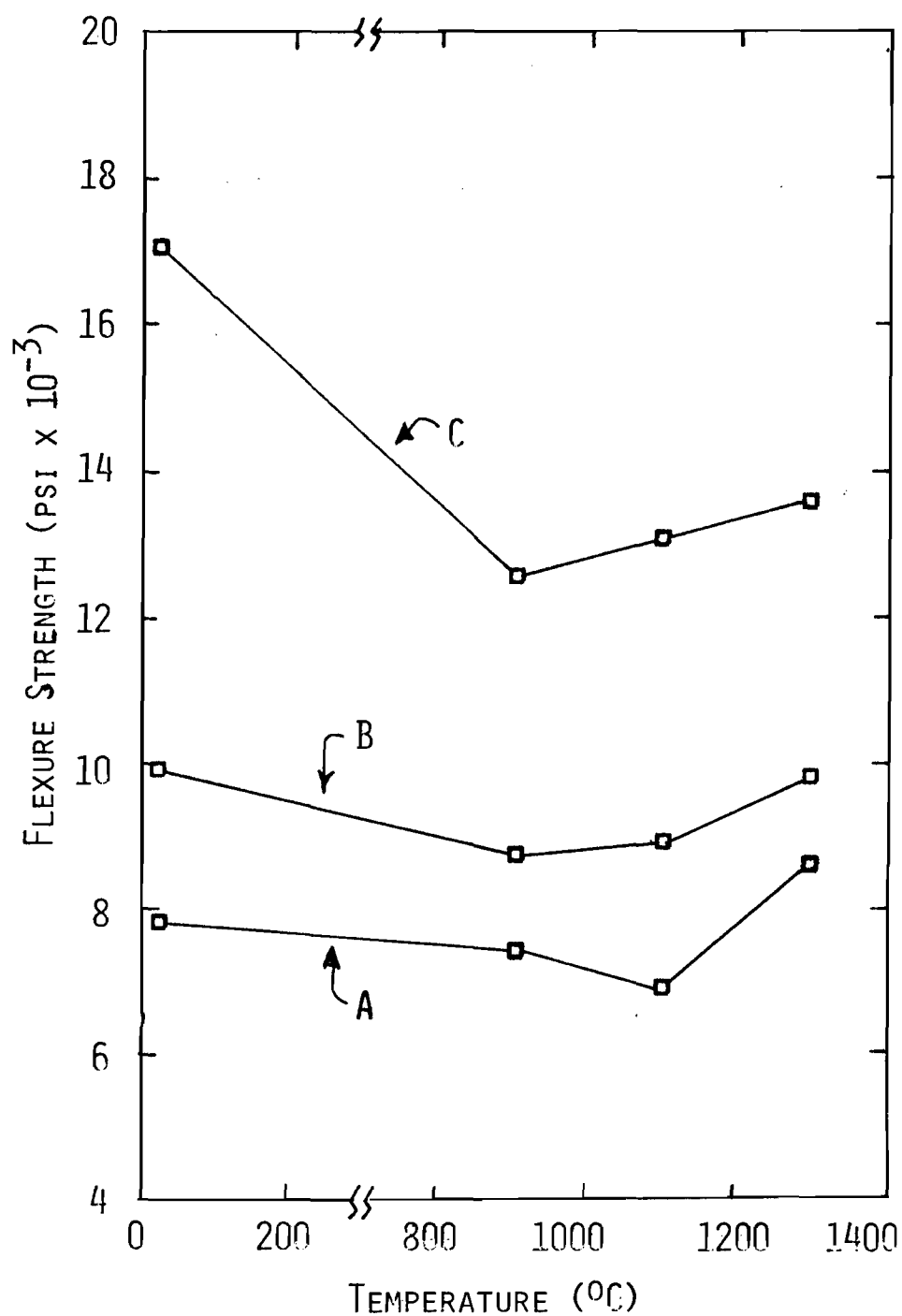


FIGURE 29. EFFECT OF TEMPERATURE ON FLEXURE STRENGTH OF  $\text{CaO-Al}_2\text{O}_3\text{-ZrO}_2$  COMPOSITIONS A, B, AND C. EACH POINT REPRESENTS THE AVERAGE OF ALL HEAT TREATMENT CONDITIONS.



of all three was relatively constant with temperature up to 1300°C showing a slight decrease at 900 and 1100°C (~10%) as compared to 20 and 1300°C strengths. A slight strength decrease is probably to be expected around the 1000°C monoclinic  $\text{ZrO}_2$  phase inversion. The higher average strength of composition C at 20°C is misleading as a strength of 27 Kpsi for samples heat treated at 1300°C for 1000 hours is included in this average and will be discussed below.

The effect of heat treatment at 900°C and 1300°C for up to 2000 hours is presented in Figures 30-32. Other than composition C-1300°C-1000 hours heat treatment, there were no significant effects produced by the heat treatments. The standard deviation of all the data points in Figures 30-32 was approximately 5 to 20% which covers the ranges of strengths produced by the heat treatments. Thus, heat treatment was not detrimental to flexure strength.

In considering the effect of monoclinic  $\text{ZrO}_2$  on flexure strength, it must be concluded that for the variations in monoclinic  $\text{ZrO}_2$  exhibited by these compositions, the effect is negligible. If increases in monoclinic  $\text{ZrO}_2$  weakened the samples, the 1300°C heat treatment should have produced weaker samples compared to the "as fired" and 900°C samples. Heat treatment at 1300°C did not

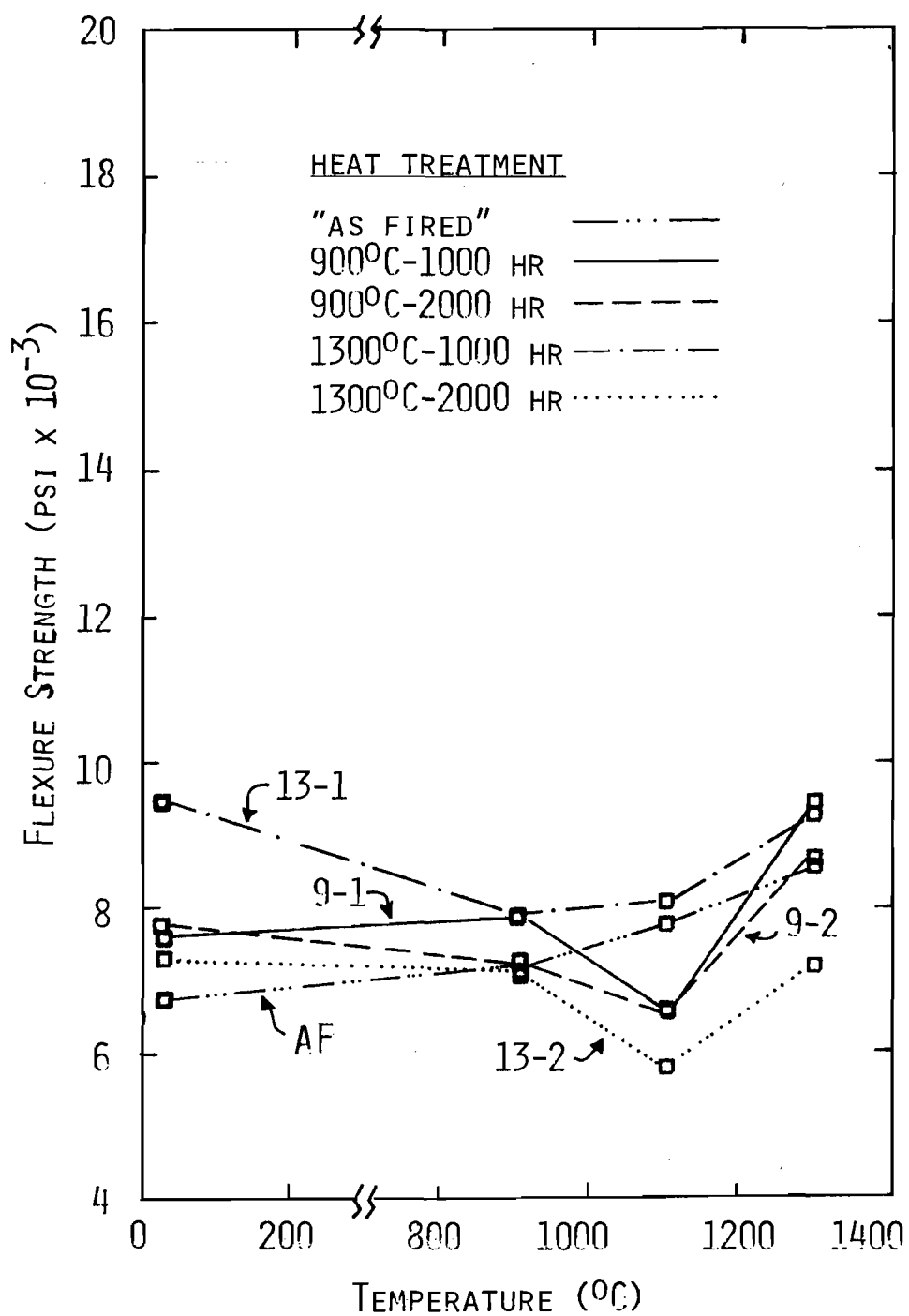


FIGURE 30. EFFECT OF TEMPERATURE ON FLEXURE STRENGTH OF  $\text{CAO-AL}_2\text{O}_3\text{-ZrO}_2$  COMPOSITION A AFTER HEAT TREATMENTS.

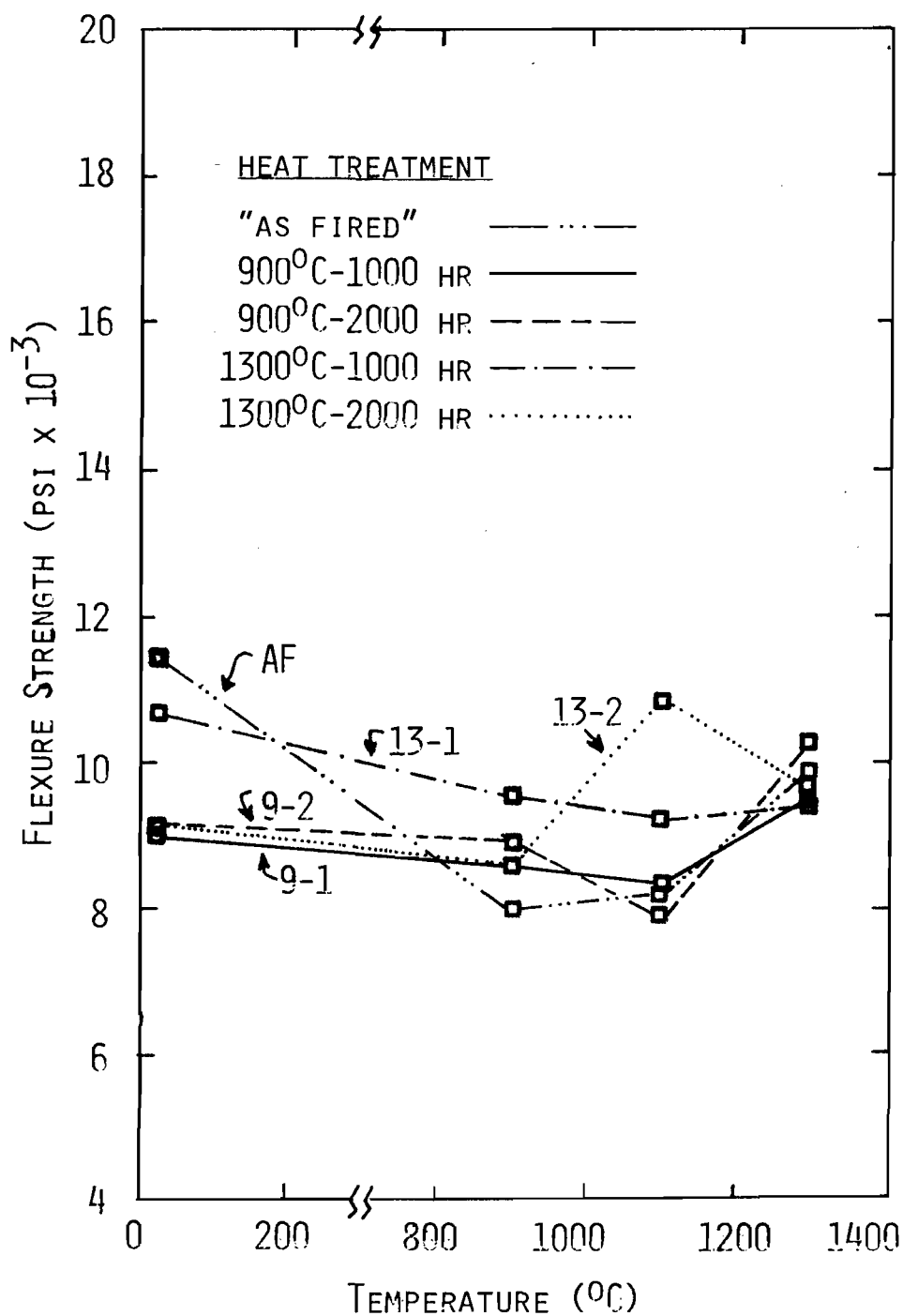


FIGURE 31. EFFECT OF TEMPERATURE ON FLEXURE STRENGTH OF  $\text{CaO-Al}_2\text{O}_3\text{-ZrO}_2$  COMPOSITION B FOR VARIOUS HEAT TREATMENT CONDITIONS.

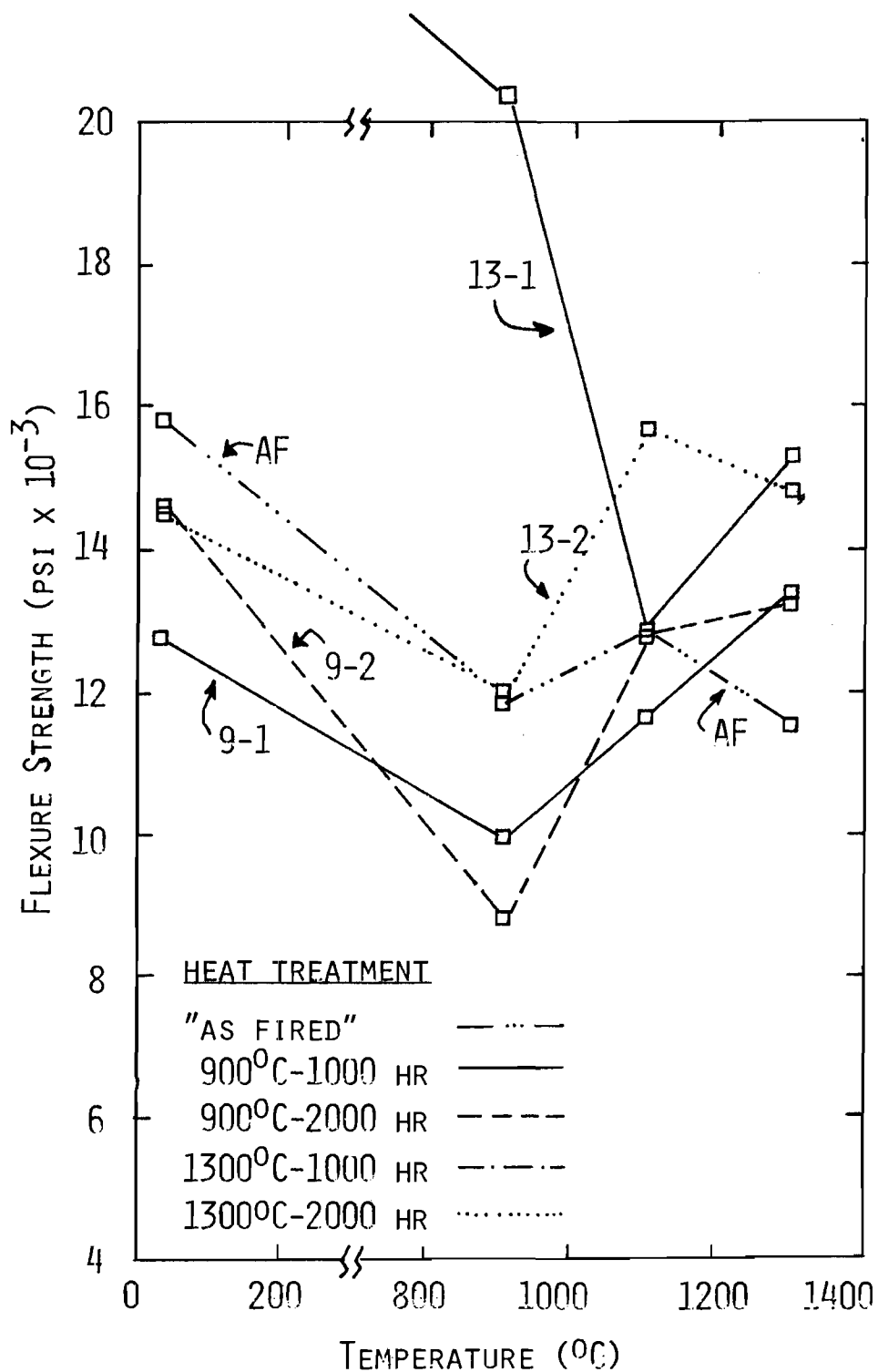


FIGURE 32. EFFECT OF TEMPERATURE ON FLEXURE STRENGTH OF  $\text{CaO-Al}_2\text{O}_3\text{-ZrO}_2$  COMPOSITION C FOR VARIOUS HEAT TREATMENT CONDITIONS.

degrade flexure strength and thus the increased monoclinic  $\text{ZrO}_2$  produced by heat treatment was not detrimental.

The strength produced by heat treatment of sample C at  $1300^\circ\text{C}$  for 1000 hours is worthy of special note. The average strength of composition C for all heat treatments was approximately 14 Kpsi. The average strength for samples of composition C heat treated at  $1300^\circ\text{C}$  for 1000 hours was 27 kpsi when broken at  $20^\circ\text{C}$  and 20.5 kpsi when broken at  $900^\circ\text{C}$ . No adequate explanation is apparent for the significantly higher strengths. They were fired and strength tested with other compositions that showed no significant variations and thus lack of control of testing procedures must be eliminated as an explanation. The most significant difference in sample history is that the "as fired" "C" contained no monoclinic  $\text{ZrO}_2$ ; on heating treating at  $1300^\circ\text{C}$  for 1000 hours, 12% monoclinic  $\text{ZrO}_2$  was formed; and cooling to room temperature was the only time that the monoclinic  $\text{ZrO}_2$  of these samples went through the tetragonal-monoclinic inversion prior to strength testing at  $20^\circ\text{C}$  and  $900^\circ\text{C}$ . For all other samples of all compositions and testing conditions, there was monoclinic  $\text{ZrO}_2$  present that went through the inversion a minimum of two times. Comparison of flexure strength of  $\text{CA}_2$  to "as fired" values for compositions A, B, and C, Figure 33 shows that  $\text{CA}_2$  values

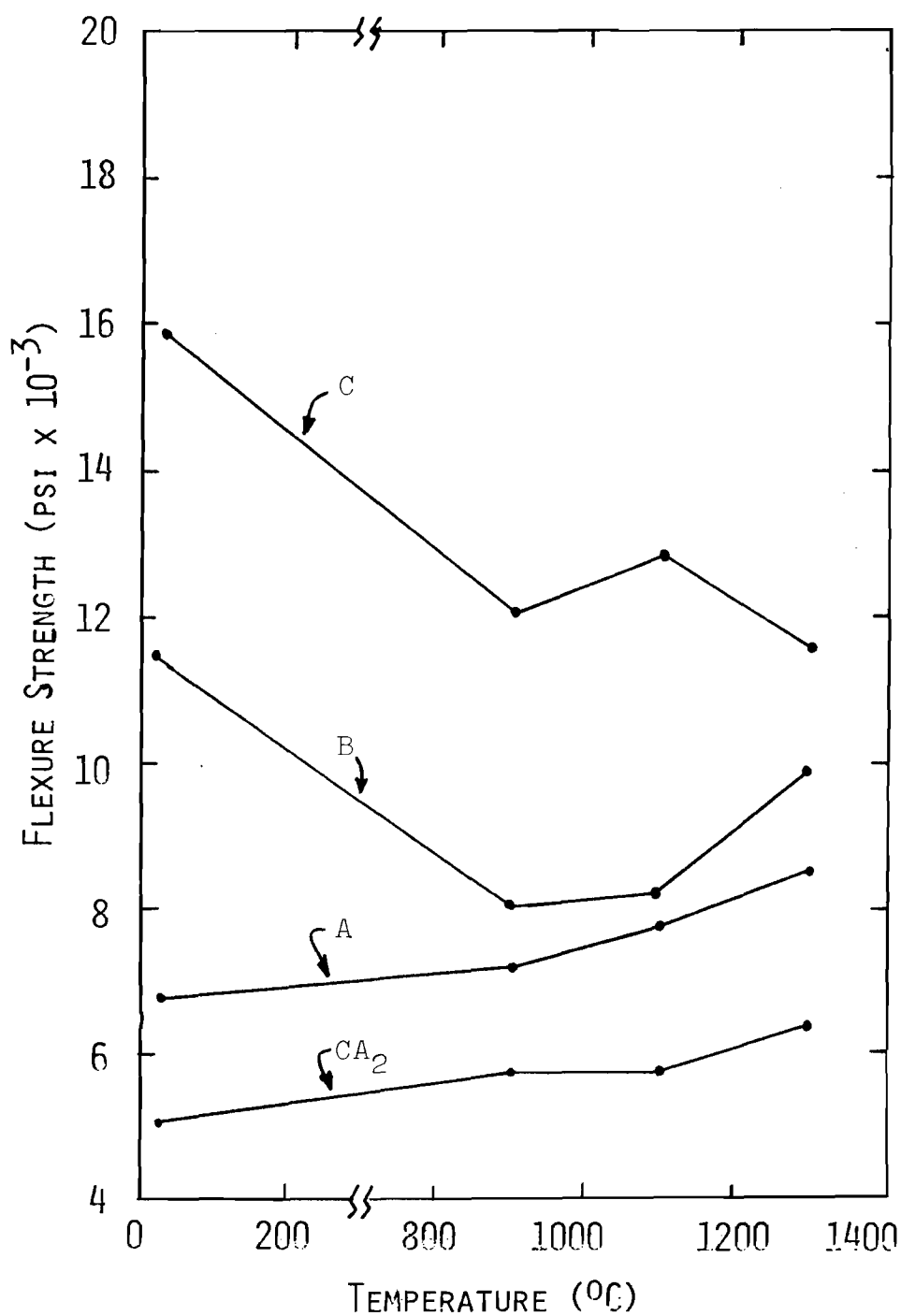


Figure 33. Flexure Strength of  $\text{CA}_2$  Compared to "As Fired" Compositions A, B and C.

were lower. This is interesting, since as  $\text{CA}_2$  content increased for compositions A, B, and C, flexure strength increased. Flexure strength may have been porosity and grain size controlled which could provide an explanation for the strength variations. Since the porosity increased in the order of strength decreases ( $\text{C} = 2.8\%$ ,  $\text{B} = 4.1\%$ ,  $\text{A} = 4.5\%$ , and  $\text{CA}_2 = 17.3\%$ ) it was very likely that microstructure controlled the strength and composition was a second order effect.

In summary, the strengths of compositions A, B, and C increased in that order. Both heat treatment at  $900^\circ\text{C}$  and  $1300^\circ\text{C}$  and breaking temperatures up to  $1300^\circ\text{C}$  had little effect on flexure strength of these  $\text{CaO-Al}_2\text{O}_3\text{-ZrO}_2$  compositions. From a practical aspect, the lack of effect of heat treatment and breaking temperature is important in that "as fired" room temperature property measurement is indicative of higher temperature properties.

### 3. Microhardness of High $\text{ZrO}_2$ Compositions

Knoop's microhardness for compositions A, B and C are presented in Figures 34-37 and tabulated in Appendix F. Microhardness of the "as-fired" compositions, Figure 34, were analogous to the flexural strength data in that hardness increased from composition A to B to C. Again, increasing the  $\text{CA}_2$  content also improved microhardness. In analyzing the effect of heat treatment on

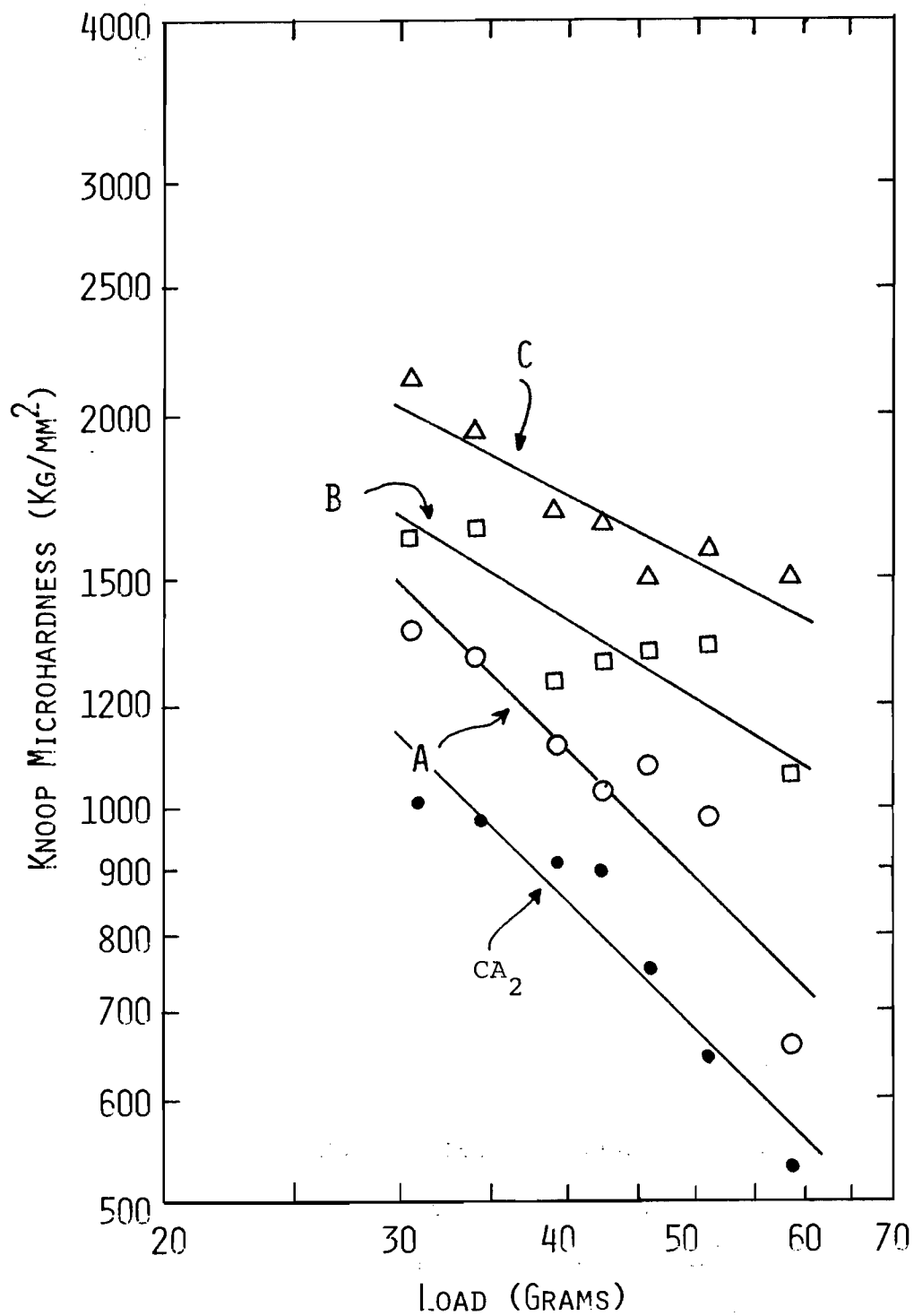


FIGURE 34. ROOM TEMPERATURE MICROHARDNESS OF "AS FIRED"  $\text{CaO-Al}_2\text{O}_3\text{-ZrO}_2$  COMPOSITIONS A, B, AND C AND COMPOUND  $\text{CA}_2$ .



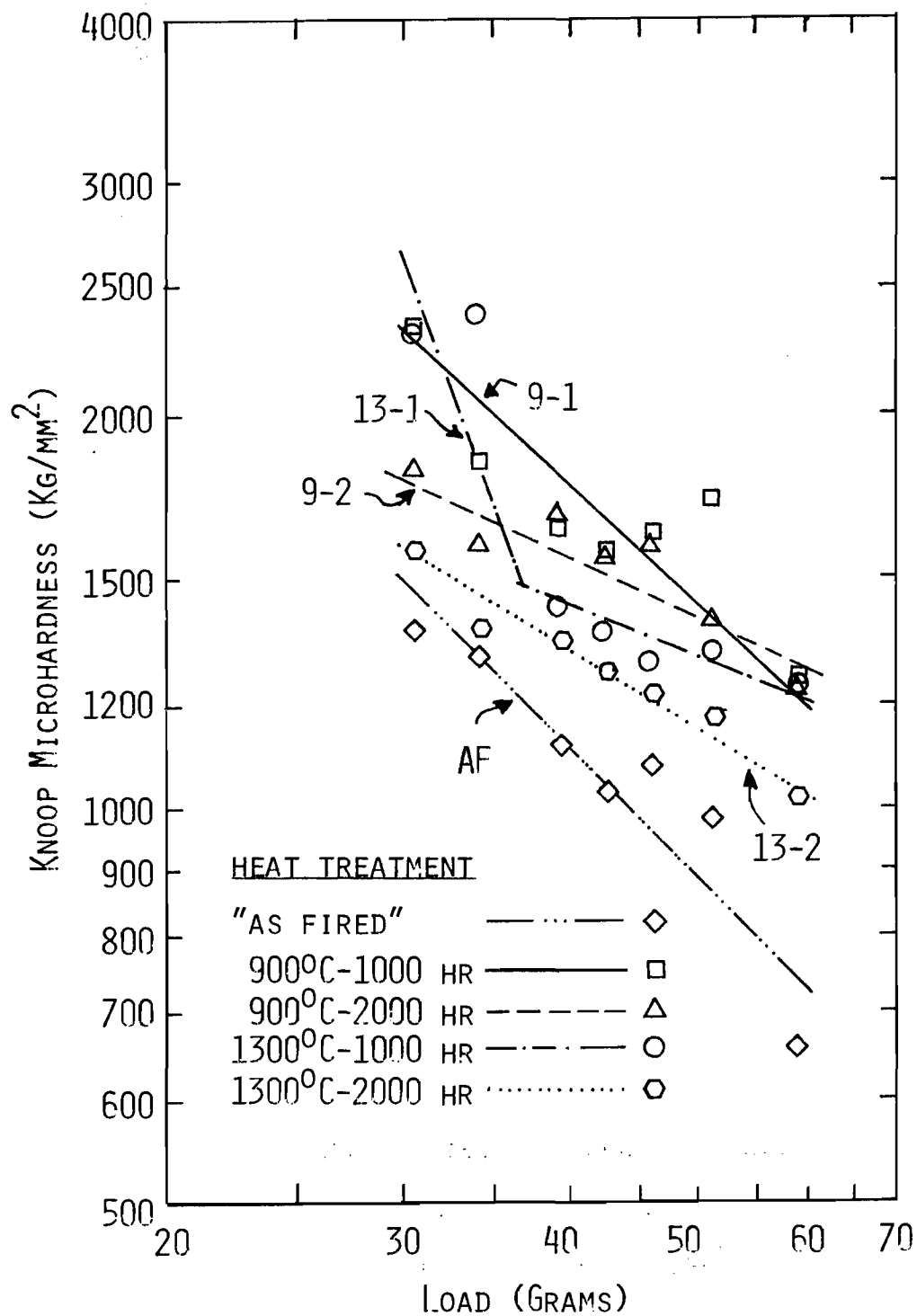


FIGURE 35. ROOM TEMPERATURE MICROHARDNESS OF  $\text{CaO-Al}_2\text{O}_3\text{-ZrO}_2$  COMPOSITION A AFTER VARIOUS HEAT TREATMENTS.

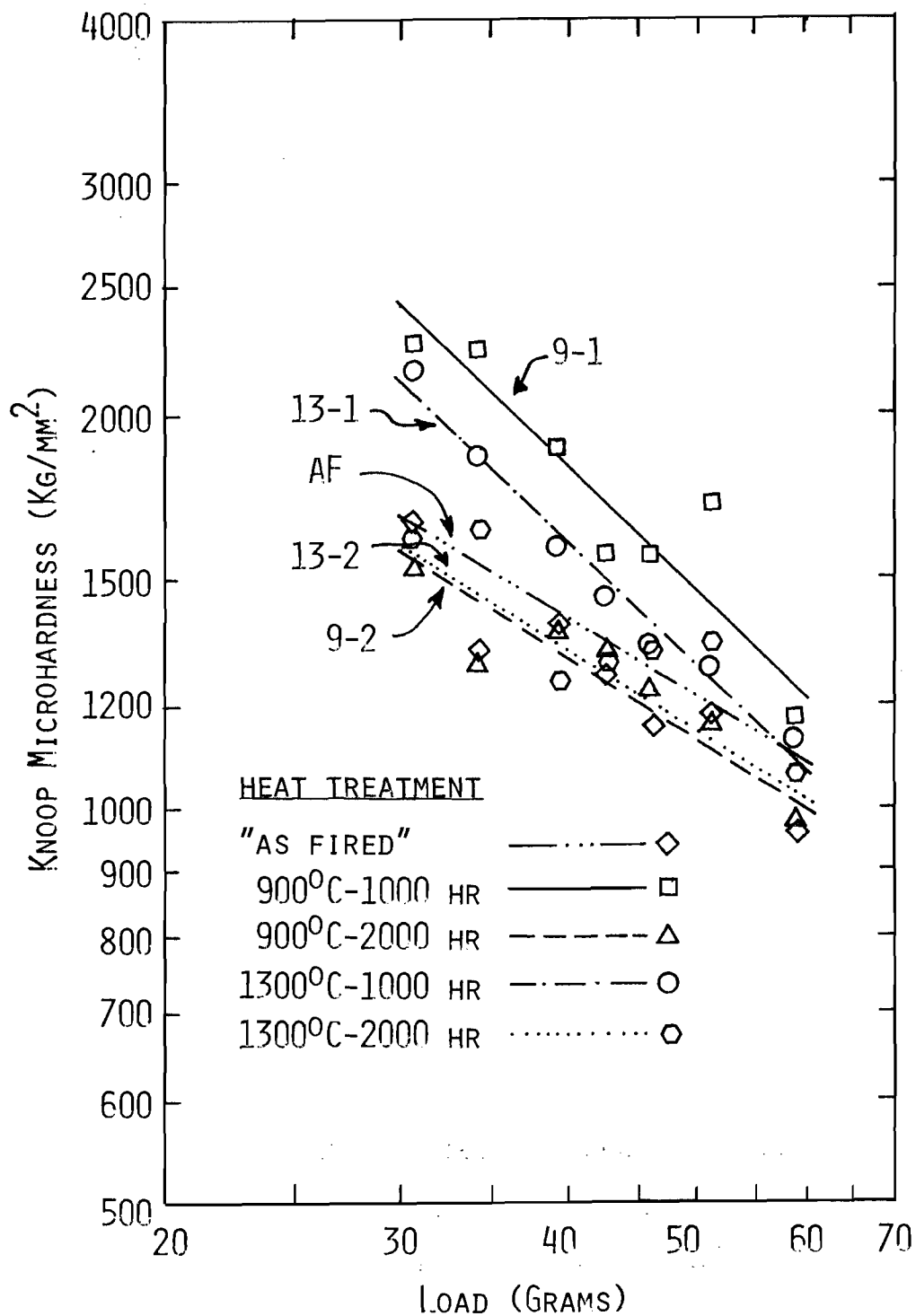


FIGURE 36. ROOM TEMPERATURE MICROHARDNESS OF  $\text{CaO-Al}_2\text{O}_3\text{-ZrO}_2$  COMPOSITION B AFTER VARIOUS HEAT TREATMENTS.

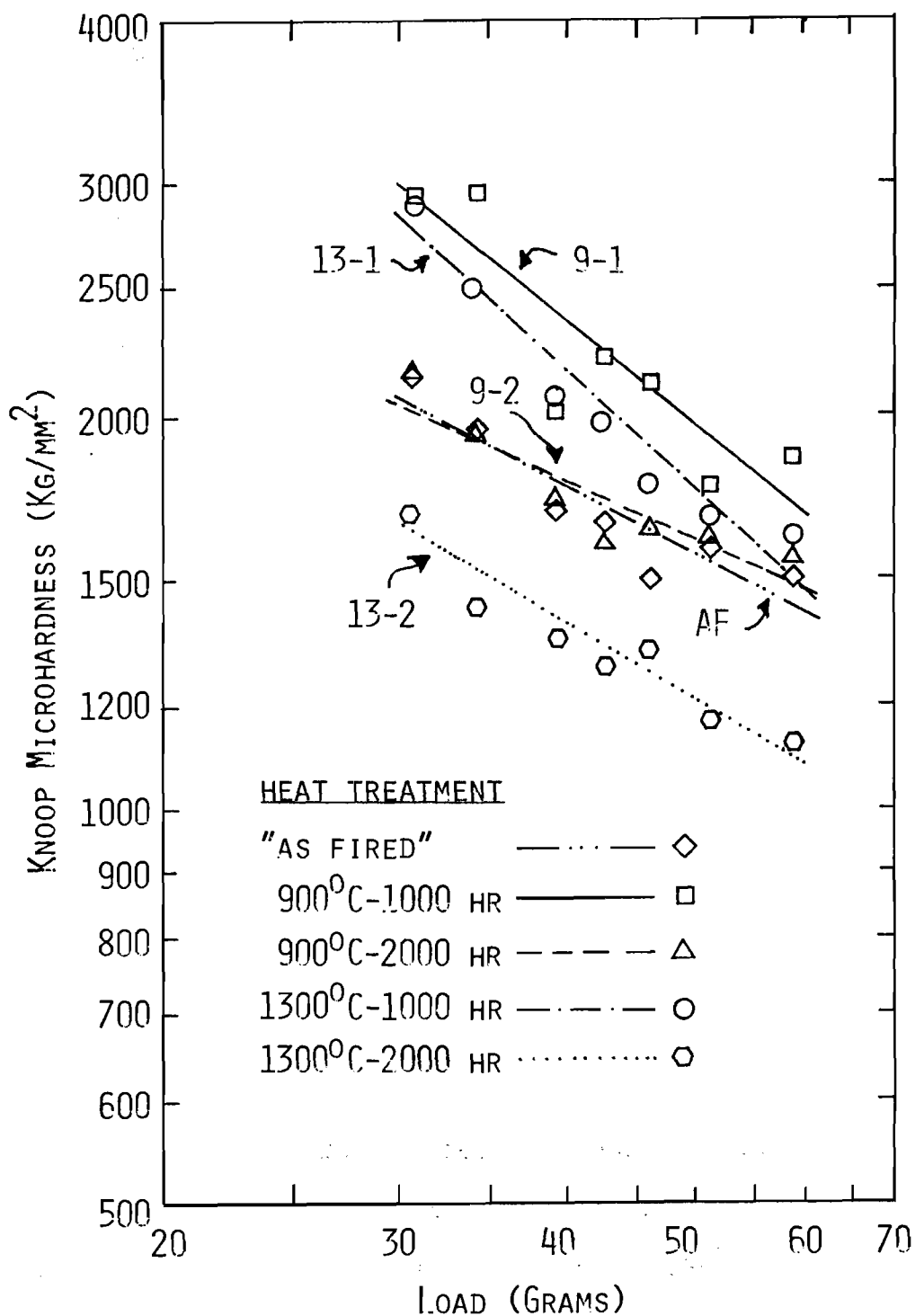


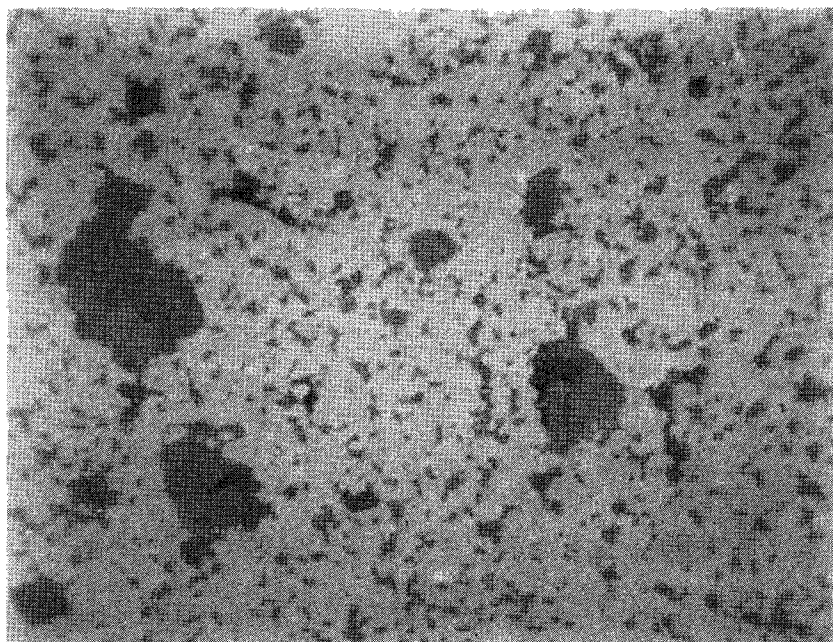
FIGURE 37. ROOM TEMPERATURE MICROHARDNESS OF  $\text{CaO-AL}_2\text{O}_3\text{-ZrO}_2$  COMPOSITION C AFTER VARIOUS HEAT TREATMENTS.

microhardness for the three compositions, Figures 35-37, there were several trends apparent. Heat treatment for 1000 hours both at 900 and 1300°C produced higher microhardness values than did heat treatment at 2000 hours. In general, heat treatment increased microhardness of compositions A, B and C possibly due to annealing. Except for the "as-fired" samples, the microhardness of compositions A and B were almost identical.

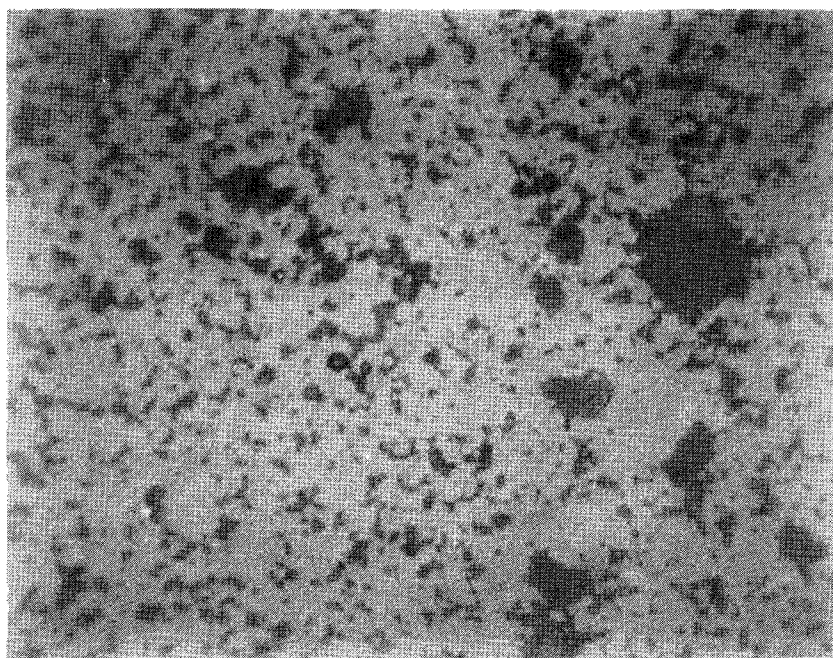
Again as for flexural strength, CA<sub>2</sub>, had a lower microhardness. The increasing microhardness of compositions A, B and C with CA<sub>2</sub> was difficult to rationalize here since microhardness was measured in nonporous areas. Perhaps microhardness measurements are dependent on microstructure in polycrystalline materials when the grain size is smaller than the indentations.

#### 4. Microstructure of High ZrO<sub>2</sub> Compositions

The microstructure of high ZrO<sub>2</sub> compositions A, B and C "as-fired" and after heat treatment at 1300°C for 2000 hours is shown in Figures 38-40. The dark gray discontinuous phase was CA<sub>2</sub> and the light continuous phase was a mixture of cubic and monoclinic ZrO<sub>2</sub>. Optical analysis indicated the volume of CA<sub>2</sub> to be 22.0 v/o in A, 39.7 v/o in B, and 52.0 v/o in C which agreed well with calculated values from the density and weight % of the phase present. It is interesting that even for

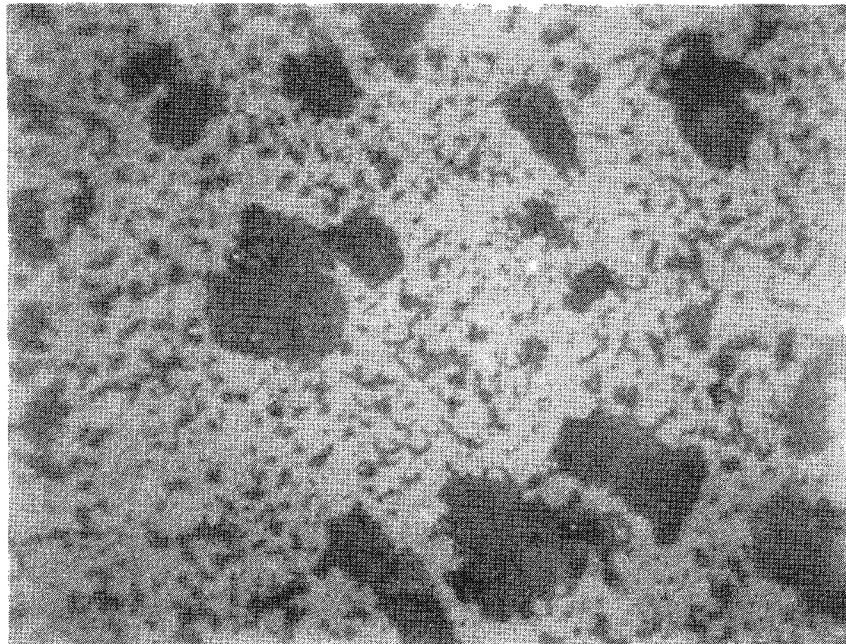


(a)

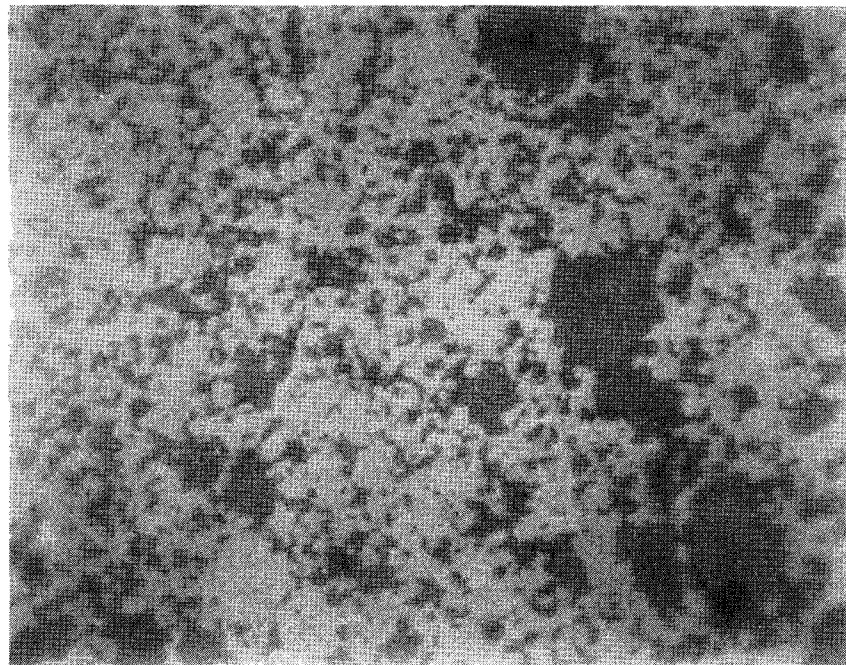


(b)

Figure 38. Reflected Light Micrograph of Microstructure of Composition A (a) "As-Fired" at  $1550^{\circ}\text{C}$  and (b) After Heat Treatment at  $1300^{\circ}\text{C}$  for 2000 Hours; 600X.

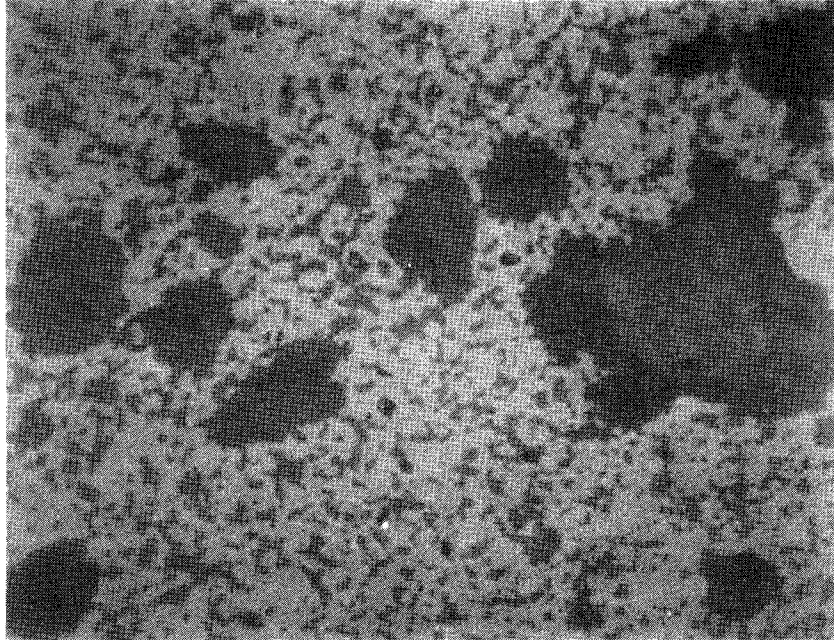


(a)

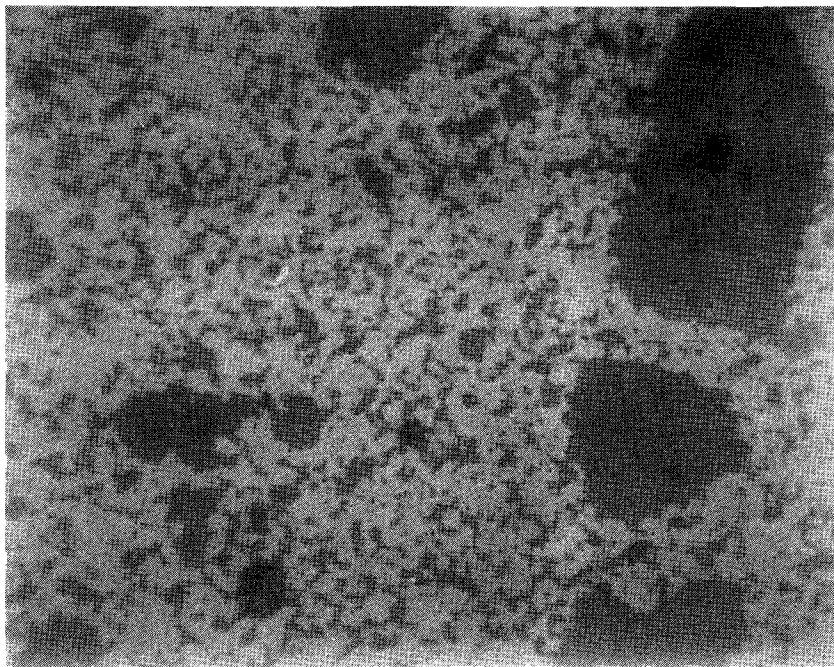


(b)

Figure 39. Reflected Light Micrograph of Micro-Structure of Composition B (a) "As-Fired" at 1550°C and (b) After Heat Treatment at 1300°C for 2000 Hours; 600X.



(a)



(b)

Figure 40. Reflected Light Micrograph of Micro-Structure of Composition C (a) "As-Fired at 1550°C and (b) After Heat Treatment at 1300°C for 2000 Hours; 600X.

composition C with 52.0 v/o  $\text{CA}_2$ ,  $\text{CA}_2$  was still the discontinuous phase. Thus, the chemical stability of these compositions would be that of the continuous  $\text{ZrO}_2$  phases. Heat treatment had no detectable effect on the microstructure. Attempts to etch grain boundaries in these samples were unsuccessful and no information on grain size was available.

##### 5. Thermal Expansion of High $\text{ZrO}_2$ Compositions

The effect of heat treatment on thermal expansion of compositions A, B, and C can be seen in Figure 41. where the expansion curves for A, B, and C "as-fired" and after 1400 hours at  $1300^\circ\text{C}$  are presented. These conditions cover the range of compositional changes and thermal expansion values measured. As shown by quantitative x-ray data earlier, heat treatment served to destabilize the cubic zirconia thereby increasing the amount of monoclinic zirconia. As would be expected, there was a correlation between the w/o monoclinic  $\text{ZrO}_2$  and the length change of the monoclinic to tetragonal contraction, Figure 42. The absence of an inversion for the "as-fired" C sample confirmed the absence of monoclinic  $\text{ZrO}_2$  in C as reported earlier from x-ray diffraction results.

Variation in thermal expansion values before the inversion was smaller than expected for the quantity



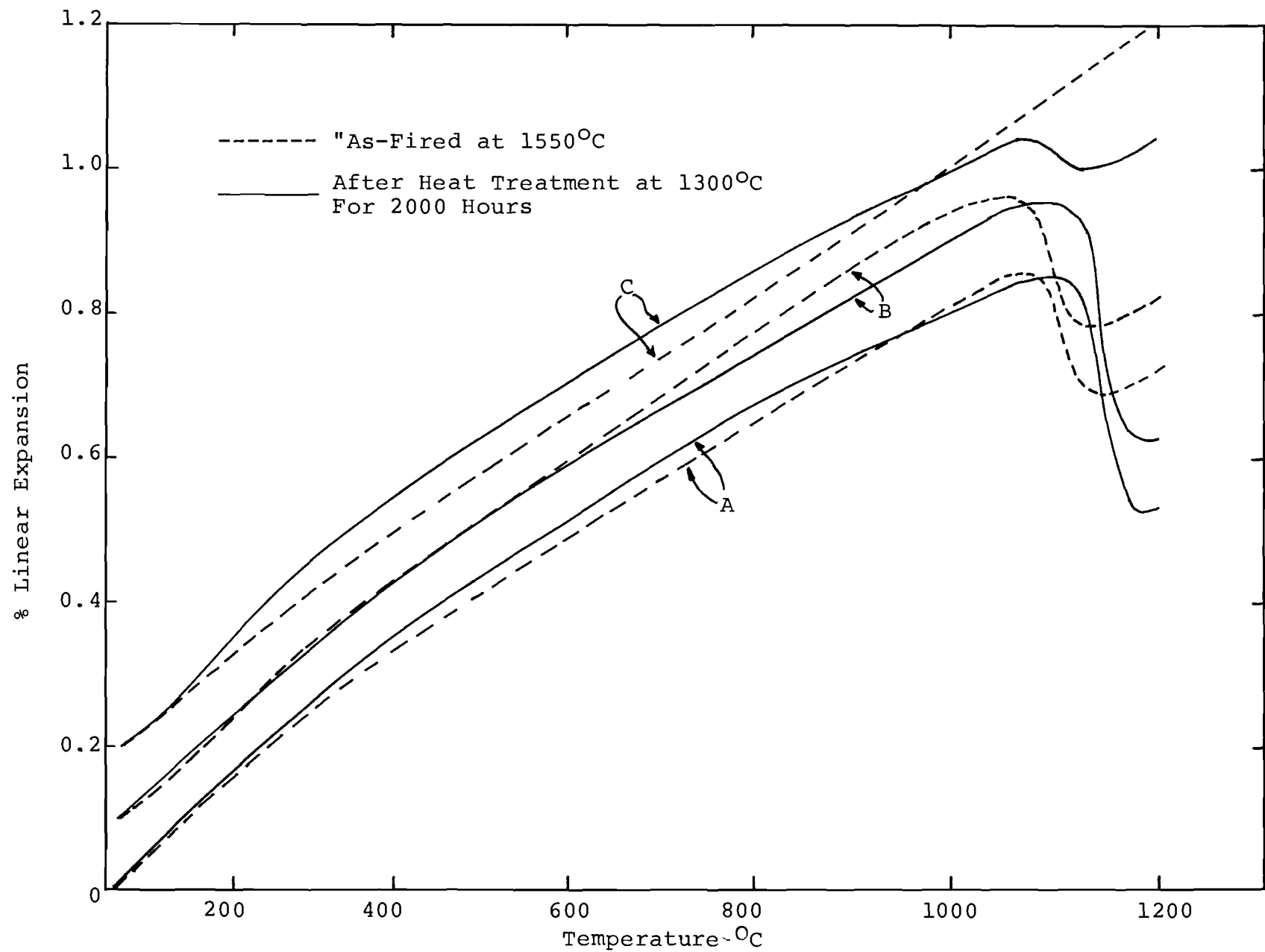


Figure 41. Comparison of Linear Thermal Expansion of Compositions A, B, and C "As-Fired at 1550°C and After Heat Treatment at 1300°C for 1400 Hours.

% Length Change For Monoclinic  $\rightarrow$  Tetragonal

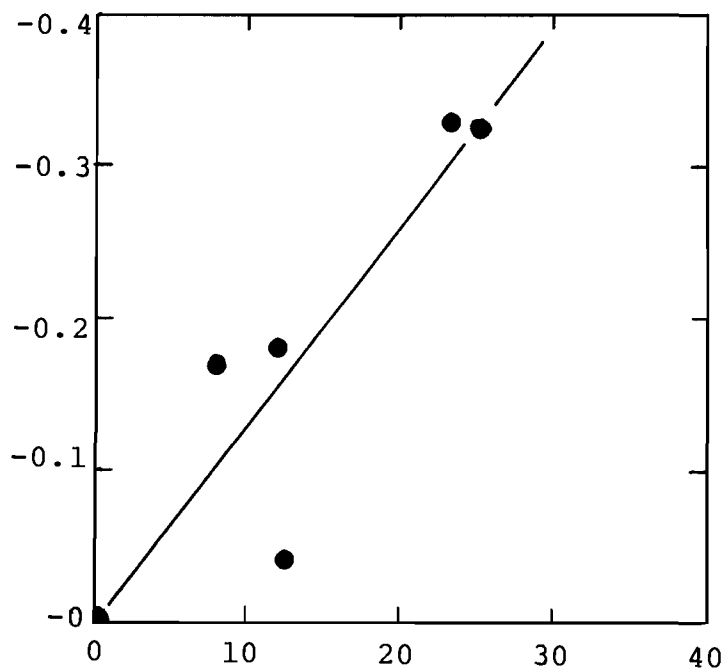


Figure 42. w/o Monoclinic  $ZrO_2$   
Length Change for Monoclinic to Tetragonal Inversion as a Function of Monoclinic  $ZrO_2$  Content for Samples Shown in Figure 41.

% Expansion at 1020°C

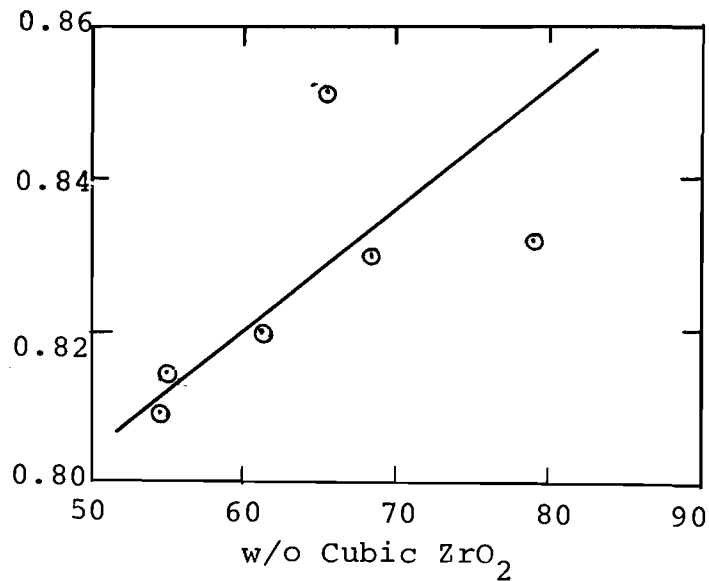
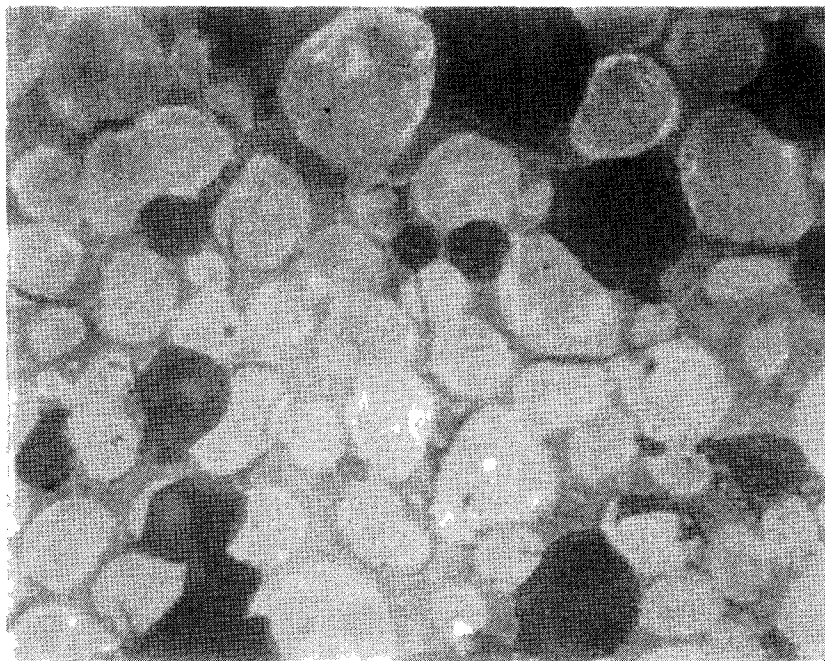


Figure 43. Expansion of Compositions A, B, and C as a Function of Cubic  $ZrO_2$  Content for Samples Shown in Figure 41.

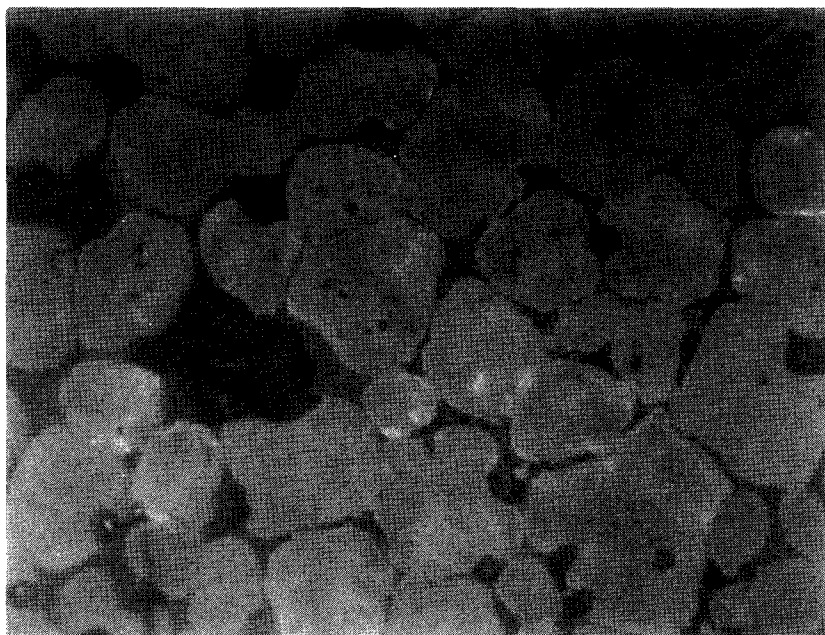
change in cubic  $\text{ZrO}_2$  for these samples. The range in engineering expansion coefficient at  $1020^\circ\text{C}$  was small ( $8.10$  to  $8.52 \times 10^{-6}/^\circ\text{C}$ ) for variations in cubic  $\text{ZrO}_2$  of  $54.4$  to  $78.6$  w/o. There was a general correlation between the expansion at  $1020^\circ\text{C}$  and cubic  $\text{ZrO}_2$  content, Figure 43. This was to be expected since cubic  $\text{ZrO}_2$  has an expansion coefficient of  $10.5 \times 10^{-6}/^\circ\text{C}$  and both monoclinic  $\text{ZrO}_2$  and  $\text{CA}_2$  have coefficients of approximately  $5 \times 10^{-6}/^\circ\text{C}$ .

#### D. Liquid Formation in $\text{CaO-Al}_2\text{O}_3\text{-ZrO}_2$ at $1700^\circ\text{C}$

When the nine samples 1-1 through 1-9 were removed from the furnace after firing to  $1700^\circ\text{C}$ , it was observed that 1-1, 1-2, and 1-4 had definitely undergone partial melting because the edges of the pellets were rounded and slumped. Photographs of samples 1-1 and 1-9 are included, Figure 44, showing large uniformly rounded grains surrounded by the secondary gray phase, which is a clear indication that melting occurred. Table 18 shows the results of the qualitative x-ray analysis and the optical analysis. It is clear from the phase analysis that the samples were not at equilibrium. The phases present do not correspond to the equilibrium phases at  $1500^\circ\text{C}$  and sample 1-1 has four phases present, an impossibility in equilibrium unless the composition was exactly at the eutectic point. Thus no phase diagram information may be taken from these results.



Sample 1-1

 $\text{ZrO}_2$  64 m/o $\text{CaO}$  16 m/o $\text{Al}_2\text{O}_3$  20 m/o

Sample 1-9

 $\text{ZrO}_2$  85.7 m/o $\text{CaO}$  9.5 m/o $\text{Al}_2\text{O}_3$  4.8 m/o

Figure 44. Photomicrographs of Series 1, 1700 °C, 600x

Table 18, Phase Composition and Optically Determined  
Phase Volume of Series 1, 1700°C

Sample Number	Crystalline Phases	Percent Porosity	Optical	
			%White	%Gray
1-1	Cubic, $CA_6$ , $CA_2$ , Mono	13	61	39
1-2	Cubic, Mono, $CA_2$	25	79	21
1-3	Cubic, Mono, $CA_6$	13	62	38
1-4	Cubic, $CA_2$ , Mono	21	76	24
1-5	Cubic, $CA_2$	7	69	31
1-6	Cubic, Mono, $CA_6$	11	78	22
1-7	Cubic, $CA_2$ , CZ	10	84	16
1-8	Cubic, Mono	10	89	11
1-9	Cubic, Mono, $CA_6$	16	94	6

The presence of  $CA_6$  is important. First of all, it corroborates the work of Takagi<sup>6</sup>, who also found melting of the samples at 1700°C, with the formation of  $CA_6$ . From the literature it has not been clear if  $CA_2$  melted congruently or incongruently. The presence of  $CA_6$  in several of the samples, where from previous phase diagram results  $CA_2$  should have been the only calcium aluminate phase, indicates that  $CA_2$  melts incongruently forming  $CA_6$  and a liquid. Thus if the samples did not attain equilibrium on cooling (which was at the relatively fast cool down rate of the gas-fired furnace), it would be reasonable for  $CA_6$  to be present.

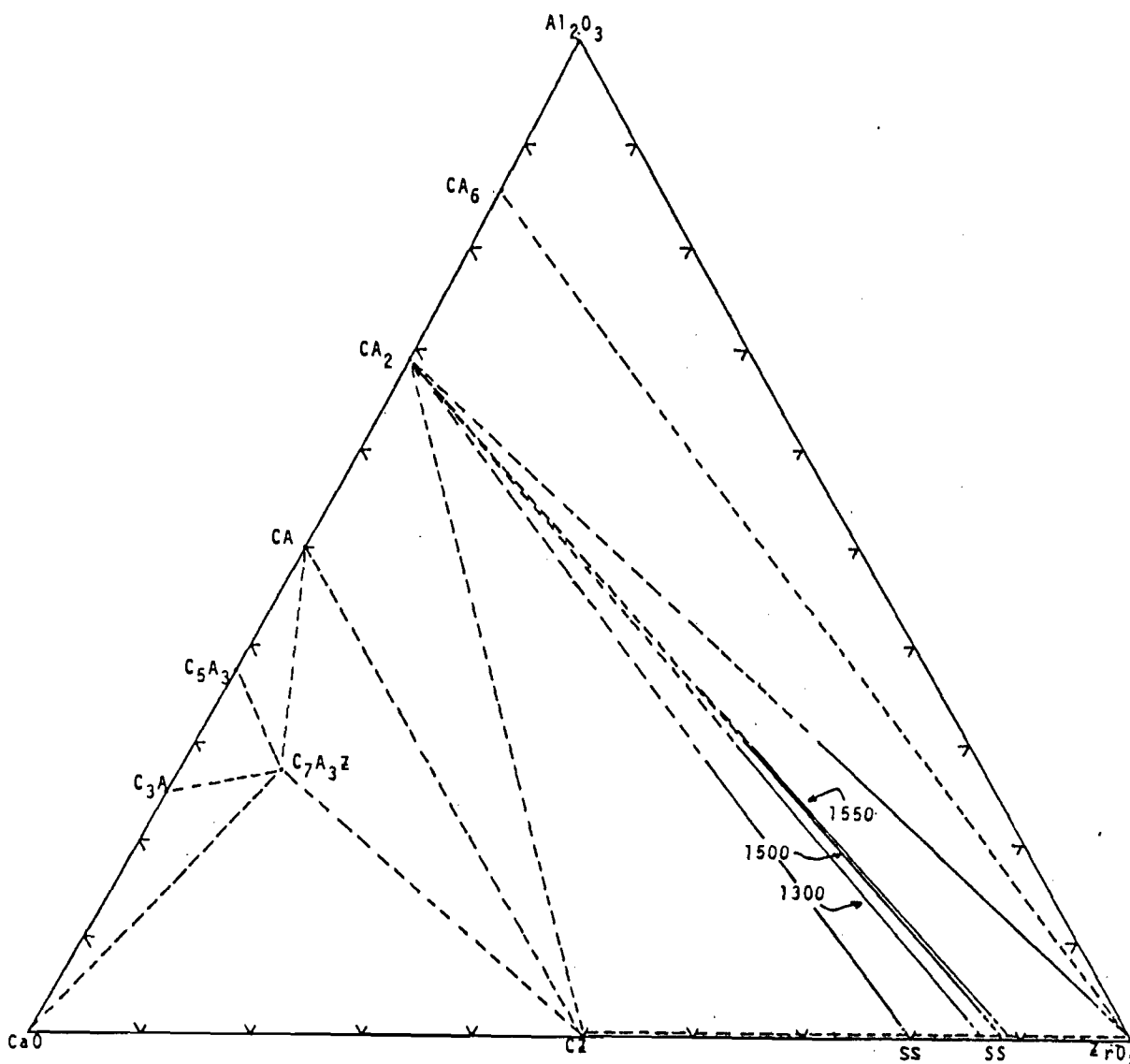
The x-ray phase analysis from sample 1-8 would suggest considerable solid solution of alumina in zirconia. However, the optical information showed that there was still a considerable amount of calcium aluminate in this sample, but that it was below the detection limits of the x-ray diffractometer.

Because equilibrium was not attained due to partial melting of the samples, it was not possible to make any determination about solid solution phenomena for either cubic zirconia or  $CA_2$  at 1700°C. The incongruent melting of  $CA_2$  was, however, more definitely established.

## SECTION V

Summary

The phase diagram for the high zirconia region of the calcia-alumina-zirconia system was determined at 1500°C and combined with available information to prepare a complete diagram of the calcia-alumina-zirconia system as shown:



Multiple firings utilizing quenching and slow cooling were used to demonstrate equilibrium for the high  $\text{ZrO}_2$  portion of the diagram. Using selected high  $\text{ZrO}_2$  compositions in the  $\text{CA}_2$ -cubic  $\text{ZrO}_2$  SS-monoclinic  $\text{ZrO}_2$  compatibility triangle, it was shown that the minimum  $\text{CaO}$  solubility needed to stabilize cubic  $\text{ZrO}_2$  varied from 11 m/o at  $1550^\circ\text{C}$  to 14 m/o at  $1300^\circ\text{C}$ . After firing at  $1550^\circ\text{C}$ , these compositions required 1000 hours to reach equilibrium at  $1300^\circ\text{C}$  and had not reached equilibrium after 2000 hours at  $900^\circ\text{C}$ . The changing  $\text{CaO}$  solubility in cubic  $\text{ZrO}_2$  was demonstrated through lattice parameter measurements on the cubic SS.

The changing  $\text{CaO}$  content in cubic  $\text{ZrO}_2$  SS with temperature, resulted in increasing monoclinic  $\text{ZrO}_2$  content with time and decreasing cubic  $\text{ZrO}_2$  contents. These phase changes were reflected in the thermal expansion characteristics of the compositions with increases in expansion accompanying increased cubic  $\text{ZrO}_2$  content and increases in the size of the monoclinic-tetragonal contraction at  $1050^\circ\text{C}$  as the monoclinic  $\text{ZrO}_2$  content increased.

Flexure strength, both room temperature and high temperature up to  $1300^\circ\text{C}$ , was shown to be independent of heat treatment at temperatures of 900 and  $1300^\circ\text{C}$  for up to 2000 hours. Likewise, the microstructure



and microhardness was not significantly changed by such heat treatment.

The presence of calcium dialuminate in partially CaO stabilized  $\text{ZrO}_2$  was shown not to be detrimental to the properties measured and if anything was beneficial. The low expansion coefficient,  $5 \times 10^{-6}/^\circ\text{C}$ , of  $\text{CA}_2$  should provide increased thermal shock resistance for the high  $\text{ZrO}_2$  compositions by lowering the thermal expansion.

Since  $\text{CA}_2$  was the discontinuous phase up to 52 v/o in the microstructure, the chemical stability of  $\text{CA}_2$ -cubic  $\text{ZrO}_2$ -monoclinic  $\text{ZrO}_2$  compositions should be close to that of the  $\text{ZrO}_2$  phases. The only detrimental aspect of  $\text{CA}_2$  in these  $\text{ZrO}_2$  bodies was the reduced refractoriness resulting from a lowering of the solidus to below  $1700^\circ\text{C}$ .

## APPENDIX A

Systematic Point Counting Technique

The systematic point counting technique was used for determining the volume fraction of calcium aluminates, porosity, and zirconia phases from optical micrographs of polished sections of the samples. Accuracy is directly related to the number of points used in the count and the method depends on the fact that the following relationship is true:<sup>28</sup>

$$P_p = V_v \quad (11)$$

where  $P_p$  is the fraction of points falling on a phase of interest, and  $V_v$  is the volume fraction of the phase of interest. Standard deviation is given by the following formula:

$$\sigma V_v = \frac{V_v}{(N)^{1/2}} \quad (12)$$

where  $N$  is the number of points falling on the phase. For a confidence factor of 95%, two standard deviations from the average value are allowed. Table 19 shows the accuracy that can be expected statistically when a total of three hundred points are counted.

Table 19. Accuracy of Systematic Point Counting Technique

$V_v$	0.01	0.05	0.1	0.2	0.4	0.6	0.8
$\sigma V_v$	0.006	0.013	0.018	0.026	0.037	0.045	0.052
$\pm$ % accuracy	120	52	36	26	18.5	15	13

Percent accuracy in Table 19 is written in terms of the volume fraction. Accuracy increases as the inverse square of the number of points counted so that, for instance, quadrupling the number of points would only halve the uncertainty. Thus 300 points were determined to be sufficient as a good balance between the time required and the accuracy obtained. A square grid of 25 points spaced on 0.25 inch centers was dropped randomly without bias on each photograph 12 times as a tally of the points in each phase was made. Randomness was required for accuracy and it was necessary that a representative sector of the sample be photographed, rather than an area with some outstanding feature. The actual numbers determined for volume fractions of the three phases in each pellet were reasonably accurate, within  $\pm 30\%$  for most cases.

## APPENDIX B

Phase Analysis of Compositions Fired at 1500°C

The phases present were determined qualitatively by x-ray diffraction. Qualitative analysis of series 2 was performed on samples fired for 20 and 40 hours. The results were the same, as listed in Table 20.

Several of the samples were polished after being fired to 1500°C and slow cooled. A small amount of porosity, which appeared as very dark areas, was observed. The major phase was white in color and was apparently, as confirmed by quantitative information, the sum of the two zirconia phases. The gray phase was the sum of the calcium aluminate phases,  $CA_2$  and  $CA_6$ . The total white and gray phases were expressed in terms of 100%, mathematically eliminating the amount of porosity.

Table 20. Phase Analysis of Series 2

Sample Number	Porosity vol%	White vol %	Gray vol %	Phases Present
2-1	6	49	51	Cubic, $CA_2$
2-2				Cubic, Mono, $CA_2$
2-3	8	52	48	Cubic, Mono, $CA_2$
2-4				Mono, Cubic, $CA_2$
2-5	13	49	51	Mono, $CA_2$ , $CA_6$
2-6				Cubic, $CA_2$
2-7				Cubic, $CA_2$
2-8				Cubic, Mono, $CA_2$
2-9	11	54	46	Cubic, Mono, $CA_2$
2-10				Mono, Cubic, $CA_2$
2-11	4	65	35	Cubic, $CA_2$
2-12				Cubic, $CA_2$
2-13				Cubic, Mono, $CA_2$
2-14				Cubic, Mono, $CA_2$
2-15				Cubic, Mono, $CA_2$
2-16				Cubic, $CA_2$
2-17				Cubic, $CA_2$
2-18				Cubic, $CA_2$
2-19				Cubic, Mono, $CA_2$
2-20				Cubic, Mono, $CA_2$
2-21	10	79	21	Cubic, $CA_2$
2-22				Cubic, $CA_2$
2-23				Cubic, $CA_2$
2-24				Cubic, Mono, $CA_2$
2-25	20	79	21	Cubic, Mono, $CA_2$

Table 21. Phase Analysis of Series 3

Sample Number	Porosity vol%	White vol %	Gray vol%	Phases Present
3-1	7	52	48	Cubic, $CA_2$ , Mono
3-2	6	56	44	Cubic, $CA_2$ , Mono
3-3	38	65	35	Mono, $CA_2$ , $CA_6$
3-4	7	67	33	Cubic, $CA_2$
3-5	24	70	30	Cubic, Mono, $CA_2$
3-6	24	71	29	Cubic, Mono, $CA_2$
3-7	9	81	19	Cubic, $CA_2$
3-8	33	87	13	Cubic, $CA_2$
3-9	26	80	20	Cubic, Mono, $CA_2$
3-10				Cubic
3-11				Cubic
3-12				Cubic, Mono

Table 22. Phase Analysis of Series 5

Sample Number	Phases Present
5-1	Cubic, $CA_2$ , CZ
5-2	Cubic, $CA_2$ , CZ
5-3	Cubic, $CA_2$ , CZ
5-4	Cubic, $CA_2$ , CZ
5-5	Cubic, $CA_2$ , CZ

Table 23. Phase Analysis of Series 6

Sample Number	Phases Present
6-1	$CA_2$ , $CA_6$
6-2	$CA_2$ , $CA_6$ , Mono, $CA^*$
6-3	$CA_2$ , $CA_6$ , Mono, $CA^*$
6-4	$CA_2$ , $CA_6$
6-5	$CA_2$ , $CA_6$ , Mono, $CA^*$
6-6	$CA_2$ , $CA_6$ , Mono, $CA^*$
6-7	$CA_2$ , CA
6-8	$CA_2$ , CA, CZ
6-9	$CA_2$ , Cubic, $CA^*$
6-10	$CA_2$ , CA
6-11	$CA_2$ , CA, CZ
6-12	$CA_2$ , CA, CZ
6-13	$CA_2$ , CA
6-14	$CA_2$ , CA, CZ
6-15	$CA_2$ , CA, CZ

\*CA present in samples -2, -3, -5, -6, and -9 indicate that equilibrium was not achieved in these samples.

## APPENDIX C

Data for Calculating  $\text{CA}_2$ -Cubic  $\text{ZrO}_2$  and  
 $\text{CA}_2$ -Monoclinic  $\text{ZrO}_2$  Alkemade Lines

In Tables 24-27 are presented the data necessary to calculate the  $\text{CA}_2$ -Cubic  $\text{ZrO}_2$  and  $\text{CA}_2$ -Monoclinic  $\text{ZrO}_2$  Alkemade lines. Columns two and three list the  $\text{Al}_2\text{O}_3$  and CaO composition of each sample on a mole percent basis. The monoclinic to cubic zirconia weight ratio as measured by quantitative x-ray diffraction is in column four. The weight ratio of column four was converted to a mole percent ratio of cubic to cubic plus monoclinic zirconia and is shown in column five. As discussed earlier, at a constant  $\text{Al}_2\text{O}_3$  mole content, the mole percent ratio of cubic zirconia varies linearly with mole percent CaO from 0 at the  $\text{CA}_2$ -Monoclinic zirconia Alkemade line to 100 at the  $\text{CA}_2$ -cubic zirconia Alkemade line. Therefore the least squares line fit of mole percent CaO (x) versus mole percent ratio of cubic to cubic plus monoclinic zirconia (y) at constant  $\text{Al}_2\text{O}_3$  content could be calculated (column six). At each  $\text{Al}_2\text{O}_3$  content the least squares



Table 24. Quantitative X-ray Data for Series 2 and 3, Slow-Cooled

Sample Number	m/o $\text{Al}_2\text{O}_3$	m/o CaO (x)	wt. mono wt. cubic	m/o cubic (y)	Equation of line	m/o CaO 100 % cubic	m/o CaO 0 % cubic
2-2	25	12.5	0.267	80.1	$y = 14.43x - 169.57$	18.68	11.75
2-3	25	15	0.926	52.8			
2-4	25	12.5	12.5	7.93			
2-8	20	15	0.345	75.7	$y = 10.83x - 90.82$	17.62	8.39
2-9	20	12.5	0.684	61.1			
2-10	20	10	6.25	14.7			
3-1	20	16	0.340	76.0			
3-2	20	12	2.78	27.9			
2-13	15	15	0.0558	95.1	$y = 9.34x - 43.95$	15.41	4.71
2-14	15	12.5	0.361	74.9			
2-15	15	10	1.149	48.4			

Table 24. Quantitative X-ray Data for Series 2 and 3, Slow-Cooled. (contd.)

Sample Number	m/o $\text{Al}_2\text{O}_3$	m/o CaO (x)	Wt. mono Wt. cubic	m/o cubic (y)	Equation of line	m/o CaO 100 % cubic	m/o CaO 0 % cubic
3-5	13	13	0.469	69.6	} $y = 10.23x - 63.42$	15.97	6.20
3-6	13	8.7	3.125	25.6			
2-19	10	12.5	0.138	88.6	} $y = 10.2x - 38.9$	13.62	3.81
2-20	10	10	0.629	63.1			
2-24	5	12.5	0.034	96.9	} $y = 9.96x - 26.82$	12.73	2.69
2-25	5	10	0.316	77.3			
3-9	5	9.5	0.606	64.0			

Table 25. Quantitative X-ray Data for Series 2, Quenched

Sample Number	m/o $\text{Al}_2\text{O}_3$	m/o CaO (x)	wt. mono wt. cubic	m/o cubic (y)	Equation of line	m/o CaO 100% cubic	m/o CaO 0 % cubic
2-2	25	17.5	0.0236	97.9	$y = 18.81x - 233.77$	17.74	12.43
2-3	25	15	1.39	43.6			
2-4	25	12.5	27.03	3.83			
2-8	20	15	0.392	73.3	$y = 8.8x - 58.7$	18.03	6.67
2-9	20	12.5	1.02	51.3			
2-13	15	15	0.0554	95.1	$y = 8.7x - 37.62$	15.82	4.32
2-14	15	12.5	0.538	66.7			
2-15	15	10	1.01	51.6			
2-19	10	12.5	0.183	85.5	$y = 10.52x - 46.0$	13.88	4.37
2-20	10	10	0.741	59.3			
2-24	5	12.5	0.0658	94.2	$y = 7.8x - 3.3$	13.24	0.42
2-25	5	10	0.365	74.7			

Table 26. Quantitative X-ray Data for Long-Term Samples at 1550°C

Sample	m/o $\text{Al}_2\text{O}_3$	m/o CaO (x)	wt. mono wt. cubic	m/o cubic (y)	Equation of line	m/o CaO 100% cubic	m/o CaO 0 % cubic
A*	10	3.91	infinite	0	} $y = 10.28x - 40.19$	13.64	3.91
A	10	12.5	0.143	88.3			
B*	17.5	7.51	infinite	0	} $y = 12.06x - 90.57$	15.80	7.51
B	17.5	14.5	14.5	0.2			
C*	25	11.11	infinite	0	} $y = 15.6x - 173.3$	17.5	11.11
C	25	17.5	0	100			

Table 27. Quantitative X-ray Data for Long-Term Samples at 1300°C

Sample	m/o $\text{Al}_2\text{O}_3$	m/o CaO (x)	wt. mono wt. cubic	m/o cubic (y)	Equation of line	m/o CaO 100% cubic	m/o CaO 0 % cubic
A*	10	3.91	infinite	0	} $y = 8.49x - 33.18$	15.7	3.91
A	10	12.5	0.47	72.9			
B*	17.5	7.51	infinite	0	} $y = 10.43x - 78.32$	17.10	7.51
B	17.5	14.5	0.47	72.9			
C*	25	11.11	infinite	0	} $y = 13.38x - 148.7$	18.6	11.11
C	25	17.5	0.235	85.5			

\* Mole percent CaO at 0 mole percent  $\text{ZrO}_2$  was calculated from Equation (10).

line was extrapolated to give the mole percent CaO at 100% cubic (column seven) and at 0% cubic (column eight), which are the CaO compositions at that  $\text{Al}_2\text{O}_3$  composition for the  $\text{CA}_2$ -cubic zirconia Alkemade line and the  $\text{CA}_2$ -monoclinic zirconia Alkemade line respectively. Linear regression analysis of mole percent CaO versus mole percent  $\text{Al}_2\text{O}_3$  for the respective lines was used to determine the best fit equations for those two lines, which are presented in Chapter IV.

Page 126 Intentionally left blank.

## APPENDIX D

Quantitative Changes in Cubic to Monoclinic Zirconia  
Contents for Long Term Firings

The weight ratio of cubic to cubic plus monoclinic zirconia contained in each of the long term fired samples was determined by x-ray diffraction and is recorded in Table 28.

Table 28. Weight Ratio of Cubic to Cubic + Monoclinic  $ZrO_2$ , Compositions A, B, and C.

Time (Hours)	900°C			1300°C		
	A	B	C	A	B	C
0	0.88	0.83	1.0	0.88	0.83	1.0
200	0.89	0.88	0.98	0.88	0.84	0.94
400	0.91	0.83	1.0	0.76	0.77	0.89
600	0.88	0.84	1.0	0.73	0.78	0.86
800	0.91	0.87	1.0	0.70	0.78	0.83
1000	0.91	0.84	1.0	0.72	0.69	0.81
1200	0.88	0.84	0.98	0.72	0.70	0.82
1400	0.89	0.81	0.97	0.71	0.69	0.88
1600	0.87	0.87	0.96	0.61	0.66	0.80
1800	0.89	0.85	0.97	0.72	0.71	0.81
2000	0.85	0.84	0.95	0.73	0.69	0.83



## APPENDIX E

Flexure Strength of High ZrO<sub>2</sub> Compositions

Flexure strength of high ZrO<sub>2</sub> compositions A, B, and C are presented in Tables 29-32. The average flexure strengths and standard deviations were the result of testing four samples for each composition, heat treatment conditions, and breaking temperature.

TABLE 29

Flexure Strength of As-Fired  $\text{CaO-Al}_2\text{O}_3\text{-ZrO}_2$   
 Compositions A, B, and C  
 As a Function of Breaking Temperature

Breaking Temperature ( $^{\circ}\text{C}$ )	Flexure Strength ( $10^3$ psi)	Standard Deviation ( $10^3$ psi)	Percent Standard Deviation
<u>Composition A</u>			
20	6.70	0.43	6.4
900	7.18	1.46	20.3
1100	7.74	1.64	21.2
1300	8.52	1.48	17.4
<u>Composition B</u>			
20	11.40	0.05	0.4
900	7.96	0.99	12.4
1100	8.14	1.80	22.1
1300	9.92	0.23	2.3
<u>Composition C</u>			
20	15.58	0.20	1.7
900	11.79	1.39	11.8
1100	12.82	2.70	21.0
1300	11.48	0.89	7.8

TABLE 30

Flexure Strength of Composition A  
As a Function of Breaking Temperature  
For Various Heat Treatment Conditions

Breaking Temperature (°C)	Flexure Strength (10 <sup>3</sup> psi)	Standard Deviation (10 <sup>3</sup> psi)	Percent Standard Deviation
<u>900°C Heat Treatment - 1000 hours</u>			
20	7.78	0.73	9.5
900	7.83	1.07	13.6
1100	6.53	0.98	15.0
1300	9.42	1.32	14.0
<u>900°C Heat Treatment - 2000 hours</u>			
20	7.75	0.56	7.3
900	7.21	0.74	10.3
1100	6.49	0.66	10.2
1300	8.63	2.68	31.1
<u>1300°C Heat Treatment - 1000 hours</u>			
20	9.42	0.77	8.2
900	7.88	1.17	14.5
1100	8.07	1.08	13.3
1300	9.25	1.84	19.9
<u>1300°C Heat Treatment - 2000 hours</u>			
20	7.23	0.42	5.8
900	7.07	0.89	12.6
1100	5.78	1.05	18.2
1300	7.20	1.20	16.7

TABLE 31

Flexure Strength of Composition B  
As a Function of Breaking Temperature  
For Various Heat Treatment Conditions

Breaking Temperature (C°)	Flexure Strength (10 <sup>3</sup> psi)	Standard Deviation (10 <sup>3</sup> psi)	Percent Standard Deviation
<u>900°C Heat Treatment - 1000 hours</u>			
20	8.99	0.61	6.8
900	8.57	0.80	9.4
1100	8.34	0.96	11.5
1300	9.54	1.69	17.7
<u>900°C Heat Treatment - 2000 hours</u>			
20	9.14	1.16	12.7
900	8.89	1.38	15.5
1100	7.93	0.69	8.7
1300	10.28	1.99	19.4
<u>1300°C Heat Treatment - 1000 hours</u>			
20	10.66	0.29	2.7
900	9.55	1.11	11.6
1100	9.22	1.61	17.5
1300	9.41	1.65	17.5
<u>1300°C Heat Treatment - 2000 hours</u>			
20	9.15	0.82	9.0
900	8.65	0.48	5.5
1100	10.85	3.84	35.4
1300	9.72	0.94	9.7

TABLE 32

Flexure Strength of Composition C  
As a Function of Breaking Temperature  
For Various Heat Treatment Conditions

Breaking Temperature (C°)	Flexure Strength (10 <sup>3</sup> psi)	Standard Deviation (10 <sup>3</sup> psi)	Percent Standard Deviation
<hr/> 900°C Heat Treatment - 1000 hours <hr/>			
20	13.71	2.87	20.9
900	9.91	0.89	9.0
1100	11.62	1.67	14.3
1300	13.33	1.37	10.3
<hr/> 900°C Heat Treatment - 2000 hours <hr/>			
20	14.55	2.79	19.2
900	8.72	0.80	9.2
1100	12.75	2.19	17.2
1300	13.21	1.64	12.4
<hr/> 1300°C Heat Treatment - 1000 hours <hr/>			
20	27.02	5.27	19.5
900	20.56	1.98	9.6
1100	12.60	4.67	37.0
1300	15.23	2.49	16.3
<hr/> 1300°C Heat Treatment - 2000 hours <hr/>			
20	14.43	1.87	13.0
900	11.97	0.40	3.8
1100	15.68	3.11	19.8
1300	14.79	2.12	14.4

## APPENDIX F

Knoop's Microhardness of High ZrO<sub>2</sub> Compositions

Microhardness of high ZrO<sub>2</sub> compositions A, B, and C as a function of load are tabulated in Tables 33-35. Each microhardness value was the result of three indentations.

Table 33. Room Temperature Microhardness of Composition C  
After Various Heat Treatments

Load (grams)	Knoop Microhardness (kg/mm <sup>2</sup> )				
	As-fired 1550°C	900°C 1000 hrs	900°C 2000 hrs	1300°C 1000 hrs	1300°C 2000 hrs
30.5	2149	2966	2159	2936	1675
34.0	1955	2988	1938	2499	1429
39.0	1697	2010	1719	2053	1384
42.5	1657	2216	1587	1970	1275
46.0	1500	2134	1616	1786	1333
51.0	1583	1765	1611	1682	1160
59.0	1506	1857	1551	1619	1119

Table 34. Room Temperature Microhardness of Composition B  
After Various Heat Treatments

Load (grams)	Knoop Microhardness (kg/mm <sup>2</sup> )				
	As-fired 1550 °C	900°C 1000 hrs	900°C 2000 hrs	1300°C 1000 hrs	1300°C 2000 hrs
30.5	1377	2294	1529	2154	1654
34.0	1309	2288	1291	1854	1316
39.0	1117	1889	1373	1592	1393
42.5	1036	1567	1334	1462	1297
46.0	1080	1562	1240	1325	1166
51.0	985	1726	1161	1299	1171
59.0	657	1175	981	1123	957



Table 35. Room Temperature Microhardness of Composition A  
After Various Heat Treatments

Load (grams)	Knoop Microhardness (kg/mm <sup>2</sup> )				
	As-fired 1550°C	900°C 1000 hrs	900°C 2000 hrs	1300°C 1000 hrs	1300°C 2000 hrs
30.5	1377	2330	1815	2409	1566
34.0	1309	1840	1592	2492	1366
39.0	1117	1639	1687	1427	1337
42.5	1036	1584	1565	1368	1271
46.0	1080	1603	1593	1297	1211
51.0	985	1771	1395	1327	1163
59.0	657	1252	1239	1237	1005

## REFERENCES

1. A.S. Berezhnoi and R.A. Kordyuk, "Melting Diagram of the System  $\text{CaO-Al}_2\text{O}_3\text{-ZrO}_2$ ," Dopovidi Akademii Nauk Ukrain-skoi RSR, No. 10, 1344-1347 (1963).
2. A.S. Berezhnoi and R.A. (Kordyuk) Tranopol'skaya, "Calcium Alumino-zirconate - A New Hydraulic Binder," Izvestiya Akademii Nauk SSSR Neorganicheskie Materialy, 4 (12) 2151-2154 (1968).
3. R.A. Tarnopol'skaya and N.V. Gul'ko, "The  $\text{CaO-SrO-Al}_2\text{O}_3\text{-ZrO}_2$  System and Its Importance for Refractories Technology," Ogneupory, No. 12, 38-42 (1967).
4. N.I. Voronin, V.S. Gorodetskii, and E.P. Fedorova, "Effect of Impurities on Stabilization of Zirconium Dioxide with Magnesium Dioxide and the Technical Properties of Zirconium Products," Trudy Vsesoyuznyi Inst. Nauch-Issled. Proekt. Rab. Ogneupory Prom., No. 37, 81 (1965). In Chemical Abstracts (66-98068p).
5. Antonio Cocco, "Sull'azione Esercitata da Piccole Percentuali de  $\text{Al}_2\text{O}_3$  sui Limiti di Composizione della Fase con Struttura Cubica Costituita da  $\text{CaO}$  e  $\text{ZrO}_2$ ," La Chimica e L'Industria, 42 (2) 142-145 (1960).
6. Hiroyoshi Takagi, et al., Effects of Alumina on Sintering of Zirconia Stabilized with Calcia," Sprechsaal fuer Keramik, Glas, Baustoffe, 107 (13) 584-588 (1974).
7. Kenneth Shaw, Refractories and Their Uses. John Wiley & Sons, New York, 1972, p. 151.
8. Pol Duwez and Francis Odell, "Phase Relationship in the System Zirconia-Ceria," Journal of the American Ceramic Society, 33 (9) 274-283 (1950).
9. Pol Duwez, Francis Odell, and Frank H. Brown, Jr., "Stabilization of Zirconia with Calcia and Magnesia," Journal of the American Ceramic Society, 51 (10) 553-556 (1968).
10. Ronald C. Garvie, "The Cubic Field in the System  $\text{CaO-ZrO}_2$ ," Journal of the American Ceramic Society, 51 (10) 553-556 (1968).
11. B.C. Weber, et al., "Observations on the Stabilization of Zirconia," Journal of the American Ceramic Society, 39 (6) 197-207 (1956).

12. A.M. Gavrish, et al., "X-ray Diffraction Investigation of the Decomposition Solid Solutions Based on Zirconium Dioxide," Izvestiya Akademii Nauk SSSR Nerorganicheskie Materialy, 5 (9) 1584-1588 (1969).
13. W.D. Kingery, Introduction to Ceramics. John Wiley & Sons, New York, 1960, p. 151.
14. R.W. Nurse, J.H. Welch, and A.J. Mujumdar, "The CaO-Al<sub>2</sub>O<sub>3</sub> System in a Moisture Free Atmosphere," Transactions of the British Ceramic Society, 64 409-418 (1965).
15. F.M. Lea and C.H. Desch, The Chemistry of Cement and Concrete, 2d. ed. Edward Arnold & Co., London, 1956, p. 52.
16. D. Brooksbank, "Thermal Expansion of Calcium-Aluminate Inclusions and Relation to Tessellated Stresses," Journal of the Iron and Steel Institute, 208 495-499 (1970).
17. A. Auriol, Phase Diagrams for Ceramists, American Ceramic Society, Columbus, Ohio, 1964, p. 102, fig. 232.
18. Powder Diffraction File, Joint Committee on Powder Diffraction Standards, Philadelphia, 1960, cards 7-82 and 1-572.
19. G.R. Rigby and A.T. Green, "The Thermal Expansion Characteristics of the Calcium Aluminates and Calcium Ferrites," Transactions of the British Ceramic Society, 42 (5) 95-103 (1943).
20. Julian R. Goldsmith, "The Compound CaO·2Al<sub>2</sub>O<sub>3</sub>," Journal of Geology, 56 80-81 (1948).
21. B. Tavischi, "Constitution of Portland Cement Clinker," Tonindustrie-Zeitung 61 717-719 (1937).
22. E.R. Boyko and L.G. Wisnyi, "The Optical Properties and Structures of CaO·2Al<sub>2</sub>O<sub>3</sub> and SrO·2Al<sub>2</sub>O<sub>3</sub>," Acta Crystallographica 11 444-445 (1958).
23. P.J. Baldock, et al., "X-ray Powder Diffraction Data for Calcium Monoaluminate and Calcium Dialuminate," Journal of Applied Crystallography, 3 188-191 (1970).
24. Woldemar A. Weyl and Evelyn C. Marboe, The Constitution of Glasses, Interscience Publishers, New York, 1962, p. 30.

25. Hans W. Hennicke and Horst Vaupel, "The Stabilization of Zirconium Dioxide with Aluminum Dioxide," Tonindustrie-Zeitung, 94 45-50 (1970).
26. R.E. Thoma, "Determination of Phase Diagrams," Handbook of X-rays E.F. Kaebler, McGraw Hill, New York, 1964, chapter 20.
27. Leonid V. Azaroff, Elements of X-ray Crystallography, McGraw-Hill, New York, 1968, p. 517.
28. S.W. Freiman, "Applied Stereology," c. 19 in Characterization of Ceramics, ed. L.L. Hench, Marcel Dekker, Inc., New York, 1971, p. 569.